

Electronic Thesis and Dissertation Repository

---

3-6-2023 11:30 AM

## The Synthesis and Characterization Studies of Modified Nucleobase in PNA and DNA

Gyeongsu Park, *The University of Western Ontario*

Supervisor: Hudson, Robert H.E., *The University of Western Ontario*

A thesis submitted in partial fulfillment of the requirements for the Doctor of Philosophy degree in Chemistry

© Gyeongsu Park 2023

Follow this and additional works at: <https://ir.lib.uwo.ca/etd>

 Part of the [Biochemistry Commons](#), and the [Organic Chemistry Commons](#)

---

### Recommended Citation

Park, Gyeongsu, "The Synthesis and Characterization Studies of Modified Nucleobase in PNA and DNA" (2023). *Electronic Thesis and Dissertation Repository*. 9228.  
<https://ir.lib.uwo.ca/etd/9228>

This Dissertation/Thesis is brought to you for free and open access by Scholarship@Western. It has been accepted for inclusion in Electronic Thesis and Dissertation Repository by an authorized administrator of Scholarship@Western. For more information, please contact [wlsadmin@uwo.ca](mailto:wlsadmin@uwo.ca).

## Abstract

Nucleic acids have been extensively studied not only for their importance in biological systems as the medium of genetic information but also for their potential uses in therapeutic, diagnostic and other biological applications. As such, modified oligonucleotides and oligonucleotide analogues have drawn the attention of researchers from various disciplines. Modification of oligonucleotides can enhance their desired characteristics and engender unique properties, such as fluorescence, giving rise to a variety of applications. Peptide nucleic acid (PNA) is an oligonucleotide mimic with a pseudo-peptide backbone based on *N*-(2-aminoethyl)glycine that is renowned for high target binding affinity and resistance to enzyme degradation. These properties of PNA are useful in their application as sequence-selective probes and other bioanalytical applications.

Thus, the overall theme of this thesis was the synthesis and evaluation of nucleobase-modified PNA and DNA monomers and the investigate of their effects on the physicochemical and photophysical characteristics of oligonucleotides and analogues.

The nucleobase modification 5-nitrouracil has only been investigated *in-silico* and these studies indicate that the 5-nitrouracil-adenine base pair is more energetically favourable than the uracil-adenine base-pair. We have constructed an experimental system to investigate the base-pairing ability of 5-nitrouracil in the context of a PNA oligomer. PNA oligomers possessing 5-nitrouracil substitution for uracil were studied in both duplex and triplex binding modes. 5-nitrouracil destabilized in the duplex forming sequence. However, in the triplex study, 5-nitrouracil formed stronger hydrogen bonds with adenine when it was incorporated into the Hoogsteen strand of a bis-PNA triplex. The discrimination of matched binding versus mismatched binding was also investigated. This study showed that 5-nitroU maintained the specificity for the matching complementary base pair.

We have also investigated the synthesis of modified nucleobases which possess dark fluorophore properties so that they act as a quencher when paired with an appropriate

fluorophore. Two fluorophore systems, that change conformation and switch between quenched and fluorescent states are known as molecular beacons. This work contributes to the design of a new model for a molecular beacon in which a base-pairing competent fluorescent nucleobase and a nucleobase quencher are incorporated in the stem region of a stem-loop sequence. An improved synthesis of the 5-(4-(*N,N*-dimethylamino)phenylazo-yl)uracil (DMPAU) PNA analog was achieved. Subsequently, its ability to hydrogen bond to adenine was determined by NMR methods, and it was found to associate with adenine as strongly as thymine, with a  $K_a \sim 120$  in chloroform. The ability of DMPAU to quench the fluorescence of the intrinsically fluorescent 6-phenylpyrrolocytosine (PhpC) and a selection of other common fluorophores was examined. These results allow us to predict that the DMPAU-PhpC make a suitable fluorophore-quencher pair for molecular beacon development.

Finally, an extension of the DMPAU base modification was developed for the 2'-deoxynucleoside, which resulted in 5-(4-(*N,N*-dimethylamino)phenylazo-yl)-2'-deoxyuridine (DMPAdU). A new synthetic route for starting with 2'-deoxyuridine was developed to avoid the need for a stereochemically-controlled glycoside bond formation which has been problematic in past syntheses from our lab. During the synthesis, the method for selective acylation of 2'-deoxyuridine was studied. The optimized condition for the diazotization of 5-amino-2'-deoxyuridine without glycosidic bond breakage was described. With the photophysical characterization of DMPAdU, the quenching ability was tested against 6-phenylpyrrolo-2'-deoxycytidine (PhpdC) fluorophore.

## Keywords

Peptide nucleic acid, duplex, triplex, hybridization, binding affinity, mismatch, molecular beacon, quenching, FRET, nucleobase quencher, nucleoside quencher

## Summary for Lay Audience

Nucleic acids have been a useful tool in biological applications; thus, many modifications have been made to nucleic acids to alter and give additional characteristics. Among the modified DNA, peptide nucleic acid (PNA) has been heavily investigated due to its excellent binding target DNA and ability to find the exact target. Such characteristics allow for PNAs to be used in therapeutic and diagnostic applications. Also, researchers have studied different modifications on a nucleobase and their backbone and their effects in adding or eliminating characteristics. This thesis focuses on the development of novel design and synthesis of PNA/DNA building blocks with structural nucleobase modifications that add novel properties. Photophysical characteristics of modified nucleobases and the binding ability of nucleic acids were investigated.

According to previous studies, the introduction of a nitro ( $-\text{NO}_2$ ) group to uracil should result in stronger pairing with its base pair partner, adenine, thereby improving binding; thus, we hypothesized 5-nitrouracil containing PNA to have better binding when it replaced natural nucleobase. Correspondingly 5-nitrouracil containing PNA monomer was made, and then the PNA chains to test their improved binding.

Molecular beacon is a useful biological tool that can detect certain sequences of nucleic acids. To create a molecular beacon, we need a light source (fluorophore) and a switch (quencher). Modified nucleobases, DMPAU, could act as the switch. After making the nucleobase switch, their ability to turn ON/OFF and to pair with its nucleobase partner was tested.



## Acknowledgments

I would like to sincerely thank my supervisor Robert H. E. Hudson for his guidance and support during my time in graduate studies. He always welcomed me in his office when I knocked on his door with problems or new ideas. He has always shown trust in me, imparting great wisdom not only in research but in life as well. I truly appreciate his contribution of knowledge, his time and his efforts. He will always be a frontier in the field of chemistry, where I always followed in his footsteps and where I am now willing to walk by his side.

Next, I would like to thank all the past and current members of the Hudson group for their support and enthusiasm during my life as a graduate student. Rachael, Atefeh, Timothy, Ali, Mason, Antony, Mria, Zi and Mohammed, you all have been a joy to work with. I hope every one of you has a bright future and happiness in your lives. I would also like to express my gratitude to the visiting professor Yoshio Saito.

I'd like to thank my family and friends who have helped me get through this important chapter of my life. I am truly fortunate to have all of you by my side, and I believe that I am where I am thanks to all of you. The many words of encouragement and support I have received from everyone, especially my family in Korea, have helped me get through this long journey.

Another group of friends that I've gained over the years is from The Western Taekwondo Club. The club was my place of rest like an oasis during difficult experimental situations. I give thanks to all of you. Special thanks go out to Tim and Kuny for their moral support during my writing of this thesis.

And now, I would like to express my deepest gratitude to my love, Jisu. Thank you for waiting and thank you for trusting in me. I thought of you to give me the encouragement that I needed, and you have been a great support. I find my motivation, my joy, and my light in you, and I look forward to seeing you soon.

# Table of Contents

Abstract.....	i
Summary for Lay Audience.....	iii
Acknowledgments.....	iv
Table of Contents.....	v
List of Tables .....	viii
List of Figures.....	ix
List of Schemes.....	xiv
List of abbreviations .....	xv
1. Introduction.....	1
1.1. Nucleic Acids.....	1
1.1.1. Peptide nucleic acid (PNA) .....	10
1.2. Nucleobase modification .....	15
1.2.1. Fluorescence nucleobase .....	17
1.3. Fluorescence spectroscopy <sup>95</sup> .....	25
1.3.1. Molecular beacon .....	27
1.4. Rationale.....	28
1.5. References.....	29
2. The Synthesis and Hybridization Study of 5-Nitrouracil PNA .....	38
2.1. Introduction.....	38
2.2. Result and Discussion.....	39
2.2.1. Computational calculation.....	39
2.2.2. Synthesis of 5-nitrouracil PNA monomer .....	40
2.2.3. Oligomerization of PNA.....	42

2.2.4.	Hybridization study .....	45
2.3.	Conclusion .....	50
2.4.	Future work.....	51
2.5.	Experimental.....	52
2.5.1.	Synthesis of 5-nitrouracil PNA monomer .....	52
2.6.	References.....	56
3.	The Synthesis and Photochemical Study of Nucleobase Quencher .....	59
3.1.	Introduction.....	59
3.2.	Result and Discussion.....	61
3.2.1.	Synthesis of DMPAU acetic acid .....	61
3.2.2.	Selection of quenchers and fluorophores.....	63
3.2.3.	The photophysical properties of quenchers and fluorophores.....	64
3.2.4.	Quenching study in EtOH.....	66
3.2.5.	Quenching study in water .....	69
3.2.6.	Hydrogen bonding study .....	70
3.3.	Conclusion .....	72
3.4.	Future work.....	72
3.5.	Experimental.....	73
3.6.	References.....	75
4.	The synthesis and Photochemical Study of Nucleoside Quencher.....	77
4.1.	Introduction.....	77
4.2.	Result and Discussion.....	78
4.2.1.	Synthesis of 5-DMPA-2' -deoxyuridine .....	78
4.2.2.	Photophysical Properties .....	85
4.3.	Conclusion .....	89
4.4.	Future work.....	89

4.5. Experimental.....	90
4.6. References.....	94
5. Conclusion .....	100
Appendix.....	102
General synthesis procedures.....	102
Instrumentation for characterization.....	102
PNA oligomerization .....	103
Quantification of PNA oligomers .....	104
Hybridization study of oligomers .....	105
Quenching study .....	105
<sup>1</sup> H NMR titration .....	105
Characterization of Fluorophores .....	107
Photophysical data of compounds .....	108
Quenching study .....	111
HPLC chromatograms .....	120
NMR Spectra .....	123

# List of Tables

Table 1-1. Structures and photophysical properties of naturally occurring fluorescent nucleobases. .....	19
Table 1-2. Structures and photophysical properties of the expanded nucleobases. ....	20
Table 1-3. Structures and photophysical properties of the extended nucleobases. ....	21
Table 1-4. Structures and photophysical properties of the isomorphous nucleobases. ....	22
Table 1-5. Structures and photophysical properties of the chromophoric nucleobases. ....	24
Table 2-1. Atomic Charges of $N^1$ -methylthymine (T) and $N^1$ -methyl-5-nitrouracil ( $U^m$ ) in different methods. ....	40
Table 2-2. PNA oligomers for duplex binding and mismatch study. ....	44
Table 2-3. DNA and RNA oligomers for the duplex formation and mismatch studies with PNA oligomers. ....	44
Table 2-4. Binding study of the PNA/DNA duplex and triplex. ....	47
Table 2-5. Mismatch study of the PNA/DNA duplex. ....	50
Table 3-1. Photophysical property of quenchers. ....	65
Table 3-2. Photophysical property of fluorophores. ....	65
Table 4-1. Stability of IV-5 under acidic conditions. ....	83
Table 4-2 Optimization of diazotization of IV-5. ....	83
Table 4-3. Photophysical properties of quenchers. ....	86
Table S1. Flow setting of HPLC for PNA purification. ....	103
Table S2. Purified PNA oligomers characterized by high-resolution mass spectroscopy. ....	104

## List of Figures

Figure 1-1. Schematic representation of a DNA-RNA duplex. ....	2
Figure 1-2. Watson-Crick complementary base pairing of nucleobases. Arrow indicates H-bond donor/acceptor interaction. ....	3
Figure 1-3. Hoogsteen base pairing for A:T and G:C <sup>+</sup> base pairs. ....	3
Figure 1-4. Wobble base pairing for I:C, G:U, I:U and I:A base pairs. ....	4
Figure 1-5. G-tetraplex; a planar guanine tetrad formed by Hoogsteen bonds and stabilized by the metal cation M <sup>+</sup> . ....	4
Figure 1-6. Antisense and antigene pathways. ....	5
Figure 1-7. Various modifications in the natural oligonucleotide. ....	6
Figure 1-8. Chemical structure of nucleic acids with backbond modification. (a) phosphate group; (b) 2'-position of ribose sugar moiety. ....	7
Figure 1-9. Chemical structure of nucleic acids with unnatural sugars or cyclic structures as backbone modification. ....	8
Figure 1-10. Chemical structure of nucleic acid analogs varying rigidity of backbone. ....	9
Figure 1-11. Chemical structure of nucleic acid with backbone modification: phosphorodiamidate morpholino (PMO) and peptide nucleic acid (PNA). ....	10
Figure 1-12. The structures of DNA (top) and PNA (bottom). ....	11
Figure 1-13. Structure of PNA complexes: side view (top) and upper view (bottom). ....	12
Figure 1-14. Fmoc-based solid-phase peptide synthesis (SPPS) cycle for PNA oligomerization. ....	14
Figure 1-15. Potential chemical modification sites of canonical pyrimidines (a) and (b). ....	16
Figure 1-16. Chemical structures of selection of modified nucleobases. ....	17
Figure 1-17. A chronicle of fluorescent nucleobase development. ....	18
Figure 1-18. The interaction of chromophoric base analogs in oligonucleotides and the wide variety of possible emission wavelengths. ....	23
Figure 1-19. Jablonski diagram. ....	26
Figure 1-20. Diagram of spectral overlap for FRET. ....	27
Figure 1-21. Structure of molecular beacon and Target-probe hybrid formation. ....	27
Figure 2-1. Hydrogen bonding between adenine (A) and 5-nitrouracils (U <sup>n</sup> ). ....	39
Figure 2-2. The electrostatic potential surface calculated of energy minimized structures computed using Hartree-Fock method 6-31+G* basis set as implemented by Wavefunction Spartan '14. (a) N <sup>1</sup> -methylthymine; (b) N <sup>1</sup> -methyl-5-nitrouracil. Red colour indicates d <sup>-</sup> regions and blue indicates d <sup>+</sup> regions. ....	40

Figure 2-3. The structure of bis-PNA and the hairpin structure formation of bis-PNA/DNA complex. (a) bis-PNA1/DN6 complex (control); (b) bis-PNA1/DN6 complex. ....	45
Figure 2-4. Potential intramolecular interactions. (a) 5-nitrouracil ( $U^n$ ) and cytosine (C); (b) 5-nitrouracil ( $U^n$ ) and protonated cytosine ( $C^+$ ). ....	48
Figure 3-1. Original and new design of molecular beacon. ....	60
Figure 3-2. Chemical structure of DABCYL acid, DMPAU and NPhpC. ....	61
Figure 3-3. Chemical structure of quenchers selected for quenching study. ....	63
Figure 3-4. Chemical structure of fluorophores selected for quenching study. ....	64
Figure 3-5. Normalized absorption spectra of DABCYL ethyl ester and DMPAU <i>tert</i> -butyl ester with normalized excitation and emission spectra of fluorophores. ....	67
Figure 3-6. Normalized absorption spectra of NPhpC ethyl ester and NPhEC ethyl ester with normalized excitation and emission spectra of fluorophores. ....	68
Figure 3-7. (a) Quenching study of PhpC acetic acid with DABCYL acid; (b) Quenching study of PhpC acetic acid with DMPAU acetic acid; (c) Stern-Volmer plots of DABCYL acid and DMPAU acetic acid. ....	69
Figure 3-8. Stacked NMR spectra of continuous variation of DMPAU <i>tert</i> -butyl ester and adenine ethyl ester mixture. ....	71
Figure 3-9. Chemical shift changes of the N4 hydrogen of adenine (a) and the C2 hydrogen (b) induced by the addition of the guest solution (DMPAU in $CDCl_3$ ) ....	71
Figure 4-1. Photophysical properties of the 6-phenylpyrrolo-2'-deoxycytidine (PhpdC) in EtOH. ....	85
Figure 4-2. Normalized absorption spectra of DMPAdU with normalized excitation and emission spectra of PhpdC in EtOH. ....	87
Figure 4-3. (a) Quenching study of DMPAdU with PhpdC in EtOH; (b) Stern-Volmer plot. ....	88
Figure S1 NMR titration of DMPAU <i>tert</i> -butyl ester(guest) and adenine ethyl ester(host). ....	107
Figure S2. UV-Vis spectra of quenchers ( $5.00 \times 10^{-5}$ M) in EtOH. ....	108
Figure S3. UV-Vis spectra of Pyrene in EtOH and Beer's law plot ( $\lambda_{ab} = 334$ nm). ....	109
Figure S4. UV-Vis spectra of PhpC ethyl ester in EtOH and Beer's law plot ( $\lambda_{ab} = 367$ nm). ....	109
Figure S5. UV-Vis spectra Acridone amide in EtOH and Beer's law plot ( $\lambda_{ab} = 398$ nm). ....	110
Figure S6. UV-Vis spectra of NBD amide in EtOH and Beer's law plot ( $\lambda_{ab} = 455$ nm). ....	110
Figure S7. Fluorescent spectra of PhpC acetic acid in 0.1% $Et_3N$ aqueous solution plot, $\lambda_{ex} = 362$ nm $\lambda_{em} = 450$ nm. ....	111
Figure S8. Quenching study of pyrene with DABCYL ethyl ester; a) Fluorescence intensities of pyrene in different concentrations of DABCYL ethyl ester, $\lambda_{excit} = 332$ nm ; b) Stern Volmer plot. ....	111

Figure S9. Quenching study of PhpC ethyl ester with DABCYL ethyl ester; a) Fluorescence intensities of PhpC ethyl ester in different concentrations of DABCYL ethyl ester, $\lambda_{\text{excit}} = 368$ nm; b) Stern Volmer plot. ....	112
Figure S10 Quenching study of acridone amide with DABCYL ethyl ester; a) Fluorescence intensities of acridone amide in different concentrations of DABCYL ethyl ester, $\lambda_{\text{excit}} = 343$ nm; b) Stern Volmer plot. ....	112
Figure S11 Quenching study of NBD amide with DABCYL ethyl ester; a) Fluorescence intensities of NBD amide in different concentrations of DABCYL ethyl ester, $\lambda_{\text{excit}} = 325$ nm; b) Stern Volmer plot. ....	113
Figure S12 Quenching study of pyrene with DMPAU <i>tert</i> -butyl ester; a) Fluorescence intensities of pyrene in different concentrations of DMPAU <i>tert</i> -butyl ester, $\lambda_{\text{excit}} = 332$ nm; b) Stern Volmer plot. ....	113
Figure S13 Quenching study of PhpC ethyl ester with DMPAU <i>tert</i> -butyl ester; a) Fluorescence intensities of PhpC ethyl ester in different concentrations of DMPAU <i>tert</i> -butyl ester, $\lambda_{\text{excit}} = 368$ nm; b) Stern Volmer plot. ....	114
Figure S14 Quenching study of acridone amide with DMPAU <i>tert</i> -butyl ester; a) Fluorescence intensities of acridone amide in different concentrations of DMPAU <i>tert</i> -butyl ester $\lambda_{\text{excit}} = 343$ nm; b) Stern Volmer plot. ....	114
Figure S15 Quenching study of NBD amide with DMPAU <i>tert</i> -butyl ester; a) Fluorescence intensities of NBD amide in different concentrations of DMPAU <i>tert</i> -butyl ester $\lambda_{\text{excit}} = 325$ nm; b) Stern Volmer plot. ....	115
Figure S16 Quenching study of pyrene with 4-NO <sub>2</sub> -PhpC ethyl ester; a) Fluorescence intensities of pyrene in different concentrations of 4-NO <sub>2</sub> -PhpC ethyl ester $\lambda_{\text{excit}} = 332$ nm; b) Stern Volmer plot. ....	115
Figure S17 Quenching study of PhpC ethyl ester with 4-NO <sub>2</sub> -PhpC ethyl ester; a) Fluorescence intensities of PhpC ethyl ester in different concentrations of 4-NO <sub>2</sub> -PhpC ethyl ester $\lambda_{\text{excit}} = 350$ nm; b) Stern Volmer plot. ....	116
Figure S18 Quenching study of NBD amide with 4-NO <sub>2</sub> -PhpC ethyl ester; a) Fluorescence intensities of NBD amide in different concentrations of 4-NO <sub>2</sub> -PhpC ethyl ester $\lambda_{\text{excit}} = 465$ nm; b) Stern Volmer plot. ....	116
Figure S19 Quenching study of pyrene with 4-NO <sub>2</sub> -PhEC ethyl ester; a) Fluorescence intensities of pyrene in different concentrations of 4-NO <sub>2</sub> -PhEC ethyl ester, $\lambda_{\text{excit}} = 316$ nm; b) Stern Volmer plot. ....	117
Figure S20 Quenching study of PhpC ethyl ester with 4-NO <sub>2</sub> -PhEC ethyl ester at different excitation wavelengths; a) c) e) Fluorescence intensities of PhpC ethyl ester in different concentrations of 4-NO <sub>2</sub> -PhEC ethyl ester; b) d) f) Stern Volmer plot. ....	118
Figure S21 Quenching study of acridone amide with 4-NO <sub>2</sub> -PhEC ethyl ester; a) Fluorescence intensities of acridone amide in different concentrations of 4-NO <sub>2</sub> -PhEC ethyl ester, $\lambda_{\text{excit}} = 267$ nm; b) Stern Volmer plot. ....	119



Figure S22 Quenching study of NBD amide with 4-NO <sub>2</sub> -PhEC ethyl ester; a) Fluorescence intensities of NBD amide in different concentrations of 4-NO <sub>2</sub> -PhEC ethyl ester, $\lambda_{\text{excit}} = 450$ nm; b) Stern Volmer plot. ....	119
Figure S23 HPLC trace of PNAd1 detected by UV absorption at 265 nm.....	120
Figure S24. HPLC trace of PNAd2 detected by UV absorption at 265 nm.....	120
Figure S25. HPLC trace of PNAd3 detected by UV absorption at 265 nm.....	121
Figure S26. HPLC trace of PNAd4 detected by UV absorption at 265 nm.....	121
Figure S27. HPLC trace of bisPNA1 detected by UV absorption at 265 nm.....	122
Figure S28. HPLC trace of bisPNA2 detected by UV absorption at 265 nm.....	122
Figure S29 <sup>1</sup> H NMR of <i>tert</i> -Butyl 2-(5-nitrouracil-1-yl)acetate (II-2).....	123
Figure S30 <sup>13</sup> C NMR of <i>tert</i> -Butyl 2-(5-nitrouracil-1-yl)acetate (II-2).....	124
Figure S31 <sup>1</sup> H NMR of 2-(5-Nitrouracil-1-yl)acetic acid (II-3).....	125
Figure S32 <sup>1</sup> H NMR of <i>tert</i> -Butyl 2-((2-aminoethyl)amino)acetate (II-5).....	126
Figure S33 <sup>1</sup> H NMR of <i>N</i> -(2-(((9 <i>H</i> -Fluoren-9-yl)methoxy)carbonyl)amino)ethyl)-2-( <i>tert</i> -butoxy)-2-oxoethanaminium chloride (II-6).....	127
Figure S34 <sup>13</sup> C NMR of <i>N</i> -(2-(((9 <i>H</i> -Fluoren-9-yl)methoxy)carbonyl)amino)ethyl)-2-( <i>tert</i> -butoxy)-2-oxoethanaminium chloride (II-6).....	128
Figure S35 <sup>1</sup> H NMR of <i>tert</i> -Butyl 2-( <i>N</i> -(2-(((9 <i>H</i> -fluoren-9-yl)methoxy)carbonyl)amino) ethyl)-2-(5-nitrouracil-1-yl)-acetamido)acetate (II-7).....	129
Figure S36 <sup>13</sup> C NMR of <i>tert</i> -Butyl 2-( <i>N</i> -(2-(((9 <i>H</i> -fluoren-9-yl)methoxy)carbonyl)amino) ethyl)-2-(5-nitrouracil-1-yl)-acetamido)acetate (II-7).....	130
Figure S37 <sup>1</sup> H NMR of 2-( <i>N</i> -(2-(((9 <i>H</i> -Fluoren-9-yl)methoxy)carbonyl)amino)ethyl)-2-(5-nitrouracil-1-yl)acetamido)acetic acid (II-8). ....	131
Figure S38 <sup>13</sup> C NMR of 2-( <i>N</i> -(2-(((9 <i>H</i> -fluoren-9-yl)methoxy)carbonyl)amino)ethyl)-2-(5-nitrouracil-1-yl)acetamido)acetic acid (II-8). ....	132
Figure S39 <sup>1</sup> H NMR of <i>tert</i> -butyl 2-(5-aminouracil-1-yl)acetate (II-9). ....	133
Figure S40 <sup>13</sup> C NMR of <i>tert</i> -butyl 2-(5-aminouracil-1-yl)acetate (II-9). ....	134
Figure S41 <sup>1</sup> H NMR of <i>tert</i> -Butyl 2-(5-[(4'( <i>N,N</i> -dimethylamino)phenyl)diazenyl])-uracil-1-yl)acetate (II-11). ....	135
Figure S42 <sup>13</sup> C NMR of <i>tert</i> -Butyl 2-(5-[(4'( <i>N,N</i> -dimethylamino)phenyl)diazenyl])-uracil-1-yl)acetate (II-11). ....	136
Figure S43 <sup>1</sup> H NMR of 2-(5-[(4'( <i>N,N</i> -dimethylamino)phenyl)diazenyl])-uracil-1-yl)acetic acid (II-12).....	137
Figure S44 <sup>13</sup> C NMR of 2-(5-[(4'( <i>N,N</i> -dimethylamino)phenyl)diazenyl])-uracil-1-yl)acetic acid (II-12).....	138
Figure S45 <sup>1</sup> H NMR of <i>tert</i> -butyl 2-(5-aminouracil-1-yl)acetate (III-3). ....	139

Figure S46 <sup>13</sup> C NMR of <i>tert</i> -butyl 2-(5-aminouracil-1-yl)acetate (III-3).....	140
Figure S47 <sup>1</sup> H NMR of <i>tert</i> -Butyl 2-(5-((4-( <i>N,N</i> -dimethylamino)phenyl)diazenyl)-uracil-1-yl)acetate (III-5).....	141
Figure S48 <sup>13</sup> C NMR of <i>tert</i> -Butyl 2-(5-((4-( <i>N,N</i> -dimethylamino)phenyl)diazenyl)-uracil-1-yl)acetate (III-5).....	142
Figure S49 <sup>1</sup> H NMR of 2-(5-((4-( <i>N,N</i> -dimethylamino)phenyl)diazenyl)-uracil-1-yl)acetic acid (III-6).....	143
Figure S50 <sup>13</sup> C NMR of 2-(5-((4-( <i>N,N</i> -dimethylamino)phenyl)diazenyl)-uracil-1-yl)acetic acid (III-6).....	144
Figure S51 <sup>1</sup> H NMR of 2'-deoxyuridine-3',5'- <i>O</i> -diacetate (IV-2).....	145
Figure S52 <sup>13</sup> C NMR of 2'-deoxyuridine-3',5'- <i>O</i> - diacetate (IV-2).....	146
Figure S53 <sup>1</sup> H NMR of 5-nitro-2'-deoxyuridine-3',5'- <i>O</i> -diacetate (IV-3).....	147
Figure S54 <sup>13</sup> C NMR of 5-nitro-2'-deoxyuridine-3',5'- <i>O</i> -diacetate (IV-3). ....	148
Figure S55 <sup>1</sup> H NMR of 5-amino-2'-deoxyuridine-3',5'- <i>O</i> -diacetate (IV-4). ....	149
Figure S56 <sup>13</sup> C NMR of 5-amino-2'-deoxyuridine-3',5'- <i>O</i> -diacetate (IV-4). ....	150
Figure S57 <sup>1</sup> H NMR of 5-((4-( <i>N,N</i> -dimethylamino)phenyl)diazenyl) -2'-deoxyuridine-3',5'- <i>O</i> -diacetate (IV-5). ....	151
Figure S58 <sup>13</sup> C NMR of 5-((4-( <i>N,N</i> -dimethylamino)phenyl)diazenyl) -2'-deoxyuridine-3',5'- <i>O</i> -diacetate (IV-5). ....	152
Figure S59. <sup>1</sup> H NMR of 5-((4-( <i>N,N</i> -dimethylamino)phenyl)diazenyl) -2'-deoxyuridine (IV-6). .....	153
Figure S60. <sup>13</sup> C NMR of 5-((4-( <i>N,N</i> -dimethylamino)phenyl)diazenyl) -2'-deoxyuridine (IV-6) .....	154

## List of Schemes

Scheme 1-1. The central dogma of molecular biology.....	1
Scheme 2-1. Synthesis of the 5-nitrouracil monomer (U <sup>n</sup> ).....	41
Scheme 3-1. Synthesis of 4-( <i>N,N</i> -dimethylamino)phenylazouracil nucleobase acetic acid derivative (III-6).....	62
Scheme 4-1. Optimized synthetic pathway for 5-DMPA-2'-deoxyuridine (IV-6). ....	79
Scheme 4-2. Acylation of 2'-deoxyuridine with acetic anhydride.....	80
Scheme 4-3. Nitration of IV-2; (a) the use of 1-nitropyrazol; (b) the use of NOBF <sub>4</sub> .....	80
Scheme 4-4. Hydrogenation of IV-3 with Pd/C catalyst. ....	81
Scheme 4-5. Diazotization of IV-4 and azo coupling.....	82
Scheme 4-6. Removal of acetate-protecting groups. ....	84

## List of abbreviations

2-AP	2-aminopurine
A	adenine
A-3Ph	2-phenylpropyl-2'-deoxyadenosine
aeg	aminoethylglycine
ANA	arabino nucleic acid
AON	antisense oligonucleotide
Bhoc	benzhydryloxycarbonyl
Boc	<i>tert</i> -butyloxycarbonyl
br	broad singlet
C	cytosine
CD	circular dichroism
CeNA	cyclohexene nucleic acid
cm	centimeter
D	2,6-diaminopurine
d	doublet
DABCYL	4-( <i>N,N</i> -dimethylamino)azobenzene- 4'-carboxylic
DCC	dicyclohexyl carbodiimide
DCM	dichloromethane
dd	doublet of doublet
ddd	doublet of doublet of doublet
DFT	density functional theory
DIPEA	<i>N,N</i> -diisopropylethylamine
DMAP	4-dimethylaminopyridine
DMF	<i>N,N</i> -dimethylformamide
DMPAdU	5-(4-( <i>N,N</i> -dimethylamino)phenylazo-yl)-2'-deoxyuridine
DMPAU	5-(4-( <i>N,N</i> -dimethylamino)phenylazo-yl)uracil
DMSO	dimethyl sulfoxide
DNA	2'-deoxyribonucleic acid
dt	doublet of triplet

dU	2'-deoxyuridine
EDC	<i>N</i> -ethyl- <i>N'</i> -(3-dimethylaminopropyl) carbodiimide
EDTA	ethylenediaminetetraacetic acid
EI	electron ionization
ESI	electrospray ionization
Et <sub>3</sub> N	triethylamine
EtOH	ethanol
EWG	electron-withdrawing group
FCC	flash column chromatography
Fmoc	fluorenylmethoxycarbonyl
Fmoc-OSu	<i>N</i> -(9-fluorenylmethoxycarbonyloxy) succinimide
FRET	fluorescence resonance energy transfer
g	gram
G	guanine
GNA	glycol nucleic acid
h	hour
HNA	hexitol nucleic acid
HOBt	<i>N</i> -hydroxybenzotriazole
HPLC	high-pressure liquid chromatography
HRMS	high resolution mass spectrometry
Hz	hertz
<i>I</i>	fluorescence intensity
I	hypoxanthine
<i>I</i> <sub>0</sub>	initial fluorescence intensity
ISC	intersystem crossing
J	pseudocytosine
<i>J</i>	coupling constant
K	lysine
K <sub>a</sub>	association constant
K <sub>sv</sub>	Stern-Volmer constant
LNA	locked nucleic acid

m	multiplet
M	mol
m/z	mass-to-charge ratio
ma.	major
MB	molecular beacon
MeO	methoxy
MeOH	methanol
MHz	megahertz
mi.	minor
min	minute
mL	milliliter
mmol	millimole
MO	molecular orbital
MOE	methoxyethyl
mRNA	messenger ribonucleic acid
N	normality
NBD	4-nitro-2,1,3-benzoxadiazole
nm	nanometer
NMP	<i>N</i> -methyl-2-pyrrolidone
NMR	nuclear magnetic resonance
NPhpC	6-(4-nitrophenyl)pyrrolocytosine
PAH	polycyclic aromatic hydrocarbon
pC	pyrrolocytosine
PEG2	8-amino-3,6-dioxaoctanoic acid
PhpC	6-phenylpyrrolocytosine
PhpdC	6-phenylpyrrolo-2'-deoxycytidine
PMO	phosphorodiamidate morpholino oligomer
PNA	peptide nucleic acid
ppm	parts per million
q	quartet
Q-TOF	quadrupole time of flight

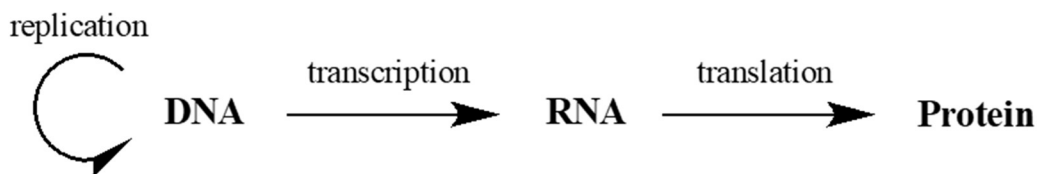
RAM	rink amide
RNA	ribonucleic acid
rot.	rotamers
s	singlet
SNPs	single-nucleotide polymorphisms
SPPS	solid-phase peptide synthesis
t	triplet
T	thymine
TcNA	tricyclo nucleic acid
TFA	trifluoroacetic acid
TfOH	trifluoromethanesulfonic acid
THF	tetrahydrofuran
TLC	thin layer chromatography
T <sub>m</sub>	melting temperature
TMS	trimethylsilyl
TNA	threose nucleic acid
tRNA	transfer ribonucleic acid
U	uracil
U <sup>n</sup>	5-nitrouracil
UNA	unlocked nucleic acid
UV	ultra violet
v/v	percent volume/volume
Vis	visible
W	watt
δ	chemical shifts
λ <sub>ab</sub>	maximum absorption wavelength
λ <sub>em</sub>	maxima emission wavelength
λ <sub>ex</sub>	maxima excitation wavelength
μM	micromole
μL	microliter
°C	degrees Celsius

# Chapter 1

## 1. Introduction

### 1.1. Nucleic Acids

Deoxyribonucleic acid (DNA) and ribonucleic acid (RNA) are biopolymers that store and transfer genetic information within biological systems in nature. In 1970, Francis Crick defined the central dogma of molecular biology as the flow of genetic information from these nucleic acids to protein. DNA, which is at the beginning of the central dogma, serves as the repository of genetic information.<sup>1</sup> The genetic information in DNA can be replicated into DNA or be transcribed into RNA such as messenger RNA (mRNA). The translation of the information in mRNA produces proteins (**Scheme 1-1**). According to this scheme, nucleic acids provide high-fidelity information transfer via the processes of replication, transcription, and translation. These system processes are the key to our existence.



**Scheme 1-1. The central dogma of molecular biology.**

Naturally occurring nucleic acids are polymers made with building blocks called nucleotides. A nucleotide is composed of a ribose sugar moiety, a phosphate group, and one of the canonical nucleobases. As the repeating unit of the nucleic acid polymer, the phosphate group and the ribose sugar link nucleotide building blocks to form a strand of nucleic acid. This repeating linkage of phosphodiester and ribose sugars is the backbone of nucleic acid. The two main classes of nucleic acids, deoxyribonucleic acid (DNA) and ribonucleic acid (RNA) are differentiated based on the existence of a hydroxyl group on the 2' position of ribose sugar (**Figure 1-1**).



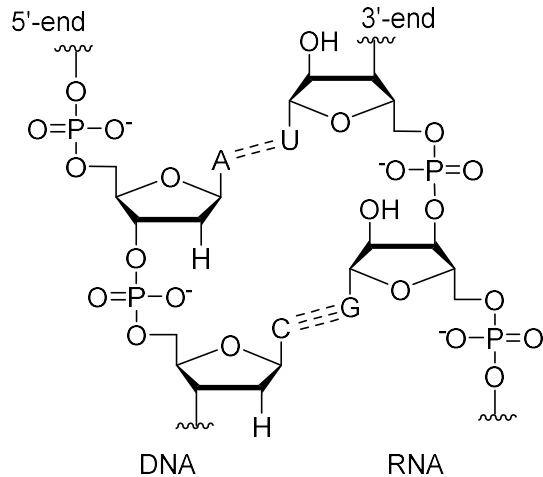


**Figure 1-1. Schematic representation of a DNA-RNA duplex.**

The nucleobase is the fundamental unit of the genetic code. The arrangement of these bases in the oligonucleotide, forming a sequence, determines what biological instructions are contained in a strand of DNA. There are five canonical nucleobases: adenine (A), guanine (G), cytosine (C), thymine (T), and uracil (U). A, G, C, and T are used in DNA, and T is replaced with U in RNA. Structurally, nucleobases are made of two heterocyclic aromatic rings: pyrimidine and purine. Nucleobases differentiated based on these two rings, form hydrogen bonds through external nitrogen and oxygen groups. This hydrogen bonding of nucleobases allows molecular recognition of nucleic acids, linking and stabilizing the nucleotide building blocks.

When nucleobases pair with each other, the hydrogen bond acceptors and donors base interact through complementary sites. Adenine (A) pairs with thymine (T) or uracil (U) by forming two hydrogen bonds, and guanine (G) pairs with cytosine (C) by forming three hydrogen bonds. These are referred to as Watson-Crick base pairs (**Figure 1-2**). In addition to Watson-Crick base pairs, there are different forms of base pairs with hydrogen bonding to form secondary DNA structures. An example of these non-Watson-Crick interactions is Hoogsteen pairing (**Figure 1-3**).<sup>2</sup> In Hoogsteen pairing, an extra thymine forms hydrogen bonds on the major groove of adenine in a Watson-Crick A-T base pair complex, and a protonated cytosine forms hydrogen bonds on the major groove of guanine in a Watson-Crick C-G base pair complex. These Watson-Crick and Hoogsteen base pairings enable the formation of three-stranded quadruplex.<sup>4,5</sup> Wobble base pairings can be found in the pairings between the anticodon of

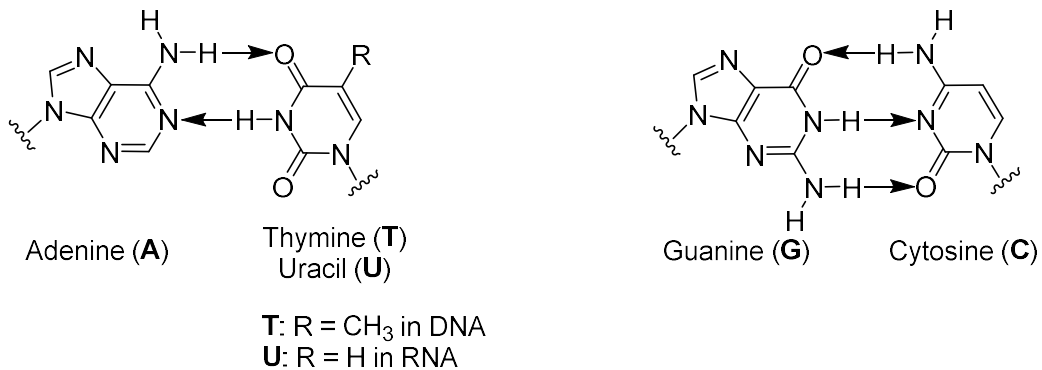


**Figure 1-2. Watson-Crick complementary base pairing of nucleobases. Arrow indicates H-bond donor/acceptor interaction.**

complexes called triplexes. Other non-Watson-Crick pairings include wobble<sup>3</sup> and G- tRNA and the codon of mRNA. There are four main base pairs: hypoxanthine-cytosine (I-C), guanine-uracil (G-U), hypoxanthine-uracil (I-U), and hypoxanthine-adenine (I-A) (**Figure 1-4**). Hypoxanthine results from deamination of adenosine. G-Quadruplex is a complex of four guanines with hydrogen bondings and a metal ion in the center (**Figure 1-5**). This can be found in telomeres at the terminal ends of chromosomes.

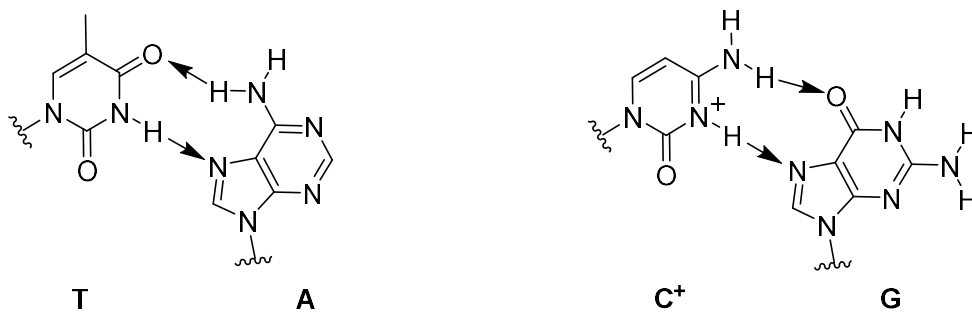


**Figure 1-3. Hoogsteen base pairing for A:T and G:C<sup>+</sup> base pairs.**

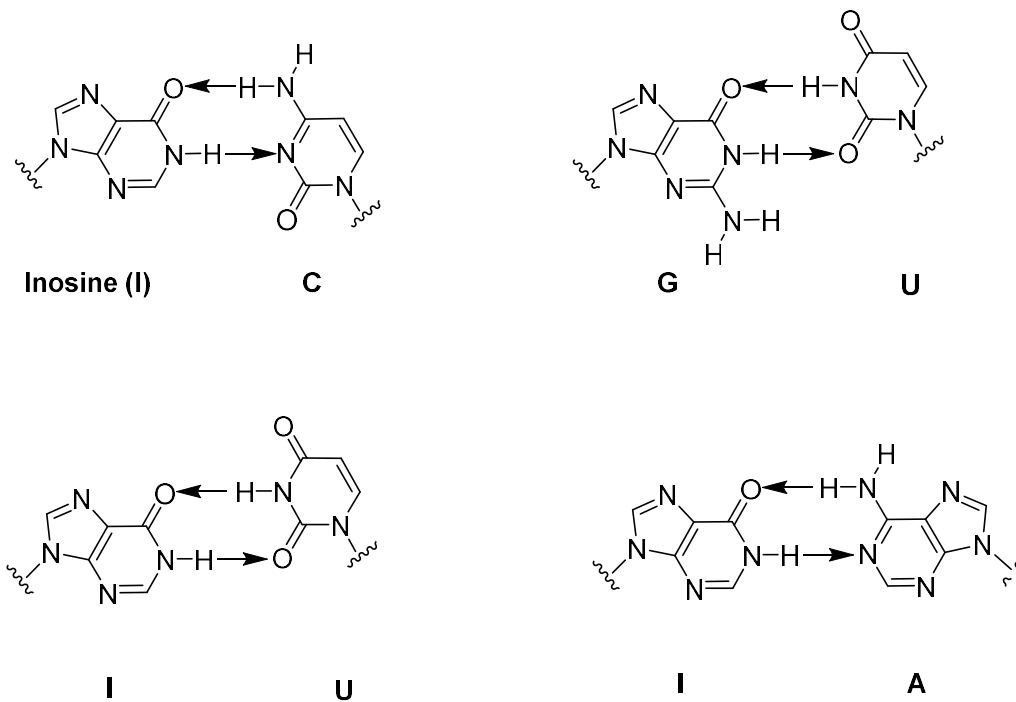


Figure 1-4. Wobble base pairing for I:C, G:U, I:U and I:A base pairs.

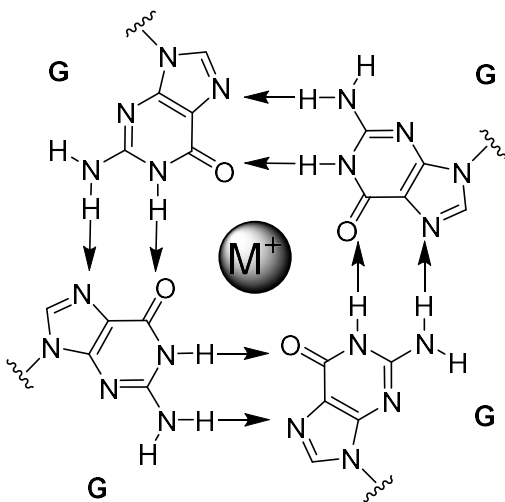
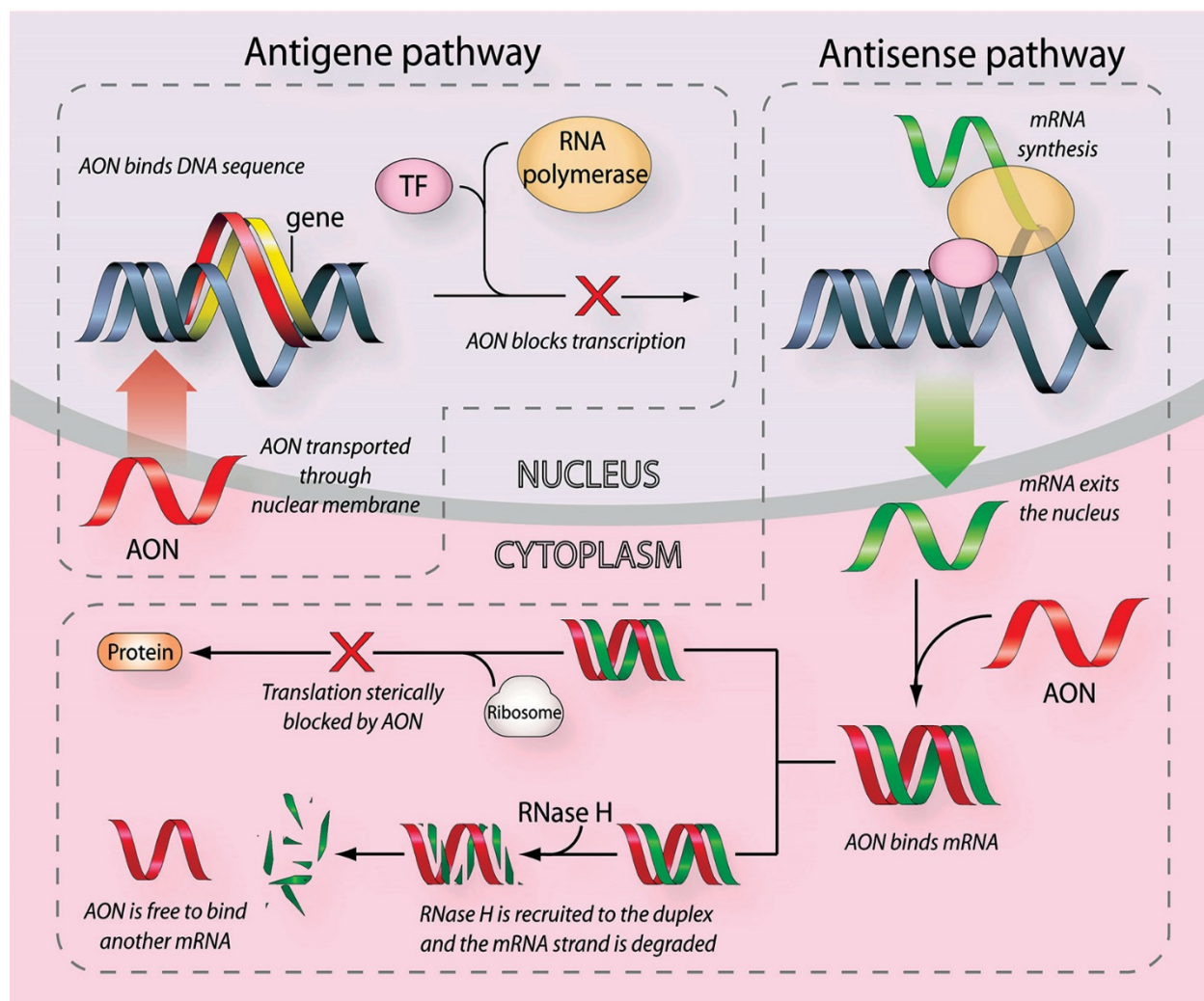


Figure 1-5. G-tetraplex; a planar guanine tetrad formed by Hoogsteen bonds and stabilized by the metal cation  $M^+$ .

The potential of nucleic acids is not limited to carrying genetic information. They also play diverse roles in numerous disciplines, including therapeutics, diagnostics, and nanotechnology.<sup>6</sup> In particular, nucleic acids have demonstrated great promise in the treatment of cancer, diabetes, cystic fibrosis, and other genetic disorders. One therapeutic approach to treat these diseases is the antisense strategy, in which gene expression is silenced by binding complementary antisense oligonucleotide (AON) to the disease-causing mRNA sequence (**Figure 1-6**). This prevents the translation of the mRNA either by sterically blocking translation or by recruiting the ribonuclease H enzyme to degrade the RNA strand in the mRNA-AON duplex.<sup>7</sup> The antigene strategy is another therapeutic approach to treat genetic diseases by interrupting transcription or replication processes. A single-stranded antigene agent enters the



**Figure 1-6. Antisense and antigene pathways.** [Reprinted with permission from (Jain, M.L.; Bruice, P. Y.; Szabo, I. E.; Bruice, T. C. *Chem. Rev.* **2011**, *112*, 1284-1309)<sup>9</sup> Copyright © (2012) American Chemical Society]

nucleus of the cell and binds to a genomic double-stranded DNA (dsDNA). This antigenic oligonucleotide binding blocks the target region on the gene to prevent DNA replication and transcription into mRNA.<sup>8,9</sup>

The use of naturally occurring DNA or RNA nucleotides in therapeutic applications comes with the challenge of improving pharmacokinetics, binding affinity, specificity, and stability against the degradation by nucleases. Modified nucleic acid analogs, however, have the potential to overcome these challenges.<sup>10</sup> Nucleic acids can be modified at the backbone, sugar, or nucleobase (**Figure 1-7**). These modified nucleic acid analogs have gained widespread use in therapeutic and diagnostic applications.<sup>9,11-14</sup>

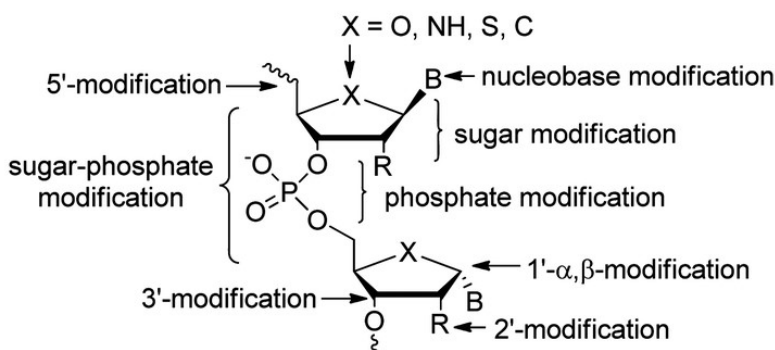


**Figure 1-7. Various modifications in the natural oligonucleotide.** [Reprinted with permission from (Sharma, V. K.; Rungta, P.; Prasad, A. K. *RSC Adv.* **2014**, 4, 16618-16631)<sup>13</sup> Copyright © (2014) of The Royal Society of Chemistry]

The first modification attempt at the backbone was the replacement of the oxygen of the phosphate linkage with sulfur<sup>15-18</sup> or a methyl group (**Figure 1-8a**).<sup>19,20</sup> Phosphorothioate oligonucleotides have shown increased resistance to nucleases and the ability to recruit RNases that degrade mRNA. Disadvantages of this modification are the production of diastereomers during synthesis, lower binding affinity during hybridization, as well as specificity that leads to undesirable side effects *in-vivo* such as cellular toxicity. Phosphoramidate oligonucleotides have nuclease resistance and high affinity but cannot recruit RNase H for mRNA degradation.<sup>21,22</sup>

The next generation of modified oligonucleotides introduced electronegative groups such as methoxy (MeO),<sup>23</sup> methoxyethyl (MOE),<sup>24,25</sup> and fluoro group<sup>26</sup> to the 2' position of ribose sugar (**Figure 1-8b**). These 2' substituted oligonucleotides also showed high binding affinity and stability against enzyme degradation. However, this modification still could not recruit RNase H for the degradation of target mRNA. When a phosphorothioate replacement was introduced with the 2' modification, these chimeric oligonucleotides showed both RNase H activity and resistance to nucleases due to the arms in the 2' position.<sup>27</sup>

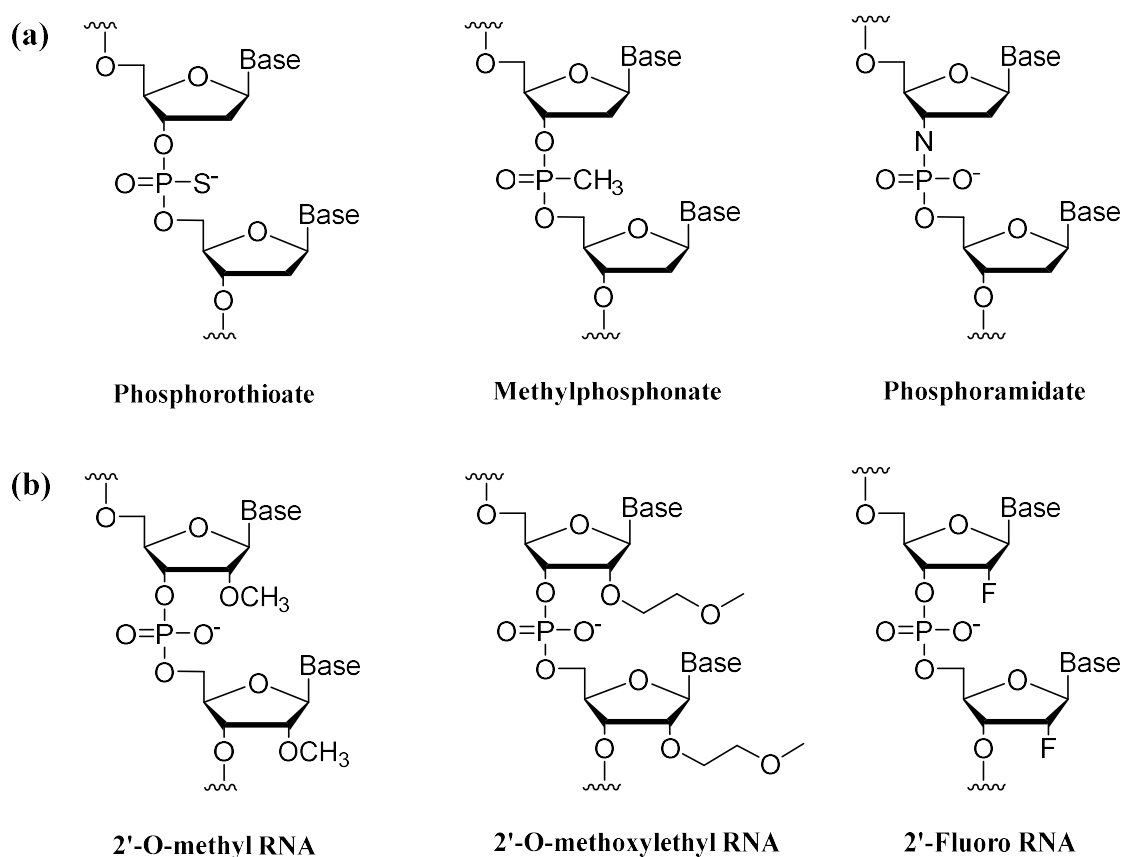


**Figure 1-8. Chemical structure of nucleic acids with backbond modification. (a) phosphate group; (b) 2'-position of ribose sugar moiety.**

The third generation of modifications came in the form of oligonucleotides with unnatural sugars or cyclic structures instead of ribose sugar (**Figure 1-9**). Arabino nucleic acid (ANA)<sup>28</sup> and 2'-fluoro-arabino nucleic acid (FANA)<sup>29,30</sup> have arabinose sugar which is an epimer

of ribose. The difference between these two sugars is the orientation of the OH group in the 2' carbon stereocentre. This stereoinversion at C2' makes ANA favor a DNA-like C2'-endo sugar pucker over the RNA-like C3'-endo sugar pucker. This conformational change allows ANA to recruit RNase H, while RNA cannot do so. Despite having C2'-endo sugar pucker, they are stable against C2'-endo nucleases.<sup>31-33</sup> Threose nucleic acid (TNA) has an unnatural four-carbon threose sugar.<sup>34</sup> This makes TNA completely refractory to nuclease digestion, so it is a promising candidate for therapeutic use as an antisense and aptamer.<sup>35-38</sup> Hexitol nucleic acid (HNA)<sup>39-41</sup> and Cyclohexene nucleic acid (CeNA)<sup>42-44</sup> have a 6-membered ring instead of a 5-member furanose sugar. HNA and CeNA also exhibit RNase H activity, high affinity to the target, and nuclease resistance.

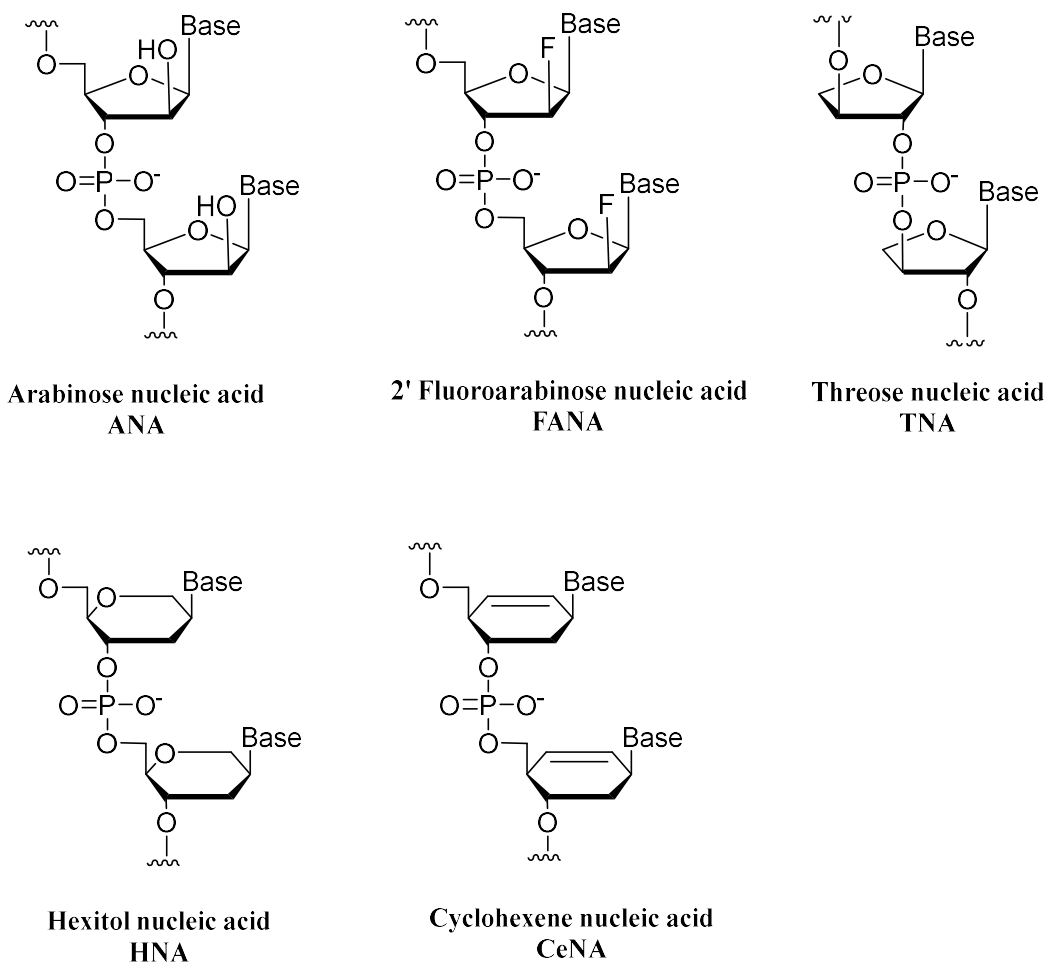


**Figure 1-9. Chemical structure of nucleic acids with unnatural sugars or cyclic structures as backbone modification.**

To achieve higher affinity, other attempts were made to reduce the degree of freedom of rotation by structurally constraining the sugar. The rigid structure reduced entropic cost in duplex formation. Locked nucleic acid (LNA)<sup>45-48</sup> and tricyclo nucleic acid (TcNA)<sup>49,50</sup> have extra ring structures in contrast to natural nucleic acids to lock the backbone (**Figure 1-10**). LNA has a methylene bridge that connects the 2'-oxygen of the ribose moiety with the 4'-carbon. This linkage fixed the sugar ring to a C3'-endo pucker only, so LNA has A-form helical structure like RNA. Therefore, LNA cannot initiate RNase H cleavage to target. Nonetheless, this locking bridge gives LNA high binding affinity and stability against nucleolytic degradation. To introduce both the strong RNase H activity of DNA and the high binding affinity of LNA, chimeric “gapmers” with LNA inserted into the central DNA portion were designed and studied.<sup>51</sup> In a contrasting approach, unlocked nucleic acids (UNA)<sup>52</sup> were investigated by removing the C2'-C3' bond to give flexibility in binding to the target (Figure 1-10). UNA shows increased discrimination of mismatch that improves hybridization specificity, though with lower

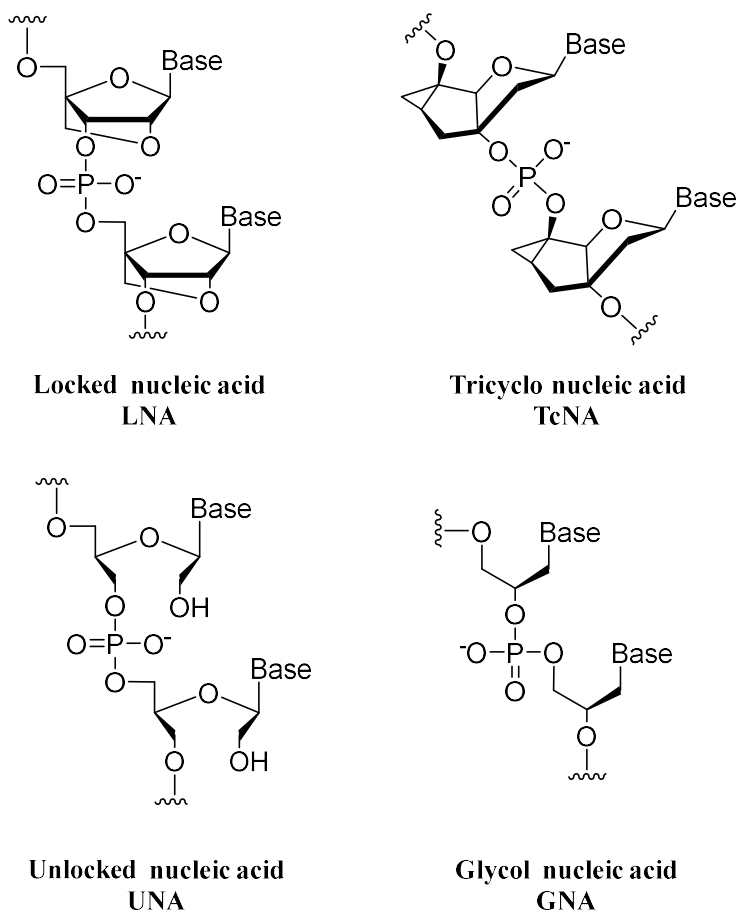


**Figure 1-10. Chemical structure of nucleic acid analogs varying rigidity of backbone.**



duplex stability. In contrast, Glycol nucleic acid (GNA)<sup>53</sup>, comprised of a backbone with just three carbons, shows high duplex stability despite having comparable flexibility.

Subsequent progress in backbone modification has led to the introduction of phosphorodiamidate morpholino oligomer (PMO)<sup>53-56</sup> and peptide nucleic acid (PNA)<sup>57-59</sup> (**Figure 1-11**). The backbone of PMO is composed of a methylenemorpholine ring and phosphorodiamidate instead of a ribose sugar and phosphodiester linkage. PMO shows excellent stability against nucleases due to the replacement of sugar to methylenemorpholine ring. Neutral phosphorodiamidate linkage removes electrostatic repulsion with the target sequence, thus PMO has a high binding affinity. Similarly, PNA has a natural charge pseudo-peptide backbone with high flexibility that gives rise to affinity and selectivity.

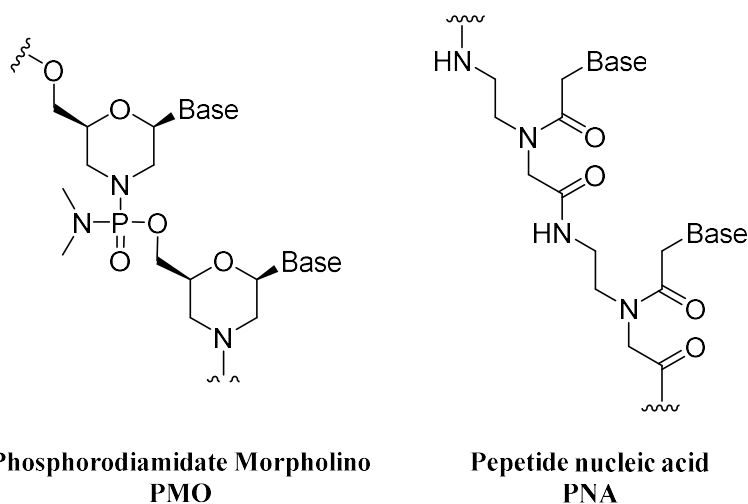


**Figure 1-11. Chemical structure of nucleic acid with backbone modification: phosphorodiamidate morpholino (PMO) and peptide nucleic acid (PNA).**

### 1.1.1. Peptide nucleic acid (PNA)

In 1991, a new nucleic acid analog was introduced by Nielsen and Buchardt.<sup>60</sup> Peptide nucleic acid (PNA)<sup>57,58,61</sup> is an oligonucleotide mimic with a pseudo-peptide backbone based on *N*-(2-aminoethyl)glycine instead of the phosphate diester and ribose sugar backbone found in natural nucleic acids (**Figure 1-12**). Due to the achiral and uncharged pseudo-peptide backbone, PNA has unique physicochemical and biochemical properties in comparison with naturally occurring DNA and RNA. The neutral character of the backbone abolishes charge repulsion

between the two strands in a PNA/nucleic acid duplex. As a result of the absence of electronic repulsion, the thermal stability of the PNA/nucleic acid duplex is mainly independent of the ion strength. Furthermore, PNA with the pseudo-peptide backbone is resistant to chemical reactions and enzyme degradation.<sup>62</sup>

The structure of PNA shares a common bond spacing framework with the structure of natural nucleic acids; however, PNA has different compositions. In DNA, repeating monomers have six covalent bonds length of the backbone, and their nucleobases are three covalent bonds length away from the backbone. This “6+3” bond spacing frame can also be found in the *N*-(2-aminoethyl)glycine backbone and methylene linker in PNA (**Figure 1-12**). PNA can act as a DNA mimic because it shares the same bond spacing frame. This has been supported by Nielsen and Egholm’s experimental data,<sup>57</sup> which showed that PNA analogs with different bond spacing recognized complementary DNA sequences with lower affinity when compared with PNA with the same bond spacing.

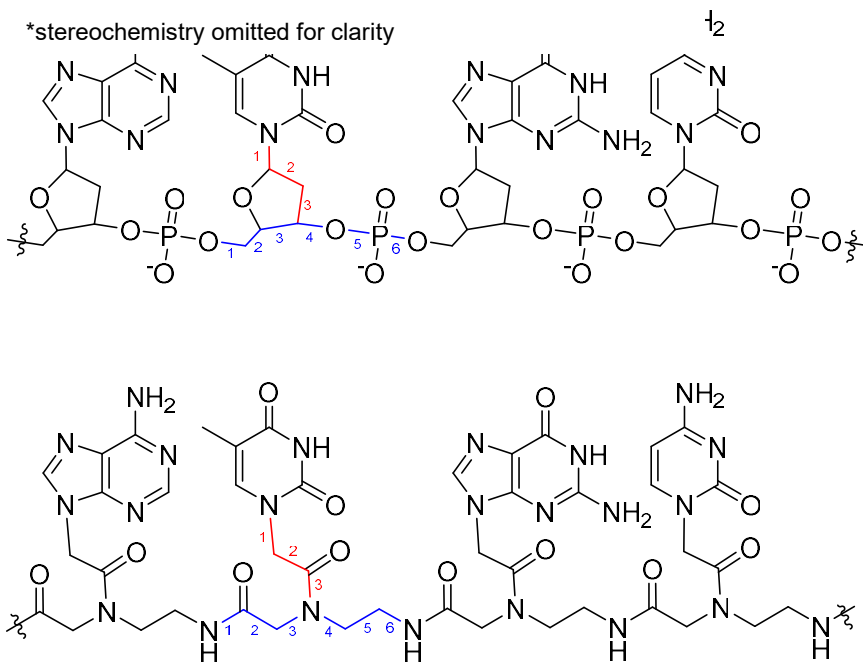


**Figure 1-12. The structures of DNA (top) and PNA (bottom).**

PNA can adapt to the helical structure favored by the target nucleic acid due to PNA's flexible backbone (**Figure 1-13**). PNA-RNA duplexes adopt the A-form helical structure favored by the RNA strand<sup>63</sup>, while PNA-DNA duplexes adopt the B-form helical structure favored by the DNA strand. However, PNA-PNA duplexes adopt a new helical conformation named P-form.<sup>64</sup> This conformation is a wide helix with a longer helical diameter (28 Å) with more base pairs (18 base pairs) per turn compared to A-form and B-form. The P-form has also been seen in the 2PNA/DNA triplex. PNA can form a duplex with complementary strands in both anti-parallel and parallel orientations,<sup>65</sup> while the anti-parallel orientation is the preferred form.

PNA has a high binding affinity to complementary nucleic acids (DNA or RNA), which has been observed experimentally as a high thermal stability of the duplex formed. High specificity is also observed due to stricter Watson-Crick base pairing and higher destabilization on mismatching strands in PNA/DNA duplex than in DNA/DNA duplex.<sup>66</sup> Because of stable and

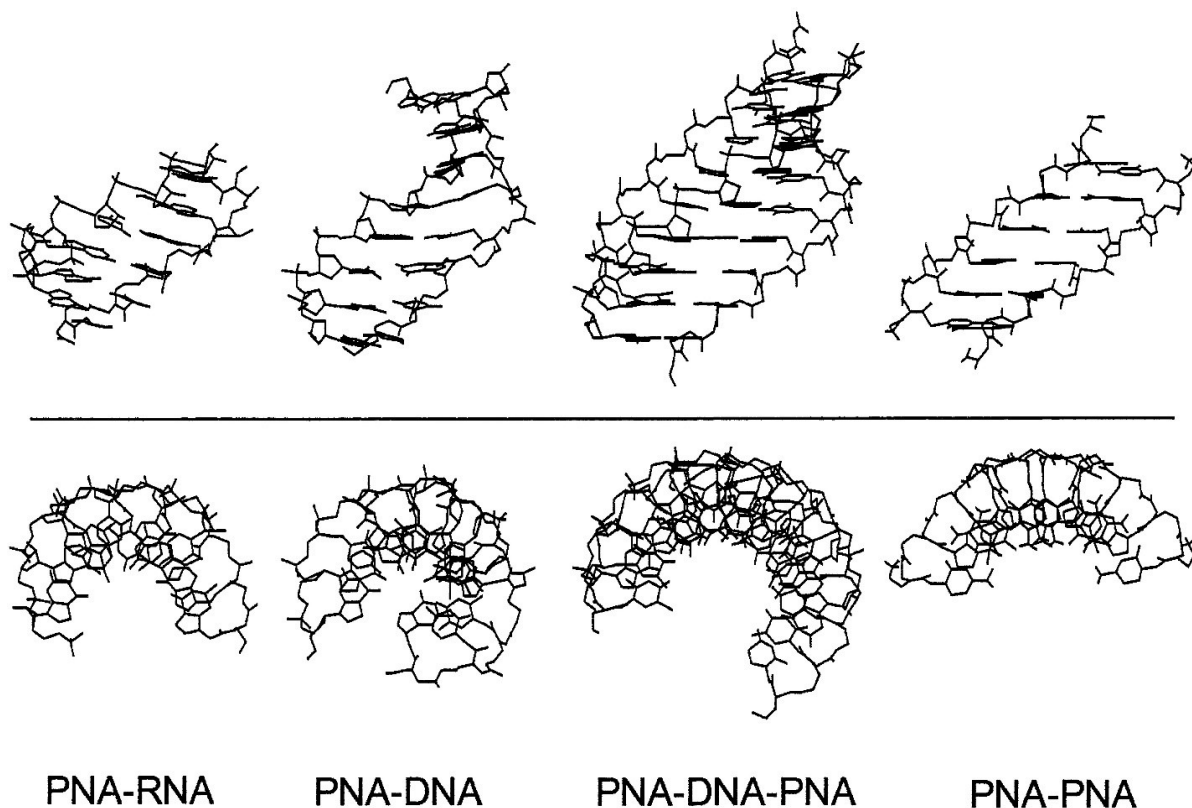


**Figure 1-13. Structure of PNA complexes: side view (top) and upper view (bottom).**  
 [Reprinted with permission from (Nielsen, P. E. *Acc. Chem. Res.* **1999**, 32, 624-630)<sup>101</sup>  
 Copyright (1999) American Chemical Society and (Eriksson, M.; Nielsen, P. E. *Q. Rev. Biophys.* **1996**, 29, 369-394)<sup>102</sup> Copyright © (1996) Cambridge University Press]

highly sequence-specific binding, as well as high biological and chemical stability, PNA is a useful biomolecular tool with an enhanced lifetime for *in vivo* and *in vitro* applications, such as molecular diagnostics and antisense therapeutics.<sup>67,68</sup> Despite its superior affinity and selectivity, chemical modifications of PNA have been studied to improve its molecular recognition and biophysical properties, such as enhancing cellular uptake and labeling it with fluorescent groups. Common modification sites in PNA are the original *N*-(2-aminoethyl)glycine PNA backbone and the nucleobase. Various backbone-modified PNA analogs were synthesized to enhance binding affinity with target and cellular delivery.

Peptide oligomerization applies solid-phase peptide synthesis (SPPS) methods.<sup>57</sup> Oligomerization of peptides by SPPS uses a selective protecting group strategy on the primary amine group and carboxylic acid group on an amino acid, and functional groups on the sidechains. Since a PNA monomer has a primary amine group and a carboxylic acid group on the backbone, the same strategy can be used. In addition, PNA has nucleobases with exocyclic amino groups which need selective protection strategy during SPPS. There are two methods for a selective protecting strategy for SPPS: Boc protecting strategy with graded acidolysis for deprotection, and Fmoc protecting strategy that uses orthogonal protecting groups. Fmoc protecting strategy is preferred to the Boc strategy due to the mild deprotection step without the hazard of hydrofluoric acid (HF) in the cleavage. To apply an orthogonal Fmoc protecting strategy in PNA oligomer synthesis,<sup>69,70</sup> PNA monomers are prepared with the terminal amine protected with the fluorenylmethyloxycarbonyl (Fmoc) group and nucleobases protected with the acid-labile *tert*-butyloxycarbonyl (Boc) or benzhydryloxycarbonyl (Bhoc) group. SPPS cycle for PNA oligomerization with Fmoc protecting strategy is present in **Figure 1-14**.

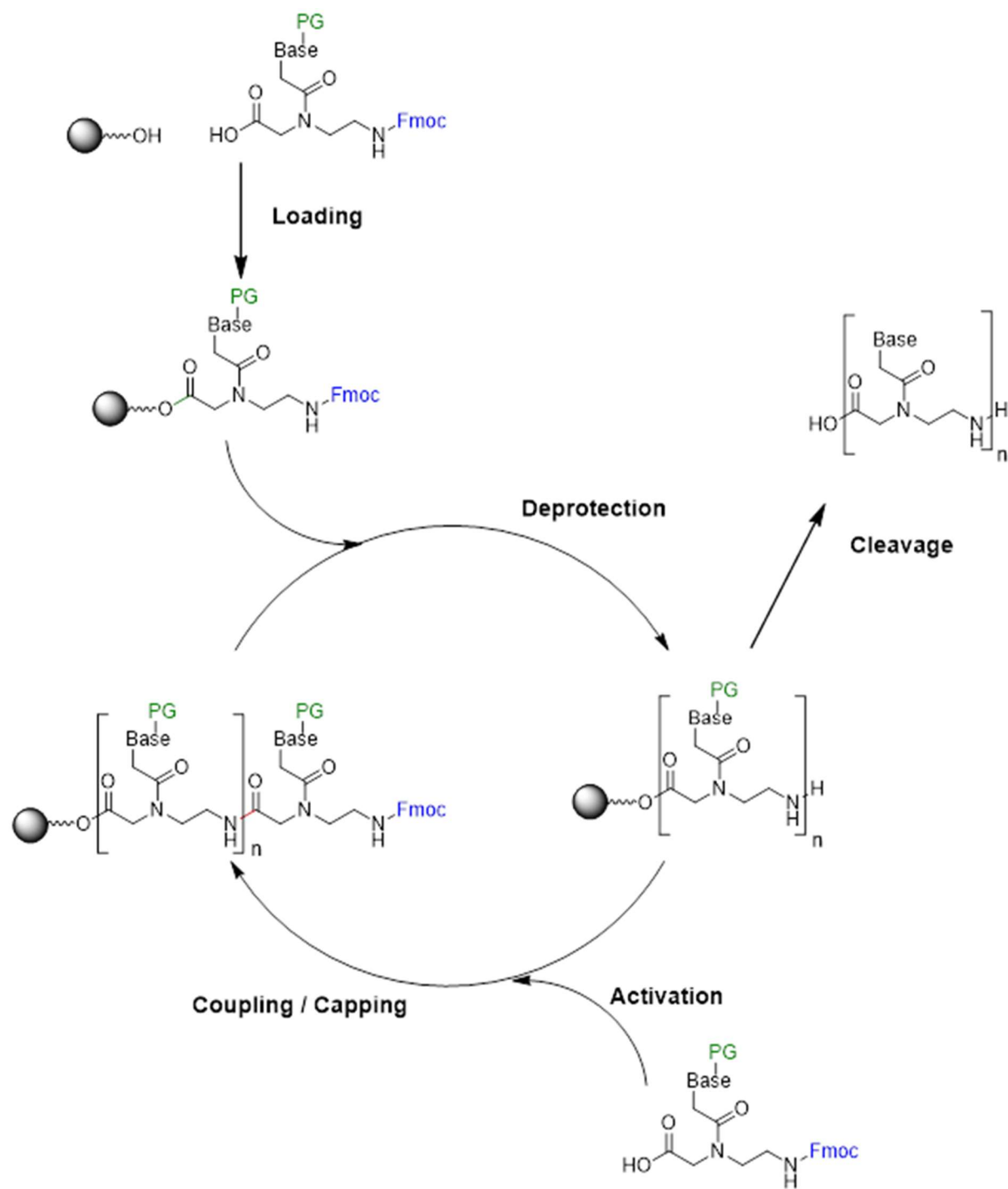


**Figure 1-14. Fmoc-based solid-phase peptide synthesis (SPPS) cycle for PNA oligomerization.**

## 1.2. Nucleobase modification

Nucleobases represent key structural motifs in biologically active molecules, including synthetic and natural products. Molecular modifications made on nucleobases or their isolation from natural sources are being widely investigated for the development of drugs with improved potency for the treatment of diseases such as cancer, as well as viral and bacterial infections. It is preferred that nucleobase modifications avoid hydrogen bonding sites and sterically hindered sites to minimize structural perturbation in hybridization (**Figure 1-15**). There are three different forms of modified nucleobases: expanded nucleobases, extended nucleobases, and isomorphous nucleobases. Expanded nucleobases have additional aromatic rings that are fused onto the pyrimidine or purine. Additional rings introduce extended conjugated bonds, which give new photophysical properties. In extended nucleobases, additional moieties are linked or conjugated to the natural nucleobases via rigid or flexible linkers. The most common extension sites are the 5-position in pyrimidine bases and the 7-position in purine bases which places the moieties at the major groove. Lastly, isomorphous nucleobases are heterocycles that are structurally similar to natural nucleobases. They have similar overall dimensions, hydrogen bonding patterns, and the ability to form Watson-Crick base pairs while having enhanced photophysical characteristics.

Nucleobase modification can change binding affinity and duplex stability by introducing a new hydrogen bond site or a new functional group. 2,6-Diaminopurine (D) is a modified adenosine with an extra amine group that forms an extra hydrogen bond with thymine (**Figure 1-16**). This gives the oligonucleotide a higher affinity when forming Watson-Crick base pairs. Similarly, 2-aminopurine (2-AP) is an adenosine analog with the amine group relocated to C4, causing changes in affinity. 2-Thiouracil is an analog of thymine and uracil that is used with 2,6-diaminopurine. Though both 2-thiouracil and 2,6-diaminopurine make base pairs with adenosine and thymine respectively, they cannot make base pairs with one another.<sup>71</sup> This characteristic can be utilized in the duplex invasion; though they are used together, they will not form base pairs with each other, allowing binding to the intended complementary strand. G-clamp<sup>72</sup> is a cytosine analog with two additional fused rings with an arm. The arm consists of an alkyl and a terminal-charged amine group, which allows the analog to act as a 'clamp' when binding to guanine by forming extra hydrogen bonds. These extra hydrogen bonds and the additional rings increase the

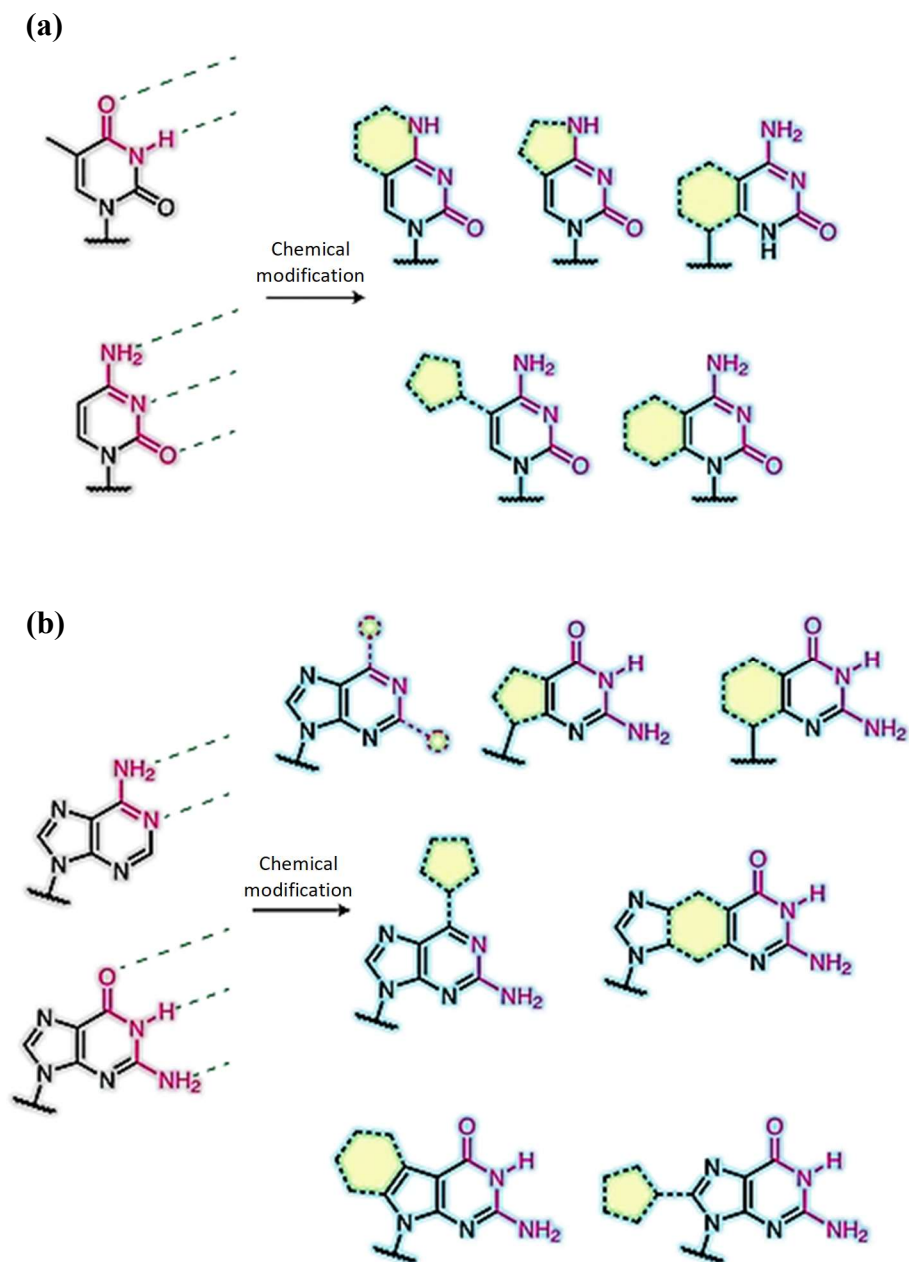


**Figure 1-15. Potential chemical modification sites of canonical pyrimidines (a) and (b). Examples cover ring substitution, conjugated linker extension and ring fusion. Yellow shading highlights modified structures and the purple bonds and atoms are base-pairing moieties.** [Reprinted with permission from (Xu, W.; Chan, K. M.; Kool, E. T. *Nat. Chem.* **2017**, *9* (11), 1043–1055)<sup>76</sup>. Copyright © 2017, Nature Publishing Group

duplex stability of the G-clamp via base pairing and base stacking. Lastly, pseudoisocytosine (J)<sup>73</sup> is a cytosine analog that can form Hoogsteen-type hydrogen bonds with guanine independent of pH. To form a Hoogsteen base pair with guanine, pseudoisocytosine provides 2 hydrogen bonds without protonation, whereas cytosine has to be protonated.

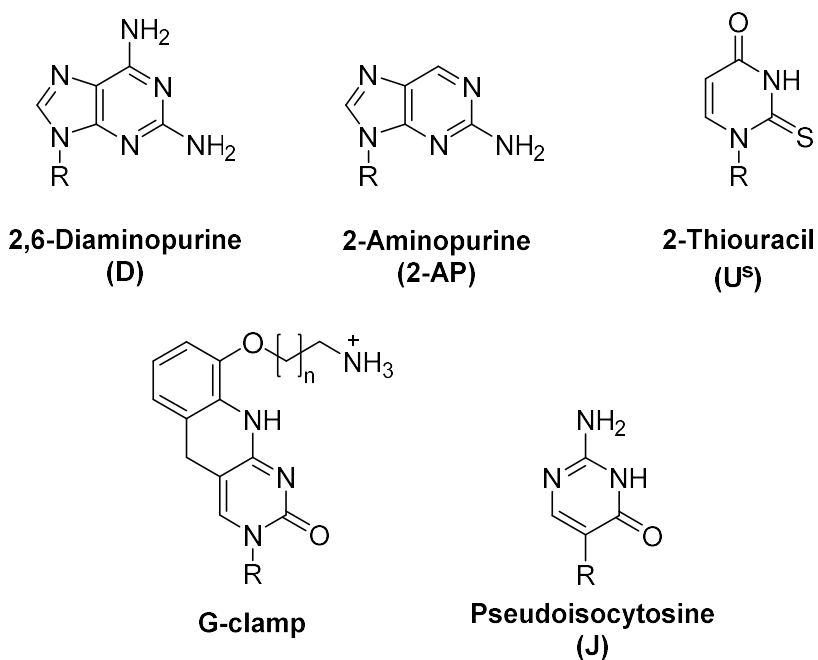
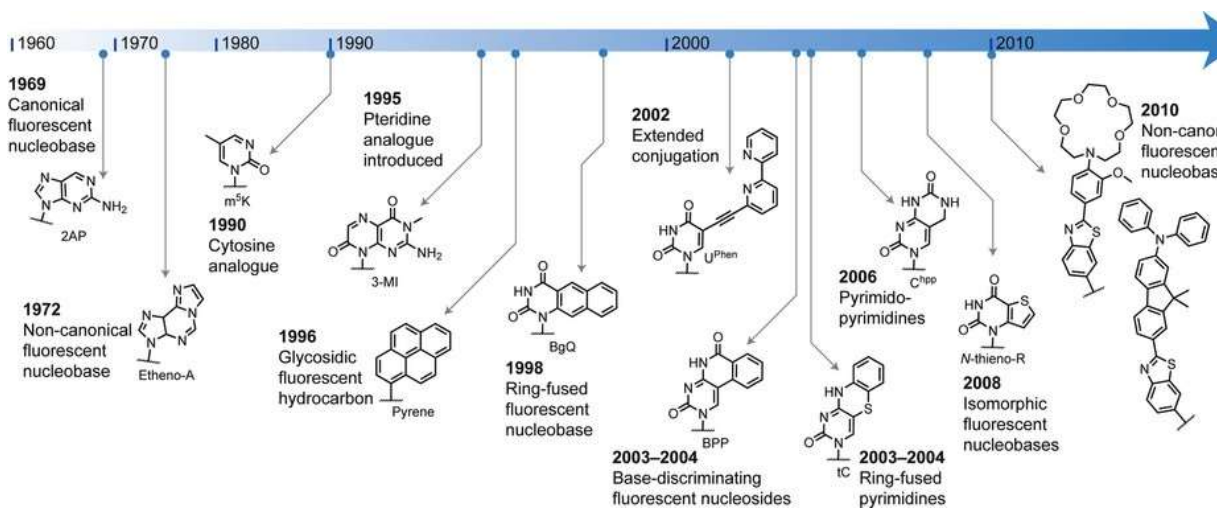


**Figure 1-16. Chemical structures of selection of modified nucleobases.**

### 1.2.1. Fluorescence nucleobase

Fluorescence spectroscopy has shown its usefulness as a tool in the detection of target nucleic acid. Indeed, there is a demand for nucleic acids possessing enhanced photophysical properties. One of the most common methods of achieving nucleic acid fluorescence has been to tag the fluorophore onto the 3' or 5' terminal end of the nucleic acid. Research is ongoing to design and synthesize a wider variety of nucleic acids with fluorescent properties. Notably, both fluorophores and native nucleobases contain an aromatic ring structure. Because of their structural similarities, attempts to modify the non-fluorescent native nucleobases to give fluorescent characteristics through chemical modification have been made<sup>74-76</sup> (**Figure 1-17**).



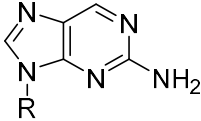
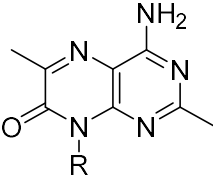
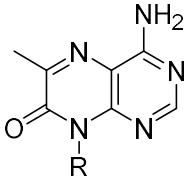
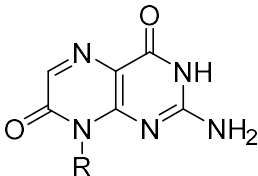
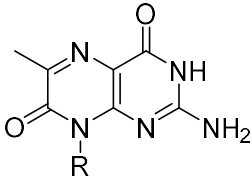


**Figure 1-17. A chronicle of fluorescent nucleobase development.** [Reprinted with permission from (Xu, W.; Chan, K. M.; Kool, E. T. *Nat. Chem.* **2017**, *9* (11), 1043–1055)<sup>76</sup>. Copyright © 2017, Nature Publishing Group]

The chemical modification can be done by mimicking the aromatic structure of the fluorophore or by tagging the fluorophore to the nucleobase. With the modification methods mentioned above, various fluorescent nucleobases were synthesized and studied.<sup>75</sup>

Native nucleobase, adenine, guanine, cytosine, thymine and uracil, are either non-fluorescent or very faintly fluorescent.<sup>77</sup> However, there are naturally occurring fluorescent nucleobases: 2-aminopurine (2-AP)<sup>78,79</sup> and pteridine analogs<sup>80,81</sup> (**Table 1-1**). These naturally occurring nucleobases have excellent photophysical properties such as high fluorescence quantum yields and longer fluorescence lifetimes. However, due to the lower abundance of these natural fluorescent nucleobases, researchers have had more interest in fluorescent nucleobases that can be chemically synthesized.

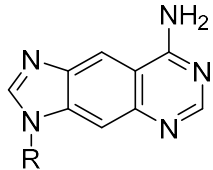
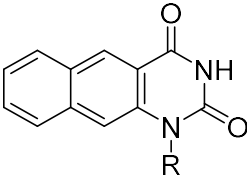
**Table 1-1. Structures and photophysical properties of naturally occurring fluorescent nucleobases.**

Structure	$\lambda_{ab}$ (nm)	$\lambda_{em}$ (nm)	$\Phi$	$\tau$ (ns)
 <p><b>2-AP</b></p>	303	370	0.68 <sup>a</sup>	7.0 <sup>a</sup>
 <p><b>DMAP</b></p>	250	430	0.48 <sup>b</sup>	4.8 <sup>b</sup>
 <p><b>6-MAP</b></p>	248	430	0.39 <sup>b</sup>	3.8 <sup>b</sup>
 <p><b>3-MI</b></p>	254	430	0.88 <sup>b</sup>	6.5 <sup>b</sup>
 <p><b>6-MI</b></p>	340	431	0.70 <sup>b</sup>	6.4 <sup>b</sup>

R = 2'-deoxyribose. <sup>a</sup> Measured in water. <sup>b</sup> Measured in Tris buffer, pH = 7.5.

Expanded fluorescent nucleobases (**Table 1-2**), such as benzoadenine<sup>82</sup> and benzo[g]quinazoline-2,4-(1H,3H)-dione (Naphthothymine),<sup>83</sup> have additional fused aromatic rings. This typically results in enhanced photophysical properties including red-shifted absorption bands compared with native nucleobases, emission wavelengths in the visible region and high quantum yields.

**Table 1-2. Structures and photophysical properties of the expanded nucleobases.**

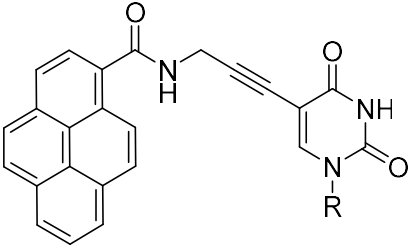
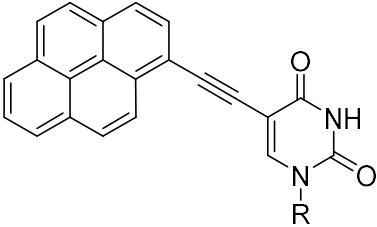
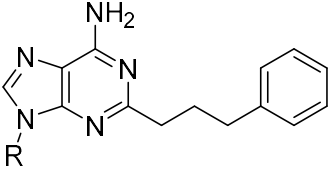
Structure	$\lambda_{ab}$ (nm)	$\lambda_{em}$ (nm)	$\Phi$	$\tau$ (ns)
 <p><b>Benzoadenosine</b><sup>a</sup></p>	340	395	0.44 <sup>a</sup>	3.7
 <p><b>Benzo[g]quinazoline-2,4-(1H,3H)-dione</b><sup>a</sup></p>	360	434	0.82 <sup>a</sup>	

R = 2'-deoxyribose. <sup>a</sup> Measured in buffer, pH = 7.0.

In extended fluorescent nucleobases (**Table 1-3**), fluorophores are linked or conjugated to the nucleobases via linkers.<sup>74</sup> This maintains the hydrogen bonding sites of native nucleobases and introduces fluorescent characteristics from the fluorophore. When fluorophores are linked with flexible nonconjugated linkers, the modified nucleobase analogs generally show photophysical properties similar to that of the original fluorophores. For example, PyU,<sup>84</sup> a uracil analog with a pyrene carbonyl fluorophore attached via a non-conjugated linker, has an absorption band and an emission band at the same region as the spectra of pyrene. When the fluorophores are conjugated with rigid linkers, absorption and emission spectra tend to be red-shifted compared to the original fluorophore, while high quantum yields remain. In 5-(1-ethynylpyrenyl)-dU, pyrene is conjugated via an ethynyl linkage to uridine. Compared to PyU, absorption and emission bands are red-shifted. As an interesting example of extended nucleobase

analogs, 2-phenylpropyl-2'-deoxyadenosine (A-3Ph) is a 2-substituted adenosine analog with a nonconjugated phenyl alkyl substituent. A-3Ph displays low fluorescence as a monomer; however, upon incorporation into RNA, it shows a surprisingly enhanced quantum yield.<sup>85</sup> As an interesting example of extended nucleobase analogs, 2-phenylpropyl-2'-deoxyadenosine (A-3Ph) is a 2-substituted adenosine analog with a nonconjugated phenyl alkyl substituent. A-3Ph displays low fluorescence as a monomer; however, upon incorporation into RNA, it shows a surprisingly enhanced quantum yield.<sup>85</sup>

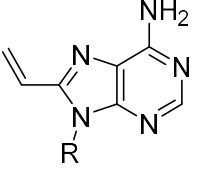
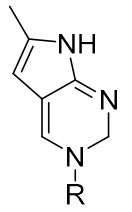
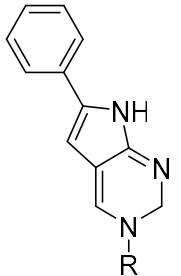
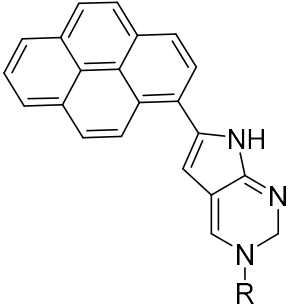
**Table 1-3. Structures and photophysical properties of the extended nucleobases.**

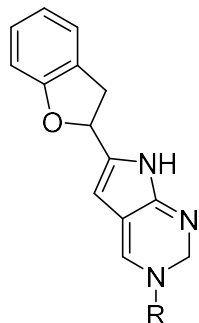
Structure	$\lambda_{ab}$ (nm)	$\lambda_{em}$ (nm)	$\Phi$	$\tau$ (ns)
 <p style="text-align: center;"><b>PyU</b></p>	341	397	0.2 <sup>a</sup>	
 <p style="text-align: center;"><b>5-(1-Ethynyl-pyrenyl)-U<sup>b</sup></b></p>	392	400, 424		
 <p style="text-align: center;"><b>2-Phenylpropyl-A</b></p>	292	385	0.011 <sup>b</sup>	6.22

R = 2'-deoxyribose. <sup>a</sup> Measured in MeOH. <sup>b</sup> Measured in water.

An isomorphous fluorescent base structurally resembles a native nucleobase but has enhanced photophysical properties. Examples of fluorescent isomorphous nucleobases include 2-aminopurine (Table 1-1), 8-vinyl-6-aminopurine<sup>86</sup> and pyrrolocytosines<sup>87,88</sup> (Table 1-4). The Hudson group has synthesized and characterized pyrrolocytosine (pC) derivatives<sup>88-91</sup>: 6-phenylpyrrolocytodine, 6-pyrenyl-pyrrolocytodine and benzo[b]furanylcytodine. pC derivatives respectively retain selectivity for guanosine and possess intrinsic fluorescence, which is very useful for labeling.

**Table 1-4. Structures and photophysical properties of the isomorphous nucleobases.**

Structure	Solvent	$\lambda_{ab}$ (nm)	$\lambda_{em}$ (nm)	$\Phi$
 <p><b>8-Vinyl-6-aminopurine</b></p>	buffer <sup>a</sup>	290	382	0.66 <sup>c</sup>
 <p><b>Pyrrolocytosine</b></p>	buffer <sup>b</sup>	350	460	0.20
 <p><b>6-Phenyl-pyrrolocytosine</b></p>	water	362	454	0.31
 <p><b>6-Pyrenyl-pyrrolocytosine</b></p>	water	377	485	0.02



water

372

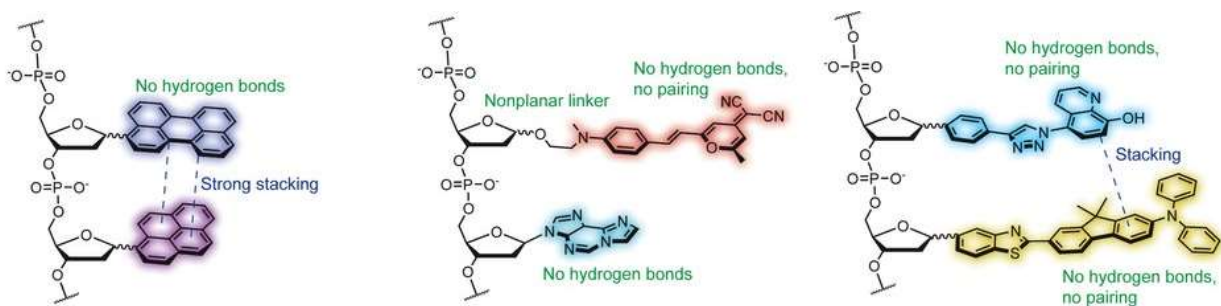
462

0.50

### Benzo[b]furan-2-ylpyrrolo[2,1-c]cytosine

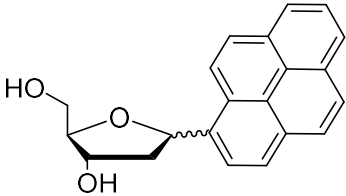
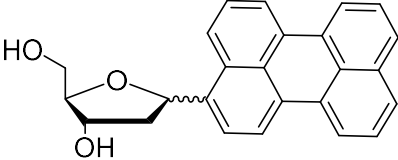
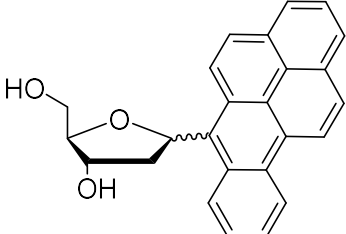
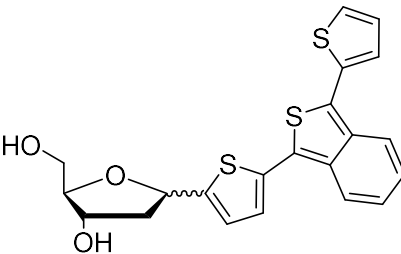
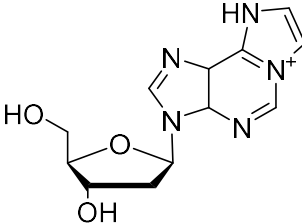
R = 2'-deoxyribose. <sup>a</sup> Measured in HEPES (N-2-hydroxyethylpiperazine-N-2-ethane sulfonic acid) buffer at pH = 7.5. <sup>b</sup> Measured in HEPES buffer at pH = 7.0

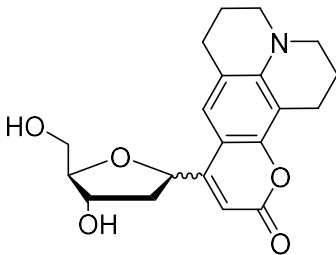
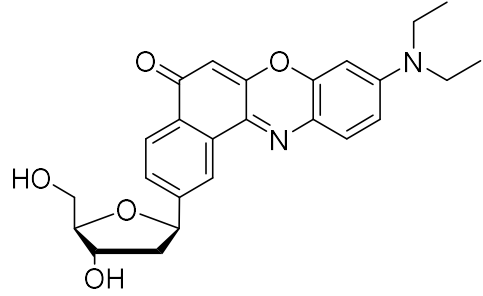
Kool and co-workers have introduced chromophoric base analogs which have polycyclic aromatic hydrocarbon (PAH) fluorophores instead of native nucleobases.<sup>92,93</sup> PAH fluorophores, such as Pyrene, perylene, benzopyrene and phenanthrene, were incorporated into the backbone with C-glycosidic bonds as chromophoric base analogs (**Table 1-5**). Though PAH cannot form the Watson-Crick hydrogen bonding, they interact with neighboring nucleobases via  $\pi$ -stacking. Chromophoric base analogs showed exotic optical phenomena that led to their applications as the biophysical probes of enzyme activity. Moreover, chromophoric bases comprising heterocyclic fluorophores, such as benzothiofene, ethenoadenosine, coumarin and Nile-red,<sup>94</sup> contributed to a broader spectrum of emission wavelengths (**Figure 1-18**).



**Figure 1-18. The interaction of chromophoric base analogs in oligonucleotides and the wide variety of possible emission wavelengths. (Depicted color on each chromophore illustrates its emission color)** [Reprinted with permission from (Xu, W.; Chan, K. M.; Kool, E. T. *Nat. Chem.* **2017**, 9 (11), 1043–1055)<sup>76</sup>. Copyright © 2017, Nature Publishing Group]

**Table 1-5. Structures and photophysical properties of the chromophoric nucleobases.**

Structure	Solvent	$\lambda_{ab}$ (nm)	$\lambda_{em}$ (nm)	$\Phi$
 <p><b>Pyrene</b></p>	MeOH	241, 345	375, 395	0.12
 <p><b>Perylene</b></p>	MeOH	440	433, 472	0.88
 <p><b>Benzopyrene</b></p>	MeOH	394	408	0.98 <sup>a</sup>
 <p><b>Benzoterthiophene</b></p>	MeOH	437	536	0.67
 <p><b>Ethenoadenosine</b></p>	buffer <sup>a</sup>	258, 265, 275, 294	415	0.6

 <p><b>Coumarin</b></p>	buffer <sup>b</sup>	40	515	
 <p><b>Nile-red</b></p>	MeOH	557	632	0.09

R = 2'-deoxyribose. <sup>a</sup>n aqueous buffer at pH 7.0. <sup>b</sup> aqueous buffer at pH 7.2.

### 1.3. Fluorescence spectroscopy<sup>95</sup>

Photoluminescence is the emission of light when an excited electron returns to the ground state from a higher energetic state. There are two types of photoluminescence: fluorescence and phosphorescence. As shown in the Jablonski diagram (**Figure 1-19**), when a photon is absorbed by a molecule, that energy makes the electron jump from the  $S_0$  ground state to a higher energy state,  $S_1$ . When it returns to the ground state after vibrational cooling, the energy can be released by heat or emission of light. In fluorescence, the excited electron at the  $S_1$  energy level immediately returns to the  $S_0$  ground state releasing energy by emitting light. In phosphorescence, the excited electron undergoes intersystem crossing (ISC) from  $S_1$  to  $T_1$  and returns to the  $S_0$  ground state releasing the energy by emitting a photon.



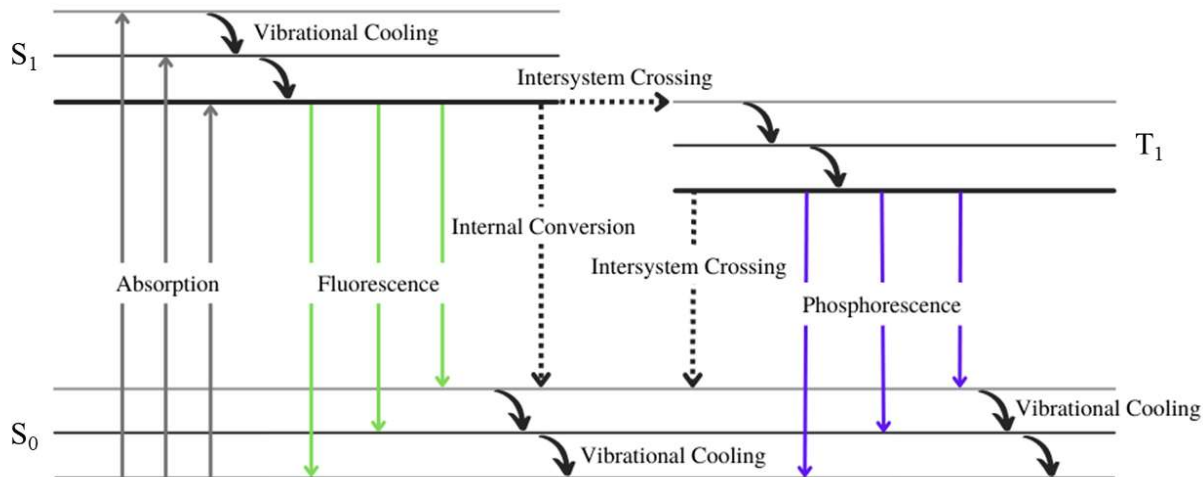


**Figure 1-19. Jablonski diagram.**

Quenching is the process that decreases the fluorescence intensity. There are two main quenching mechanisms by which the release of energy from a donor molecule can be captured by acceptor molecules: static quenching and dynamic quenching. Static quenching occurs when the fluorophore and the quencher form a complex by a stacking interaction. The complex has a non-fluorescent ground state with a unique absorption spectrum. Dynamic quenching mechanism includes energy exchange between donor and acceptor, such as fluorescence resonance energy transfer (FRET). FRET occurs when the emission spectrum of the donor overlaps with the absorption spectrum of the acceptor (**Figure 1-20**). Notably, the rate of FRET is distance dependent.<sup>96,97</sup> The quenching efficiency can be measured by the Stern-Volmer equation (**Equation 1**), a linear relationship between the concentration of the quencher and the change in fluorescent intensity.  $K_{SV}$  is the Stern-Volmer quenching constant and  $I_0$  is the initial fluorescent intensity of fluorophore,  $I$  is the decreased intensity by quenchers, and  $[Q]$  is the quencher concentration.

$$\frac{I_0}{I} = K_{SV}[Q] + 1$$

**Equation 1**

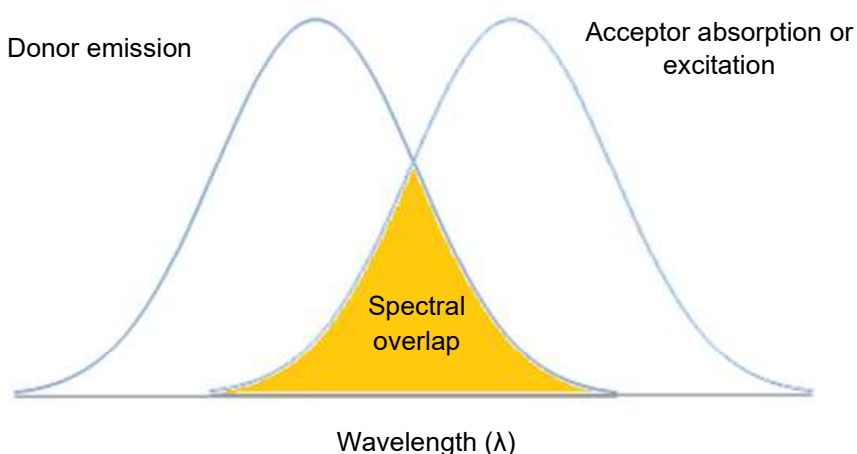


**Figure 1-20. Diagram of spectral overlap for FRET.**

### 1.3.1. Molecular beacon

A molecular beacon is a single-stranded oligonucleotide hybridization probe that forms a stem-and-loop structure (**Figure 1-21**).<sup>98</sup> The loop contains a probe sequence that is complementary to a target sequence. The stem is formed by the annealing of complementary arm sequences that are located on either side of the probe sequence. A fluorophore is covalently linked to the end of one arm, and a quencher is covalently linked to the end of the other arm. In the absence of the target sequence, the proximity between the fluorophore and the quencher prevents the fluorophore from emitting light. When the beacon hybridizes with the target, a conformational change occurs such that the distance between the fluorophore and the quencher increases, thus, light is emitted.

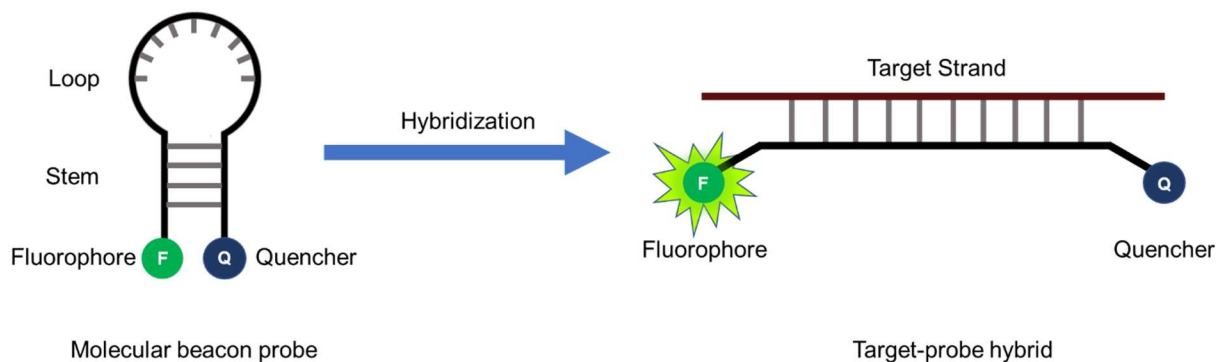


**Figure 1-21. Structure of molecular beacon and Target-probe hybrid formation.**

## 1.4. Rationale

DNA oligonucleotides have been a useful tool in biological applications; thus, many modifications have been made to oligonucleotides to alter and give additional characteristics. Among the modified DNA oligonucleotide, peptide nucleic acid (PNA) has been heavily investigated due to its excellent affinity and specificity. Such characteristics allow for PNAs to be used in therapeutic and diagnostic applications. Also, researchers have studied different nucleobase modifications and their effects in adding or eliminating characteristics. This thesis focuses on the development of novel design and synthesis of PNA/DNA monomers with structural nucleobase modifications that add novel properties. Photophysical characteristics of modified nucleobases and the duplex stability of their oligomers are investigated.

According to computational studies,<sup>99,100</sup> the introduction of an electronegative nitro group to uracil should result in stronger hydrogen bonding with adenine thereby improving base pairing; thus, we hypothesized 5-nitrouracil containing PNA to have enhanced affinity at oligomer level compared to thymine containing PNA. Correspondingly, in Chapter 2, 5-nitrouracil containing PNA monomer was synthesized and then used to synthesize PNA oligomers. Thermal stabilities of DNA-PNA and DNA-bisPNA complex with the PNA oligomers were investigated to evaluate binding affinity in the context of duplex and triplex sequences, and specificity.

To create a molecular beacon with a novel design in which the fluorophore and the quencher are embedded in the stem region, a nucleobase with quenching ability was required. In Chapter 3, 5-(4-(N,N-dimethylamino)phenylazo-yl)uracil (DMPAU) and 6-(4-Nitrophenyl) pyrrolocytosine (NPhpC) were selected as candidates for such quenching nucleobases. A new synthesis pathway of DMPAU PNA analogs was developed. A hydrogen bonding study of newly synthesized DMPAU with adenine was conducted followed by the quenching study of nucleobase quenchers with different fluorophores.

Compared to PNA, DNA is studied by a wider audience and research community regarding its use in the development of therapeutic applications. Naturally, our studies also led to a DNA-based study for a broader application in the nucleotide research field. In Chapter 4, 5-(4-(N,N-dimethylamino)phenylazo-yl)-2'-deoxyuridine (DMPAdU) was synthesized and then studied to characterize the photophysical properties and quenching ability of DMPA-uridine.

## 1.5. References

- (1) Crick, F. Central Dogma of Molecular Biology. *Nature* **1970**, 227 (5258), 561–563.
- (2) Hoogsteen, K. The Crystal and Molecular Structure of a Hydrogen-Bonded Complex between 1-Methylthymine and 9-Methyladenine. *Acta. Crystallogr.* **1963**, 16 (9), 907–916.
- (3) Crick, F. H. C. Codon—Anticodon Pairing: The Wobble Hypothesis. *J. Mol. Biol.* **1966**, 19 (2), 548–555.
- (4) Gellert, M.; Lipsett, M. N.; Davies, D. R. Helix Formation by Guanylic Acid. *Proc. Natl. Acad. Sci. USA* **1962**, 48 (12), 2013–2018.
- (5) Williamson, J. R. G-Quartet Structures in Telomeric DNA. *Annu. Rev. Biophys. Biomol. Struct.* **1994**, 23, 703–730.
- (6) Pushpendra, S.; Arvind, P.; Anil, B. Nucleic Acids as Therapeutics. In *From Nucleic Acids Sequences to Molecular Medicine*; Erdmann, V. A., Barciszewski, J., Eds; Springer: Berlin 2012; pp 19–45.
- (7) Stephenson, M. L.; Zamecnik, P. C. Inhibition of Rous Sarcoma Viral RNA Translation by a Specific Oligodeoxyribonucleotide. *Proc. Natl. Acad. Sci. USA* **1978**, 75 (1), 285–288.
- (8) Hélène, C. The Anti-Gene Strategy: Control of Gene Expression by Triplex-Forming-Oligonucleotides. *Anticancer. Drug. Des.* **1991**, 6 (6), 569–584.
- (9) Jain, M. L.; Bruice, P. Y.; Szabó, I. E.; Bruice, T. C. Incorporation of Positively Charged Linkages into DNA and RNA Backbones: A Novel Strategy for Antigene and Antisense Agents. *Chem. Rev.* **2012**, 112 (3), 1284–1309.
- (10) Bennett, C. F.; Swayze, E. E. RNA Targeting Therapeutics: Molecular Mechanisms of Antisense Oligonucleotides as a Therapeutic Platform. *Annu. Rev. Pharmacol. Toxicol.* **2010**, 50, 259–293.
- (11) de Mesmaeker, A.; HÄner, R.; Martin, P.; Moser, H. E. Antisense Oligonucleotides. *Acc. Chem. Res.* **1995**, 28 (9), 366–374.
- (12) Chan, J. H. P.; Lim, S.; Wong, W. S. F. Antisense Oligonucleotides: from Design to Therapeutic Application. *Clin. Exp. Pharmacol. Physiol.* **2006**, 33 (5–6), 533–540.
- (13) Sharma, V. K.; Rungta, P.; Prasad, A. K. Nucleic. Acid. Ther.apeutics: Basic Concepts and Recent Developments. *RSC. Adv.* **2014**, 4 (32), 16618–16631.
- (14) Lipi, F.; Chen, S.; Chakravarthy, M.; Rakesh, S.; Veedu, R. N. In Vitro Evolution of Chemically-Modified Nucleic Acid Aptamers: Pros and Cons, and Comprehensive Selection Strategies. *RNA. Biol.* **2016**, 13 (12), 1232–1245.

- (15) de Clercq, E.; Wells, R. D.; Grant, R. C.; Merigan, T. C. Thermal Activation of the Antiviral Activity of Synthetic Double-Stranded Polyribonucleotides. *J. Mol. Biol.* **1971**, *56* (1), 83–100.
- (16) Vu, H.; Hirschbein, B. L. Internucleotide Phosphite Sulfurization with Tetraethylthiuram Disulfide. Phosphorothioate Oligonucleotide Synthesis via Phosphoramidite Chemistry. *Tetrahedron Lett.* **1991**, *32* (26), 3005–3008.
- (17) Xie, X.; Liang, J.; Pu, T.; Xu, F.; Yao, F.; Yang, Y.; Zhao, Y. L.; You, D.; Zhou, X.; Deng, Z.; Wang, Z. Phosphorothioate DNA as an Antioxidant in Bacteria. *Nucleic Acids Res.* **2012**, *40* (18), 9115–9124.
- (18) Rahman, S. M. A.; Baba, T.; Kodama, T.; Islam, M. A.; Obika, S. Hybridizing Ability and Nuclease Resistance Profile of Backbone Modified Cationic Phosphorothioate Oligonucleotides. *Bioorg. Med. Chem.* **2012**, *20* (13), 4098–4102.
- (19) Shoji, Y.; Akhtar, S.; Periasamy, A.; Herman, B.; Juliano, R. L. Mechanism of Cellular Uptake of Modified Oligodeoxynucleotides Containing Methylphosphonate Linkages. *Nucleic Acids Res.* **1991**, *19* (20), 5543–5550.
- (20) Monn, S. T. M.; Schürch, S. New Aspects of the Fragmentation Mechanisms of Unmodified and Methylphosphonate-Modified Oligonucleotides. *J. Am. Soc. Mass. Spectrom.* **2007**, *18* (6), 984–990.
- (21) Froehler, B.; Ng, P.; Matteucci, M. Phosphoramidate Analogues of DNA: Synthesis and Thermal Stability of Heteroduplexes. *Nucleic Acids Res.* **1988**, *16* (11), 4831–4839.
- (22) Gryaznov, S. M. Oligonucleotide N3'→p5' Phosphoramidates and Thio-Phosphoramidates as Potential Therapeutic Agents. *Chem Biodivers* **2010**, *7* (3), 477–493.
- (23) Majlessi, M.; Nelson, N. C.; Becker, M. M. Advantages of 2'-O-Methyl Oligoribonucleotide Probes for Detecting RNA Targets. *Nucleic Acids Res.* **1998**, *26* (9), 2224.
- (24) Kawasaki, A. M.; Casper, M. D.; Prakash, T. P.; Manalili, S.; Sasmor, H.; Manoharan, M.; Cook, P. D. Synthesis, Hybridization, and Nuclease Resistance Properties of 2'-O-Aminoxyethyl (2'-O-AOE) Modified Oligonucleotides. *Tetrahedron Lett.* **1999**, *40* (4), 661–664.
- (25) Teplova, M.; Minasov, G.; Tereshko, V.; Inamati, G. B.; Cook, P. D.; Manoharan, M.; Egli, M. Crystal Structure and Improved Antisense Properties of 2'-O-(2-Methoxyethyl)-RNA. *Nat. Struct. Biol.* **1999**, *6* (6), 535–539.
- (26) Kawasaki, A. M.; Casper, M. D.; Freier, S. M.; Lesnik, E. A.; Zounes, M. C.; Cummins, L. L.; Gonzalez, C.; Dan Cook, P. Uniformly Modified 2'-Deoxy-2'-Fluoro Phosphorothioate Oligonucleotides as Nuclease-Resistant Antisense Compounds with High Affinity and Specificity for RNA Targets. *J. Med. Chem.* **1993**, *36* (7), 831–841.

- (27) Geary, R. S.; Yu, R. Z.; Watanabe, T.; Henry, S. P.; Hardee, G. E.; Chappell, A.; Matson, J.; Sasmor, H.; Cummins, L.; Levin, A. A. Pharmacokinetics of a Tumor Necrosis Factor- $\alpha$  Phosphorothioate 2'-O-(2-Methoxyethyl) Modified Antisense Oligonucleotide: Comparison across Species. *Drug Metabolism and Disposition* **2003**, *31* (11), 1419–1428.
- (28) Damha, M. J.; Wilds, C. J.; Noronha, A.; Brukner, I.; Borkow, G.; Arion, D.; Parniak, M. A. Hybrids of RNA and Arabinonucleic Acids (ANA and 2'F-ANA) Are Substrates of Ribonuclease H. *J. Am. Chem. Soc.* **1998**, *120* (49), 12976–12977
- (29) Wilds, C. J.; Damha, M. J. 2'-Deoxy-2'-Fluoro- $\beta$ -d-Arabinonucleosides and Oligonucleotides (2'F-ANA): Synthesis and Physicochemical Studies. *Nucleic Acids Res.* **2000**, *28* (18), 3625–3635.
- (30) Dowler, T.; Bergeron, D.; Tedeschi, A. L.; Paquet, L.; Ferrari, N.; Damha, M. J. Improvements in SiRNA Properties Mediated by 2'-Deoxy-2'-Fluoro-Beta-D-Arabinonucleic Acid (FANA). *Nucleic Acids Res.* **2006**, *34* (6), 1669–1675.
- (31) Noronha, A.; Damha, M. J. Triple Helices Containing Arabinonucleotides in the Third (Hoogsteen) Strand: Effects of Inverted Stereochemistry at the 2'-Position of the Sugar Moiety+. *Nucleic Acids Res.* **1998**, *26* (11), 2665–2671.
- (32) Noronha, A. M.; Wilds, C. J.; Lok, C. N.; Viazovkina, K.; Arion, D.; Parniak, M. A.; Damha, M. J. Synthesis and Biophysical Properties of Arabinonucleic Acids (ANA): Circular Dichroic Spectra, Melting Temperatures, and Ribonuclease H Susceptibility of ANA-RNA Hybrid Duplexes. *Biochemistry* **2000**, *39* (24), 7050–7062.
- (33) Martín-Pintado, N.; Yahyaee-Anzahae, M.; Campos-Olivas, R.; Noronha, A. M.; Wilds, C. J.; Damha, M. J.; González, C. The Solution Structure of Double Helical Arabino Nucleic Acids (ANA and 2'F-ANA): Effect of Arabinoses in Duplex-Hairpin Interconversion. *Nucleic Acids Res.* **2012**, *40* (18), 9329.
- (34) Schoning, K. U.; Scholz, P.; Guntha, S.; Wu, X.; Krishnamurthy, R.; Eschenmoser, A. Chemical Etiology of Nucleic Acid Structure: The Alpha-Threofuranosyl-(3'-->2') Oligonucleotide System. *Science* **2000**, *290* (5495), 1347–1351.
- (35) Yu, H.; Zhang, S.; Chaput, J. C. Darwinian Evolution of an Alternative Genetic System Provides Support for TNA as an RNA Progenitor. *Nat. Chem.* **2012**, *4* (3), 183–187.
- (36) Mei, H.; Liao, J. Y.; Jimenez, R. M.; Wang, Y.; Bala, S.; McCloskey, C.; Switzer, C.; Chaput, J. C. Synthesis and Evolution of a Threose Nucleic Acid Aptamer Bearing 7-Deaza-7-Substituted Guanosine Residues. *J. Am. Chem. Soc.* **2018**, *140* (17), 5706–5713.
- (37) Liu, L. S.; Leung, H. M.; Tam, D. Y.; Lo, T. W.; Wong, S. W.; Lo, P. K.  $\alpha$ -1-Threose Nucleic Acids as Biocompatible Antisense Oligonucleotides for Suppressing Gene Expression in Living Cells. *ACS Appl. Mater. Interfaces* **2018**, *10* (11), 9736–9743.

- (38) Yu, H.; Zhang, S.; Dunn, M. R.; Chaput, J. C. An Efficient and Faithful in Vitro Replication System for Threose Nucleic Acid. *J. Am. Chem. Soc.* **2013**, *135* (9), 3583–3591.
- (39) Hendrix, C.; Rosemeyer, H.; de Bouvere, B.; van Aerschot, A.; Seela, F.; Herdewijn, P. 1',5'-Anhydrohexitol Oligonucleotides: Hybridisation and Strand Displacement with Oligoribonucleotides, Interaction with RNase H and HIV Reverse Transcriptase. *Chem. Eur. J.* **1997**, *3* (9), 1513–1520.
- (40) Hendrix, C.; Rosemeyer, H.; Verheggen, I.; Seela, F.; van Aerschot, A.; Herdewijn, P. 1',5'-Anhydrohexitol Oligonucleotides: Synthesis, Base Pairing and Recognition by Regular Oligodeoxyribonucleotides and Oligoribonucleotides. *Chem. Eur. J.* **1997**, *3* (1), 110–120.
- (41) Vandermeeren, M.; Préveral, S.; Janssens, S.; Geysen, J.; Saison-Behmoaras, E.; van Aerschot, A.; Herdewijn, P. Biological Activity of Hexitol Nucleic Acids Targeted at Ha-Ras and Intracellular Adhesion Molecule-1 mRNA. *Biochem. Pharmacol.* **2000**, *59* (6), 655–663.
- (42) Wang, J.; Herdewijn, P. Enantioselective Synthesis and Conformational Study of Cyclohexene Carbocyclic Nucleosides. *J. Org. Chem.* **1999**, *64* (21), 7820–7827.
- (43) Wang, J.; Verbeure, B.; Luyten, I.; Froeyen, M.; Hendrix, C.; Rosemeyer, H.; Seela, F.; van Aerschot, A.; Herdewijn, P. Cyclohexene Nucleic Acids (CeNA) Form Stable Duplexes with RNA and Induce RNase H Activity. *Nucleosides Nucleotides Nucleic Acids* **2001**, *20* (4–7), 785–788.
- (44) Gu, P.; Schepers, G.; Rozenski, J.; van Aerschot, A.; Herdewijn, P. Base Pairing Properties of D- and L-Cyclohexene Nucleic Acids (CeNA). *Oligonucleotides* **2003**, *13* (6), 479–489.
- (45) Obika, S.; Nanbu, D.; Hari, Y.; Morio, K. I.; In, Y.; Ishida, T.; Imanishi, T. Synthesis of 2'-O,4'-C-Methylenuridine and -Cytidine. Novel Bicyclic Nucleosides Having a Fixed C3, -Endo Sugar Puckering. *Tetrahedron Lett.* **1997**, *38* (50), 8735–8738.
- (46) Obika, S.; Nanbu, D.; Hari, Y.; Andoh, J. I.; Morio, K. I.; Doi, T.; Imanishi, T. Stability and Structural Features of the Duplexes Containing Nucleoside Analogues with a Fixed N-Type Conformation, 2'-O,4'-C-Methylenribonucleosides. *Tetrahedron Lett.* **1998**, *39* (30), 5401–5404.
- (47) Koshkin, A. A.; Singh, S. K.; Nielsen, P.; Rajwanshi, V. K.; Kumar, R.; Meldgaard, M.; Olsen, C. E.; Wengel, J. LNA (Locked Nucleic Acids): Synthesis of the Adenine, Cytosine, Guanine, 5-Methylcytosine, Thymine and Uracil Bicyclonucleoside Monomers, Oligomerisation, and Unprecedented Nucleic Acid Recognition. *Tetrahedron* **1998**, *54* (14), 3607–3630.

- (48) Hildebrandt-Eriksen, E. S.; Aarup, V.; Persson, R.; Hansen, H. F.; Munk, M. E.; Ørum, H. A Locked Nucleic Acid Oligonucleotide Targeting MicroRNA 122 Is Well-Tolerated in Cynomolgus Monkeys. *Nucleic Acid Ther.* **2012**, *22* (3), 152–161.
- (49) Leumann, C. J. DNA Analogues: From Supramolecular Principles to Biological Properties. *Bioorg. Med. Chem.* **2002**, *10* (4), 841–854.
- (50) Renneberg, D.; Bouliong, E.; Reber, U.; Schuümperli, D.; Leumann, C. J. Antisense Properties of Tricyclo-DNA. *Nucleic Acids Res.* **2002**, *30* (13), 2751–2757.
- (51) Kurreck, J.; Wyszko, E.; Gillen, C.; Erdmann, V. A. Design of Antisense Oligonucleotides Stabilized by Locked Nucleic Acids. *Nucleic Acids Res.* **2002**, *30* (9), 1911–1918.
- (52) Campbell, M. A.; Wengel, J. Locked vs. Unlocked Nucleic Acids (LNA vs. UNA): Contrasting Structures Work towards Common Therapeutic Goals. *Chem. Soc. Rev.* **2011**, *40* (12), 5680–5689.
- (53) Meggers, E.; Zhang, L. Synthesis and Properties of the Simplified Nucleic Acid Glycol Nucleic Acid. *Acc. Chem. Res.* **2010**, *43* (8), 1092–1102.
- (54) Heasman, J. Morpholino Oligos: Making Sense of Antisense? *Dev. Biol.* **2002**, *243* (2), 209–214.
- (55) Amantana, A.; Iversen, P. L. Pharmacokinetics and Biodistribution of Phosphorodiamidate Morpholino Antisense Oligomers. *Curr. Opin. Pharmacol.* **2005**, *5* (5), 550–555.
- (56) Schnell, F. J.; Crumley, S. L.; Mourich, D. v.; Iversen, P. L. Development of Novel Bioanalytical Methods to Determine the Effective Concentrations of Phosphorodiamidate Morpholino Oligomers in Tissues and Cells. *Biores. Open. Access.* **2013**, *2* (1), 61–66.
- (57) Nielsen, P. E.; Egholm, M. An Introduction to Peptide Nucleic Acid. *Cur. Issues Mol. Biol.* **1999**, *1* (2), 89–104.
- (58) Nielsen, P. E. PNA Technology. *Mol. Biotechnol.* **2004**, *26* (3), 233–248.
- (59) Reid Corey, D.; Elayadi, A. N.; Corey, D. R. Application of PNA and LNA Oligomers to Chemotherapy. *Curr. Opin. Investig. Drugs* **2001**, *2* (4).
- (60) Nielsen, P. E.; Egholm, M.; Berg, R. H.; Buchardt, O. Sequence-Selective Recognition of DNA by Strand Displacement with a Thymine-Substituted Polyamide. *Science* **1991**, *254* (5037), 1497–1500.
- (61) Egholm, M.; Buchardt, O.; Nielsen, P. E.; Berg, R. H. Peptide Nucleic Acids (PNA). Oligonucleotide Analogues with an Achiral Peptide Backbone. *J. Am. Chem. Soc.* **1992**, *114* (5), 1895–1897.



- (62) Demidov, V. v.; Potaman, V. N.; Frank-Kamenetskii, M. D.; Egholm, M.; Buchard, O.; Sönnichsen, S. H.; Nielsen, P. E. Stability of Peptide Nucleic Acids in Human Serum and Cellular Extracts. *Biochem. Pharmacol.* **1994**, *48* (6), 1310–1313.
- (63) Brown, S. C.; Thomson, S. A.; Veal, J. M.; Davis, D. G. NMR Solution Structure of a Peptide Nucleic Acid Complexed with RNA. *Science* **1994**, *265* (5173), 778–780.
- (64) Rasmussen, H.; Kastrop, S. J.; Nielsen, J. N.; Nielsen, J. M.; Nielsen, P. E. Crystal Structure of a Peptide Nucleic Acid (PNA) Duplex at 1.7 Å Resolution. *Nat. Struct. Biol.* **1997**, *4* (2), 98–101.
- (65) Nielsen, P. E. Peptide Nucleic Acid. A Molecule with Two Identities. *Acc. Chem. Res.* **1999**, *32* (7), 624–630.
- (66) Ratilainen, T.; Holmén, A.; Tuite, E.; Nielsen, P. E.; Nordén, B. Thermodynamics of Sequence-Specific Binding of PNA to DNA. *Biochemistry* **2000**, *39* (26), 7781–7791.
- (67) Janson, C.; Düring, M. *Peptide Nucleic Acids, Morpholinos and Related Antisense Biomolecules*, Springer, **2006**.
- (68) Nielsen, P. E. *Peptide Nucleic Acids: Protocols and Applications*, 2nd ed.; Horizon Bioscience: Wymondham, 2004.
- (69) Wu, Y.; Xu, J. C. Synthesis of Chiral Peptide Nucleic Acids Using Fmoc Chemistry. *Tetrahedron* **2001**, *57* (38), 8107–8113.
- (70) Wojciechowski, F.; Hudson, R. H. E. A Convenient Route to N-[2-(Fmoc)Aminoethyl]Glycine Esters and PNA Oligomerization Using a Bis-N-Boc Nucleobase Protecting Group Strategy. *J. Org. Chem.* **2008**, *73* (10), 3807–3816.
- (71) Lohse, J.; Dahl, O.; Nielsen, P. E. Double Duplex Invasion by Peptide Nucleic Acid: A General Principle for Sequence-Specific Targeting of Double-Stranded DNA. *Proc. Natl. Acad. Sci. USA* **1999**, *96* (21), 11804–11808.
- (72) Rajeev, K. G.; Maier, M. A.; Lesnik, E. A.; Manoharan, M. High-Affinity Peptide Nucleic Acid Oligomers Containing Tricyclic Cytosine Analogues. *Org. Lett.* **2002**, *4* (25), 4395–4398.
- (73) Egholm, M.; Christensen, L.; Deulholm, K. L.; Buchardt, O.; Coull, J.; Nielsen, P. E. Efficient pH-Independent Sequence-Specific DNA Binding by Pseudoisocytosine-Containing Bis-PNA. *Nucleic Acids Res.* **1995**, *23* (2), 217–222.
- (74) Dodd, D. W.; Hudson, R. H. E. Intrinsically Fluorescent Base-Discriminating Nucleoside Analogs. *Mini. Rev. Org. Chem.* **2009**, *6* (4), 378–391.
- (75) Sinkeldam, R. W.; Greco, N. J.; Tor, Y. Fluorescent Analogs of Biomolecular Building Blocks: Design, Properties, and Applications. *Chem. Rev.* **2010**, *110* (5), 2579–2619.

- (76) Xu, W.; Chan, K. M.; Kool, E. T. Fluorescent Nucleobases as Tools for Studying DNA and RNA. *Nat. Chem.* **2017**, *9* (11), 1043–1055.
- (77) Peon, J.; Zewail, A. H. DNA/RNA Nucleotides and Nucleosides: Direct Measurement of Excited-State Lifetimes by Femtosecond Fluorescence up-Conversion. *Chem. Phys. Lett.* **2001**, *348* (3–4), 255–262.
- (78) Ward, D. C.; Reich, E.; Stryer, L. Fluorescence Studies of Nucleotides and Polynucleotides. *J. Biol. Chem.* **1969**, *244* (5), 1228–1237.
- (79) Evans, K.; Xu, D.; Kim, Y.; Nordlund, T. M. 2-Aminopurine Optical Spectra: Solvent, Pentose Ring, and DNA Helix Melting Dependence. *J. Fluoresc.* **1992**, *2* (4), 209–216.
- (80) Hawkins, M. E. Fluorescent Pteridine Nucleoside Analogs: A Window on DNA Interactions. *Cell Biochem. Biophys.* **2001**, *34* (2), 257–281.
- (81) Hawkins, M. E. Chapter 10 Fluorescent Pteridine Probes for Nucleic Acid Analysis. *Methods Enzymol.* **2008**, *450*, 201–231.
- (82) Scopes, D. I. C.; Barrio, J. R.; Leonard, N. J. Defined Dimensional Changes in Enzyme Cofactors: Fluorescent “Stretched-Out” Analogs of Adenine Nucleotides. *Science* (1979) **1977**, *195* (4275), 296–298.
- (83) Godde, F.; Aupeix, K.; Moreau, S.; Toulmé, J. J. A Fluorescent Base Analog for Probing Triple Helix Formation. *Antisense Nucleic Acid Drug Dev.* **1998**, *8* (6), 469–476.
- (84) Okamoto, A.; Saito, Y.; Saito, I. Design of Base-Discriminating Fluorescent Nucleosides. *J. Photochem. Photobiol. C* **2005**, *6* (2–3), 108–122.
- (85) Zhao, Y.; Knee, J. L.; Baranger, A. M. Characterization of Two Adenosine Analogs as Fluorescence Probes in RNA. *Bioorg. Chem.* **2008**, *36* (6), 271–277.
- (86) Gaied, N. ben; Glasser, N.; Ramalanjaona, N.; Beltz, H.; Wolff, P.; Marquet, R.; Burger, A.; Mély, Y. 8-Vinyl-Deoxyadenosine, an Alternative Fluorescent Nucleoside Analog to 2'-Deoxyribosyl-2-Aminopurine with Improved Properties. *Nucleic Acids Res.* **2005**, *33* (3), 1031–1039.
- (87) Berry, D. A.; Jung, K. Y.; Wise, D. S.; Sercel, A. D.; Pearson, W. H.; Mackie, H.; Randolph, J. B.; Somers, R. L. Pyrrolo-DC and Pyrrolo-C: Fluorescent Analogs of Cytidine and 2'-Deoxycytidine for the Study of Oligonucleotides. *Tetrahedron Lett.* **2004**, *45* (11), 2457–2461.
- (88) Hudson, R. H. E.; Dambeniek, A. K.; Viirre, R. D. Fluorescent 7-Deazapurine Derivatives from 5-Iodocytosine via a Tandem Cross-Coupling-Annulation Reaction with Terminal Alkynes. *Synlett* **2004**, *2004* (13), 2400–2402.

- (89) Hudson, R. H. E.; Choghamarani, A. G. The 6-Methoxymethyl Derivative of Pyrrolo-DC for Selective Fluorometric Detection of Guanosine-Containing Sequences. *Nucleosides Nucleotides Nucleic Acids* **2007**, *26* (6–7), 533–537.
- (90) Hudson, R. H. E.; Ghorbani-Choghamarani, A. Selective Fluorometric Detection of Guanosine-Containing Sequences by 6-Phenylpyrrolocytidine in DNA. *Synlett* **2007**, *2007* (6), 870–873.
- (91) Elmehriki, A. A. H.; Suchý, M.; Chicas, K. J.; Wojciechowski, F.; Hudson, R. H. E. Synthesis and Spectral Characterization of Environmentally Responsive Fluorescent Deoxycytidine Analogs. *Artif. DNA PNA XNA* **2014**, *5* (2), e29174.
- (92) Kool, E. T. Replacing the Nucleobases in DNA with Designer Molecules. *Acc. Chem. Res.* **2002**, *35* (11), 936–943.
- (93) Wilson, J. N.; Kool, E. T. Fluorescent DNA Base Replacements: Reporters and Sensors for Biological Systems. *Org. Biomol. Chem.* **2006**, *4* (23), 4265–4274.
- (94) Okamoto, A.; Tainaka, K.; Fujiwara, Y. Nile Red Nucleoside: Design of a Solvatofluorochromic Nucleoside as an Indicator of Micropolarity around DNA. *J. Org. Chem.* **2006**, *71* (9), 3592–3598.
- (95) Lakowicz, J. R. Principles of Fluorescence Spectroscopy. *Principles of Fluorescence Spectroscopy* **2006**, 1–954.
- (96) Förster, Th. Zwischenmolekulare Energiewanderung Und Fluoreszenz. *Ann. Phys.* **1948**, *437* (1–2), 55–75.
- (97) Cardullo, R. A.; Agrawal, S.; Flores, C.; Zamecnik, P. C.; Wolf, D. E. Detection of Nucleic Acid Hybridization by Nonradiative Fluorescence Resonance Energy Transfer. *Proc. Natl. Acad. Sci. USA* **1988**, *85* (23), 8790–8794.
- (98) Tyagi, S.; Kramer, F. R. Molecular Beacons: Probes That Fluoresce upon Hybridization. *Nat. Biotechnol.* **1996**, *14* (3), 303–308.
- (99) Kawahara, S.; Uchamaru, T. Theoretical Investigation on the Substitution Effect of the Hydrogen Bond Energy of the Watson-Crick Type Base Pair between Substituted 1-Methyluracil and 9-Methyladenine. *J. Mol. Struct-Theochem.* **2002**, *588* (1–3), 29–35.
- (100) Kawahara, S.; Wada, T.; Kawauchi, S.; Uchamaru, T.; Sekine, M. Ab Initio and Density Functional Studies of Substituent Effects of an A - U Base Pair on the Stability of Hydrogen Bonding. *J. Phys. Chem. A* **1999**, *103* (42), 8516–8523.
- (101) Nielsen, P. E. Peptide Nucleic Acid. A Molecule with Two Identities. *Acc. Chem. Res.* **1999**, *32* (7), 624–630.

- (102) Eriksson, M.; Nielsen, P. E. PNA-Nucleic Acid Complexes. Structure, Stability and Dynamics. *Q. Rev. Biophys.* **1996**, *29* (4), 369–394.

## Chapter 2

### 2. The Synthesis and Hybridization Study of 5-Nitrouracil

#### PNA

#### 2.1. Introduction

The nitro group is hydrophilic and a strong electron-withdrawing group (EWG). The 5-nitro modification constitutes a relatively minor structural change to the nucleobases, representing the replacement of a methyl group on 5-methyluracil (thymine). The resulting 5-substituent is placed in the major groove of double-stranded nucleic acids; thus, it is expected to be sterically well tolerated. Other advantages are that the chemistry is accessible and that uracil does not require protection.

Hydrogen bonds in crystalline 5-nitrouracil were studied computationally by density functional theory (DFT) calculations. These studies show that 5-nitrouracil crystal has stronger hydrogen bonding interactions in comparison with uracil and related 5-uracil derivatives.<sup>1-3</sup> Kawahara and Uchimaru have also calculated the hydrogen bond energy between 9-methyladenine and 5-substituted 1-methyluracil derivatives in the gas phase and in the solvent using molecular orbital (MO) theory and DFT methods.<sup>4,5</sup> According to their calculations, uracil base derivatives possessing a strong EWG, such as the nitro group, in the 5-position will form more stable base pairs with adenine nucleobases than the natural nucleobases. The hydrogen bond energies in 9-methyladenine and 5-substituted 1-methyluracil derivatives are reinforced by introduction of an EWG group, and electrostatic energy contributes significantly to stabilization of the base pair. Moreover, although the tautomerism of an uracil base derivative is possible, the imide tautomer was calculated to be much more stable than the enol tautomer; thus, the tautomerism does not appear to play an important role in the base pairing.<sup>2</sup>

However, no experimental studies have been performed with nucleobases, nucleosides or nucleic acids. Thus, the goal of this research is to synthesize the 5-nitrouracil ( $U^n$ ) PNA monomer and PNA oligomers including  $U^n$ , as well as to examine the hydrogen bonding of 5-

nitroureil via Watson-Crick base pairing and Hoogsteen base pairing (**Figure 2-1**) by PNA/DNA duplex and bis-PNA/DNA triplex hybridization studies.

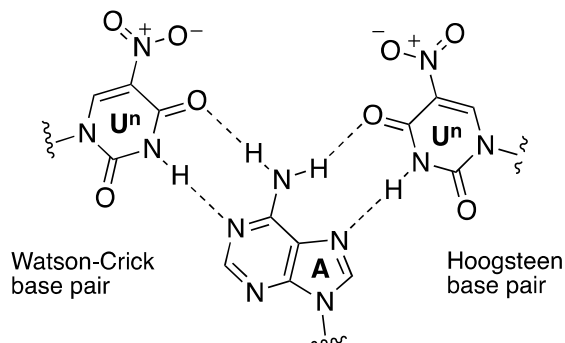


**Figure 2-1. Hydrogen bonding between adenine (A) and 5-nitroureils (U<sup>n</sup>).**

## 2.2. Result and Discussion

### 2.2.1. Computational calculation

Atomic charges of 5-nitroureil were calculated with Moller-Plesset MP2 with 6-31+G\* basis set which is same condition as Kawahara's calculation.<sup>5</sup> The partial charges of hydrogen in N3 position (N3-H) were calculated with three different sets of atomic charge analyses: electrostatic potential charge, Mulliken charge and natural charge. (**Table 2-1**) In each analysis, compare to thymine, the N3-H of 5-nitroureil showed a greater partial positive charge one which is expected due to the electron withdrawing effect from nitro substituent. This greater partial positive charge can be expected to make N3-H a better hydrogen bond donor. Based on the electrostatic potential map in **Figure 2-2**, nitro group substitution affects the polarization of the aromatic ring, and this could lead to changes in  $\pi$ - $\pi$  stacking properties with other nucleobases.

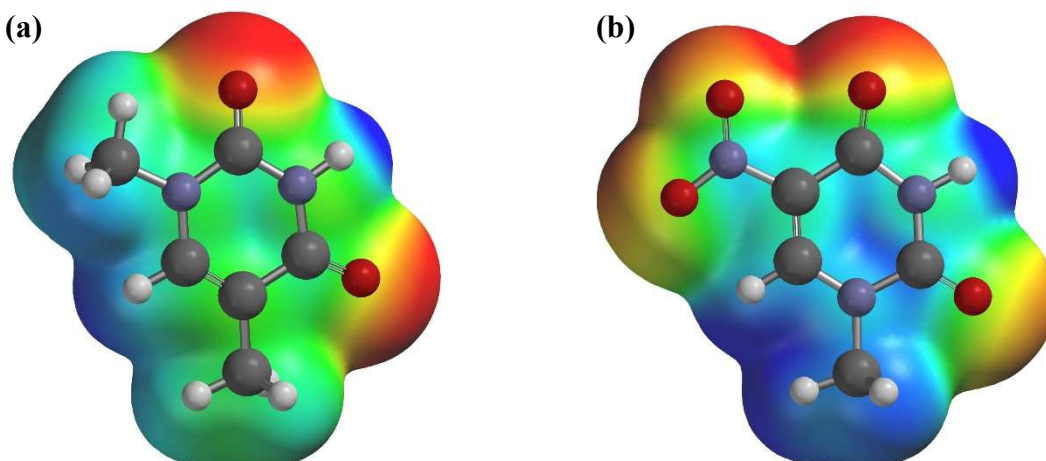


**Figure 2-2.** The electrostatic potential surface calculated of energy minimized structures computed using Hartree-Fock method 6-31+G\* basis set as implemented by Wavefunction Spartan '14. (a) *N*<sup>1</sup>-methylthymine; (b) *N*<sup>1</sup>-methyl-5-nitrouracil. Red colour indicates d<sup>-</sup> regions and blue indicates d<sup>+</sup> regions.

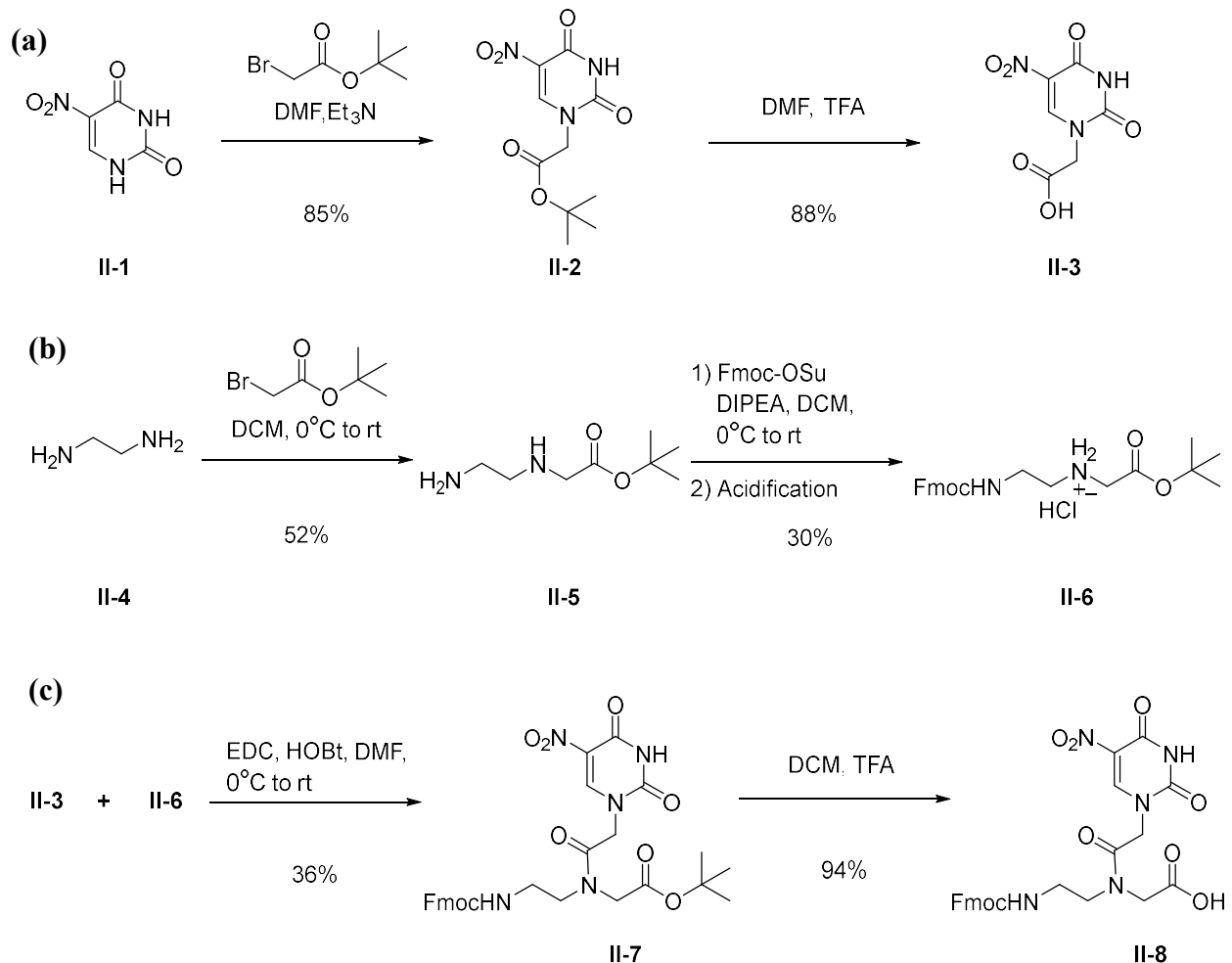
**Table 2-1.** Atomic Charges of *N*<sup>1</sup>-methylthymine (T) and *N*<sup>1</sup>-methyl-5-nitrouracil (U<sup>n</sup>) in different methods.

	Electrostatic charge	Mulliken charge	Natural charge
	N3-H	N3-H	N3-H
T	+0.404	+0.483	+0.454
U <sup>n</sup>	+0.406	+0.490	+0.461

\*Calculated at Hartree-Fock method 6-31+G\* level

### 2.2.2. Synthesis of 5-nitrouracil PNA monomer

The synthesis of the 5-nitrouracil PNA monomer (U<sup>n</sup>), which is compatible with Fmoc-based peptide chemistry, is divided into 3 steps (**Scheme 2-1**): the synthesis of 5-nitrouracil with methyl carbonyl linker (a), the synthesis of 9-fluorenylmethoxycarbonyl (Fmoc) and *tert*-butyl protected *N*-(2-aminoethyl)glycine PNA backbone (b) and the coupling of the two subunits followed by the removal of the protecting group (c).



**Scheme 2-1. Synthesis of the 5-nitrouracil monomer ( $U^n$ ).** (a) Synthesis of 2-(5-nitrouracil-1-yl)acetic acid; (b) Synthesis of Fmoc and *tert*-butyl protected *N*-(2-aminoethyl)glycine PNA backbone; (c) Amide coupling reaction of 5-nitrouracil with linker and PNA backbone, followed by removal of *tert*-butyl ester protecting group.

The synthesis started with 5-nitrouracil, **II-1**, which is a commercially available material. In the first step, the N1 position of 5-nitrouracil was alkylated with *tert*-butyl bromoacetate in the presence of a base. Control of the reaction temperature and proper choice of the base were critical factors to prevent the formation of a di-substituted compound. Due to the electron-withdrawing effect from the nitro group, both the N1 and N3 positions of 5-nitrouracil were readily alkylated under conventional conditions ( $K_2CO_3$ /DMF). However, the proton in the N1 position is more acidic than the proton in the N3 position; therefore, a weaker base like triethylamine was able to give regioselectivity. After N-alkylation, the *tert*-butyl protecting



group was removed by acidolysis with trifluoroacetic acid (TFA) to produce the 5-nitrouracil-based acetic acid derivative **II-3**.

Next, the *N*-(2-aminoethyl)glycine PNA backbone with protecting groups on the amine and carboxylic acid was prepared. For the oligomerization of PNA via solid-phase peptide synthesis (SPPS) using Fmoc chemistry, the Fmoc group for the amine side was chosen as protecting group. In addition, the *tert*-butyl group was selected for masking the carboxyl acid to prevent from an undesired reaction during the coupling step with the **II-3** submonomer. The *N*-(2-(((9*H*-fluoren-9-yl)methoxy)carbonyl)aminoethyl)glycine-*tert*-butyl ester PNA backbone was obtained according to the synthetic pathway outlined in Scheme 2-1 following the method reported in the literature.<sup>6</sup> *tert*-Butyl-*N*-(2-aminoethyl)glycinate **II-5** was obtained by the reaction of ethylenediamine with *tert*-butyl bromoacetate in dichloromethane (DCM). The primary amino group was protected using *N*-(9-fluorenylmethoxycarbonyloxy)succinimide (Fmoc-OSu) to yield the fully protected backbone submonomer. The free base is a liquid that is less stable to storage than the salt form; therefore, the Fmoc and *tert*-butyl protected backbone **II-5** was isolated as a hydrochloride salt form **II-6** by acidifying it with an HCl aqueous solution.

The condensation of the backbone submonomer **II-6** with the modified nucleobases **II-3** was achieved by the use of the carbodiimide reagent *N*-ethyl-*N'*-(3-dimethylaminopropyl) carbodiimide (EDC) with a hydroxybenzotriazole (HOBt) additive. The HCl salt of the backbone submonomer was used in slight excess (1.1 equivalent) because of the loss during the neutralization and extractive workup. From several trials, compound **II-7** was synthesized in sufficient yield to continue further reactions; therefore, no effort has been made to optimize the coupling reaction. However, excess use of the acid component **II-3** relative to the equivalent of the free base form of the backbone submonomer would help to improve yields. The *tert*-butyl protecting group on the backbone was removed under the same reaction conditions as the previous deprotection step for **II-3**, only with a different solvent.

### 2.2.3. Oligomerization of PNA

PNA oligomers were synthesized on a 5  $\mu$ mol scale using the Fmoc-based FastMoc module on an ABI 433 SPPS synthesizer. Rink amide (RAM) resin was selected as the solid

support. Upon cleavage, the rink amide resin yields an amide C-terminal, rather than a carboxylic acid C-terminal. The amide C-terminal prevents undesired negative charge at the terminus. The loading of the resin at 0.19 mmol/g was too high for solid-phase PNA synthesis. Therefore, downloading of resin was required before the oligomerization due to the growing PNA's tendency to aggregate during SPPS. The resin was downloaded to approximately 0.04 mmol/g by coupling it to a sub-stoichiometric amount of Fmoc-L-Lys(Boc)-OH, followed by capping. Due to preloading, all synthesized PNA oligomers possessed a lysine (K) at the C-terminus. The presence of lysine helps to improve water solubility of PNA. For this reason, a second lysine was added at the N-terminus of PNA oligomers. For Fmoc-based SPPS, PNA monomers with nucleobases protected by acid labile groups such as Boc or Bhoc groups were used. After the synthesis, PNA oligomers were cleaved with TFA that cleaves oligomers from the solid support and removes protecting groups on nucleobases at the same time. Cleaved PNA oligomers were purified with high-pressure liquid chromatography (HPLC) and characterized by high-resolution mass spectroscopy.

For duplex binding and mismatch studies with target DNA and RNA, PNA oligomers were designed and synthesized (**Table 2-2 and Table 2-3**). For the duplex study, PNA sequences were designed to be complementary to the sequence of DNA 1 (Table 2-3). PNA1 was a control sequence without a 5-nitrouracil base. PNA2 was the oligomer used for the mismatch study with matching (DNA1) and mismatching DNA oligomers (DNA2, DNA3 and DNA4). In each of PNA3, PNA4, PNA5 and PNA6, one or more thymine bases were replaced with 5-nitrouracil bases to examine their effects on the binding affinity of PNA oligomers.

To test the Hoogsteen base pairing ability of 5-nitrouracil, bis-PNA oligomers for the triplex study were prepared (**Figure 2-3**). The target DNA (DNA6) for the triplex study had the same sequence as Nielson's novel bis-PNA:DNA complex sequence<sup>7</sup> for comparison with other data that use this sequence with different modified nucleobases. bis-PNA has two PNA strands which are linked to each other with a linker; one strand is for Watson-Crick recognition, and the other strand is for Hoogsteen recognition of the target. In this study, the two PNA strands were composed only with pyrimidine nucleobases which bind with the purine-rich region of target DNA sequence (5' CGC AAA GAG ACG C 3'). Three 8-amino-3,6-dioxaoctanoic acid (PEG2) linkers were used to connect the Watson-Crick PNA strand with the Hoogsteen PNA strand. This

flexible linker allowed bis-PNA to form a hairpin shape triplex with the target DNA strand. For recognition of guanines in the target, cytosines were used in the Watson-Crick PNA strand, and pseudoisocytosine (J) bases were used in the Hoogsteen PNA strand. The use of J bases allowed for a pH-independent triplex study. bis-PNA1 was a control sequence without a 5-nitrouracil base which has the same sequence as Nielson's. In bis-PNA2, a 5-nitrouracil was placed instead of the thymine in the Hoogsteen bonding site (**Figure 2-3**).

**Table 2-2. PNA oligomers for duplex binding and mismatch study.**

Oligomer	Sequence* (N → C)		
PNA1	K-GTA GAT CCC T-K		Control
PNA3	K-GTA GAU <sup>n</sup> CCC T-K	Duplex binding study	1 replacement
PNA4	K-GU <sup>n</sup> A GAU <sup>n</sup> CCC T-K		2 replacements
PNA5	K-GU <sup>n</sup> A GAU <sup>n</sup> CCC U <sup>n</sup> -K		3 replacements
PNA2	K-GTA GAT CU <sup>n</sup> C T-K	Mismatch study	

\* U<sup>n</sup> = 5-nitrouracil, K = L-lysine.

Sequences possess an amide group at the C-terminus and Fmoc-protected amine at the N-terminus

**Table 2-3. DNA and RNA oligomers for the duplex formation and mismatch studies with PNA oligomers.**

Oligomer	Sequence (5' → 3')	
DNA1	5' AGG GAT CTA C 3'	PNA/DNA binding study
RNA1	5' AGG GAU CUA C 3'	PNA/RNA binding study
DNA2	5' AG <u>A</u> GAT CTA C 3'	Mismatch study - Match
DNA3	5' AG <u>G</u> GAT CTA C 3'	Mismatch study - Mismatch G
DNA4	5' AG <u>T</u> GAT CTA C 3'	Mismatch study - Mismatch T
DNA5	5' AG <u>C</u> GAT CTA C 3'	Mismatch study - Mismatch C

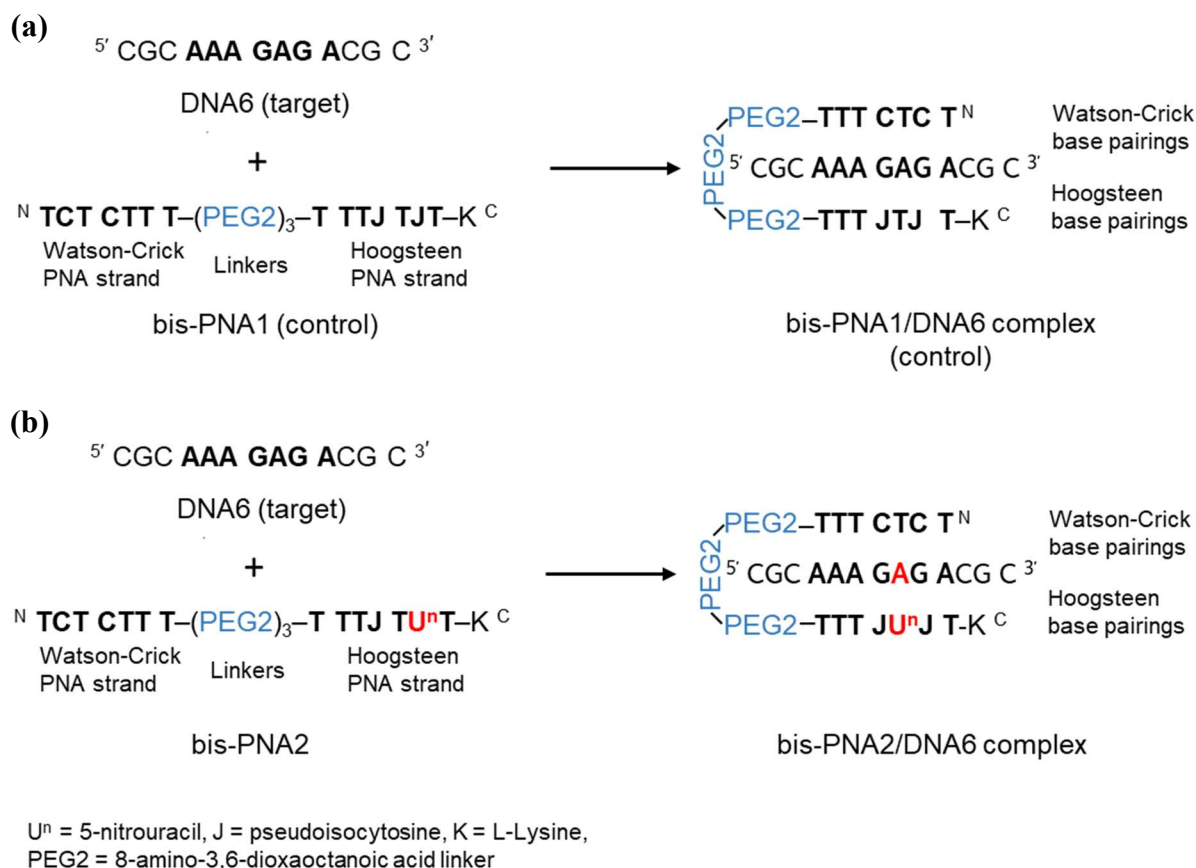


**Figure 2-3. The structure of bis-PNA and the hairpin structure formation of bis-PNA/DNA complex. (a) bis-PNA1/DN6 complex (control); (b) bis-PNA1/DN6 complex.**

#### 2.2.4. Hybridization study

In order to study the binding affinity of PNA oligomer to the target DNA strand, a thermal stability analysis was performed by measuring the melting temperature ( $T_m$ ) for each duplex. Samples for the thermal stability analysis were prepared by dissolving PNA oligomer strands and target DNA strands in the standard buffer (10 mM Na<sub>2</sub>HPO<sub>4</sub>, 100 mM NaCl, 0.1 mM EDTA, pH 7.0). Each experimental duplex was formed by base pairing experimental PNA with target DNA; for instance, in the case of PNA3, the duplex formation would result in PNA3/DNA duplex. In the annealing process, prepared samples were heated to 90 °C and slowly cooled down to 25 °C for the hybridization of PNA and DNA strands. After annealing, the stability of PNA/DNA complexes was measured by thermal denaturation.  $T_m$  values of samples were

measured by temperature-dependent UV-Vis spectrophotometry using a computer-controlled Peltier device cuvette holder with the heating block.

#### 2.2.4.1 Duplex binding study

Based on the computational study<sup>4,5</sup>, which predicted 5-nitrouracil to have stronger hydrogen bonds with adenine at the monomeric level, the binding affinity of PNA containing 5-nitrouracil was expected to be better than PNA without modification. However, experimental data showed different results. PNA with 5-nitrouracil had a lower  $T_m$  value than the control PNA when it was denatured from the duplex.

The control duplex, PNA1/DNA1, had a  $T_m$  value of 52.8 °C at pH 7. At the same pH, PNA3/DNA1 duplex had a  $T_m$  value of 42.2 °C, 10.6 °C lower than the control duplex (Table 2-4). PNA4/DNA1 duplex also had a  $T_m$  value of 42.3 °C at pH 7. PNA5/DNA1 complex did not show the melting pattern during denaturation measurement. Comparing the  $T_m$  values of the control and the experimental complexes, the results suggest that the binding affinity of PNA with 5-nitrouracil was decreased. However, various limitations to the study should be discussed prior to making a conclusive statement. The decrease in  $T_m$  values may be a result of different experimental limitations, such as the self-aggregation of PNA molecules and undesired hydrogen bond formations with a target.

To determine whether the ionization of 5-nitrouracil contributes to the destabilization of hybridization, duplex samples were prepared with a pH 5 buffer providing acidic condition (**Table 2-4**). At pH 5, the control duplex had a  $T_m$  value of 50.8 °C. This suggests that there was no significant pH effect on the control complex, as predicted. However, at pH 5, PNA3/DNA1 and PNA4/DNA1 duplexes showed even lower  $T_m$  values of 29.8 °C and 38.1 °C, respectively. PNA5/DNA1 duplex, on the other hand, still did not show evidence of denaturation which further suggests that PNA5 failed to form a duplex complex with the target DNA at both pH 7 and 5.

**Table 2-4. Binding study of the PNA/DNA duplex and triplex.**

<i>Duplex</i>		$T_m^a$ (°C)	
		pH 7	pH 5
Target DNA1	3' CAT CTA GGG A 5'		
PNA1 (control)	<sup>N</sup> GTA GAT CCC T <sup>C</sup>	52.8	50.8
PNA3	<sup>N</sup> GTA GAU <sup>n</sup> CCC T <sup>C</sup>	42.2	29.8
PNA4	<sup>N</sup> GU <sup>n</sup> A GAU <sup>n</sup> CCC T <sup>C</sup>	42.3	38.1
PNA5	<sup>N</sup> GU <sup>n</sup> A GAU <sup>n</sup> CCC U <sup>n</sup> <sup>C</sup>	.	.
<i>Triplex</i>			
Target DNA	3' CGC <u>ACA GAA ACG</u> C 5'		
bis-PNA1 (control)	<sup>N</sup> TCT CTT T – (PEG2) <sub>3</sub> – T TTJ TJT <sup>C</sup>	61.2	61.3
bis-PNA2	<sup>N</sup> TCT CTT T – (PEG2) <sub>3</sub> – T TTJ U <sup>n</sup> JT <sup>C</sup>	63.3	62.5

<sup>a</sup> Buffer: 100 mM NaCl, 10 mM Na<sub>2</sub>HPO<sub>4</sub>, 0.1 mM EDTA. Heating rate: 0.5 °C/min at 5-90 °C

Based on these data, there was a disruption when PNA3, PNA4 and PNA5 strands formed duplexes with DNA strands, and this disruption was exaggerated at pH 5. We hypothesized that there is some intermolecular and/or intramolecular interaction involving 5-nitrouracil. To check for self-aggregation, a thermal stability experiment without target DNA was performed. However, there was no significant evidence of self-aggregation of PNA strands.

Although the nitro groups are known to be poor hydrogen bond acceptors, hydrogen bonding to the neutral nitro group has been reported in solution<sup>8-12</sup> and crystal.<sup>13-19</sup> Especially, the nitro group in a nitroaromatic compound can form a hydrogen bond with a hydrogen atom, albeit a weak hydrogen bond due to the slightly longer distance.<sup>20</sup> Moreover, the nitro groups of 5-nitrouracil could have acted as good hydrogen bond acceptors because of the electron delocalization from N1 of uracil which makes oxygen atoms of the nitro group more basic with an anionic nitro intermediate. An anionic nitro group is known to act as a good hydrogen bonding acceptor.<sup>21,22</sup> In Portalone's study,<sup>23</sup> the nitro group of 5-nitrouracil made bonds with

both cytosine and protonated cytosine. Therefore, there is a chance that 5-nitrouracil interacted with both cytosine and protonated cytosine and formed an undesired complex. Protonated cytosine has two hydrogen bonding donors which can interact with hydrogen acceptor sites (O4 and O of the nitro group) which are located on the opposite side of the Watson-Crick base pairing site. Because of this, 5-nitrouracil is predicted to have a higher chance of interaction with protonated cytosine than with cytosine. (Figure 2-4)

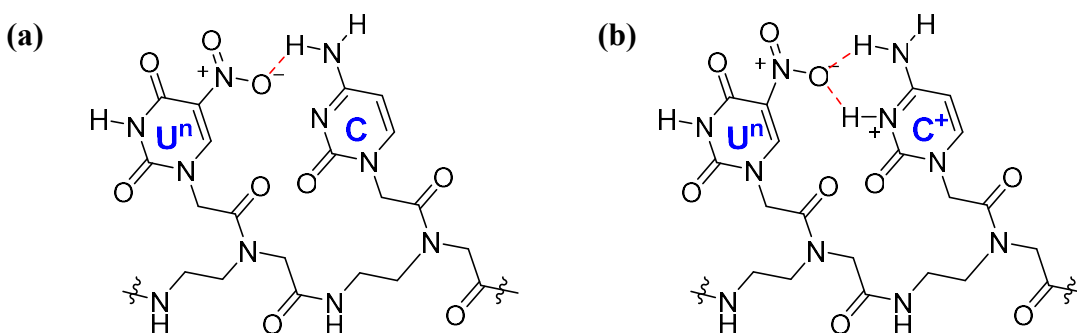


**Figure 2-4. Potential intramolecular interactions. (a) 5-nitrouracil (U<sup>n</sup>) and cytosine (C); (b) 5-nitrouracil (U<sup>n</sup>) and protonated cytosine (C<sup>+</sup>).**

The sequence of PNA3 had 5-nitrouracil adjacent to cytosine which may have interacted with the nitro group of 5-nitrouracil. This may have caused a disruption in duplex formation. When cytosine was protonated at pH 5, the interaction between 5-nitrouracil and the adjacent cytosine would have strengthened, resulting in a stronger disruption. This was reflected in the drop in  $T_m$ . The sequence of PNA4 added an extra 5-nitrouracil replacement to the sequence of PNA3. Because this new replacement site was not adjacent to a cytosine nucleobase, there was no additional disruption effect on duplex formation. Compared to PNA3, PNA4 showed an improved affinity in both pH conditions, which is a reflection of the stronger hydrogen bonding ability of 5-nitrouracil. PNA5, which did not form a duplex, had an extra insertion of 5-nitrouracil compared to PNA4. This insertion was adjacent to cytosine; thus, there would have been extra disruptions caused by the formation of 5-nitrouracil:cytosine complex. Another possible explanation for the destabilizing effect of 5-nitrouracil is due to changes to solvation of the PNA single strand versus the PNA/DNA duplex. The effect may be due to the nature of the sequence examined. Further studies would be required to delineate these effects.

#### 2.2.4.2 Mismatch study

To analyze the specificity of 5-nitrouracil, a PNA oligomer containing 5-nitrouracil (PNA2) was hybridized with a perfectly matched (DNA2) or one-base mismatched DNA strands (DNA3, DNA4 and DNA5). The match duplex, PNA2/DNA2, exhibited a  $T_m$  value of 40.2 °C (**Table 2-5**). Interestingly, this value was close to the  $T_m$  value (42.2 °C) of PNA3/DNA1 complex which was found as the result of the duplex binding study. This may be because PNA2 and PNA3 have very similar sequences, each with only one 5-nitrouracil replacement. Like in the sequence of PNA3, the replacement in PNA2 also placed 5-nitrouracil adjacent to cytosine nucleobases. This may have led to a similar disruption on duplex formation. Nevertheless, under the same experimental conditions, the G mismatch duplex exhibited a  $T_m$  value that is 8.4 °C lower than that of the match duplex. The T mismatch duplex exhibited a  $T_m$  value that is 10.5 °C lower than that of the match duplex. Lastly, C mismatch duplex yielded a  $T_m$  value that is 14.7 °C lower than that of the match duplex. In short, the duplexes containing mismatch base pairs against 5-nitrouracil exhibited lower  $T_m$  values compared to the match duplex. This indicates that 5-nitrouracil selectively binds to adenine with the discriminatory ability against mismatched bases.

#### 2.2.4.3 Triplex binding study

The reference triplex which is the complex of bis-PNA1 and target DNA had  $T_m$  values of 61.2 °C at pH 7, and 61.3 °C at pH 5 (**Table 2-4**). These values were close to previously reported values.<sup>7</sup> This proves that the low affinity was caused by the installation of 5-nitrouracil nucleobase and not by an instrumentation or technique issue.

At pH 7, the bis-PNA2 triplex had a  $T_m$  value of 63.3 °C which is 2.1 °C higher than the  $T_m$  of the bis-PNA1 triplex. At pH 5, it had a  $T_m$  value of 62.5 °C, which is 1.2 °C higher than the reference triplex. This shows 5-nitrouracil can have slightly better Hoogsteen bonds with adenine relatively independent of pH. It showed that the nitro group enhanced the hydrogen bonding between uracil and adenine nucleobases, in this particular context.



Contrary to the PNA sequences used in duplexes, the sequence used in the triplex does not have a cytosine base adjacent to 5-nitrouracil nucleobase. Therefore, there could not have been unintended weak hydrogen bonding between adjacent 5-nitrouracil and cytosine.

**Table 2-5. Mismatch study of the PNA/DNA duplex.**

PNA <i>Mismatch</i>		$T_m^a$ (°C)	$\Delta T_m$ (°C)
DNA2 (Match) PNA2	5' AGA GAT CTA C 3' C TCU <sup>m</sup> CTA GAT G <sup>N</sup>	40.2	
DNA3 (G mismatch) PNA2	5' AGG GAT CTA C 3' C TCU <sup>m</sup> CTA GAT G <sup>N</sup>	31.8	-8.4
DNA4 (T mismatch) PNA2	5' AGT GAT CTA C 3' C TCU <sup>m</sup> CTA GAT G <sup>N</sup>	29.7	-10.5
DNA5 (C mismatch) PNA2	5' AGC GAT CTA C 3' C TCU <sup>m</sup> CTA GAT G <sup>N</sup>	25.5	-14.7

<sup>a</sup> Buffer: 100 mM NaCl, 10 mM Na<sub>2</sub>HPO<sub>4</sub>, 0.1 mM EDTA. Heating rate: 0.5 °C/min at 5-90 °C.

## 2.3. Conclusion

Based on computational DFT calculations, 5-nitrouracil was predicted to have strong hydrogen bonds with complementary adenine nucleobase due to the electron-withdrawing effect from the nitro group. In this chapter, we sought experimental data to confirm the prediction. By studying the effects of inserting 5-nitrouracil in PNA strands, experimental data was acquired that characterized the binding affinity and specificity of complexes containing 5-nitrouracil nucleobases. The 5-nitrouracil PNA monomer was synthesized with Fmoc protecting group for SPPS using the Fmoc-based peptide chemistry. Then, PNA oligomers with various sequences were synthesized and characterized for hybridization study with target complementary DNA

strands. Hybridization study showed that the PNA/DNA duplexes with 5-nitrouracil insertions in the PNA strands exhibited a lower  $T_m$  compared to the control duplex. Additional tests were performed to rule out the possibility of self-aggregation and pH dependency. The mismatch study showed that 5-nitrouracil has discriminatory ability against mismatched bases. To check the Hoogsteen base pairing ability of 5-nitrouracil, bis-PNA oligomer was synthesized. In contrast to the duplex study, the bis-PNA2 complex which had 5-nitrouracil nucleobase in the Hoogsteen recognition strand had slightly higher  $T_m$  values compared to the reference triplex. As a result, 5-nitrouracil nucleobase improved the binding affinity of PNA oligomer when it was inserted in Hoogsteen strands in bis-PNA.

## 2.4. Future work

Further studies are required to investigate the cause of the duplex destabilization of 5-nitrouracil in PNA/DNA complexes. Duplex PNA sequences without adjacent 5-nitrouracils and cytosines should be examined to eliminate the possibility that unwanted interactions between the nitro group and cytosine occur during the duplex binding study.

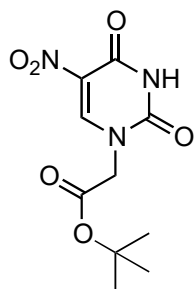
Even though no significant evidence of self-aggregation was found by the UV-melting study, there remains the possibility that the PNA strands with 5-nitrouracil fold upon itself. This can be investigated in depth with other analytical methods.

Regarding the triplex study, bis-PNA with two or more 5-nitrouracil nucleobases in the Hoogsteen region can be made in search of further improved binding affinity. Additionally, bis-PNA with 5-nitrouracil replacement(s) in the Watson-Crick strand should be examined for its binding characteristics. This 5-nitrouracil replacement could avoid the site adjacent to cytosine. Lastly, bis-PNA in which 5-nitrouracil nucleobases are inserted in both the Watson-Crick strand and the Hoogsteen strand should be synthesized, so two 5-nitrouracil nucleobases can form a triplex with an adenine nucleobase, such as presented in **Figure 2-1**.

## 2.5. Experimental

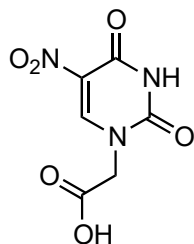
### 2.5.1. Synthesis of 5-nitrouracil PNA monomer

#### *tert*-Butyl 2-(5-nitrouracil-1-yl)acetate (**II-2**)



5-Nitrouracil, **II-1** (4.71 g, 30.0 mmol) and triethylamine (4.18 mL, 30.0 mmol) were dissolved in dry DMF (200 mL). A solution of *tert*-butyl bromoacetate (4.33 mL, 30.0 mmol) in dry DMF (100 mL) was added dropwise to the above solution. The resulting solution was stirred under nitrogen atmosphere, at room temperature for 24 hours. The solvent was removed by rotary evaporation and the crude product was dissolved in ethyl acetate, washed sequentially with pH 4 HCl solution and brine, dried over Na<sub>2</sub>SO<sub>4</sub> and evaporated to white powder product (7.20 g, 89 %): <sup>1</sup>H NMR (600 MHz, DMSO-d<sub>6</sub>) δ: 12.22 (s, 1 H), 9.35 (s, 1 H), 4.60 (s, 2 H), 1.43 (s, 9 H). <sup>13</sup>C NMR (150 MHz, DMSO-d<sub>6</sub>) δ: 166.2, 154.8, 142.7, 149.1, 124.9, 82.5, 50.2, 27.6. HRMS (EI) m/z: [M]<sup>+</sup> Calculated for C<sub>10</sub>H<sub>13</sub>N<sub>3</sub>O<sub>6</sub> 271.0804, found 271.0814.

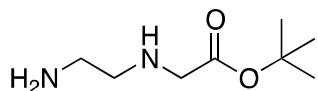
#### 2-(5-Nitrouracil-1-yl)acetic acid (**II-3**)



Compound **II-2** (2.71 g, 10 mmol) was dissolved in dry DMF (10 mL) before the addition of 5 mL of TFA. The solution was stirred for 2 hours at room temperature. After flushing with a nitrogen stream for 30 min, the solvent was removed by lyophilization to give a

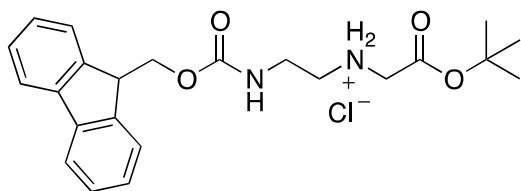
white powdery solid (1.88 g, 88 %). Compound **II-3** was used without further purification:  $^1\text{H}$  NMR (400 MHz, DMSO- $d_6$ )  $\delta$ : 12.21 (s, 1 H), 9.36 (s, 1 H), 4.61 (s, 2 H), 3.33 (br s, 1 H). HRMS (ESI/TOF)  $m/z$ :  $[\text{M}+\text{Na}]^+$  Calculated for  $\text{C}_6\text{H}_5\text{N}_3\text{O}_6\text{Na}$   $[\text{M}]^+$  238.0076, found 238.0083.

### ***tert*-Butyl 2-((2-aminoethyl)amino)acetate (II-5)**



A solution of *tert*-butyl bromoacetate (14.4 mL, 100 mmol) in DCM (80 mL) was added dropwise to a solution of ethylenediamine (60.1 mL, 900 mmol) in DCM (100 mL) at 0 °C over a period of 5 hours. The mixture was warmed slowly to room temperature and then stirred for a period of 48 hours. The reaction mixture was washed with water 3 times, and the combined aqueous wash was back-extracted with DCM. The combined organic layers were dried with  $\text{Na}_2\text{SO}_4$  and concentrated in vacuo to give a yellow clear oil. (9.02 g, 52 %):  $^1\text{H}$  NMR ( $\text{CDCl}_3$ , 400 MHz,  $\delta$ ): 3.21 (s, 2H), 2.71 (t, 2 H), 2.58 (t, 2H), 1.73 (br s, 3H), 1.38 (s, 9H). The spectra correspond to the literature.<sup>24</sup>

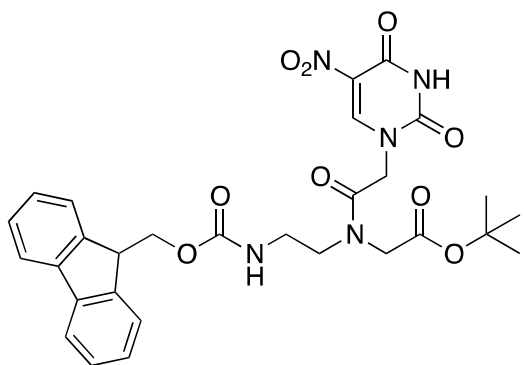
### ***N*-2-(((9*H*-Fluoren-9-yl)methoxy)carbonyl)amino)ethyl)-2-(*tert*-butoxy)-2-oxoethanaminium chloride (II-6)**



A solution of *N*-(9-fluorenylmethoxycarbonyloxy)succinimide (16.30 g, 48.32 mmol) in DCM (100 mL) was added to a solution of compound **II-5** (5.00 g, 29 mmol) and *N,N*-diisopropylethylamine (8.4 mL, 48.3 mmol) in DCM (350 mL) at room temperature over a period of 1 hour. The reaction mixture was stirred for 48 hours and then washed with 100 mL of HCl (1 M) five times and once with 100 mL of brine. The organic layer was dried with  $\text{Na}_2\text{SO}_4$

and partially concentrated to about 50 mL in vacuo. Cooling to -20 °C for a period of 12 hours gave the desired compound as a white solid (6.37 g 30 %), which was isolated by filtration, washed with ice-cold DCM and dried. Compound **II-6** exists in solution as a pair of slowly exchanging rotamers: <sup>1</sup>H NMR (600 MHz, DMSO-d<sub>6</sub>) δ: 9.46 (br s 2 H), 7.89 (d, 2 H), 7.70 (t, 2 H), 7.66 (s, 1 H), 7.41 (t, 2 H), 7.33 (t, 2 H), 4.30 (d, 2 H), 4.22 (m, 1 H), 3.84 (s, 2 H), 3.34 (t, 2 H), 3.01 (t, 2H), 1.45 (s, 9H). <sup>13</sup>C NMR (150 MHz, DMSO-d<sub>6</sub>) δ: 165.6, 156.2, 143.8, 140.7, 127.6, 127.0, 125.0, 120.0, 82.8, 65.6, 54.9, 47.3, 46.6, 46.4, 36.7, 27.6. The spectra correspond to the literature.<sup>24</sup>

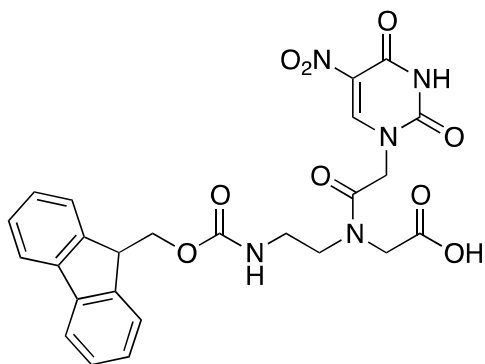
***tert*-Butyl 2-(*N*-(2-(((9*H*-Fluoren-9-yl)methoxy)carbonyl)amino)ethyl)-2-(5-nitouracil-1-yl)-acetamido)acetate (**II-7**)**



An HCl salt form of **II-6** (0.95 g, 2.2 mmol) was dissolved in DCM (10 mL) and washed with a saturated NaHCO<sub>3</sub> solution (30 mL) three times. The organic layer was dried with Na<sub>2</sub>SO<sub>4</sub> and concentrated in vacuo to give the yellow clear oil which is free base form of *N*-[2-(Fmoc)aminoethyl]glycine-*tert*-butyl ester back bone. To a solution of **II-3** (0.43 g, 2 mmol) in DMF (5 mL), the prepared free base form of the backbone (1.04 g, 1.9 mmol) and HOBt (0.92 g, 6 mmol) were added, and the solution was stirred for 10 min at 0 °C. EDC (0.38 g, 2 mmol) in DMF (10 mL) was added to the mixture solution dropwise and stirred for 48 hours under N<sub>2</sub> gas in room temperature. The solvent was removed by rotary evaporation, and the crude product was purified by column chromatography using ethyl acetate: hexane (2:1 to 4:1 v/v) as the eluent to give the monomer ester **II-7** (0.43 g, 36%) as a yellowish white solid. Compound **II-7** exists in solution as a pair of slowly exchanging rotamers: <sup>1</sup>H NMR (600 MHz, DMSO-d<sub>6</sub>) δ: 12.16 (br s

1 H), 9.25(s, 0.6 H, ma.), 9.17 (s, 0.4, mi.), 7.89 (d, 2 H), 7.67 (t, 2 H), 7.41 (t, 2 H), 7.38 (s, 1 H), 7.33 (t, 2 H), 4.93 (s, 1.2 H, ma.), 4.73 (s, 0.8 H, mi.), 4.34 (d, 1.2 H, ma.), 4.31 (d, 0.8 H, mi.), 4.23 (m, 1 H), 4.19 (s, 0.8 H, mi.), 3.96 (s, 1.2 H, ma.), 3.40 (m, 0.8 H, ma.), 3.23 (m, 1.2 H, mi.), 3.25 (m, 1.2 H, ma.), 3.11 (m, 0.8 H, mi.), 1.46 (s, mi 3.6 H), 1.39 (s, ma 5.4 H). <sup>13</sup>C NMR (150 MHz, DMSO-d<sub>6</sub>) δ: (168.2, 167.8, rot.), (166.7, 166.3, rot.), (156.3, 156.1, rot.), (154.83, 154.81, rot.), 151.3, 149.1, (143.85, 143.83, rot.), (140.73, 140.71, rot.), 127.6, 127.0, 125.0, (124.78, 124.71, rot.), 120.0, (82.8, 81.0, rot.), (65.44, 65.37, rot.), 49.9, 48.9, (47.1, 46.9, rot.), 46.7, 38.7, (27.64, 27.60, rot HRMS (ESI/TOF) m/z: [M+Na]<sup>+</sup> calculated for C<sub>29</sub>H<sub>31</sub>N<sub>5</sub>O<sub>9</sub>Na 616.2020, found 616.2027.

**2-(N-(2-(((9H-Fluoren-9-yl)methoxy)carbonyl)amino)ethyl)-2-(5-nitrouracil-1-yl)acetamido)acetic acid (II-8)**



A suspension of compound **II-7** (0.20 g, 0.27 mmol) with dry DCM (50 mL) was cooled to 0 °C followed by dropwise addition of TFA (5 mL). The reaction was stirred for 30 minutes in 0 °C and an additional 2 hours at room temperature. The mixture was evaporated by nitrogen stream, and the remaining volatiles were removed by co-evaporation with DCM and diethyl ether. The compound was dissolved in DCM (3 mL), the diethyl ether (50 mL) was added and cooled to 0 °C overnight. The precipitated product was collected by filtration and was dried under vacuum to obtain as orange solid (0.167 g, 90%). Compound **II-8** exists in solution as a pair of slowly exchanging rotamers: <sup>1</sup>H NMR (600 MHz, DMSO-d<sub>6</sub>) δ: 12.17 (s, 0.6 H, ma.), 12.16 (s, 0.4 H, mi.), 9.25 (s, 0.6 H, ma.), 9.18 (s, 0.4 H, mi.), 7.89 (d, 2 H), 7.68 (t, 2 H), 7.41 (t, 2 H), 7.40 (s, 1 H), 7.33 (t, 2 H), 4.95 (s, 1.2 H, ma.), 4.77 (s, 0.8 H, mi.), 4.35 (d, 1.2 H, ma.), 4.30 (d,

0.8 H, mi.), 4.23 (m, 1 H), 4.22 (s, 0.8 H, mi.), 4.01 (s, 1.2 H, ma.), 3.43 (m, 1.2 H, ma.), 3.37 (m, 0.8 H, mi.), 3.28 (m, 1.2 H, ma.), 3.14 (m, 0.8 H, mi.).  $^{13}\text{C}$  NMR (150 MHz, DMSO- $d_6$ )  $\delta$ : (170.6, 170.2, rot.), (166.7, 166.3, rot.), (156.4, 156.1, rot.), (154.85, 154.81, rot.), (151.34, 151.28, rot.), 149.2, 143.86 (140.74, 140.72, rot.), 127.6, 127.1, 125.0, (124.79, 124.75, rot.), 120.1, (65.48, 65.41, rot.), (49.01, 48.95, rot.), 47.9, (47.0, 46.8, rot.), 46.7, (38.7, 37.8, rot.). HRMS (ESI/TOF)  $m/z$ :  $[\text{M}+\text{Na}]^+$  calculated for  $\text{C}_{25}\text{H}_{23}\text{N}_5\text{O}_9\text{Na}$  560.1393, found 560.1390.

## 2.6. References

- (1) Kattan, D.; Alcolea Palafox, M.; Rathor, S. K.; Rastogi, V. K. A DFT Analysis of the Molecular Structure, Vibrational Spectra and Other Molecular Properties of 5-Nitrouracil and Comparison with Uracil. *J. Mol. Struct.* **2016**, *1106*, 300–315.
- (2) Kennedy, A. R.; Okoth, M. O.; Sheen, D. B.; Sherwood, J. N.; Vrcelj, R. M. Two New Structures of 5-Nitrouracil. *Acta. Crystallogr. C* **1998**, *54* (4), 547–550.
- (3) Mirzaei, M.; Hadipour, N. L. Study of Hydrogen Bonds in Crystalline 5-Nitrouracil. Density Functional Theory Calculations of the O-17, N-14, and H-2 Nuclear Quadrupole Resonance Parameters. *J. Iran. Chem. Soc. 2009 6:1* **2009**, *6* (1), 195–199.
- (4) Kawahara, S.; Wada, T.; Kawauchi, S.; Uchimaru, T.; Sekine, M. Ab Initio and Density Functional Studies of Substituent Effects of an A - U Base Pair on the Stability of Hydrogen Bonding. *J. Phys. Chem. A* **1999**, *103* (42), 8516–8523.
- (5) Kawahara, S.; Uchimaru, T. Theoretical Investigation on the Substitution Effect of the Hydrogen Bond Energy of the Watson-Crick Type Base Pair between Substituted 1-Methyluracil and 9-Methyladenine. *J Mol. Struct:THEOCHEM* **2002**, *588* (1–3), 29–35.
- (6) Bondebjerg, J.; Grunnet, M.; Jespersen, T.; Meldal, M. Solid-Phase Synthesis and Biological Activity of a Thioether Analogue of Conotoxin G1. *ChemBioChem* **2003**, *4* (2–3), 186–194.

- (7) Egholm, M.; Christensen, L.; Deuholm, K. L.; Buchardt, O.; Coull, J.; Nielsen, P. E. Efficient PH-Independent Sequence-Specific DNA Binding by Pseudoisocytosine-Containing Bis-PNA. *Nucleic Acids Res.* **1995**, *23* (2), 217.
- (8) Zheng, W. R.; Xu, J. L.; Huang, T.; Yang, Q.; Chen, Z. C. Hydrogen Bonding Interaction between Ureas or Thioureas and Nitro-Compounds. *Res. Chem. Intermed.* **2011**, *37* (1), 31–45.
- (9) West-Nielsen, M.; Dominiak, P. M.; Wozniak, K.; Hansen, P. E. Strong Intramolecular Hydrogen Bonding Involving Nitro- and Acetyl Groups. Deuterium Isotope Effects on Chemical Shifts. *J. Mol. Struct.* **2006**, *789* (1–3), 81–91.
- (10) Ungnade, H. E.; Roberts, E. M.; Kissinger, L. W. Hydrogen Bonding in Nitro Compounds. *J. Phys. Chem.* **2002**, *68* (11), 3225–3228.
- (11) Dubis, A. T.; Łotowski, Z.; Siergiejczyk, L.; Wilczewska, A. Z.; Morzycki, J. W. Study of Hydrogen Bonding in Nitro Enamides. *J. Chem. Res. Synop.* **1998**, No. 4, 170–171.
- (12) Kelly, T. R.; Kim, M. H. Relative Binding Affinity of Carboxylate and Its Isosteres: Nitro, Phosphate, Phosphonate, Sulfonate, and  $\delta$ -Lactone. *J. Am. Chem. Soc.* **1994**, *116* (16), 7072–7080.
- (13) Saeed, A.; Simpson, J. N-(2-Nitro-Phen-Yl)Benzamide. *Acta. Crystallogr. E* **2009**, *65* (Pt 8).
- (14) Wardell, J. L.; Skakle, J. M. S.; Low, J. N.; Glidewell, C. Contrasting Three-Dimensional Frame-Work Structures in the Isomeric Pair 2-Iodo-N-(2-Nitrophenyl)Benzamide and N-(2-Iodophenyl)-2-Nitrobenzamide. *Acta. Crystallogr. C* **2005**, *61* (11).
- (15) Sharma, C. V. K.; Desiraju, G. R. C–H  $\cdots$  O Hydrogen Bond Patterns in Crystalline Nitro Compounds: Studies in Solid-State Molecular Recognition. *J. Chem. Soc. Perkin Trans 2* **1994**, *2* (11), 2345–2352.
- (16) Panunto, T. W.; Urbinczyk-lipkowska, Z.; Johnson, R.; Etter, M. C. Hydrogen-Bond Formation in Nitroanilines: The First Step in Designing Acentric Materials. *J. Am. Chem. Soc.* **1987**, *109* (25), 7786–7797.



- (17) Allen, F. H.; Baalham, C. A.; Lommerse, J. P. M.; Raithby, P. R.; Sparr, E. Hydrogen-Bond Acceptor Properties of Nitro-O Atoms: A Combined Crystallographic Database and Ab Initio Molecular Orbital Study. *Acta. Crystallogr. B* **1997**, *53* (6), 1017–1024.
- (18) Baitinger, W. F.; Schleyer, P. von R.; Murty, T. S. S. R.; Robinson, L. Nitro Groups as Proton Acceptors in Hydrogen Bonding. *Tetrahedron* **1964**, *20* (7), 1635–1647.
- (19) Lemmerer, A.; Michael, J. P. Extensive Hydrogen and Halogen Bonding, and Absence of Intramolecular Hydrogen Bonding between Alcohol and Nitro Groups in a Series of Endo-Nitronorbornanol Compounds. *Acta. Crystallogr. C* **2011**, *67* (Pt 8).
- (20) Shugrue, C. R.; Defrancisco, J. R.; Metrano, A. J.; Brink, B. D.; Nomoto, R. S.; Linton, B. R. Detection of Weak Hydrogen Bonding to Fluoro and Nitro Groups in Solution Using H/D Exchange. *Org. Biomol. Chem.* **2016**, *14* (7), 2223–2227.
- (21) Linton, B. R.; Goodman, M. S.; Hamilton, A. D. Nitronate Anion Recognition and Modulation of Ambident Reactivity by Hydrogen-Bonding Receptors. *Chem. Eur. J.* **2000**, *6* (13), 2449–2455.
- (22) Kelly-Rowley, A. M.; Lynch, V. M.; Anslyn, E. v. Molecular Recognition of Enolates of Active Methylene Compounds in Acetonitrile. The Interplay between Complementarity and Basicity, and the Use of Hydrogen Bonding to Lower Guest PKas. *J. Am. Chem. Soc.* **1995**, *117* (12), 3438–3447.
- (23) Portalone, G. Solid-Phase Molecular Recognition of Cytosine Based on Proton-Transfer Reaction. Part II. Supramolecular Architecture in the Cocrystals of Cytosine and Its 5-Fluoroderivative with 5-Nitrouracil. *Chem. Cent. J.* **2011**, *5* (1), 51.
- (24) Kim, P. H.; Switzer, C. Synthesis and Characterization of Cationic PNA Bearing 5- $\omega$ -Aminopropyl-Uracil. *Tetrahedron Lett.* **2014**, *55* (40), 5580–5582.

## Chapter 3

### 3. The Synthesis and Photochemical Study of Nucleobase Quencher

#### 3.1. Introduction

A molecular beacon (MB)<sup>1-3</sup> is a single-stranded oligonucleotide hybridization probe that has been used for genotyping single nucleotide polymorphisms (SNPs) and other applications. A molecular beacon forms a stem-and-loop structure. The loop contains a probe sequence that is complementary to a target sequence. The stem is formed by the annealing of complementary arm sequences that are located on either side of the probe sequence. A fluorophore is covalently linked to the end of one arm, and a quencher is covalently linked to the end of the other arm. In the absence of the target sequence, the stem brings the fluorophore close to the nonfluorescent quencher resulting in the quenching through fluorescence resonance energy transfer (FRET). This results in the quenching of the light emitted by the fluorophore. However, when the beacon hybridizes with a nucleic acid strand containing the target sequence, it undergoes a conformational change involving unfolding of the stem domain. This results in an increase in the distance between the fluorophore and the quencher, effectively disengaging FRET between the fluorophore and the quencher, which ultimately leads to fluorescence of the fluorophore. The efficiency of FRET is majorly dependent on the distance between an electron donor and an acceptor.<sup>4-7</sup> When the acceptor molecule is close to the donor molecule, more electrons can be efficiently shared producing the FRET effect. For this reason, it is important to ensure that the distance is rigidly controlled when performing FRET analysis.

In the original design of MB<sup>1</sup>, the fluorophore and quencher are conventionally placed as overhanging residues. This overhanging design allows enough mobility in the fluorophore and the quencher, such strict distance control is limited. To improve control of the distance between the donor (fluorophore) and the acceptor (quencher) for efficient FRET, a new molecular beacon design was proposed (**Figure 3-1**). In this design, the fluorophore and the quencher are embedded in the stem region, instead of the terminal end of the molecular beacon as overhanging

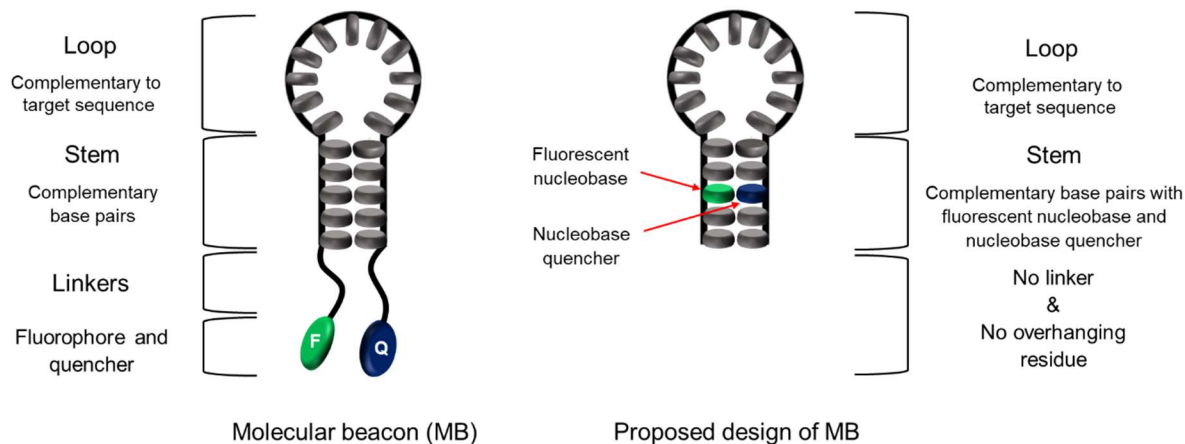


**Figure 3-1. Original and new design of molecular beacon.**

residues. This design ensures a short distance between the donor and the acceptor which increases the efficiency of FRET. Moreover, it allows for static quenching and the quenching from  $\pi$ - $\pi$  stacking to occur.

4-Dimethylaminoazobenzene-4'-carboxylic (DABCYL) acid (**Figure 3-2**) is commonly used as a universal dark quencher for molecular beacons.<sup>8</sup> In a previous study<sup>9</sup> by the Hudson group, the DABCYL moiety was inserted within PNA MB and acted as a fluorophore switch with FRET. The inserted DABCYL could contribute to the hybridization of the stem with  $\pi$ - $\pi$  stacking. However, DABCYL is unable to form base pairs with canonical nucleobases, and it isomerizes from *trans*-form to *cis*-form in response to irradiation. This photoisomerization of DABCYL destabilizes the binding of the two strands.

To overcome these limitations of DABCYL, there was a need for a nucleobase quencher that could form hydrogen bonds with canonical nucleobases while possessing the quenching ability to be embedded into the stem region of MB.

4-(*N,N*-Dimethylamino)phenylazouracil (DMPAU) and 4-nitrophenylpyrrolocytosine (NPhpC) are the modified nucleobase quenchers which can be inserted as a quencher in the stem probe of the MB with the fluorescent nucleobase and can form hydrogen bonds with the complementary nucleobase (**Figure 3-2**). DMPAU is a structural mimic of DABCYL; however, it is able to form hydrogen bonds with adenine thereby successfully base pairing without introducing base pair mismatches. X-Ray crystallography showed that DMPAU predominantly exists in *trans*-form and is unlikely to undergo photoisomerization, keeping the  $\lambda_{ab}$  constant.<sup>10</sup>

NPhpC is one of the phenylpyrrolocytosine (PhpC) derivatives. Its synthesis was reported by the Hudson group previously.<sup>11,12</sup> In contrast to other PhpC compounds, NPhpC has a very weak fluorescent emission. However, it has a great molar absorption coefficient since most of the excitation energy is dissipated as heat. Therefore, NPhpC is a cytosine-based quencher, which should form a complementary base pair with guanine, while DMPAU is a modified form of thymine nucleobase, which should make a complementary base pair with adenine.

Herein, we present a novel synthesis pathway for DMPAU, as well as quenching studies and hydrogen bonding studies with DMPAU using different fluorophores. Along with DMPAU, another nucleobase quencher, 4-nitrophenylpyrrolocytosine (NPhpC), was selected.

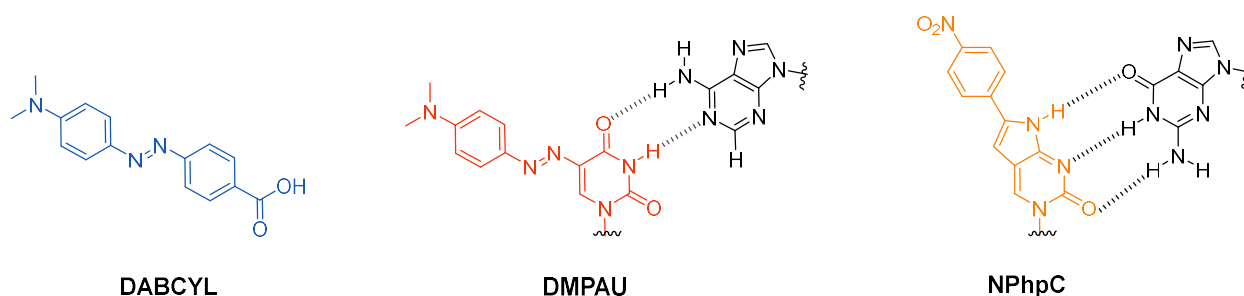


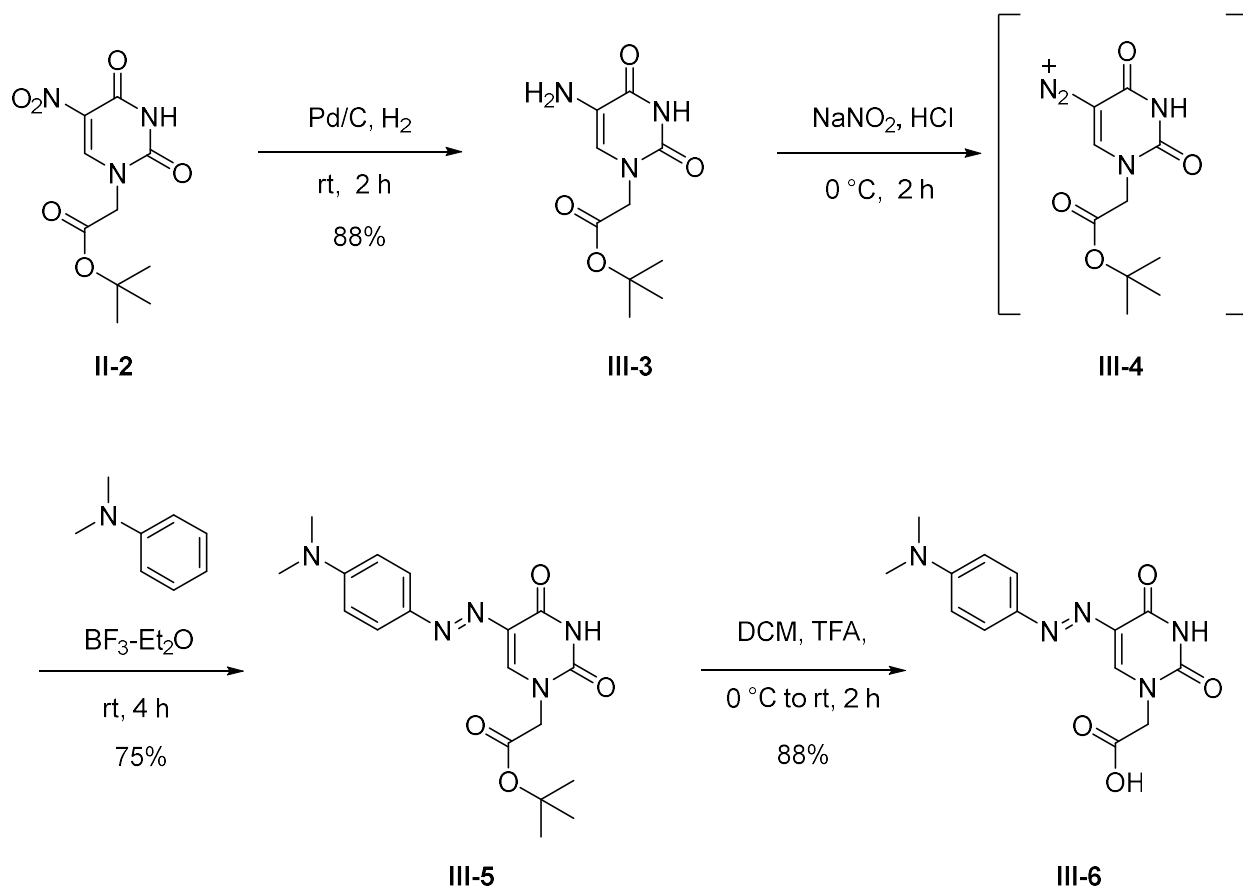
**Figure 3-2. Chemical structure of DABCYL acid, DMPAU and NPhpC.**

## 3.2. Result and Discussion

### 3.2.1. Synthesis of DMPAU acetic acid

The synthesis of the DMPAU PNA monomer analog is outlined in **Scheme 3-1**. The synthesis was started from *tert*-butyl 2-(5-nitrouracil-1-yl)acetate (**II-2**). First, the nitro group was reduced to an amino group by catalytic hydrogenation. DMPAU *tert*-butyl ester, **II-5** was obtained from compound **III-3** through two steps: a diazotization step with sodium nitrite under acidic conditions, and an azo coupling step with *N,N*-dimethylaniline. In diazotization, a good proton source such as a strong acid is required to form the diazonium salt; conversely, a strong acid causes deprotection of *tert*-butyl ester. The key point of this reaction was to find a proper pH range for diazotization without deprotection. After several trials of diazotization, pH 1.5 was defined as the optimal pH. The diazonium ion in an aqueous solution at temperatures above 5 °C

tended to be lost as N<sub>2</sub>. Due to this unstable intermediate, the reaction temperature was kept at 0 °C. During the azo coupling step with *N,N*-dimethylaniline, the boron trifluoride etherate acted as a Lewis acid catalyst, more efficiently activating of diazo intermediate compounds (**III-4**). It may operate as a dehydrating agent, transforming the hydrated diazonium intermediate into a more active form (**III-5**). On the other hand, BF<sub>3</sub> may coordinate with the nucleophilic sites of the molecules of the diazonium intermediate. When *N,N*-dimethylaniline was added to the reaction solution, an interesting color change was observed. The mixture of **III-4** and boron trifluoride etherate in acetonitrile had an orange color. After the addition of *N,N*-dimethylaniline, the color of the solution slowly changed to bright blue and turned to a dark violet color after 10 minutes. This color change comes from the protonation of product **III-5**. In the last step, the deprotection of *tert*-butyl group on **III-5** with TFA produced the DMPAU PNA monomer analog, **III-6**.



**Scheme 3-1. Synthesis of 4-(*N,N*-dimethylamino)phenylazouracil nucleobase acetic acid derivative (**III-6**).**

### 3.2.2. Selection of quenchers and fluorophores

Along with the previously synthesized DMPAU, three additional quenchers were prepared to be examined for their photophysical properties and be used in the quenching study: DABCYL, NPhpC and NPhEC (5-(4-nitrophenyl)ethynylcytosine) (**Figure 3-3**). DABCYL was prepared as a reference for a comparative study with DMPAU. NPhpC and its synthetic precursor, NPhEC, were prepared following procedures reported in the literature.<sup>11, 12</sup>

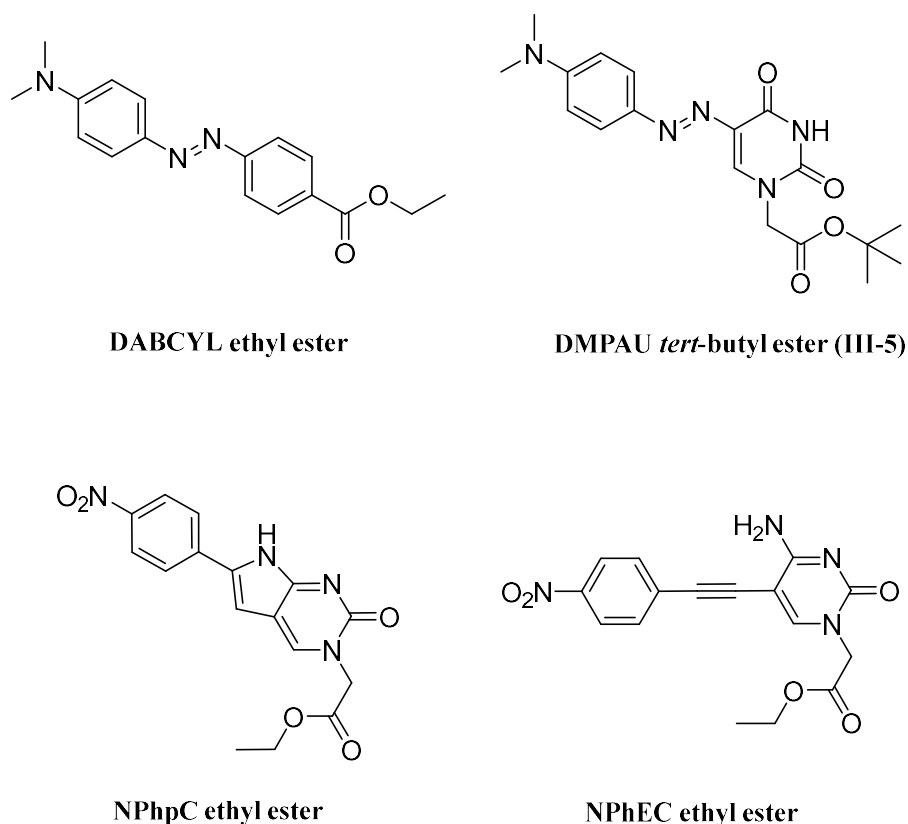


**Figure 3-3. Chemical structure of quenchers selected for quenching study.**

Pyrene, acridone amide, NBD amide and PhpC ethyl ester were prepared as fluorophores. The four selected fluorophores have different emission spectra near the absorption spectra of the quenchers (**Figure 3-4**). Out of the four, PhpC ethyl ester is a nucleobase-derived fluorophore, which can be inserted in the stem sequence of the new design of a molecular beacon.

Due to the structural similarity between the ester and amide links in the nucleobase and PNA backbone, ester derived quenchers and fluorophores were used for quenching studies; therefore, their photophysical properties in EtOH were determined.

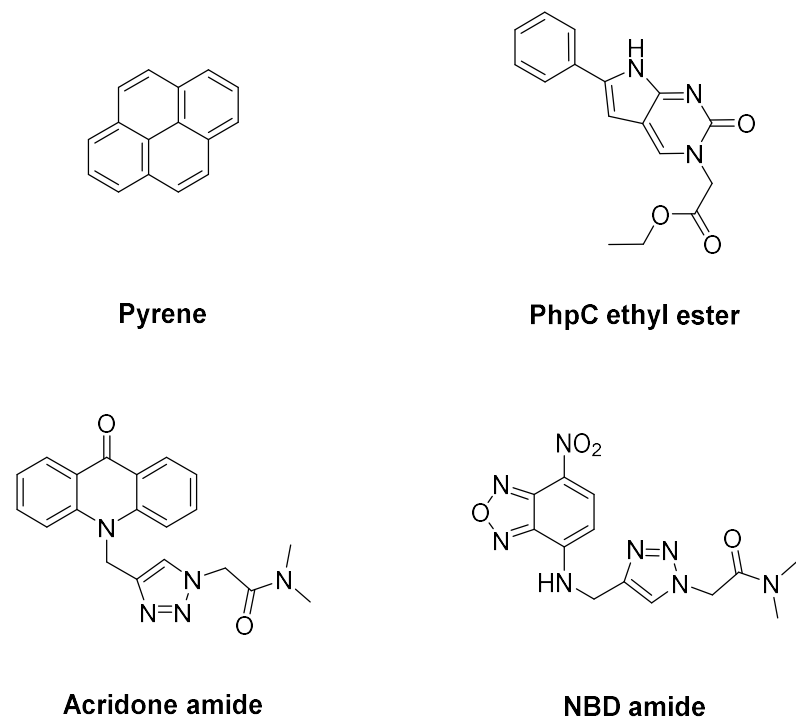


**Figure 3-4. Chemical structure of fluorophores selected for quenching study.**

### 3.2.3. The photophysical properties of quenchers and fluorophores.

The photophysical properties of quenchers were determined by UV-vis spectrometer (Table 3-1). DMPAU *tert*-butyl ester, **III-5**, has the  $\lambda_{ab}$  at 439 nm, which is similar to DABCYL ethyl ester; however, the molar extinction coefficient of DMPAU is smaller than the value of DABCYL ethyl ester. In an aqueous solution, DMPAU acetic acid has the  $\lambda_{ab}$  at 467 nm, which is also similar to DABCYL acid. The molar extinction coefficient of DMPAU acid is also smaller than DABCYL acid in an aqueous solution. Notably, both DMPAU and DABCYL display a trend in their  $\lambda_{ab}$  where there is a red shift in wavelength between the ester form and the carboxylic acid form. NPhpC and NPhEC have  $\lambda_{ab}$  values at 397 nm and 347 nm, respectively. Moreover, NPhEC has a smaller molar extinction coefficient compared to NPhpC. Overall, by

observing the molar extinction coefficients, it can be concluded that DMPAU and NPhC have better potential as quenchers.

The photophysical properties of the four different fluorophores were also measured (Table 3-2). Pyrene is excited at 333 nm and emits at 389 nm. PhpC ethyl ester is excited at 368 nm and emits at 439 nm. Acridone amide is excited at 395 nm and emits at 413 nm. NBD amide is excited at 466 nm and emits at 522 nm. Apart from NBD amide, which emitted yellow light, all other fluorophores emitted blue to violet light. Notably, acridone amide had a small stoke shift, which is similar to acridone.

**Table 3-1. Photophysical property of quenchers.**

	$\lambda_{ab}$ (nm)	$\epsilon$ (M <sup>-1</sup> cm <sup>-1</sup> )
DABCYL ethyl ester (III-5)	453 <sup>a</sup>	32,000 <sup>a</sup>
DABCYL acid (III-6)	464 <sup>a</sup>	27,400 <sup>a</sup>
	418 <sup>b</sup>	19,000 <sup>b</sup>
DMPAU <i>tert</i> -butyl ester	439 <sup>a</sup>	27,500 <sup>a</sup>
DMPAU acid	467 <sup>b</sup>	20,900 <sup>b</sup>
4-NO <sub>2</sub> -PhpC ethyl ester	397 <sup>a</sup>	18,500 <sup>a</sup>
4-NO <sub>2</sub> -PhEC ethyl ester	351 <sup>a</sup>	10,000 <sup>a</sup>

<sup>a</sup> measured in EtOH, <sup>b</sup> measured in 0.1% Et<sub>3</sub>N aqueous solution.

**Table 3-2. Photophysical property of fluorophores.**

	$\lambda_{ab}$ (nm)	$\epsilon$ (M <sup>-1</sup> cm <sup>-1</sup> )	$\lambda_{em}$ (nm)	$\Phi$ (s <sup>-1</sup> )
Pyrene	334	38,600	389	0.65
PhpC ethyl ester	367	11,000	439	0.63
Acridone amide	398	11,000	413	0.41
NBD amide	455	12,600	522	0.75

measured in EtOH.



### 3.2.4. Quenching study in EtOH

The ideal pair of fluorophore and quencher would display great spectral overlap between the emission spectrum of the fluorophore and the absorption spectrum of the quencher. Moreover, there should not be an overlap between the excitation spectrum of the fluorophore and the absorption of the quencher. The graphs illustrating the normalized absorption spectrum of a quencher with normalized excitation and emission spectra of a fluorophore are shown in **Figure 3-5** and **Figure 3-6**.

DABCYL ethyl ester and DMPAU *tert*-butyl ester quench PhpC ethyl ester most efficiently, as shown by the highest Stern-Volmer constant,  $K_{sv}$ , followed by pyrene. The excitation spectrum of acridone amide overlaps with the absorption spectrum of DABCYL and DMPAU, signifying direct absorption. There is a small overlap between the spectra of NBD amide and DABCYL and DMPAU, which results in low quenching efficiency. Although DABCYL and DMPAU display similar trends in quenching, the  $K_{sv}$  values of DMPAU with fluorophores are smaller compared to DABCYL, which had been predicted before as DMPAU has a smaller molar extinction coefficient than DABCYL.

NPhpC ethyl ester has the best quenching ability with pyrene, followed by PhpC ethyl ester as shown by their spectral overlap. A quenching study was not performed for the NPhpC ethyl ester and acridone amide pair, as the excitation and emission spectra of acridone amide completely overlap with NPhpC ethyl ester. There was only a slight overlap between the emission spectrum of NBD amide and the absorption spectrum of NPhpC ethyl ester, which resulted in minimal quenching.

Overall, NPhEC ethyl ester had the lowest quenching ability due to its small molar extinction coefficient as discussed before. It had the highest  $K_{sv}$  of  $7500 \text{ M}^{-1}$  with pyrene followed by PhpC ethyl ester. Like NPhpC ethyl ester, a quenching study with acridone amide was not performed due to the complete overlap of the absorption spectrum of NPhEC ethyl ester and the emission spectrum of acridone amide. No quenching was observed with NBD amide, which is evident from the lack of overlap between the absorption spectrum of NPhEC ethyl ester and the emission spectrum of NBD amide.

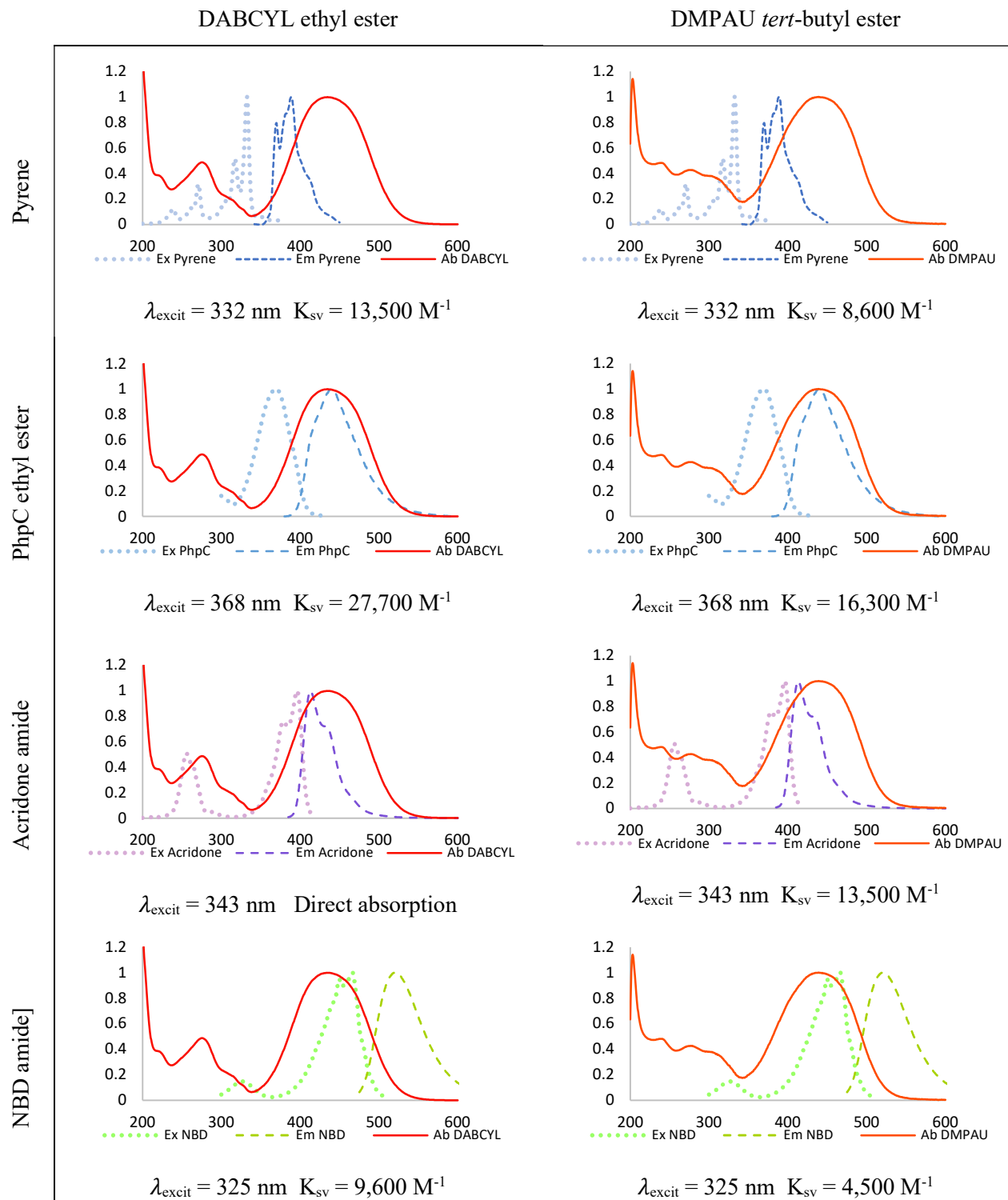


**Figure 3-5. Normalized absorption spectra of DABCYL ethyl ester and DMPAU *tert*-butyl ester with normalized excitation and emission spectra of fluorophores;  $K_{sv}$  values of the fluorophore-quencher pairs.**

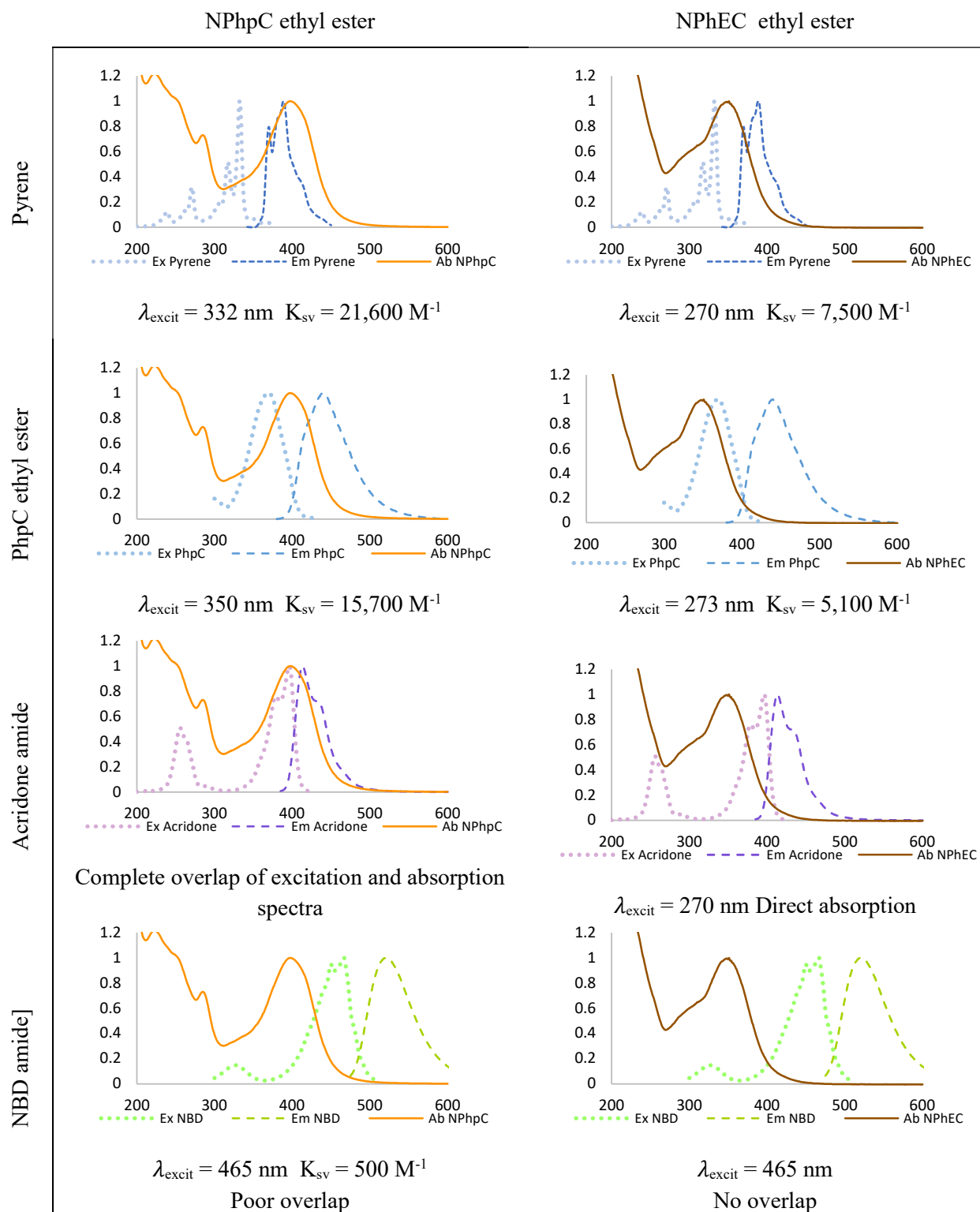


**Figure 3-6. Normalized absorption spectra of NPhpC ethyl ester and NPhEC ethyl ester with normalized excitation and emission spectra of fluorophores;  $K_{sv}$  values of the fluorophore-quencher pairs.**

### 3.2.5. Quenching study in water

Since the DMPAU and PhpC pair shows the best quenching ability in EtOH, DABCYL acid and DMPAU acetic acid were prepared for a quenching study with PhpC acetic acid in 0.1% Et<sub>3</sub>N aqueous solution. (Figure 3-7) Studies involving molecular beacons are done under aqueous buffer condition, which is better represented in 0.1% Et<sub>3</sub>N aqueous solution compared to ethanol. DABCYL acid quenched PhpC acetic acid with a  $K_{sv}$  of 30,000 M<sup>-1</sup>. DMPAU acetic acid quenched PhpC acetic acid with a  $K_{sv}$  of 16,500 M<sup>-1</sup>, which is slightly lower compared to DABCYL acid.

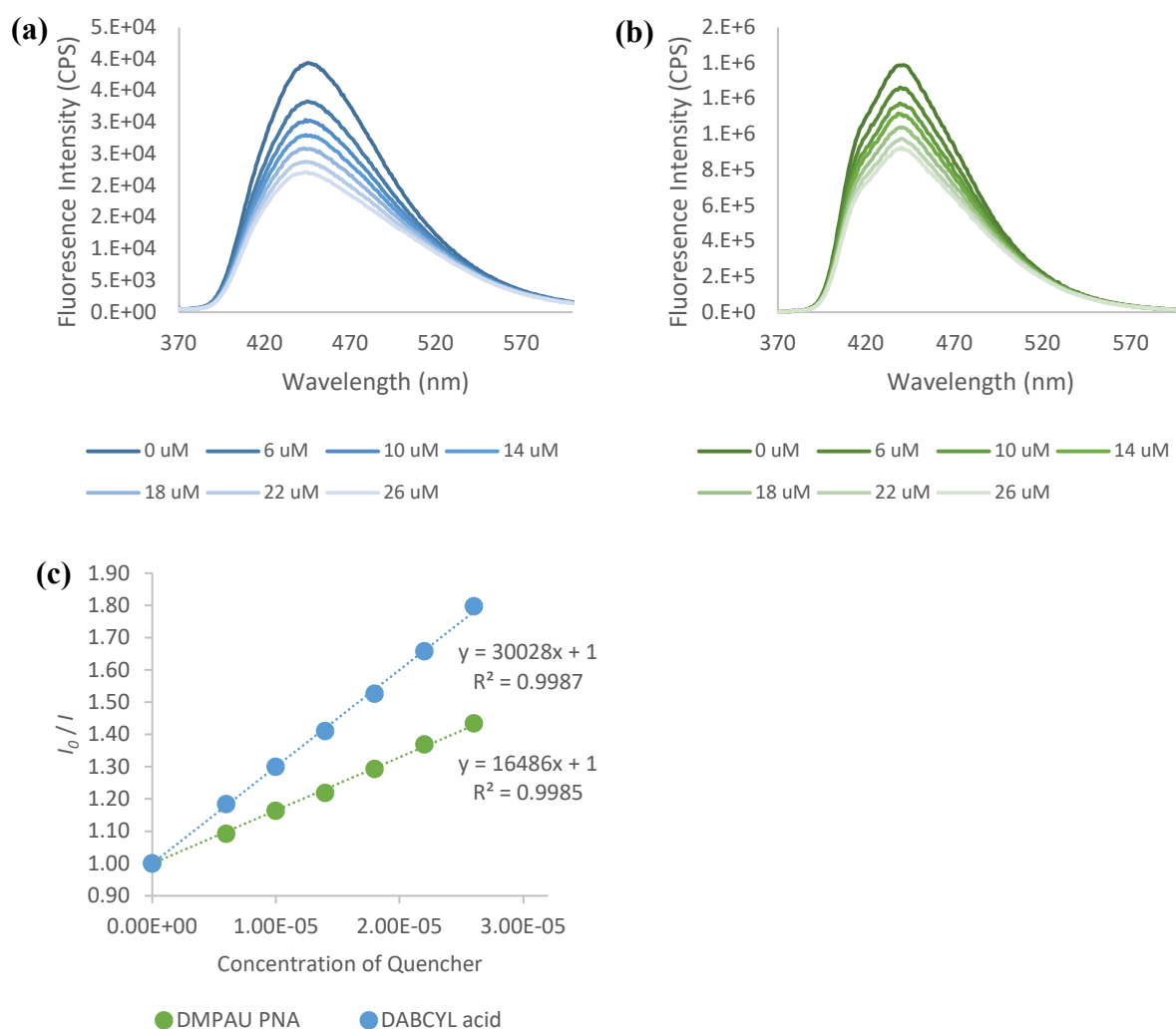


**Figure 3-7. (a) Quenching study of PhpC acetic acid with DABCYL acid; (b) Quenching study of PhpC acetic acid with DMPAU acetic acid; (c) Stern-Volmer plots of DABCYL acid and DMPAU acetic acid.**

### 3.2.6. Hydrogen bonding study

Using NMR spectroscopy, a hydrogen bonding study of DMPAU ethyl ester with adenine ethyl ester was performed. When the molar fraction of adenine ethyl ester and DMPAU *tert*-butyl ester were changed, the N4 and C2 hydrogens of adenine and N3 hydrogen of DMPAU were shifted due to hydrogen bonding, as shown in the **Figure 3-8**. Taking this phenomenon into consideration, NMR titrations were performed with adenine ethyl ester in CDCl<sub>3</sub>, as the host, and DMPAU *tert*-butyl ester in CDCl<sub>3</sub> as the guest. With the addition of the guest aliquots into the host adenine solution, chemical shifts of N4 hydrogen and C2 hydrogen of adenine were monitored. (**Figure 3-9**) The N4 hydrogen peak was shifted from 5.5 to 6.3 ppm when the concentration of DMPAU increased to 12 mM. Under the same condition, the peak of C2 hydrogen, which forms a pseudo-hydrogen bond with O2 of DMPAU, was shifted from 7.87 to 7.99 ppm. These peaks of the two hydrogens were shifted downfield as a result of donating electron density to the oxygens of DMPAU through hydrogen bonding. Using the curve fitting method<sup>12,13</sup> and a computer fitting program, the binding stoichiometry of the host and guest complex and the association constant,  $K_a$ , were determined. The curve fitting showed that DMPAU and adenine form 1:1 complex representing the canonical Watson-Crick base pair.  $K_a$  of the hydrogen bonding between N4 hydrogen of adenine with O4 of DMPAU was calculated to be 111 M<sup>-1</sup>.  $K_a$  of the pseudo-hydrogen bonding between C2 hydrogen of adenine with O2 of DMPAU was calculated to be 117 M<sup>-1</sup>. These two calculated  $K_a$  values can be compared to the  $K_a$  of canonical A-T base pair (120 M<sup>-1</sup>),<sup>13,14</sup> demonstrating the similar binding energy of DMPAU and thymine with adenine.

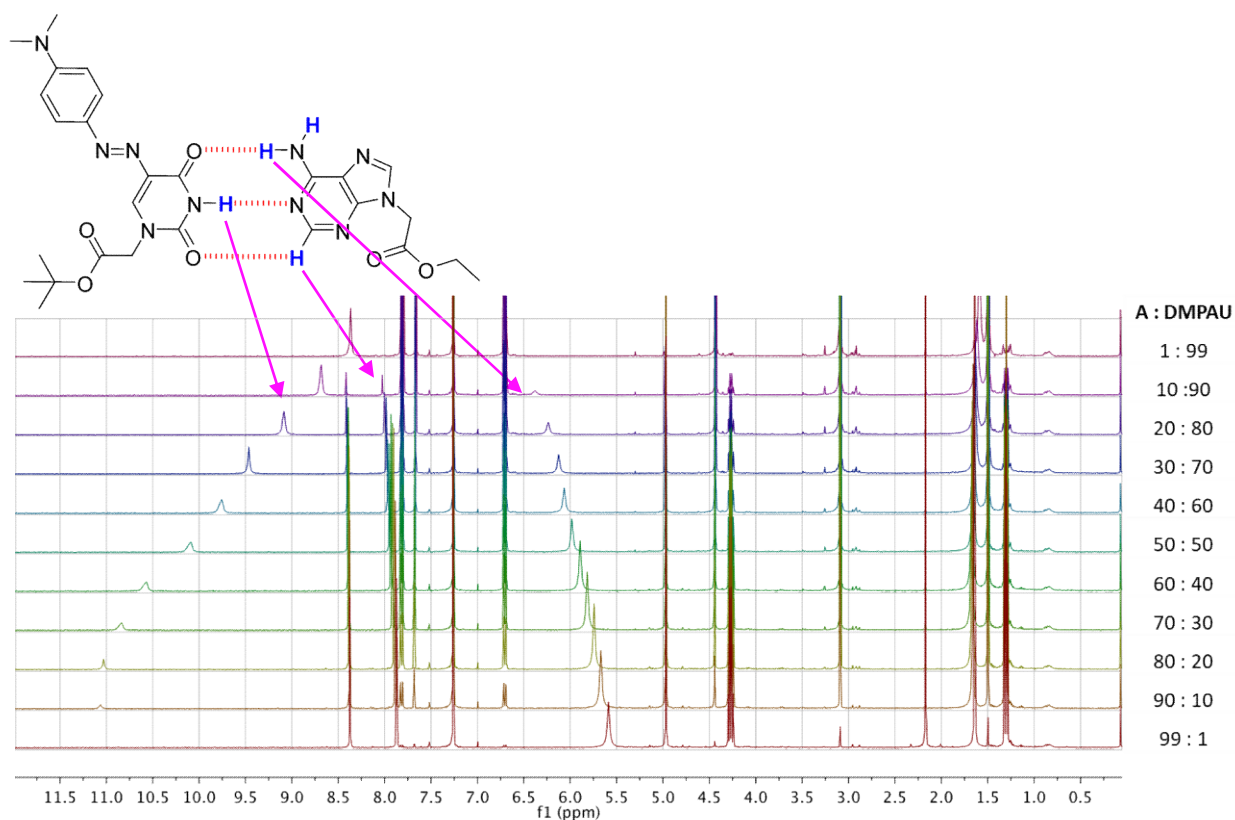


**Figure 3-8. Stacked NMR spectra of continuous variation of DMPAU *tert*-butyl ester and adenine ethyl ester mixture.**

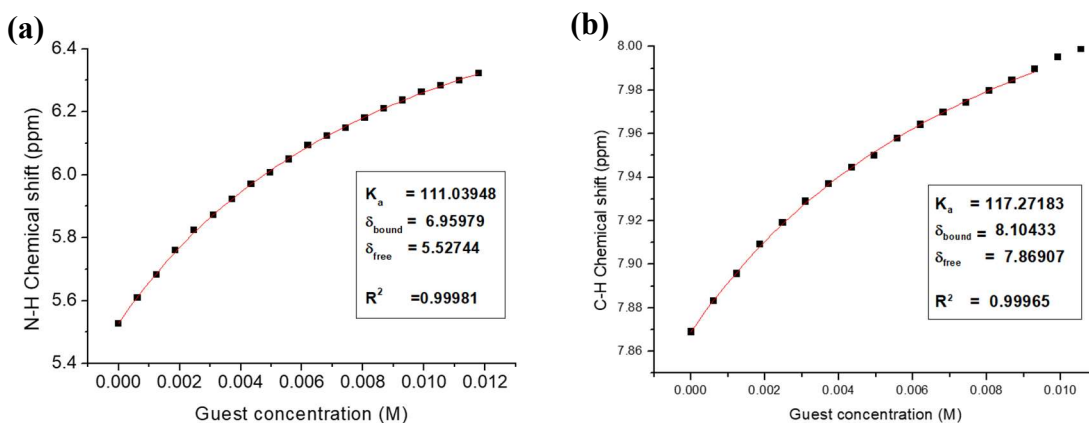


**Figure 3-9. Chemical shift changes of the N4 hydrogen of adenine (a) and the C2 hydrogen (b) induced by the addition of the guest solution (DMPAU in  $\text{CDCl}_3$ ).**

### 3.3. Conclusion

This chapter outlined a novel synthetic pathway of DMPAU which is a base-pairable uracil-derivatized quencher. In addition, NPhpC was also prepared as a cytosine-derivatized quencher. Their photophysical properties were determined, and their quenching abilities were measured using four different fluorophores: pyrene, PhpC, acridone amide and NBD amide. In quenching studies in ethanol, two fluorophores that worked the best with each of the quenchers were determined. DMPAU best matched with PhpC, quenching the fluorophore with  $K_{sv}$  of  $16,300 \text{ M}^{-1}$ , while NPhpC best matched with pyrene, quenching the fluorophore with  $K_{sv}$  of  $23,000 \text{ M}^{-1}$ . DMPAU-PhpC pair was further evaluated under aqueous conditions. The quenching ability of DMPAU in an aqueous solution was reduced but not to a great extent; it was predicted to still be a feasible candidate for molecular beacon studies. Using NMR titration, hydrogen bonding between DMPAU and adenine was examined. The plot from the curve fitting model demonstrated the formation of a 1:1 complex; furthermore,  $K_a$  was calculated to be approximately  $114 \text{ M}^{-1}$ , which is similar to the  $K_a$  of adenine-thymine base pairing.

### 3.4. Future work

From the DMPAU acid, **III-6**, a DMPAU PNA monomer can be synthesized. Using this monomer, the proposed PNA molecular beacon can be synthesized by automated SPPS. As a FRET partner of DMPAU, PhpC can be inserted to the other side of the stem region. With the complementary target sequence, hybridization studies can be conducted to check the molecular beacon function. Since the distance between the fluorophore and quencher can be controlled more accurately in the stem region, effective quenching distance can be determined. Also, this PNA beacon can enable us to determine whether extra quenching effects such as static quenching and  $\pi$ - $\pi$  stacking take place.

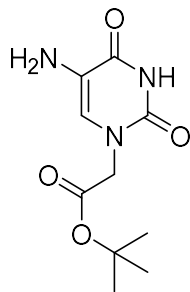
Even though DMPAU and PhpC are an appropriate quencher/fluorophore pair, they cannot form base pairs with each other. There are adenine-derived fluorophores with blue fluorescence (400 to 500 nm) which is within the quenching coverage of DMPAU. One example is 6-MAP<sup>15,16</sup>, which is a naturally occurring fluorescent pteridine derivative, and which has the same hydrogen bonding pattern as adenine. 6-MAP has an emission wavelength of 430 nm with a  $\Phi$  of 0.39. 6-MAP and DMPAU can be inserted as the fluorophore-quencher pair and as the Watson-

Crick base pair in the stem region of the PNA molecular beacon. With this PNA molecular beacon, the effects of base pairing on quenching can be investigated. Enhanced quenching is predicted because of the most rigid structure and the shortest FRET distance.

To overcome the limited spectral coverage of DABCYL acid and to provide enhanced quenching strength, many different quenchers were introduced with the brand name “blackhole quencher (BHQ)”.<sup>17,18</sup> These quenchers have a variety of spectrum coverage for quenching. New nucleobase quenchers can be designed by mimicking these blackhole quenchers to have wide and/or various regions of quenching coverage against different fluorophores. Having a series of nucleobase quenchers with different quenching regions will provide researchers a great toolbox of fluorophores for new molecular beacon studies.

### 3.5. Experimental

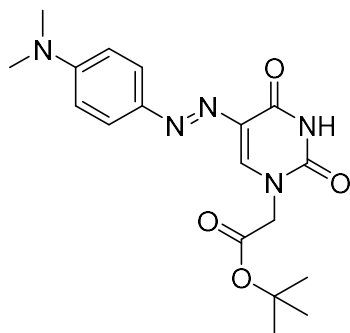
#### *tert*-Butyl 2-(5-aminouracil-1-yl)acetate (III-3)



*tert*-Butyl 2-(5-nitrouracil-1-yl)acetate **II-2** (2.94 g, 10.83 mmol) was dissolved in MeOH (250 mL). The reaction flask was covered with aluminum foil and flushed with nitrogen gas. After the addition of 10 % Pd/C catalyst (398 mg), hydrogen gas balloon was placed to top of the sealed flask. The mixture was stirred vigorously at room temperature for two hours. The reaction solution was filtered through Celite. The Celite was washed with methanol, and the filtrate was evaporated in vacuum to give yellowish white powder product. (2.58 g, 99 %): <sup>1</sup>H NMR (400 MHz, DMSO-d<sub>6</sub>) δ: 11.40 (s, 1 H), 6.75 (s, 1 H), 4.31 (s, 2 H), 4.16 (s, 2 H), 1.43 (s, 9 H). <sup>13</sup>C NMR (100 MHz, CDCl<sub>3</sub>) δ: 166.7, 161.1, 152.7, 149.5, 122.3, 82.2, 49.3, 28.0. HRMS (EI) m/z: [M]<sup>+</sup> calculated for C<sub>10</sub>H<sub>15</sub>N<sub>3</sub>O<sub>4</sub> 241.1062, found 241.1060.

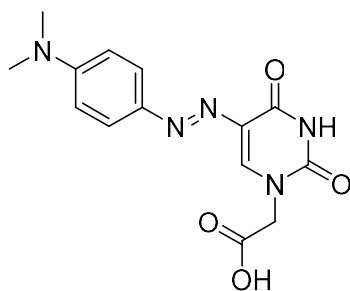


***tert*-Butyl 2-(5-((4-(*N,N*-dimethylamino)phenyl)diazenyl)uracil-1-yl)acetate (III-5)**



The solution of *tert*-butyl 2-(5-aminouracil-1-yl)acetate, **III-3** (1.04 g, 4.3 mmol) in pH 1.5 HCl (400 mL) was vigorously stirred for 15 minutes at 0 °C. A solution of sodium nitrite (593 mg 8.6 mmol) in water (50 mL) was slowly added dropwise to the solution at 0 °C with vigorously stirring in the dark for 2 hours. The solvent was removed by freeze-dry method overnight. Diazonium intermediate salt (1.76 g) was collected. A suspension of the diazonium intermediate in anhydrous acetonitrile (160 mL) was purged with nitrogen gas for 10 min, and borontrifluoride etherate (0.53 mL, 4.3 mmol) and *N,N*-dimethylaniline (0.54 mL, 4.3 mmol) were added to the mixture, which was then stirred for 4 hours. The solvent was removed with rotary evaporation. The red crude solid was purified via flash chromatography using ethyl acetate/*n*-hexane as the eluting solvent (7:3 v/v) to yield **III-5** (1.20 g, 75 %) as brown-red solid: <sup>1</sup>H NMR (600 MHz, DMSO-*d*<sub>6</sub>) δ: 11.79 (s, 1H), 8.07 (s, 1H), 7.66 (d, *J* = 9.4 Hz, 2H), 6.81 (d, *J* = 9.4 Hz, 2H), 4.54 (s, 2H), 3.05 (s, 6H). <sup>13</sup>C NMR (150 MHz, DMSO-*d*<sub>6</sub>) δ: 167.0, 160.8, 152.2, 150.2, 142.9, 134.0, 128.9, 124.4, 111.6, 49.8, 39.8, 27.7. HRMS (EI) *m/z*: [*M*]<sup>+</sup> calculated for C<sub>18</sub>H<sub>23</sub>N<sub>5</sub>O<sub>4</sub> 373.1750, found 373.1743.

**2-(5-((4-(*N,N*-dimethylamino)phenyl)diazenyl)uracil-1-yl)acetic acid (III-6)**



TFA (3 mL) was added dropwise to a cold solution of **III-5** (0.90 g, 2.41 mmol) in dry DCM (3 mL). The reaction mixture was stirred for 4 hours at room temperature under nitrogen gas. Diethyl ether (15 mL) cooled to 0 °C was added and the mixture was kept overnight at 4 °C. The resultant solid was collected by filtration, washed with cold diethyl ether, and dried to give **III-6** (0.69 g, 90 %) as a yellowish brown solid: <sup>1</sup>H NMR (600 MHz, DMSO-d<sub>6</sub>) δ: 11.69 (s, 1H), 8.01 (s, 1H), 7.65 (d, J = 8.8 Hz, 2H), 6.80 (d, J = 8.8 Hz, 2H), 4.43 (s, 2H), 3.03 (s, 6H). <sup>13</sup>C NMR (150 MHz, DMSO-d<sub>6</sub>) δ: 170.0, 160.8, 152.1, 150.3, 142.9, 134.6, 128.6, 124.3, 111.6, 50.0, 39.8. HRMS (EI) m/z: [M]<sup>+</sup> calculated for C<sub>14</sub>H<sub>15</sub>N<sub>5</sub>O<sub>4</sub> 317.1124, found 317.1115.

### 3.6. References

- (1) Tyagi, S.; Kramer, F. R. Molecular Beacons: Probes That Fluoresce upon Hybridization. *Nat. Biotechnol.* **1996**, *14* (3), 303–308.
- (2) Xi, C.; Balberg, M.; Boppart, S. A.; Raskin, L. Use of DNA and Peptide Nucleic Acid Molecular Beacons for Detection and Quantification of rRNA in Solution and in Whole Cells. *Appl. Environ. Microbiol.* **2003**, *69* (9), 5673–5678.
- (3) Ortiz, E.; Estrada, G.; Lizardi, P. M. PNA Molecular Beacons for Rapid Detection of PCR Amplicons. *Mol. Cell. Probes.* **1998**, *12* (4), 219–226.
- (4) Förster, Th. Zwischenmolekulare Energiewanderung Und Fluoreszenz. *Ann. Phys.* **1948**, *437* (1–2), 55–75.
- (5) Marras, S. A. E. Efficiencies of Fluorescence Resonance Energy Transfer and Contact-Mediated Quenching in Oligonucleotide Probes. *Nucleic Acids Res.* **2002**, *30* (21), 122e–1122.
- (6) Cardullo, R. A.; Agrawal, S.; Flores, C.; Zamecnik, P. C.; Wolf, D. E. Detection of Nucleic Acid Hybridization by Nonradiative Fluorescence Resonance Energy Transfer. *Proc. Natl. Acad. Sci. USA* **1988**, *85* (23), 8790–8794.
- (7) Johansson, M. K. Choosing Reporter-Quencher Pairs for Efficient Quenching through Formation of Intramolecular Dimers. *Methods Mol. Biol.* **2006**, *335*, 17–29.
- (8) Tyagi, S.; Bratu, D. P.; Kramer, F. R. Multicolor Molecular Beacons for Allele Discrimination. *Nat. Biotechnol.* **1998**, *16* (1), 49–53.

- (9) Moustafa, M. E.; Hudson, R. H. E. An Azo-Based PNA Monomer: Synthesis and Spectroscopic Study. *Nucleoside Nucleotide Nucleic Acids* **2011**, *30* (9), 740–751.
- (10) Hudson, R. H. E.; Moustafa, M. E.; Boyle, P. D. (E)-Tert-Butyl 2-(5-{[4-(Dimethylamino) Phenyl]Diazenyl}-2,6-Dioxo-1H-Pyrimidin-3-Yl)Acetate Dichloromethane Monosolvate. *Acta. Crystallogr. E* **2014**, *70* (5), 556–557.
- (11) Hudson, R. H. E.; Dambeniaks, A. K.; Moszynski, J. M. New Fluorescent Nucleobases Derived from 5-Alkynylpyrimidines. *Proc. Of SPIE* **2005**, *5969*, 59690J1–J10
- (12) Hudson, R. H. E.; Dambeniaks, A. K.; Viirre, R. D. Fluorescent 7-Deazapurine Derivatives from 5-Iodocytosine via a Tandem Cross-Coupling-Annulation Reaction with Terminal Alkynes. *Synlett* **2004**, *2004* (13), 2400–2402.
- (13) Fielding, L. Determination of Association Constants (K<sub>a</sub>) from Solution NMR Data. *Tetrahedron* **2000**, *56* (34), 6151–6170.
- (14) Thordarson, P. Determining Association Constants from Titration Experiments in Supramolecular Chemistry. *Chem. Soc. Rev.* **2011**, *40* (3), 1305–1323.
- (15) Hawkins, M. E. Fluorescent Pteridine Nucleosides: A Window on DNA Interactions. *Cell Biochem. Biophys.* **2001**, *34* (2), 257–281.
- (16) Hawkins, M. E. Chapter 10 Fluorescent Pteridine Probes for Nucleic Acid Analysis. *Methods Enzymol.* **2008**, *450*, 201–231.
- (17) Cook, R. M.; Lyttle, M.; Dick, D. Synthesis and Methods for Dark Quencher Probes for Donor-Acceptor Energy Transfer. EP2316974A1, November 15, 2001.
- (18) Chevalier, A.; Renard, P. Y.; Romieu, A. Azo-Based Fluorogenic Probes for Biosensing and Bioimaging: Recent Advances and Upcoming Challenges. *Chem. Asian J.* **2017**, *12* (16), 2008–2028.

# Chapter 4

## 4. The synthesis and Photochemical Study of Nucleoside Quencher

### 4.1. Introduction

Modified nucleosides have garnered considerable interest in various fields of study, including biochemistry, biotechnology, and medicinal chemistry.<sup>1-5</sup> Nucleosides are fundamental building blocks of nucleic acids, and their modifications play a vital role in the regulation of cellular processes, gene expression, and disease development. Additionally, modified nucleosides have significant potential in diagnostics and therapeutics due to their unique properties, such as fluorescence, enzymatic stability, and base-pairing selectivity.

Fluorescent nucleosides, which exhibit fluorescence nucleobases, have been extensively studied due to their ability to act as powerful tools in molecular biology, imaging, and diagnostics.<sup>6-8</sup> Additionally, there is increasing interest in nucleosides with fluorescence-quenching abilities, which can be used as molecular sensors and imaging probes.<sup>9-12</sup> While several nucleosides with fluorescent nucleobases have been identified, only a few nucleobases with fluorescence-quenching abilities have been reported. These nucleosides are usually modified by labeling either the sugar or nucleobase to develop quenching properties. Alternatively, some studies<sup>13,14</sup> have explored the direct modification of the nucleobase within the nucleoside. This approach involves synthesizing modified nucleobases with quenching capabilities and then using these modified nucleobases to produce nucleosides. However, this method has several challenges, including low overall yield and the undesired formation of  $\alpha$  anomers during the glycosylation step.

To address these issues, this study proposes a novel approach that starts with a nucleoside and introduces a modified nucleobase with quenching capabilities. Specifically, we focus on the use of 5-(4-(*N,N*-dimethylamino)phenylazo-yl)uracil (DMPAU) as the modified nucleobase quencher. DMPAU has shown potential for quenching capability with fluorophores and its ability to form hydrogen bonds with complementary nucleobases.

The present study investigated the synthesis of 5-DMPA-2-deoxyuridine (DMPAdU) and its potential as a fluorescence quencher. We overcame the challenges associated with producing DMPAdU by developing a novel synthetic approach that eliminates the glycosylation step, which is the primary cause of the anomeric formation and low yield in previous studies. We also address the issues related to the acidic-labile glycosidic bond and the high polarity of nucleotide.

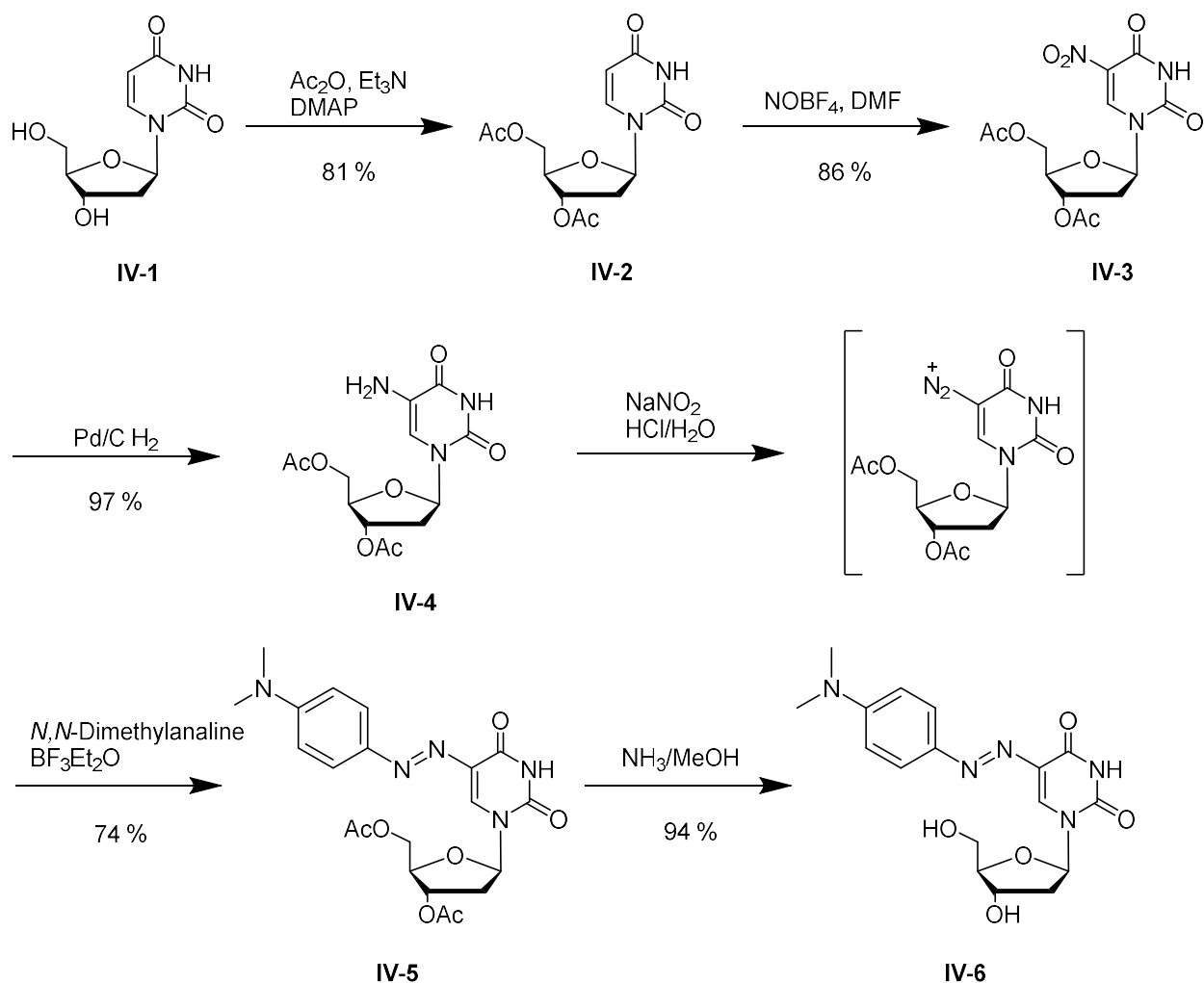
Overall, this study presents a new method for developing a nucleoside quencher that contributes to hybridization and fluorescence switching via FRET. This is promising implications for the stem-modified DNA molecular beacon (MB), which encompasses a fluorescent nucleobase and a nucleobase quencher in the stem region.

## 4.2. Result and Discussion

### 4.2.1. Synthesis of 5-DMPA-2'-deoxyuridine

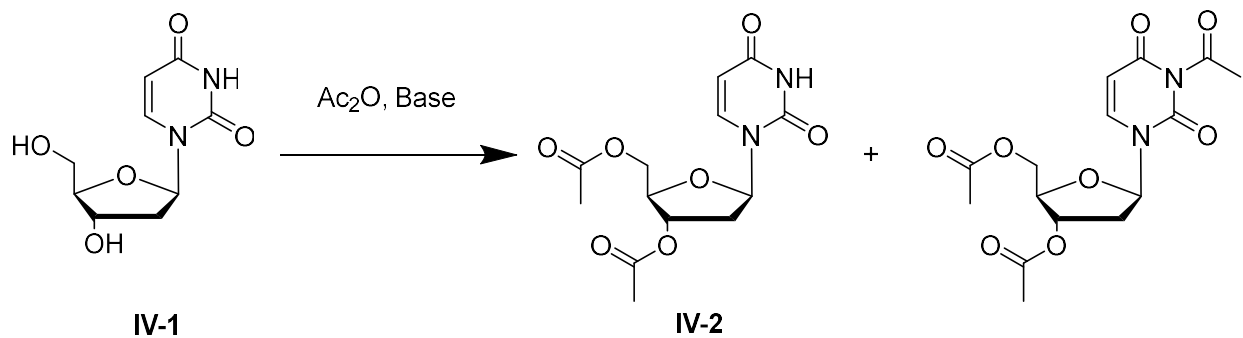
Overall chemistry for the synthesis of 5-DMPA-2'-deoxyuridine was similar to DMPAU PNA analog synthesis. (**Scheme 4-1**) However, 5-DMPA-2'-deoxyuridine has 2'-deoxyribose sugar that has many polar groups and labile bonds that could pose new challenges in the synthesis. As mentioned above, the research focus of this project is finding the synthesis route without  $\alpha$ -nucleoside formation. Thus, the synthesis started with  $\beta$ -2-deoxyuridine (**IV-1**).

In the first step, the 3' OH and 5' OH groups were acylated to avoid unwanted reactions during subsequent nucleobase modification. The OH groups were transformed by acylation with acetic anhydride in the presence of a base. Using acetic anhydride with pyridine has been a common method for the acylation of a nucleoside<sup>15-18</sup>. However, when this method was applied to 2-deoxyuridine, tri-acylation (3' OH, 5' OH and N3 on uracil) was observed (**Scheme 4-2**). The acylation of N3 is irreversible, so it is a loss of starting material. The use of extra acetic anhydride (4 eq.) and prolonged reaction time were presumed to be the cause of tri-acylation. The use of four equivalents of acetic anhydride to acylate two OH groups may serve two purposes: improving the reaction kinetics by using excess reactant and compensating for the amount of acetic anhydride that reacts with water present in the solvent. However, this extra amount of acetic anhydride gives a chance for tri-acylation to occur. Moreover, pyridine acted as



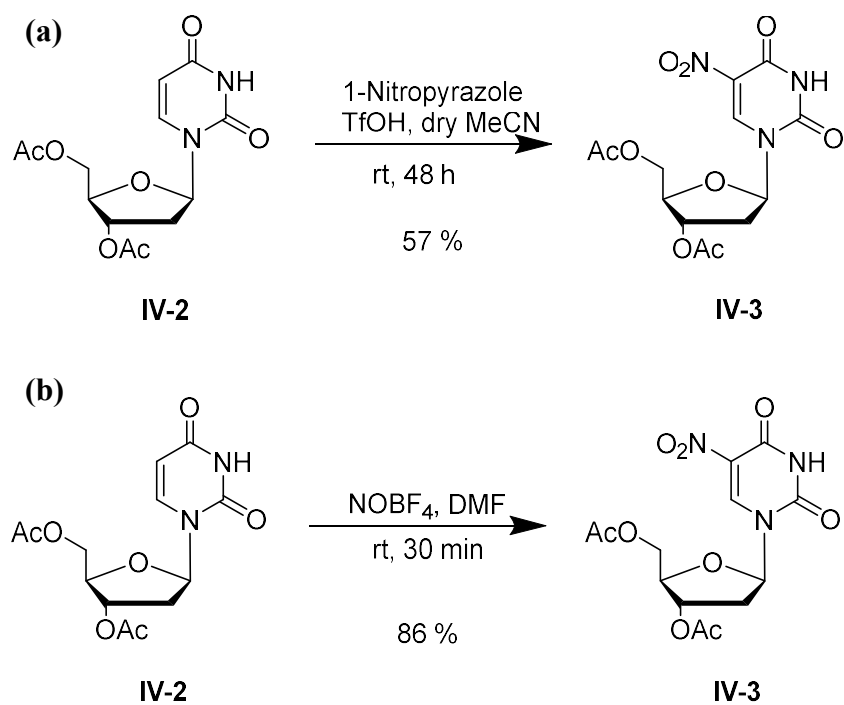
**Scheme 4-1. Optimized synthetic pathway for 5-DMPA-2'-deoxyuridine (IV-6).**

the base, the catalyst and as the solvent in this reaction condition. A reaction condition with a stoichiometric amount of base and a different solvent system was required to avoid tri-acylation formation. 4-dimethylaminopyridine (DMAP) was selected as the catalyst for this reaction since the catalytic efficiency of DMAP in acylation is approximately 10,000 times better than pyridine.<sup>19</sup> In addition, DMAP catalyst selectively induces esterification with 3' and 5' alcohols instead of amide formation with N3 of the uracil base due to steric hindrance of *N*-substituted 4-dimethylaminopyridium salt intermediate.



**Scheme 4-2. Acylation of 2'-deoxyuridine with acetic anhydride.**

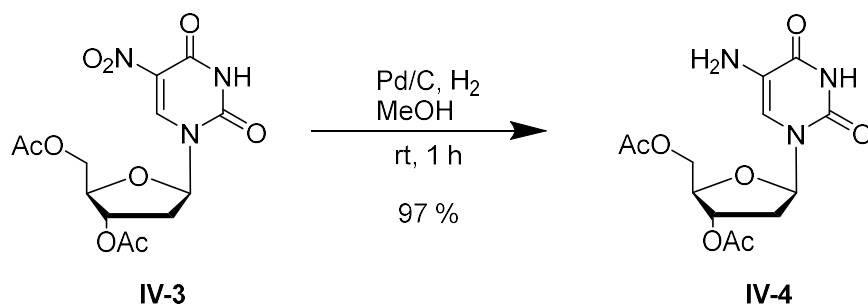
Two different methods were studied for the nitration of the C5 position of **IV-2**. The first method was nitration with 1-nitropyrazole as a nitrating reagent (**Scheme 4-3a**).<sup>20</sup> 1-Nitropyrazole was prepared by the reaction of 1H-pyrazole with fuming nitric acid. With prepared 1-nitropyrazole, **IV-2** was nitrated with the addition of trifluoromethanesulfonic acid (TfOH). This method was economical; however, it has a risk of handling a superacid TfOH.



**Scheme 4-3. Nitration of IV-2; (a) the use of 1-nitropyrazole; (b) the use of NOBF<sub>4</sub>.**

Furthermore, this method is more time-consuming due to the preparation of 1-nitropyrazole and the long nitration reaction time (48 hours). The second method was using nitrosonium tetrafluoroborate (NOBF<sub>4</sub>) (**Scheme 4-3b**).<sup>21,22</sup> The advantages of this method are the short reaction time (30 minutes) and easy work-up. It also gave a higher yield (86%) compared to the nitration with 1-nitropyrazole (57%). The only drawback is the use of expensive chemicals in excess equivalent (5 equivalents). This could be an issue for scale-up reactions.

Subsequently, the 5-amino compound, **IV-4**, was synthesized by hydrogenation using Pd/C catalyst that reduced the nitro group of **IV-3** to an amino group.<sup>23</sup> (**Scheme 4-4**) The experimental procedure of this step was almost identical to the production of *tert*-butyl 2-(5-aminouracil-1-yl)acetate, **III-3**, in Chapter 3. However, the reaction time was increased from 2 hours to 4 hours till the completion of hydrogenation was observed. In addition, the reaction gave almost theoretical yield without any side-product formation or decomposition.

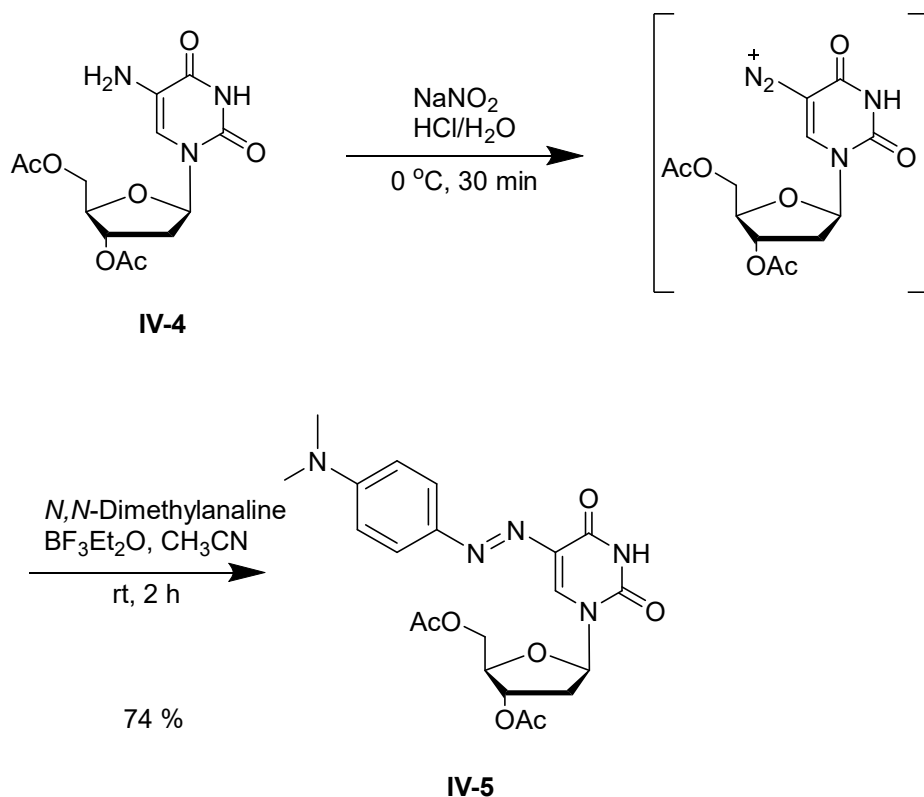


**Scheme 4-4. Hydrogenation of IV-3 with Pd/C catalyst.**

The synthesis of **IV-5** is two step reactions; a diazotization reaction with sodium nitrite (NaNO<sub>2</sub>) under acidic conditions and an azo coupling with *N,N*-dimethylaniline (**Scheme 4-5**). As mentioned in Chapter 3, a sufficient proton source is required for nitrosonium ion (NO<sup>+</sup>) formation from NaNO<sub>2</sub> and the acid catalytic conditions during diazotization. However, there is an *N*-glycosidic bond between ribose sugar and nucleobase which is acid labile. *N*-glycosidic bond cleavage happened with the protonation of nucleobase. Since the uracil nucleobase has a much lower proton affinity (by ~70–80 kJ mol<sup>-1</sup>) than the adenine, cytosine and guanine nucleobases, uracil is far less likely to be protonated than the other nucleobases. However,



protonated uracil still undergoes facile N-glycosidic bond cleavage.<sup>24</sup> In addition, the nature of the substituent at positions 2' and 3' in the carbohydrate moiety of the nucleoside affect the stability of the glycosidic bond. Ribonucleosides are 100-1000 times more stable toward hydrolysis than the corresponding deoxynucleosides.<sup>25</sup> **IV-4** has acyl-protecting OH groups. This can affect the stability of the N-glycosidic bond and acetyl protecting groups on 3' OH and 5' OH.



**Scheme 4-5. Diazotization of IV-4 and azo coupling.**

For these reasons, a stability test of **IV-4** under acidic conditions was performed before the diazotization. (**Table 4-1**) In each trial, 5 mg of **IV-4** was dissolved in 2 mL of HCl solution with different pH at 0 °C. The solutions were kept at 0 °C with continuous stirring, and the change was monitored by TLC analysis. A trace of the decomposed compound peak was monitored on Trial 1 (pH 0.5) and trial 2 (pH 1). In contrast, **IV-4** was stable above pH 1.5 over 1 hour when the diazotization step is done in 30 minutes.

**Table 4-1. Stability of IV-4 under acidic conditions.**

Trial	pH <sup>a</sup>	Time		
		5 min	30 min	1 hour
1	0.5	stable	evidence of decomposition	.
2	1.0	stable	stable	evidence of decomposition
3	1.5	stable	stable	stable
4	2.0	stable	stable	stable

<sup>a</sup> pH of HCl aqueous solution.

**Table 4-2 Optimization of diazotization of IV-4.**

Trial	pH <sup>a</sup>	Volume <sup>b</sup>	Equivalent of NaNO <sub>2</sub>	Result
1	1.0	10 mL	2 eq	reaction completed, but a decomposition peak was observed after lyophilization
2	1.5	10 mL	1 eq	reaction incomplete
3	1.5	10 mL	2 eq	reaction completed
4	1.5	10 mL	4 eq	reaction incomplete
5	1.5	40 mL	4 eq	reaction complete
6	2.0	10 mL	2 eq	reaction incomplete

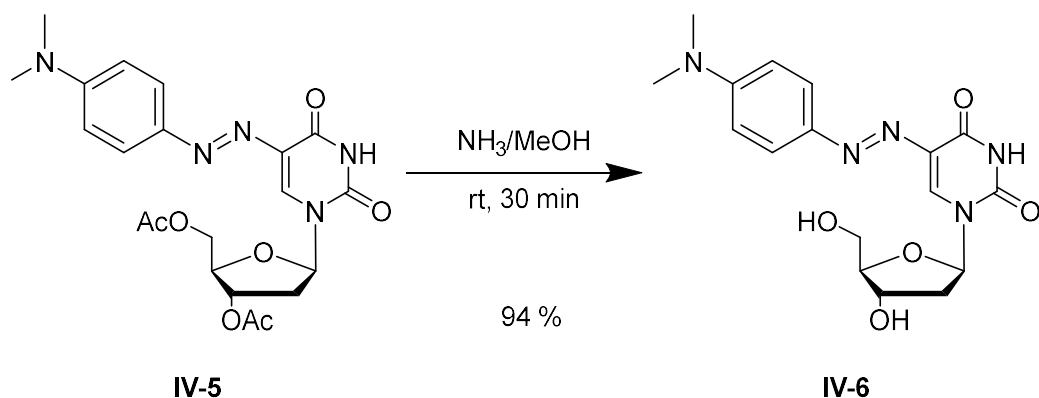
<sup>a</sup> pH of HCl aq solution; <sup>b</sup> volume of HCl aqueous solution.

Following the optimization study of the diazotization condition (**Table 4-2**), pH 1.5 was identified optimal pH. Moreover, the addition of 2 equivalents of NaNO<sub>2</sub> gave the best results for diazotization. The reaction was incomplete with 1 equivalent of NaNO<sub>2</sub> due to instability of

nitrosonium ion. In contrast, too much  $\text{NaNO}_2$  causes a pH increase in the solution which detrimentally affected the acid-catalyzed reaction. pH change can be resisted by increasing the volume of HCl solution used; however, the increase of solvent volume would slow the reaction due to the dilution effect, and also increase the time required for lyophilization after diazotization.

To remove the acetyl protecting group on the sugar, hydrolysis was done under basic condition instead of acid condition because of the acid-sensitive glycosyl bond between sugar and nucleobase. Many bases such as  $\text{NaOMe}$ <sup>26-28</sup>,  $\text{NaOH}$ <sup>29,30</sup>,  $\text{K}_2\text{CO}_3$ <sup>31-33</sup>, triethylamine<sup>34,35</sup> and  $\text{NH}_3$ <sup>36-40</sup> have been used as reagents. Among these bases, ammonia ( $\text{NH}_3$ ) was selected for deacylation. Since ammonia is a weak base, it won't react or change other functionality of the product. Moreover, the reaction using 7M  $\text{NH}_3$  in MeOH is a change functional group from ester to amide, so it gives the acetamide as a byproduct when the hydrolysis method gives acetic acid as a by-product. Acetamide can be removed easily from water-soluble nucleosides with free OH groups by extraction. Timothy Martin-Chan, a former group member, tried the deprotection of **IV-5** in different conditions such as  $\text{K}_2\text{CO}_3/\text{MeOH}$  and  $\text{NH}_3/\text{H}_2\text{O}$ ; however, the reaction was incomplete caused decomposition. However, 7M  $\text{NH}_3$  in MeOH made a complete reaction in 4 hours without any formation of side-product. (**Scheme 4-6**)

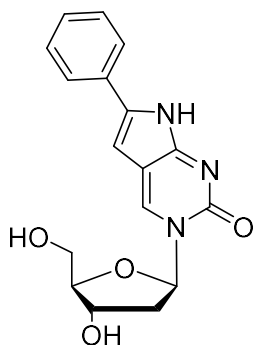
5-DMPA-2'-deoxyuridine (**IV-6**) was synthesized from 2'-deoxyuridine in 6 steps of reactions with 47% of the overall yield.



**Scheme 4-6. Removal of acetate-protecting groups.**

#### 4.2.2. Photophysical Properties

From the previous chapter, DMPAU nucleobase and PhpC nucleobase were determined as an ideal pair of fluorophore and quencher because the absorption spectrum of the DMPAU overlaps with the emission spectrum of the PhpC avoiding significant overlap with the excitation spectrum. For the quenching study of DMPAdU, 6-phenylpyrrolo-2'-deoxycytidine (PhpdC) was prepared as a fluorophore (**Figure 4-1**).



$$\lambda_{\text{ex}} = 364 \text{ nm}$$

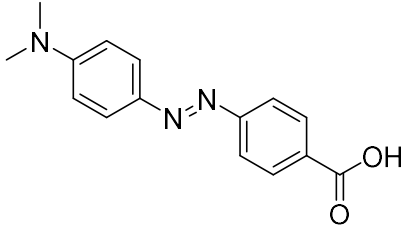
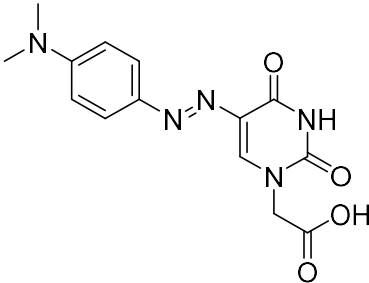
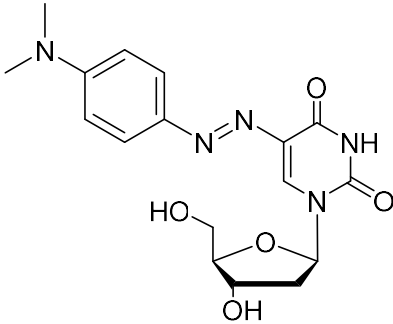
$$\lambda_{\text{em}} = 446 \text{ nm}$$

$$\Phi_{\text{EtOH}} = 0.40^{41}$$

**Figure 4-1. Photophysical properties of the 6-phenylpyrrolo-2'-deoxycytidine (PhpdC) in EtOH.**

The photophysical properties of the DMPAdU and PhpdC were determined in EtOH (**Table 4-3**). The maximum excitation wavelength ( $\lambda_{\text{ex}}$ ) was found at 364 nm and maximum emission wavelength ( $\lambda_{\text{em}}$ ) was found at 446 nm which are identical to the reported values.<sup>41</sup> The DMPAdU exhibits an absorption maximum at 462 nm which is similar to DABCYL acid and DMPAU acetic acid. However, the molar extinction coefficient of DMPAdU is smaller than DABCYL acid.

**Table 4-3. Photophysical properties of quenchers.**

	$\lambda_{ab}$ (nm)	$\epsilon$ (M <sup>-1</sup> cm <sup>-1</sup> )
 DABCYL acid <sup>a</sup>	464	27,400
 DMPAU acetic acid ( <b>III-6</b> ) <sup>a</sup>	467 <sup>†</sup>	20,900 <sup>†</sup>
 DMPAdU ( <b>IV-6</b> ) <sup>a</sup>	462	14,700

<sup>a</sup> Measured in 0.1% Et<sub>3</sub>N aqueous solution.

Based on photophysical study, DMPAdU and PhpdC were predicted as a good quencher-fluorophore pair because the absorption spectrum of the DMPAdU overlaps with most of the emission spectrum of the PhpC without the direction absorption that caused by a significant overlap with the excitation spectrum. (**Figure 4-2**).

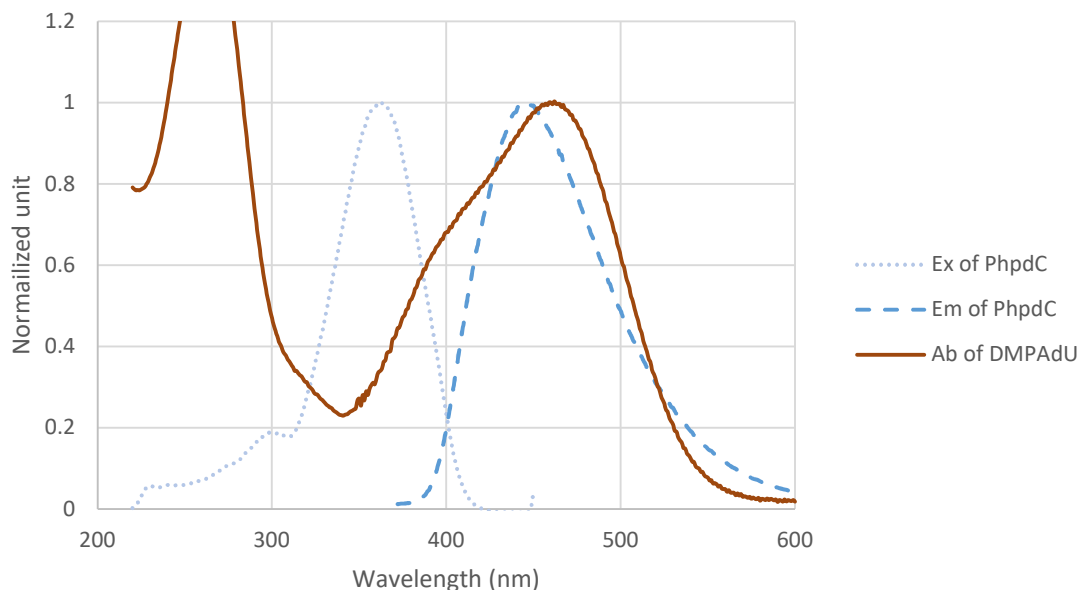


**Figure 4-2. Normalized absorption spectra of DMPAdU with normalized excitation and emission spectra of PhpdC in EtOH.**

A quenching study was performed in which a 1  $\mu\text{M}$  solution of the fluorophore PhpdC in EtOH was mixed with different concentration (0 – 26  $\mu\text{M}$ ) of the DMPAdU. The fluorescence emission from the PhpdC was decreased with increasing concentrations of DMPAdU quencher (**Figure 4-3a**). From this data, a Stern-Volmer plot was constructed, and the Stern-Volmer quenching constant,  $K_{sv}$ , was determined from the plot (**Figure 4-3b**). The  $K_{sv}$  for the quenching of PhpdC with DMPAdU was found to be 17,900  $\text{M}^{-1}$ . In addition,  $K_{sv}^{-1}$ , the concentration of the quencher at which half of the intensity of the fluorophore is quenched, was calculated to be  $5.62 \times 10^{-5}$  M. Based on  $K_{sv}$  values for quenching PhpdC fluorophores in the previous chapter, DMPAdU is shown similar quenching ability as DMPAdU PNA analogs. However, it is less effective than

DABCYL acid and DABCYL ethyl ester due to smaller molar coefficient. The reason why DMPAdU derivatives has smaller molar extinction coefficients than that of DABCYL acid may be a change in the conjugate system due to structural modification. DABCYL acid has an amine group at one end and a carboxylic acid group at the other end of the compound.

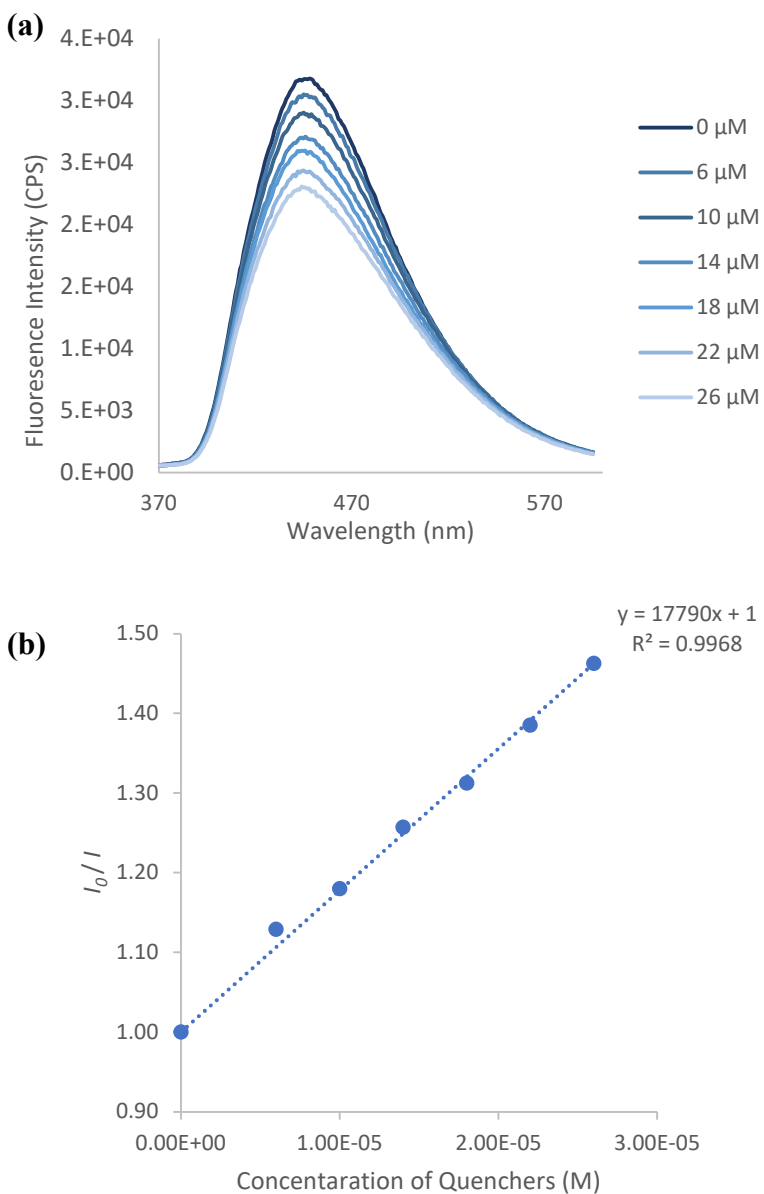


**Figure 4-3. (a) Quenching study of DMPAdU with PhpdC in EtOH; (b) Stern-Volmer plot.**

In the conjugated system of DABCYL acid, the delocalized electron moves from the electron-donating amine group to the electron-withdrawing carboxylic acid group. When DMPAU nucleobase was modified from DABCYL acid, the amine group remained, but the carboxylic acid group was removed. In the addition, the phenyl ring with the carboxylic acid group is replaced with the uracil pyrimidine ring in which nitrogen in the N1 position can act as another

electron donor. This structural modification changes the conjugated system, and this would change the molar extinction coefficients which relates to quenching ability.

### 4.3. Conclusion

To conclude, the present study discloses a novel method starting with 2'-deoxyuridine to synthesize 5-DMPA-2'-deoxyuridine. This new synthetic pathway avoids the formation of glycosidic bond which cause the loss of overall yield from  $\alpha$  anomer formation. For capping 3', 5'-OH groups of 2'-deoxyuridine, selective acylation method with DMAP catalyst was determined to avoid acylation on N3 nitrogen. Two aromatic nitration methods were explored for nitration of uracil nucleobase. While the standard protocol for diazotization involves the use of strong acid to form  $\text{NO}^+$  ion and to provide acidic-catalyst, optimization was required as the glycosidic bond in nucleoside is acid sensitive and breaks in acidic environment.

In order to determine a feasible FRET pair formation with a fluorescent nucleobase in stem region of DNA molecular beacon, quenching study were performed with 6-phenylpyrrolo-2'-deoxycytidine (PhpdC).  $K_{sv}$  for the quenching of PhpdC with DMPAdU was calculated to be  $17,900 \text{ M}^{-1}$ .

### 4.4. Future work

Major advantages of DMPAU are stable under both mildly acidic and base conditions, and it is not a strong nucleophile nor a strong electrophile. The neutral aspect of DMPAU would be the most advantageous for further synthesis requiring further modification.

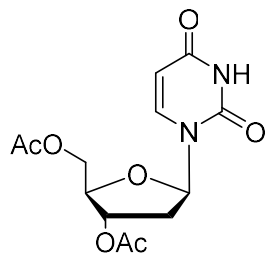
Starting with 5-DMPA-2'-deoxyuridine, both phosphoramidite DNA monomer for solid phase synthesis and triphosphate monomer for enzymatic synthesis can be prepared for oligomerization. By oligomerization with the DMPAdU building block, proposed DNA MB that has nucleobase fluorophore and quencher in stem region can be synthesized and its photophysical properties can be investigated.



Furthermore, the synthesis of 5-DMPAuridine (RNA) can be investigated by applying the reported synthetic pathway since 5-DMPAuridine can be a starting molecule for further sugar modifications such as morpholino and LNA.

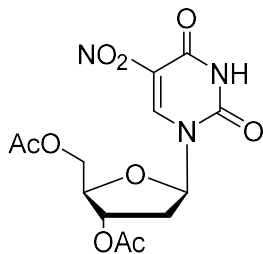
## 4.5. Experimental

### 2'-Deoxyuridine-3',5'-*O*-diacetate (IV-2)



To a suspension of 2'-deoxyuridine, **IV-1**, (2.28 g, 10.0 mmol) in dry CH<sub>3</sub>CN (50 mL), 2.2 equivalents of acetic anhydride (2.10 mL) were added in the presence of triethylamine (5.56 mL, 40 mmol) and a catalytic amount of 4-dimethylaminopyridine (0.12 g, 1 mmol). After 30 min stirring, the reaction solution was quenched by the addition of 1 mL of methanol and stirred for 10 min. Then, the solvent was evaporated under reduced pressure. The resulting yellowish oil residue was partitioned between 250 mL of dichloromethane and 150 mL of water. The collected organic layer was washed with water (4 x 100 mL), dried over Na<sub>2</sub>SO<sub>4</sub>, filtered and concentrated in vacuo. The crude product was purified by column chromatography with Hex:EtOAc = 3:7 to yield white powder **IV-2** (2.52g 81 %): <sup>1</sup>H NMR (600 MHz, DMSO-*d*<sub>6</sub>) δ 11.33 (s, 1H), 7.61 (d, *J* = 8.1 Hz, 1H), 6.11 (dd, *J* = 8.2, 6.1 Hz, 1H), 5.66 (d, *J* = 8.1 Hz, 1H), 5.14 (dd, *J* = 6.3, 3.1 Hz, 1H), 4.23 – 4.09 (m, 3H), 2.43 (s, 1H), 2.38 (ddd, *J* = 14.7, 8.2, 6.8 Hz, 1H), 2.27 (ddd, *J* = 14.4, 6.2, 2.6 Hz, 1H), 2.02 (s, 3H), 2.01 (s, 3H). <sup>13</sup>C NMR (101 MHz, Chloroform-*d*) δ 170.35, 170.18, 163.14, 150.29, 138.78, 138.34, 102.93, 85.27, 82.30, 74.03, 63.76, 37.77, 20.83, 20.74. HRMS (ESI/Q-TOF) *m/z*: [M+Na]<sup>+</sup> Calculated for C<sub>13</sub>H<sub>16</sub>N<sub>2</sub>O<sub>7</sub>Na 335.0855; Found 335.0875.

### 5-Nitro-2'-deoxyuridine-3',5'-O-diacetate (IV-3)



#### Method 1 : Nitration with 1-nitropyrazole

A solution of 1H-pyrazole (1.00 g, 14.5 mmol) in glacial acetic acid (7 mL) was cooled to 0 °C with continuous stirring. Fuming nitric acid (4.5 mL) was added dropwise to the 1H-pyrazole solution. Acetic anhydride (10.5 mL, 110 mmol) was added dropwise slowly to the flask, and the mixture was stirred for 2.5 h at the ambient temperature. The reaction was quenched with the addition of ice water (5 mL), and potassium carbonate was added until the pH of the solution increased to pH 5. The precipitate was isolated by vacuum filtration and washed with water. After air drying, a white solid was yielded (1.08g, 57%): <sup>1</sup>H NMR (400 MHz, DMSO-d<sub>6</sub>) δ: 8.81 (d, 1H), 7.88 (d, 1H), 6.71 (t, 1H).

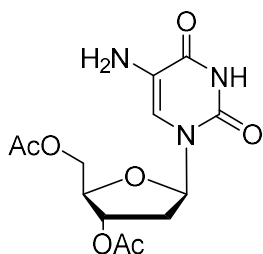
The acetylated nucleoside, **IV-2** (1.00 g, 3.20 mmol) and 1-nitropyrazole (0.50 g) was dissolved in dry acetonitrile. Under a nitrogen atmosphere, trifluoromethanesulfonic acid, TfOH, (0.90 mL, 10.1 mmol) was added to the solution dropwise. After 48 hours of vigorous stirring, the solvent was evaporated under reduced pressure. The crude was purified by column chromatography with 1% MeOH in DCM. a yellow oil product was yielded (0.86 g, 2.41 mmol, 75.0%).

#### Method 2 : Nitration with nitrosonium tetrafluoroborate

The acetylated nucleoside, **IV-2** (0.312 g, 1.00 mmol) was dissolved in 7 mL of DMF and treated with nitrosonium tetrafluoroborate (0.586 g, 5.00 mmol) for 30 min. The reaction was terminated by the addition of cold water (1 mL). The reaction mixture was diluted with ethyl acetate (45 mL). The organic layer was washed with ice-cold water (50 mL x 5 times). The organic layer was separated and dried over sodium sulfate. The crude product was purified on a silica gel column using ethyl acetate/*n*-hexanes (1:1 v/v). Fractions containing the product were

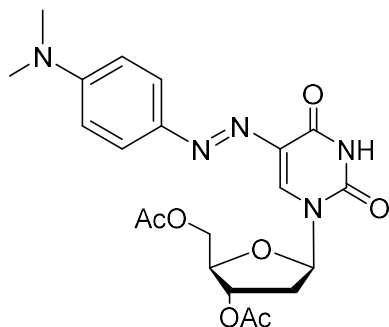
combined and evaporated to give 0.307 g (0.861 mmol, 86%):  $^1\text{H}$  NMR (400 MHz, Chloroform-*d*)  $\delta$  9.84 (s, 1H), 9.07 (s, 1H), 6.24 (t,  $J = 6.6$  Hz, 1H), 5.25 (d,  $J = 6.5$  Hz, 1H), 4.46 – 4.27 (m, 3H), 2.69 (ddd,  $J = 14.7, 5.9, 2.4$  Hz, 1H), 2.37 (dt,  $J = 14.3, 7.0$  Hz, 1H), 2.14 (s, 3H), 2.11 (s, 3H).  $^{13}\text{C}$  NMR (101 MHz, Chloroform-*d*)  $\delta$  170.69, 170.47, 154.69, 148.35, 144.37, 125.74, 87.09, 83.37, 73.89, 63.46, 38.61, 20.77, 20.53. HRMS (ESI/Q-TOF)  $m/z$ :  $[\text{M}+\text{Na}]^+$  Calculated for  $\text{C}_{13}\text{H}_{15}\text{N}_3\text{O}_9\text{Na}$  380.0706; Found 380.0718.

#### 5-Amino-2'-deoxyuridine-3',5'-*O*-diacetate (IV-4)



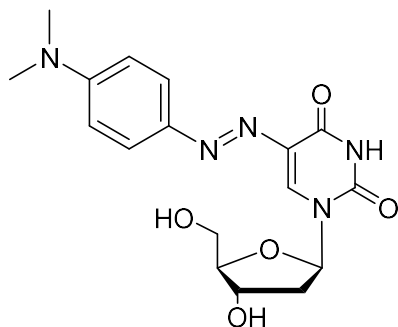
5-Nitro-2'-deoxyuridine-3',5'-*O*-diacetate, **IV-3**, (0.815 g, 2.28 mmol) was dissolved in MeOH (100 mL). The reaction flask was covered with aluminum foil and flushed with nitrogen gas. After a catalytic amount (0.158 g) of 10 % Pd/C was added, the flask was charged with hydrogen balloon with vigorously stirring at room temperature for 4 hours. The reaction solution was filtered through Celite. The solid residue on Celite was washed with methanol, and the filtrate was evaporated under vacuum. A grey powder product was yielded. (0.721 g, 97 %):  $^1\text{H}$  NMR (400 MHz, DMSO-*d*<sub>6</sub>)  $\delta$  11.35 (s, 1H), 6.76 (s, 1H), 6.16 (dd,  $J = 8.6, 5.8$  Hz, 1H), 5.12 (dd,  $J = 5.7, 2.8$  Hz, 1H), 4.23 – 4.03 (m, 5H), 2.30 – 2.16 (m, 2H), 2.02 (s, 3H), 2.01 (s, 3H).  $^{13}\text{C}$  NMR (101 MHz, Chloroform-*d*)  $\delta$  170.46, 170.42, 160.55, 148.94, 122.76, 116.15, 84.75, 81.89, 74.05, 63.85, 36.93, 20.87, 20.85. HRMS (ESI/Q-TOF)  $m/z$ :  $[\text{M}+\text{H}]^+$  Calculated for  $\text{C}_{13}\text{H}_{18}\text{N}_3\text{O}_7$  328.1145; Found 328.1150.

**5-((4-(*N,N*-dimethylamino)phenyl)diazenyl)-2'-deoxyuridine-3',5'-*O*-diacetate (IV-5)**



The solution of 5-amino-2'-deoxyuridine-3',5'-*O*-diacetate (**IV-4**) (0.10 g, 0.31 mmol) in pH 1.5 HCl (25 mL) was vigorously stirred for 30 minutes at 0 °C. A solution of sodium nitrite (0.042 g, 0.61 mmol) in water (5 mL) was slowly added dropwise to the solution at 0 °C with vigorous stirring in the dark for 2 hours. The solvent was removed by freeze-dry method, overnight. The intermediate diazonium salt (0.113 g) was collected. A suspension of the diazonium intermediate in anhydrous acetonitrile (20 mL) was purged with nitrogen gas for 10 min, and borontrifluoride etherate (40  $\mu$ L, 0.31 mmol) and *N,N*-dimethylaniline (40  $\mu$ L, 0.31 mmol) were added to the mixture, then stirred for 4 hours. The solvent was evaporated under reduced pressure. A red crude oil was purified via flash chromatography using ethyl acetate/*n*-hexane as the eluting solvent (7:3 v/v) to yield an orange solid product (0.104 g, 0.23 mmol, 74 %):  $^1\text{H}$  NMR (400 MHz, Chloroform-*d*)  $\delta$  8.86 (s, 1H), 8.08 (s, 1H), 7.80 (d,  $J$  = 9.1 Hz, 2H), 6.72 (d,  $J$  = 9.2 Hz, 2H), 6.42 (dd,  $J$  = 8.6, 5.6 Hz, 1H), 5.30 (dt,  $J$  = 6.4, 1.9 Hz, 1H), 4.47 – 4.33 (m, 3H), 3.10 (s, 6H), 2.61 (ddd,  $J$  = 14.2, 6.2, 1.6 Hz, 1H), 2.29 (ddd,  $J$  = 14.6, 8.5, 6.4 Hz, 1H), 2.15 (s, 4H), 2.05 (s, 3H).  $^{13}\text{C}$  NMR (101 MHz, Chloroform-*d*)  $\delta$  170.44, 170.34, 160.27, 152.74, 149.39, 143.49, 130.56, 126.44, 125.51, 111.39, 85.98, 82.85, 74.77, 64.18, 40.26, 38.30, 21.03, 20.94. HRMS (ESI/Q-TOF)  $m/z$ :  $[\text{M}+\text{Na}]^+$  Calculated for  $\text{C}_{21}\text{H}_{25}\text{N}_5\text{O}_7\text{Na}$  482.1651; Found 482.1658.

### 5-((4-(*N,N*-dimethylamino)phenyl)diazenyl)-2'-deoxyuridine (IV-6)



Ammonia (7 N) in MeOH (4 mL) was added to a solution of **IV-5** (0.100 mg, 0.22 mmol) in MeOH (4 mL) at 0 °C. the solution was stirred for 6 h at room temperature. The solvent was then removed under a vacuum. The remaining acetamide was removed by heating in vacuum at 100 °C for 2 h to yield a red solid product (0.080 g, 98%): <sup>1</sup>H NMR (400 MHz, Methanol-*d*<sub>4</sub>) δ 8.51 (s, 1H), 7.82 (d, *J* = 9.1 Hz, 2H), 6.80 (d, *J* = 9.1 Hz, 2H), 6.35 (m, 1H), 4.45 (m, 1H), 4.00 – 3.97 (m, 1H), 3.84 – 3.77 (m, 2H), 3.09 (s, 6H), 2.40 – 2.33 (m, 2H). <sup>13</sup>C NMR (101 MHz, Methanol-*d*<sub>4</sub>) δ 163.39, 154.25, 144.99, 131.09, 129.97, 128.78, 126.26, 112.55, 89.13, 87.32, 72.02, 62.64, 41.72, 40.39. HRMS (ESI/Q-TOF) *m/z*: [M+Na]<sup>+</sup> Calculated for C<sub>17</sub>H<sub>21</sub>N<sub>5</sub>O<sub>5</sub>Na 398.1440; Found 398.1436.

## 4.6. References

- (1) Pushpendra, S.; Arvind, P.; Anil, B. Nucleic Acids as Therapeutics. *From Nucleic Acids Sequences to Molecular Medicine* **2012**, 19–45.
- (2) Lundin, K. E.; Gissberg, O.; Smith, C. I. E. Oligonucleotide Therapies: The Past and the Present. *Hum. Gene. Ther.* **2015**, 26 (8), 475.
- (3) Bennett, C. F.; Swayze, E. E. RNA Targeting Therapeutics: Molecular Mechanisms of Antisense Oligonucleotides as a Therapeutic Platform. *Annu. Rev. Pharmacol. Toxicol.* **2010**, 50, 259–293.
- (4) Chan, J. H. P.; Lim, S.; Wong, W. S. F. Antisense Oligonucleotides: from Design to Therapeutic Application. *Clin. Exp. Pharmacol. Physiol.* **2006**, 33 (5–6), 533–540.

- (5) Sharma, V. K.; Rungta, P.; Prasad, A. K. Nucleic Acid Therapeutics: Basic Concepts and Recent Developments. *RSC Adv.* **2014**, *4* (32), 16618–16631.
- (6) Wilson, J. N.; Kool, E. T. Fluorescent DNA Base Replacements: Reporters and Sensors for Biological Systems. *Org. Biomol. Chem.* **2006**, *4* (23), 4265–4274.
- (7) Xu, W.; Chan, K. M.; Kool, E. T. Fluorescent Nucleobases as Tools for Studying DNA and RNA. *Nat. Chem.* **2017**, *9* (11), 1043–1055.
- (8) Wilhelmsson, L. M.; Tor, Y. *Fluorescent Analogs of Biomolecular Building Blocks: Design and Applications*; Wiley, 2016.
- (9) Tyagi, S.; Kramer, F. R. Molecular Beacons: Probes That Fluoresce upon Hybridization. *Nat. Biotechnol.* **1996**, *14*:3 **1996**, *14* (3), 303–308.
- (10) Ortiz, E.; Estrada, G.; Lizardi, P. M. PNA Molecular Beacons for Rapid Detection of PCR Amplicons. *Mol. Cell. Probes* **1998**, *12* (4), 219–226.
- (11) Hurley, D. J.; Tor, Y. Donor/Acceptor Interactions in Systematically Modified RuII-OsII Oligonucleotides. *J. Am. Chem. Soc.* **2002**, *124* (44), 13231–13241.
- (12) Kodama, S.; Asano, S.; Moriguchi, T.; Sawai, H.; Shinozuka, K. Novel Fluorescent OligoDNA Probe Bearing a Multi-Conjugated Nucleoside with a Fluorophore and a Non-Fluorescent Intercalator as a Quencher. *Bioorg. Med. Chem. Lett.* **2006**, *16* (10), 2685–2688.
- (13) Börjesson, K.; Preus, S.; El-Sagheer, A. H.; Brown, T.; Albinsson, B.; Wilhelmsson, L. M. Nucleic Acid Base Analog FRET-Pair Facilitating Detailed Structural Measurements in Nucleic Acid Containing Systems. *J. Am. Chem. Soc.* **2009**, *131* (12), 4288–4293.
- (14) Freeman, N. S.; Moore, C. E.; Wilhelmsson, L. M.; Tor, Y. Chromophoric Nucleoside Analogues: Synthesis and Characterization of 6-Aminouracil-Based Nucleodyes. *J. Org. Chem.* **2016**, *81* (11), 4530–4539.

- (15) Kim, K. N.; Lee, J.; Kim, D. H.; Yoo, J. S.; Kwon, H. J. A New Synthetic Analogue of Thymidine, 7-(3-Bromo-Phenoxy)-Thymidine, Inhibits the Proliferation of Tumor Cells. *Bioorg. Med. Chem. Lett.* **2005**, *15* (1), 77–79.
- (16) Bdour, H. M.; Kao, J. L. F.; Taylor, J. S. Synthesis and Characterization of a [3-<sup>15</sup>N]-Labeled Cis-Syn Thymine Dimer-Containing DNA Duplex. *J. Org. Chem.* **2006**, *71* (4), 1640–1646.
- (17) Kamaike, K.; Takahashi, M.; Utsugi, K.; Tomizuka, K.; Okazaki, Y.; Tamada, Y.; Kinoshita, K.; Masuda, H.; Ishido, Y. An Efficient Method for the Synthesis of [4-<sup>15</sup>N]Cytidine, 2'-Deoxy[4-<sup>15</sup>N]Cytidine, [6-<sup>15</sup>N]Adenosine, and 2'-Deoxy [6-<sup>15</sup>N]Adenosine Derivatives. *Nucleoside Nucleotide Nucleic Acids* **2006**, *15* (1–3), 749–769.
- (18) Gorchs, O.; Hernández, M.; Garriga, L.; Pedroso, E.; Grandas, A.; Farràs, J. A New Method for the Preparation of Modified Oligonucleotides. *Org. Lett.* **2002**, *4* (11), 1827–1830.
- (19) Höfle, G.; Steglich, W.; Vorbrüggen, H. 4-Dialkylaminopyridines as Highly Active Acylation Catalysts. [New Synthetic Method (25)]. *Angew. Chem. Int. Ed. Engl.* **1978**, *17* (8), 569–583.
- (20) Olah, G. A.; Narang, S. C.; Fung, A. P. Aromatic Substitution. 47.1 Acid-Catalyzed Transfer Nitration of Aromatics with N-Nitropyrazole, a Convenient New Nitrating Agent. *J. Org. Chem.* **1981**, *46* (13), 2706–2709.
- (21) Kovaliov, M.; Weitman, M.; Major, D. T.; Fischer, B. Phenyl-Imidazolo-Cytidine Analogues: Structure-Photophysical Activity Relationship and Ability to Detect Single Dna Mismatch. *J. Org. Chem.* **2014**, *79* (15), 7051–7062.
- (22) Gong, Y.; Chen, L.; Zhang, W.; Salter, R. Transglycosylation in the Modification and Isotope Labeling of Pyrimidine Nucleosides. *Org. Lett.* **2020**, *22* (14), 5577–5581.
- (23) Gourdain, S.; Petermann, C.; Harakat, D.; Clivio, P. Highly Efficient and Facile Synthesis of 5-Azido-2'-Deoxyuridine. *Nucleoside Nucleotide Nucleic Acids* **2010**, *29* (7), 542–546.

- (24) Wu, R. R.; Rodgers, M. T. Tautomerization Lowers the Activation Barriers for N-Glycosidic Bond Cleavage of Protonated Uridine and 2'-Deoxyuridine. *Phys. Chem. Chem. Phys.* **2016**, *18* (35), 24451–24459.
- (25) Kochetkov, N. K. Nikolaï K.; Budovskii, E. I. *Organic Chemistry of Nucleic Acids*; Plenum Press, **1972**.
- (26) Asakura, J. I.; Robins, M. J. Cerium(IV)-Mediated Halogenation at C-5 of Uracil Derivatives. *J. Org. Chem.* **1990**, *55* (16), 4928–4933.
- (27) Kim, K. N.; Lee, J.; Kim, D. H.; Yoo, J. S.; Kwon, H. J. A New Synthetic Analogue of Thymidine, 7-(3-Bromo-Phenoxy)-Thymidine, Inhibits the Proliferation of Tumor Cells. *Bioorg. Med. Chem. Lett* **2005**, *15* (1), 77–79.
- (28) Abdo, M.; Zhang, Y.; Schramm, V. L.; Knapp, S. Electrophilic Aromatic Selenylation: New OPRT Inhibitors. *Org. Lett.* **2010**, *12* (13), 2982–2985.
- (29) Escuret, V.; Aucagne, V.; Joubert, N.; Durantel, D.; Rapp, K. L.; Schinazi, R. F.; Zoulim, F.; Agrofoglio, L. A. Synthesis of 5-Haloethynyl- and 5-(1,2-Dihalo)Vinyluracil Nucleosides: Antiviral Activity and Cellular Toxicity. *Bioorg. Med. Chem.* **2005**, *13* (21), 6015–6024.
- (30) Ries, A.; Kumar, R.; Lou, C.; Kosbar, T.; Vengut-Climent, E.; Jørgensen, P. T.; Morales, J. C.; Wengel, J. Synthesis and Biophysical Investigations of Oligonucleotides Containing Galactose-Modified DNA, LNA, and 2'-Amino-LNA Monomers. *J. Org. Chem.* **2016**, *81* (22), 10845–10856.
- (31) Cho, S. J.; Ghorbani-Choghamarani, A.; Saito, Y.; Hudson, R. H. E. 6-Phenylpyrrolocytidine: An Intrinsically Fluorescent, Environmentally Responsive Nucleoside Analogue. *Curr. Protoc. Nucleic Acid Chem.* **2019**, *76* (1), e75.
- (32) Peyron, C.; Benhida, R.; Bories, C.; Loiseau, P. M. Synthesis and in Vitro Antileishmanial Activity of 5-Substituted-2'-Deoxyuridine Derivatives. *Bioorg. Chem.* **2005**, *33* (6), 439–447.



- (33) Lusic, H.; Young, D. D.; Lively, M. O.; Deiters, A. Photochemical DNA Activation. *Org. Lett.* **2007**, *9* (10), 1903–1906.
- (34) Ivanov, A. v.; Simonyan, A. R.; Belanov, E. F.; Aleksandrova, L. A. Synthesis and Antiviral Activity of New 5-Substituted 2'-Deoxyuridine Derivatives. *Russ. J. Bioorganic Chem.* **2005**, *31* (6), 556–562.
- (35) Sawai, H.; Ozaki-Nakamura, A.; Mine, M.; Ozaki, H. Synthesis of New Modified DNAs by Hyperthermophilic DNA Polymerase: Substrate and Template Specificity of Functionalized Thymidine Analogues Bearing an Sp<sup>3</sup>-Hybridized Carbon at the C5  $\alpha$ -Position for Several DNA Polymerases. *Bioconjug. Chem.* **2002**, *13* (2), 309–316.
- (36) Bdour, H. M.; Kao, J. L. F.; Taylor, J. S. Synthesis and Characterization of a [3-<sup>15</sup>N]-Labeled Cis-Syn Thymine Dimer-Containing DNA Duplex. *J. Org. Chem.* **2006**, *71* (4), 1640–1646.
- (37) Mudgal, M.; Dang, T. P.; Sobczak, A. J.; Lumpuy, D. A.; Dutta, P.; Ward, S.; Ward, K.; Alahmadi, M.; Kumar, A.; Sevilla, M. D.; Wnuk, S. F.; Adhikary, A. Site of Azido Substitution in the Sugar Moiety of Azidopyrimidine Nucleosides Influences the Reactivity of Aminyl Radicals Formed by Dissociative Electron Attachment. *J. Phys. Chem. B* **2020**, *124* (50), 11357–11370.
- (38) van Daele, I.; Munier-Lehmann, H.; Froeyen, M.; Balzarini, J.; van Calenbergh, S. Rational Design of 5'-Thiourea-Substituted  $\alpha$ -Thymidine Analogues as Thymidine Monophosphate Kinase Inhibitors Capable of Inhibiting Mycobacterial Growth. *J. Med. Chem.* **2007**, *50* (22), 5281–5292.
- (39) Weng, L.; Horvat, S. M.; Schiesser, C. H.; Greenberg, M. M. Deconvoluting the Reactivity of Two Intermediates Formed from Modified Pyrimidines. *Org. Lett.* **2013**, *15* (14), 3618–3621.
- (40) Kuwahara, M.; Nagashima, J. I.; Hasegawa, M.; Tamura, T.; Kitagata, R.; Hanawa, K.; Hososhima, S. I.; Kasamatsu, T.; Ozaki, H.; Sawai, H. Systematic Characterization of 2'-Deoxynucleoside- 5'-Triphosphate Analogs as Substrates for DNA Polymerases by

Polymerase Chain Reaction and Kinetic Studies on Enzymatic Production of Modified DNA. *Nucleic Acids Res.* **2006**, *34* (19), 5383–5394.

- (41) Elmehriki, A. A. H.; Suchý, M.; Chicas, K. J.; Wojciechowski, F.; Hudson, R. H. E. Synthesis and Spectral Characterization of Environmentally Responsive Fluorescent Deoxycytidine Analogs. *Artif. DNA PNA XNA* **2014**, *5* (2), e29174.

# Chapter 5

## 5. Conclusion

Nucleic acids have been widely used in therapeutics, diagnostics and research because they are an essential component involved in the fundamental processes in biological systems. Modified oligonucleotides have been developed and will be continuously developed to overcome the limitations of natural nucleic acids. Peptide nucleic acid (PNA), which is a backbone-modified oligonucleotide, has been studied for therapeutic applications. Due to the flexible neutral backbone, PNA has high affinity and specificity to the target DNA/RNA strand. In addition, nucleobase modification has been used to engender new characteristics, such as photophysical, physicochemical and biochemical properties to oligonucleotides. Especially, the oligonucleotides with fluorophores have been very useful tools to detect the nucleic acid sequence of interest.

In this thesis, PNA/DNA monomers with modified nucleobases were synthesized to introduce new characteristics to oligonucleotides. Their photophysical and physicochemical characteristics were investigated.

In Chapter 2, the effects of inserting 5-nitrouracil nucleobase in PNA oligomers were studied. To gather experimental data of this effect on base pairing, 5-nitrouracil PNA monomers and oligomers were prepared. The Fmoc-protected 5-nitrouracil PNA monomer was synthesized for the oligomerization by Fmoc-based SPPS. PNA oligomers were designed and synthesized for PNA/DNA duplex binding, bis-PNA/DNA triplex binding and mismatch studies. In the duplex binding study, PNA oligomers with 5-nitrouracil showed a decreased binding affinity compared to the control PNA. One explanation for the destabilizing effect of 5-nitrouracil is the interaction between 5-nitrouracil and adjacent cytosine nucleobases. In the triplex binding study, 5-nitrouracil showed enhanced Hoogsteen binding with adenine compared to thymine. In the mismatch study, 5-nitrouracil showed specificity with adenine and discrimination against mismatched base pairs. Further binding studies are required with different PNA sequences to clarify the enhanced binding and destabilization depending on the sequence.

In Chapter 3, a nucleobase quencher, which can be embedded in the stem region of the molecular beacon with a fluorescent nucleobase, was studied. Its ability to form a base pair with a canonical nucleobase and to quench the fluorescence efficiently by FRET were tested. A DMPAU PNA analog which is the mimic of DABCYL was synthesized using a novel synthetic route. Four quenchers (DABCYL, DMPAU, NPhpC and NPhEC) and four fluorophores (pyrene, PhpC, acridone and NBD) were selected for the quenching study. After the characterization of their photophysical properties, quenching study was performed on each of the 16 possible pairs. Based on the spectral overlap between the fluorophore and the quencher, DMPAU was best matched with PhpC, while NPhpC best matched with pyrene. The DMPAU-PhpC pair had excellent quenching even in aqueous conditions, indicating good quenching ability of the pair at the oligomer level as well. The  $K_a$  value calculated from the NMR titration study indicates that DMPAU can form a base pair with adenine with a similar hydrogen bonding strength as thymine. Overall, the results indicate that DMPAU and NPhpC are good nucleobase quencher candidates for the newly designed molecular beacon. PNA molecular beacons with these fluorescent nucleobase/nucleobase quencher pairs can be synthesized and studied for their FRET ability.

In Chapter 4, the nucleoside quencher, 5-DMPA-2'-deoxyuridine was synthesized. The synthetic route did not include glycosidic bond formation and therefore gave a high overall yield. To avoid tri-acylation, selective acylation methods were investigated. Two different methods of 2'-deoxyuridine nitration were tested. Moreover, the pH conditions for the diazotization step were optimized to prevent glycosylic bond breakage. The photophysical properties of 5-DMPA-2'-deoxyuridine were determined, and an excellent quenching ability against the PhpC fluorophore was found. Using the defined synthetic route of 5-DMPA-2'-deoxyuridine, phosphoramidite DNA monomer or triphosphate monomer can be prepared for oligomer synthesis. Once this nucleoside quencher monomer is made, it will be applied in various DNA molecular beacon and FRET studies.

# Appendix

## General synthesis procedures

All chemicals were obtained from commercial sources of ACS reagent grade or higher were used without further purification. Solvents for solution-phase chemistry were dried by passing through columns of activated alumina. Anhydrous and HPLC-grade solvents for PNA synthesis and chromatography were purchased from Caledon Laboratories. Thin-layer chromatography was performed on Silicycle Silica Gel TLC F-254 plates. Flash column chromatography (FCC) was performed on Merck Kieselgel 60, 230–400 mesh. Thin layer chromatography (TLC) was performed on Merck Kieselgel 60 TLC plates. Chemical shifts ( $\delta$ ) are reported in parts per million (ppm), were measured from tetramethylsilane (0 ppm) and are referenced to the solvent  $\text{CDCl}_3$  (7.26 ppm),  $\text{DMSO-d}_6$  (2.50 ppm) methanol- $\text{d}_4$  (3.31 ppm) for  $^1\text{H}$  NMR and  $\text{CDCl}_3$  (77.0 ppm),  $\text{DMSO-d}_6$  (39.5 ppm) methanol- $\text{d}_4$  (3.31 ppm) for  $^{13}\text{C}$  NMR. Multiplicities are described as s (singlet), d (doublet), t (triplet), q (quartet), m (multiplet) and br s (broad singlet). Resonances due to restricted rotation around the amide bond (rotamers) are reported as major (ma.) and minor (mi.) for  $^1\text{H}$  NMR, and notated as rotamers (rot.) for  $^{13}\text{C}$  NMR. Coupling constants (J) are reported in Hertz (Hz). Spectra were obtained on Bruker-400, Bruker-600, Varian INOVA-400 and Varian INOVA-600 instruments. High-resolution mass spectra (HRMS) were obtained using electron ionization (EI) or electrospray ionization (ESI).

## Instrumentation for characterization

The fluorescence measurements were implemented on a Photon Technology International (PTI)QM/TM-40 fluorometer equipped with a 75 W Xenon lamp, and the excitation and emission slits were set at 6 nm. The Cary 300 spectrophotometer was used to measure the UV–Vis absorption spectra. The 1 cm width quartz cuvette was used for all spectral detections. Varian INOVA 600 Hz NMR spectrometer was used for characterization and NMR titration.

## PNA oligomerization

PNA oligomers were synthesized on a 5  $\mu$ mol scale using the standard FastMoc module on an Applied Biosystems 433A synthesizer. For automated SPPS, commercially available Fmoc protected PNA monomers, amino acids and a linker were used, such as Fmoc-A(Bhoc)-AEG-OH, Fmoc-G(Bhoc)-AEG-OH, Fmoc-C(Bhoc)-AEG-OH, Fmoc-T(Bhoc)-AEG-OH (purchased from PolyOrg, Inc.), Fmoc-Lys(Boc)-OH and Fmoc-8-amino-3,6-dioxaoctanoic acid (purchased from Chem-Impex International Inc.). Lab-Fmoc-C(Bhoc)-AEG-OH Tentagel R Rink amide (RAM) was selected as the solid support. The resin was downloaded to approximately 0.04 mmol/g by coupling it to a sub-stoichiometric amount of L-lysine. 4-methylpiperidine in dimethylformamide (20%) solution was used for Fmoc deprotection. The capping solution was prepared with the ratio of 1:25:25 = acetic anhydride:pyridine:NMP(N-methyl-2-pyrrolidone). As coupling reagents, DIPEA in DMF and HBTU in NMP solutions were used. Each monomer was dissolved in NMP and stocked into cartridge for automated SPPS. PNA oligomers were cleaved from the solid support by 95% TFA and 5% of triethylsilane. The solvent was then evaporated under a nitrogen stream, the resulting residue was washed twice with cold ether. Cleaved PNA oligomers were dissolved in a solution of 0.05% trifluoroacetic acid in water and then purified by reverse-phase HPLC. Reverse-phase HPLC was performed on an Agilent Microsorb-MV 100-5 C18 250  $\times$  4.6 mm column heated to 50  $^{\circ}$ C. The purified PNA oligomer was eluted using a gradient (Mobile phase A: H<sub>2</sub>O containing 0.1% TFA. Mobile phase B: acetonitrile containing 0.1% TFA). The flow rate was 1 mL/min.

**Table S1. Flow setting of HPLC for PNA purification.**

Time	Flow	%A	%B	Curve
	1.00	99	1	
5.00	1.00	60	40	6
15.00	1.00	45	55	6
15.01	1.00	0	100	6
19.99	1.00	0	100	6
20.00	1.00	100	0	6
30.00	1.00	100	0	6

**Table S2. Purified PNA oligomers characterized by high-resolution mass spectroscopy.**

Oligomer	Sequence* (N → C)	Calculated m/z	Found m/z
PNA_d1	H-K-GTAGATCCCT-K-NH <sub>2</sub>	986.7640 [M + 3H] <sup>3+</sup>	987.0867
PNA_d2	H-K-GTAGATC <sup>U<sup>n</sup></sup> CT-K-NH <sub>2</sub>	1002.7589 [M + 3H] <sup>3+</sup>	1002.6729
PNA_d3	H-K-GTAGA <sup>U<sup>n</sup></sup> CCCT-K-NH <sub>2</sub>	997.7591 [M + 3H] <sup>3+</sup>	996.3821
PNA_d4	H-K-G <sup>U<sup>n</sup></sup> AGA <sup>U<sup>n</sup></sup> CCCT-K-NH <sub>2</sub>	1008.7541 [M + 3H] <sup>3+</sup>	1008.5773
Bis-PNA1	H-TCTCTTT(PEG2) <sub>3</sub> TTTJTJT-K-NH <sub>2</sub>	2123.8906 [M + 2H] <sup>2+</sup>	2124.9036
Bis-PNA2	H-TCTCTTT(PEG2) <sub>3</sub> TTTJU <sup>n</sup> JT-K-NH <sub>2</sub>	1427.2580 [M + 3H] <sup>3+</sup>	1427.0921

\*<sup>U<sup>n</sup></sup> = 5-nitrouracil, J = pseudoisocytosine, K = L-Lysine, PEG2 = 8-amino-3,6-dioxaoctanoic acid linker

\*Sequences possess an amide group at the C-terminus and an amine group at the N-terminus

## Quantification of PNA oligomers

The concentrations of PNA solutions were determined using the UV-Vis spectrophotometer. PNA oligomers were dissolved into water and that stock solution was 100 times diluted for UV-Vis measurement. The absorbance of diluted samples was measured at 260 nm. If absorbance was more than 1.5, extra dilution was required. The concentration of PNA solution was calculated from measured absorbance and the  $\epsilon_{260}$  constants of PNA monomers.  $\epsilon_{260}$  values of A, T, G, C and 5-nitrouracil are 13700, 8800, 6600, 11700 and 10950 M<sup>-1</sup>cm<sup>-1</sup>, respectively. The  $\epsilon_{260}$  value of 5-nitrouracil was found from UV-Vis measurement of 5-nitrouracil PNA monomer (**II-8**).

## Hybridization study of oligomers

$T_m$  values of oligomers were measured by temperature-dependent UV-Vis spectrophotometry using a computer-controlled Peltier device cuvette holder with the heating block in Varian 300 Bio UV-Vis Spectrometer at the wavelength of 260 nm. For melting samples, PNA strands and DNA strands were dissolved in the standard buffer (10 mM  $\text{Na}_2\text{HPO}_4$ , 100 mM NaCl, 0.1 mM EDTA, pH 7) with 2  $\mu\text{M}$  concentrations. For pH controlled experiment, samples were prepared with the same buffer at pH 5. Before the measurement, samples were heated to 90 °C and slowly cooled down to 25 °C for the annealing process. The sample was transferred to a 1 mL quartz cuvette with 1 cm path length. For the measurement, the temperature was increased from 5 °C to 90 °C with a heating rate of 0.5 °C/min and then cooled down to 5 °C at the same rate for subsequent measurements. Each sample had 2 cycles of melting and cooling. To prevent condensation at low temperatures, dried air was used to purge the sample chamber. A thin layer of silicone oil was used to prevent evaporation of the sample during measurement.

## Quenching study

Sixteen quenching studies were performed with all possible fluorophore-quencher pairs. For each fluorophore-quencher pair, a series of 1  $\mu\text{M}$  of a fluorophore in EtOH or 0.1%  $\text{Et}_3\text{N}$  in water sample with different concentrations (0 – 26  $\mu\text{M}$ ) of a quencher was prepared. After 10 minutes of equilibration, the fluorescent emission spectra were measured at 25 °C. A Stern-Volmer plot was constructed with the ratio of the initial fluorescence intensity ( $I_0$ ) divided by the quenched fluorescence intensity ( $I$ ) in each concentration of quencher.  $K_{sv}$  values were calculated from the slope of the linear relationship between  $I_0/I$  and the quencher concentration.

## $^1\text{H}$ NMR titration

With anhydrous  $\text{CDCl}_3$ , 2 mL of 20 mM adenine ethyl ester solution (Host) and 3 mL of 1 mM DMPAU *tert*-butyl ester solution (Guest) were prepared. At first, 500  $\mu\text{L}$  of the host solution was transferred into a clean and over-dried NMR tube and capped with a rubber septa. 8



scans of the  $^1\text{H}$  NMR spectrum were run to check the initial chemical shifts ( $\Delta\delta$ ) of hydrogen bond donors, N4 and C2 hydrogens of adenine. In each addition, 4  $\mu\text{L}$  of the guest solution was added into the tube using a syringe without opening the cap, and the mixture was shaken for 10 seconds with a vortex machine before running the NMR spectrum. Titration was stopped when the chemical shift changes were dropped under 0.02 ppm. Titrations were repeated 3 times. Collected  $\Delta\delta$  and concentrations were inserted into the computational curve fitting program with Benesi-Hildebrand equation (**Equation S1**)<sup>18</sup> to determine  $K_a$  and stoichiometry. The curve showed the best fitting with the equation (**Equation S2**) for 1:1 complex than other cubic equations for 1:2 complex and 2:1 complex, therefore, adenine ethyl ester and DMPAU tert-butyl ester formed only the Watson-Crick base pair in this titration condition.

$$1/\Delta\delta = 1/(K_a\Delta\delta_{\max}[\text{H}]_0) + 1/\Delta\delta_{\max} \quad \text{Equation S1}$$

$$[\text{HG}] = \frac{(K_a[\text{H}]_0 + K_a[\text{G}]_0 + 1) - \sqrt{(K_a[\text{H}]_0 + K_a[\text{G}]_0)^2 - 2K_a[\text{H}]_0 + 2K_a[\text{G}]_0 + 1}}{2K_a} \quad \text{Equation S2}$$

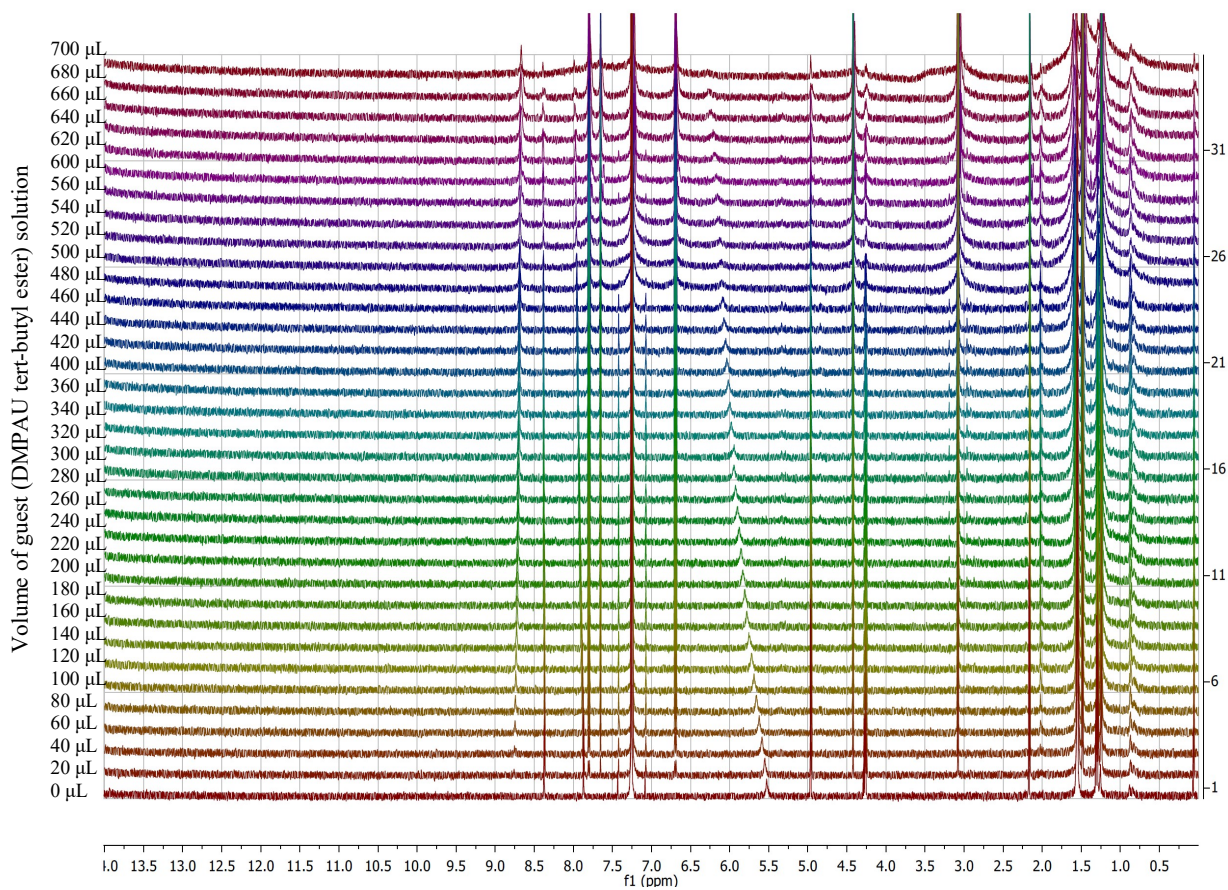
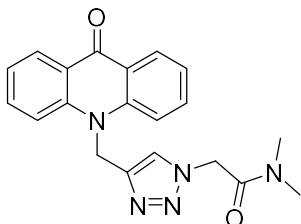


**Figure S1** NMR titration of DMPAU *tert*-butyl ester(guest) and adenine ethyl ester(host).

## Characterization of Fluorophores

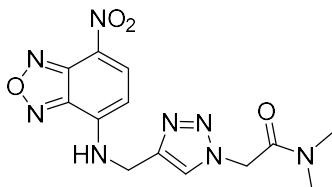
### 2-(4-((9-acridone)methyl)-1,2,3-triazol-1-yl)-*N,N*-dimethylacetamide (Acridone amide)



$^1\text{H}$  NMR (600 MHz,  $\text{DMSO-d}_6$ )  $\delta$ : 8.37 (d, 2H), 7.99 (s, 2H), 7.98 (s, NH), 7.83 (t, 2H), 7.35 (t, 2H), 5.83 (s, 2H), 5.37 (s, 2H), 2.99 (s, 3H), 2.81 (s, 3H).  $^{13}\text{C}$  NMR (151 MHz,  $\text{DMSO}$ )  $\delta$

177.07, 165.87, 142.25, 134.65, 127.12, 125.46, 122.18, 121.99, 116.85, 51.20, 41.95, 36.27, 35.66. HRMS (ESI) calculated for  $\text{NaC}_{20}\text{H}_{19}\text{N}_5\text{O}_2$   $[\text{M}]^+$  384.1436, found 384.1459.

**2-(4-(((7-nitro-2,1,3-benzooxadiazol-4-yl)amino)methyl)-1,2,3-triazol-1-yl) N,N-dimethyl-acetamide (NBD amide)** *N,N*-



$^1\text{H}$  NMR (600 MHz,  $\text{DMSO-d}_6$ )  $\delta$ : 9.89 (s, NH), 8.51 (d, 1H), 8.01 (s, 1H), 6.56 (d, 1H), 5.40 (s, 2H), 4.78 (s, 2H), 3.03 (s, 3H), 2.84 (s, 3H).  $^{13}\text{C}$  NMR (151 MHz,  $\text{DMSO}$ )  $\delta$  165.90, 145.10, 144.96, 144.54, 142.74, 138.24, 125.57, 121.92, 100.33, 51.20, 36.33, 35.68. HRMS (ESI) calculated for  $\text{NaC}_{13}\text{H}_{14}\text{N}_8\text{O}_4$   $[\text{M}]^+$  369.1036, found 369.1056.

## Photophysical data of compounds

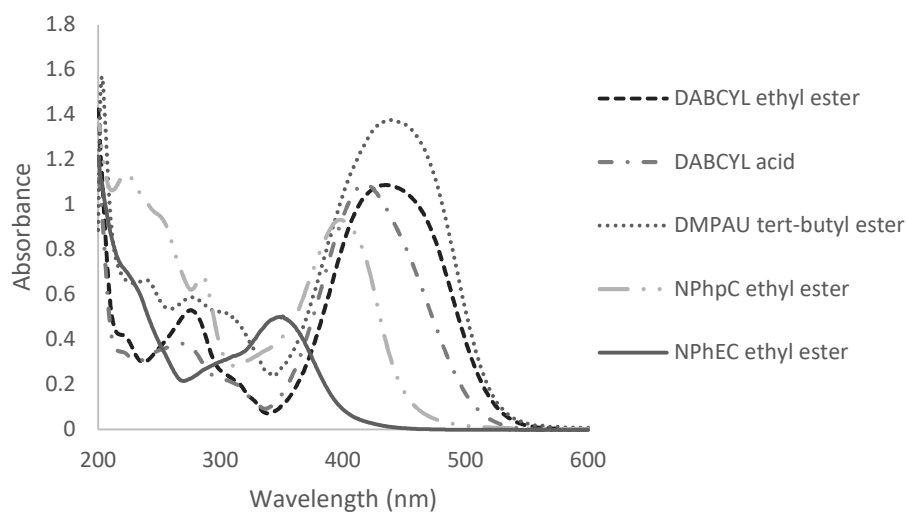


**Figure S2.** UV-Vis spectra of quenchers ( $5.00 \times 10^{-5}$  M) in EtOH.

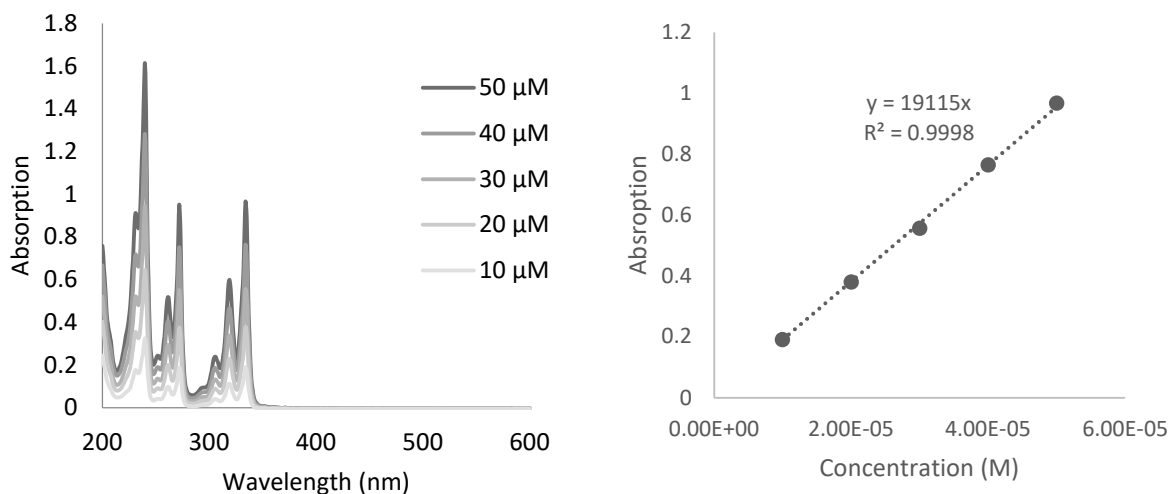


**Figure S3.** UV-Vis spectra of Pyrene in EtOH and Beer's law plot ( $\lambda_{ab} = 334$  nm).

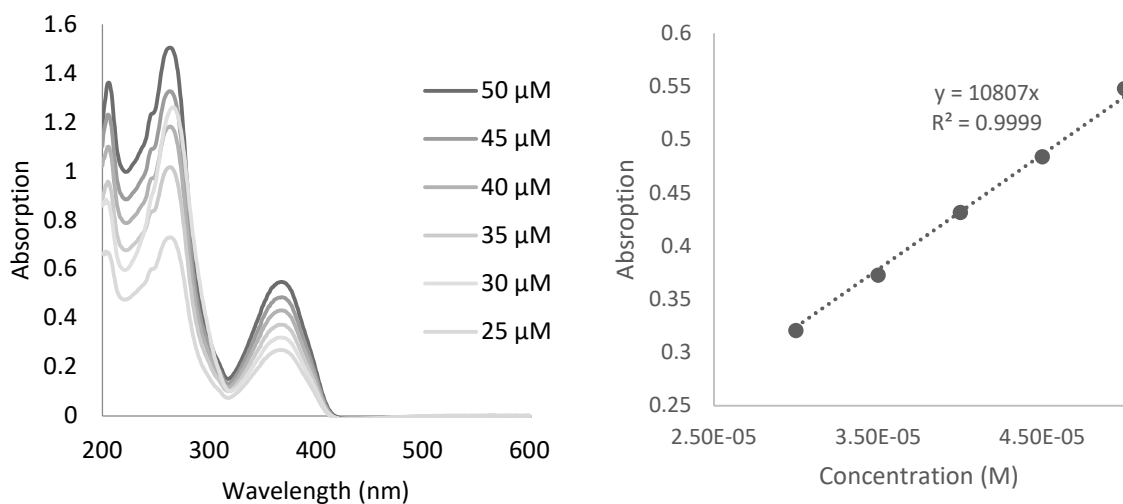


**Figure S4.** UV-Vis spectra of PhpC ethyl ester in EtOH and Beer's law plot ( $\lambda_{ab} = 367$  nm).

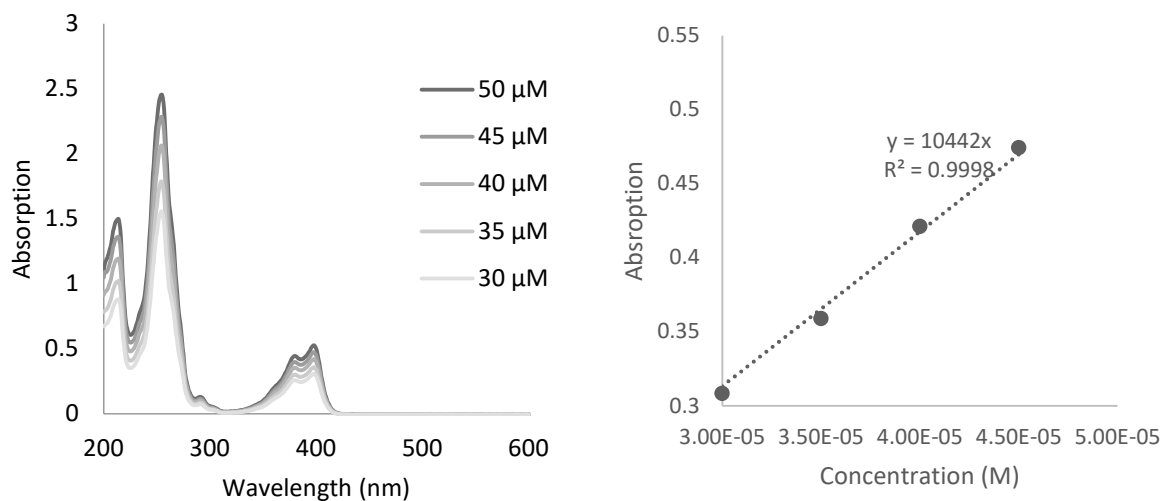


**Figure S5.** UV-Vis spectra Acridone amide in EtOH and Beer's law plot ( $\lambda_{ab} = 398$  nm).

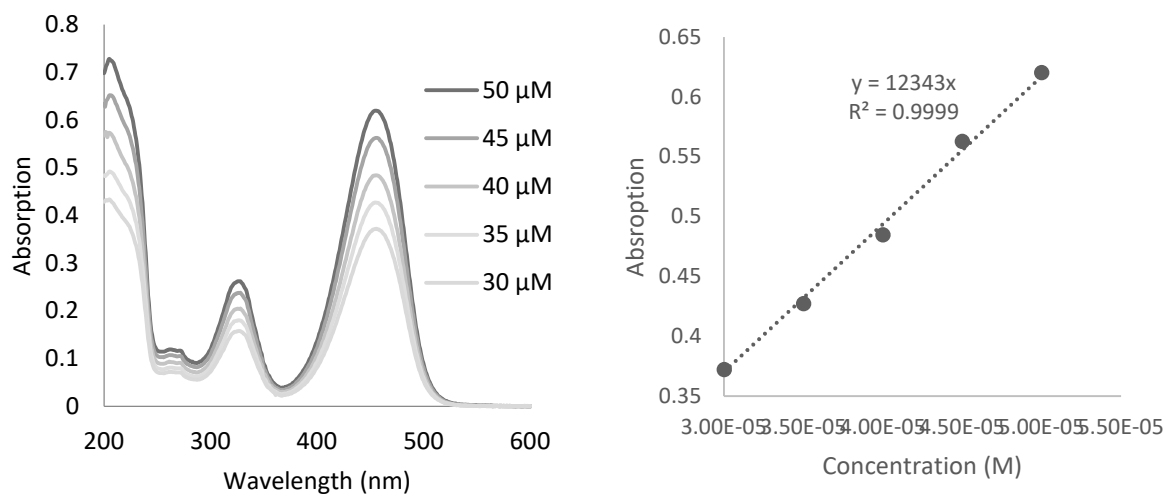


**Figure S6.** UV-Vis spectra of NBD amide in EtOH and Beer's law plot ( $\lambda_{ab} = 455$  nm).

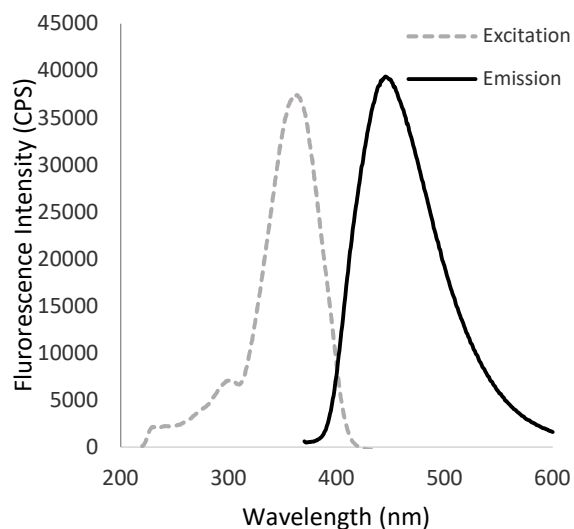


**Figure S7.** Fluorescent spectra of PhpC acetic acid in 0.1% Et<sub>3</sub>N aqueous solution plot,  $\lambda_{\text{ex}} = 362 \text{ nm}$   $\lambda_{\text{em}} = 450 \text{ nm}$ .

## Quenching study

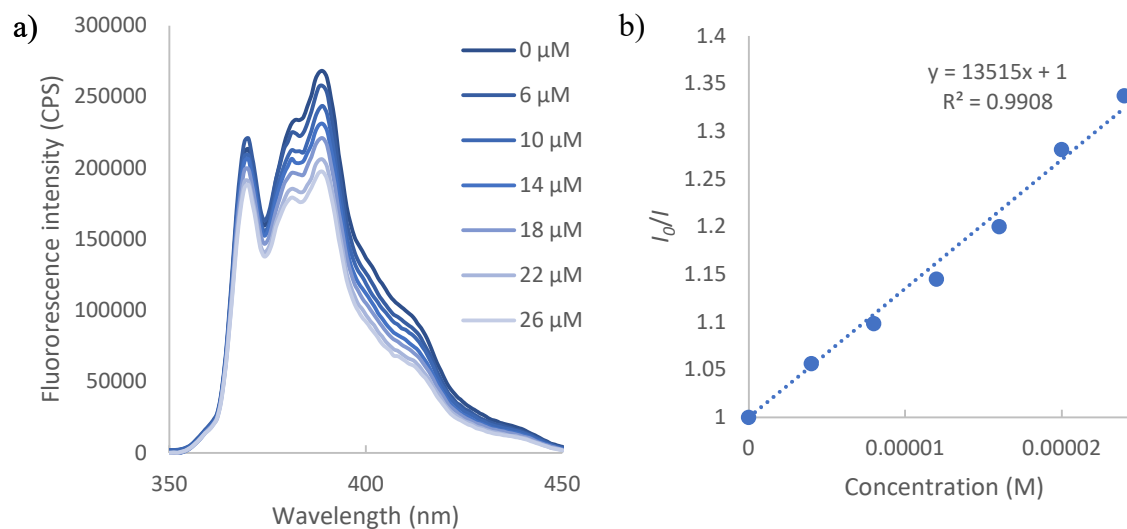


**Figure S8.** Quenching study of pyrene with DABCYL ethyl ester; a) Fluorescence intensities of pyrene in different concentrations of DABCYL ethyl ester,  $\lambda_{\text{excit}} = 332 \text{ nm}$ ; b) Stern Volmer plot.

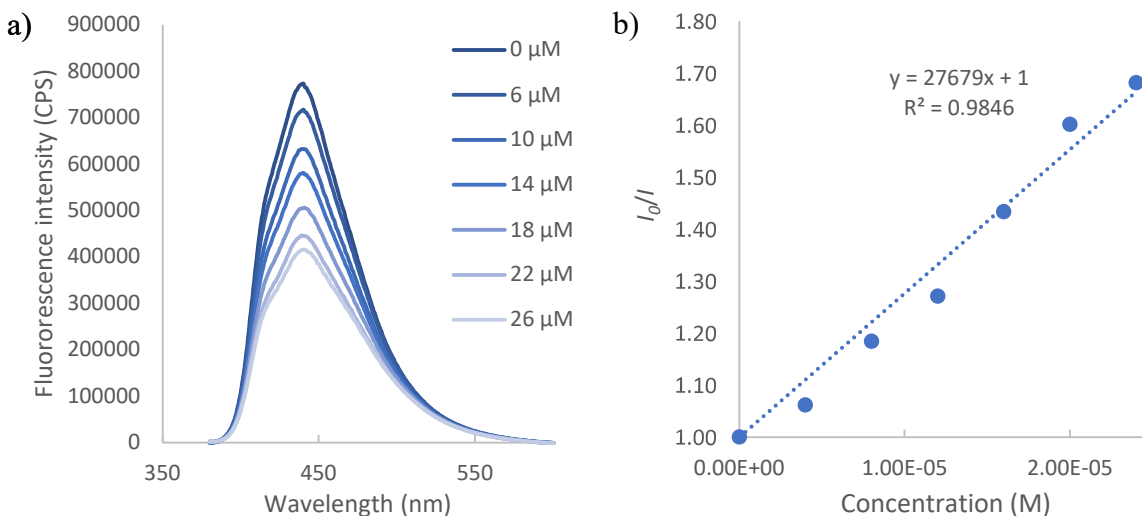


**Figure S9.** Quenching study of PhpC ethyl ester with DABCYL ethyl ester; a) Fluorescence intensities of PhpC ethyl ester in different concentrations of DABCYL ethyl ester,  $\lambda_{\text{excit}} = 368$  nm; b) Stern Volmer plot.

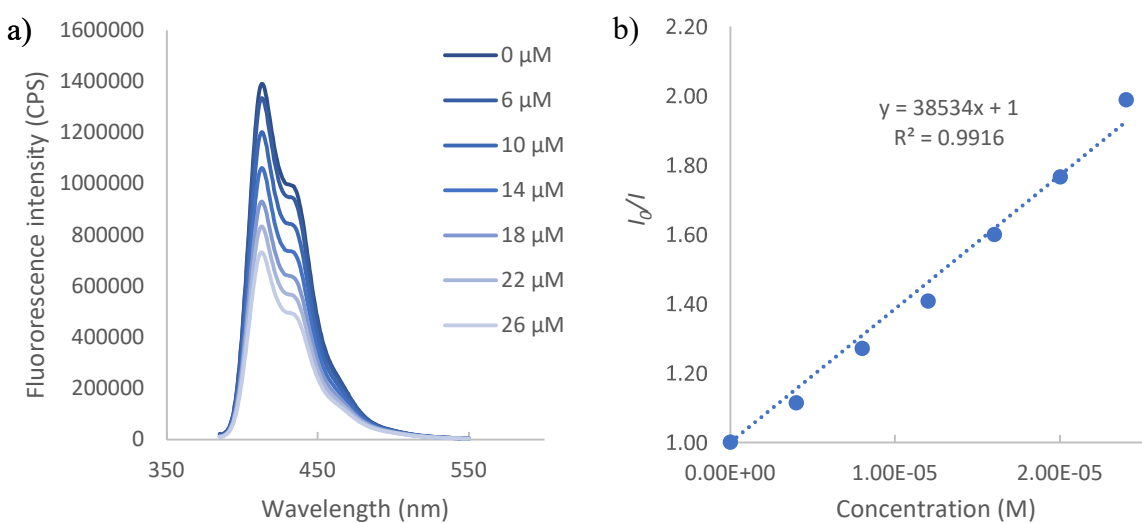


**Figure S10** Quenching study of acridone amide with DABCYL ethyl ester; a) Fluorescence intensities of acridone amide in different concentrations of DABCYL ethyl ester,  $\lambda_{\text{excit}} = 343$  nm; b) Stern Volmer plot.

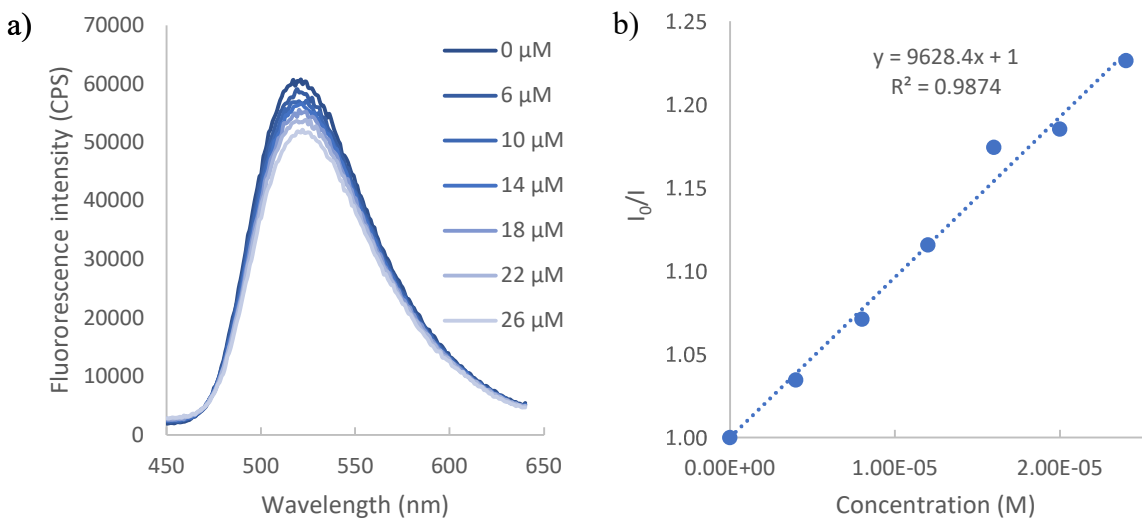


**Figure S11** Quenching study of NBD amide with DABCYL ethyl ester; a) Fluorescence intensities of NBD amide in different concentrations of DABCYL ethyl ester,  $\lambda_{\text{excit}} = 325 \text{ nm}$ ; b) Stern Volmer plot.

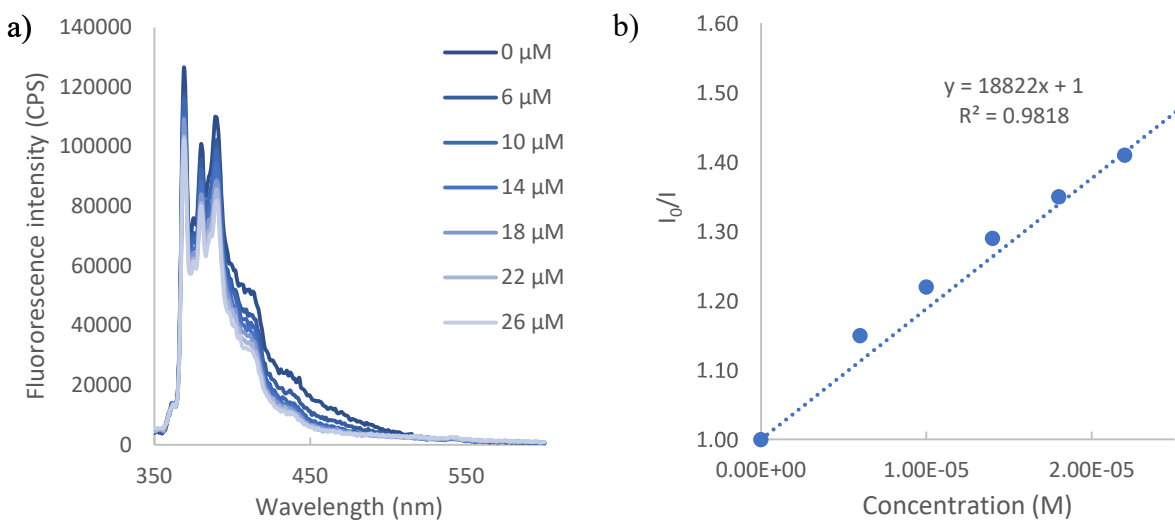


**Figure S12** Quenching study of pyrene with DMPAU *tert*-butyl ester; a) Fluorescence intensities of pyrene in different concentrations of DMPAU *tert*-butyl ester,  $\lambda_{\text{excit}} = 332 \text{ nm}$ ; b) Stern Volmer plot.



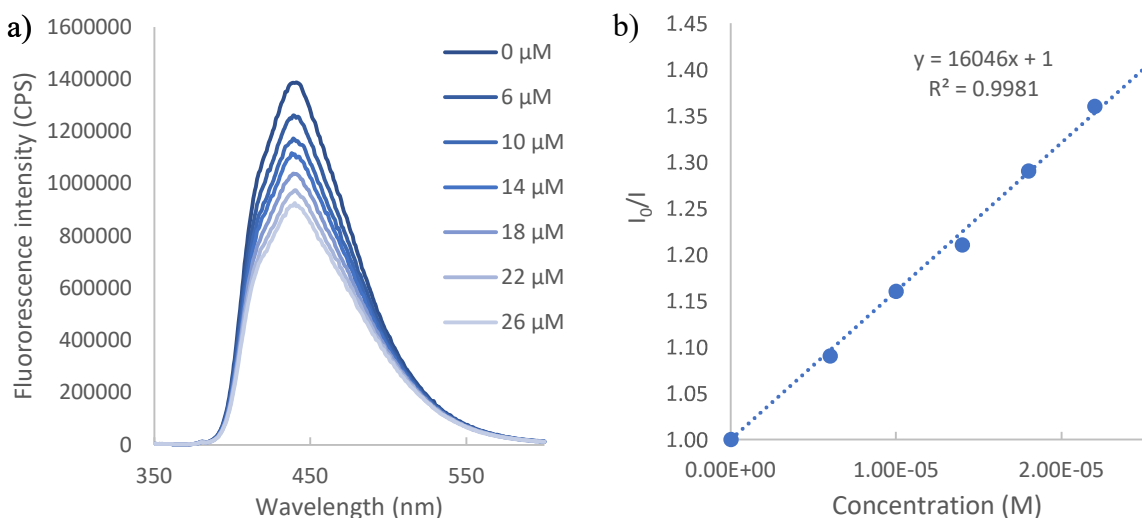


**Figure S13** Quenching study of PhpC ethyl ester with DMPAU *tert*-butyl ester; a) Fluorescence intensities of PhpC ethyl ester in different concentrations of DMPAU *tert*-butyl ester,  $\lambda_{\text{excit}} = 368$  nm; b) Stern Volmer plot.

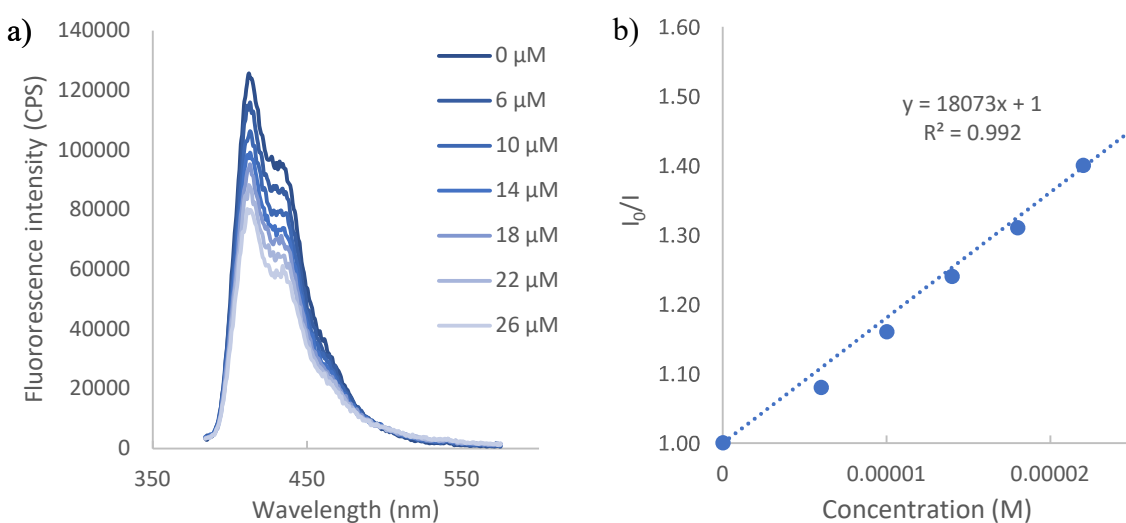


**Figure S14** Quenching study of acridone amide with DMPAU *tert*-butyl ester; a) Fluorescence intensities of acridone amide in different concentrations of DMPAU *tert*-butyl ester  $\lambda_{\text{excit}} = 343$  nm; b) Stern Volmer plot.

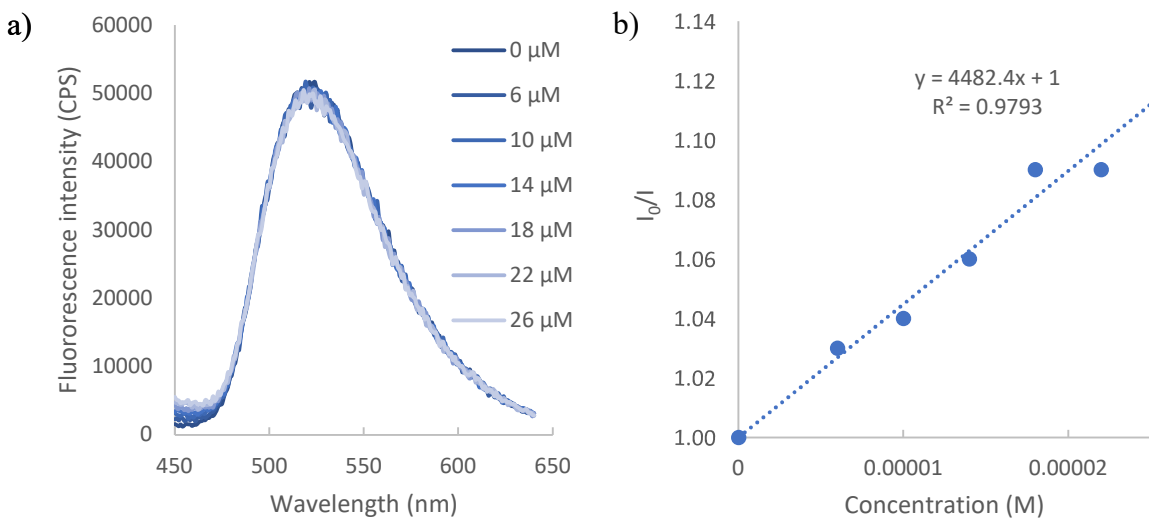


**Figure S15** Quenching study of NBD amide with DMPAU *tert*-butyl ester; a) Fluorescence intensities of NBD amide in different concentrations of DMPAU *tert*-butyl ester  $\lambda_{\text{excit}} = 325$  nm; b) Stern Volmer plot.

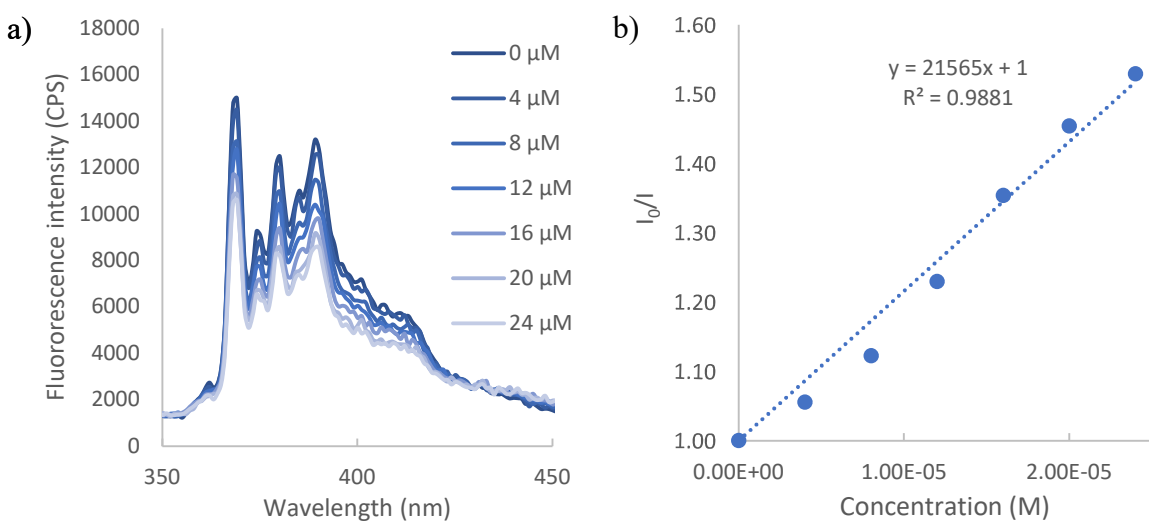


**Figure S16** Quenching study of pyrene with 4-NO<sub>2</sub>-PhpC ethyl ester; a) Fluorescence intensities of pyrene in different concentrations of 4-NO<sub>2</sub>-PhpC ethyl ester  $\lambda_{\text{excit}} = 332$  nm; b) Stern Volmer plot.

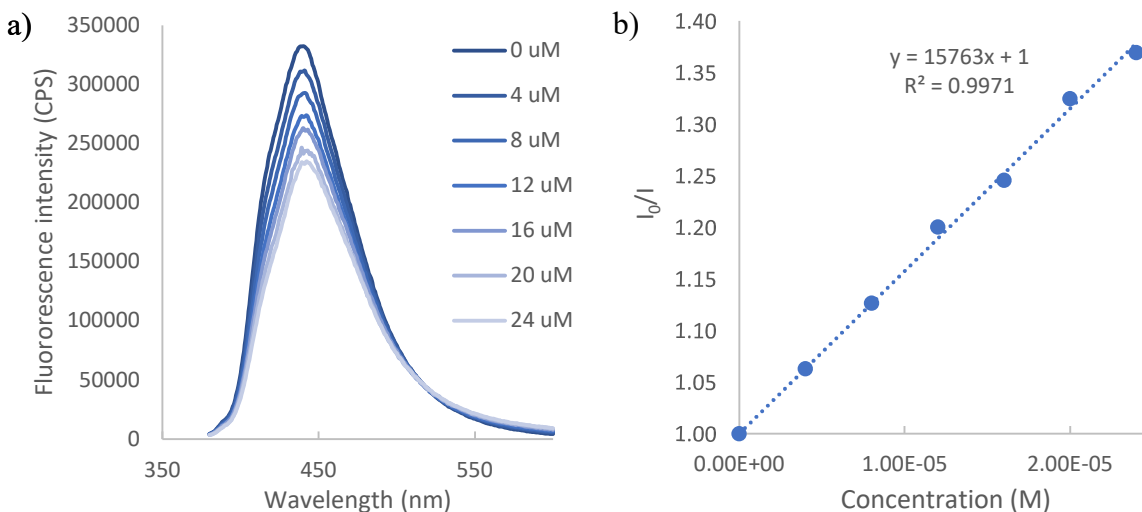


**Figure S17** Quenching study of PhpC ethyl ester with 4-NO<sub>2</sub>-PhpC ethyl ester; a) Fluorescence intensities of PhpC ethyl ester in different concentrations of 4-NO<sub>2</sub>-PhpC ethyl ester  $\lambda_{\text{excit}} = 350$  nm; b) Stern Volmer plot.

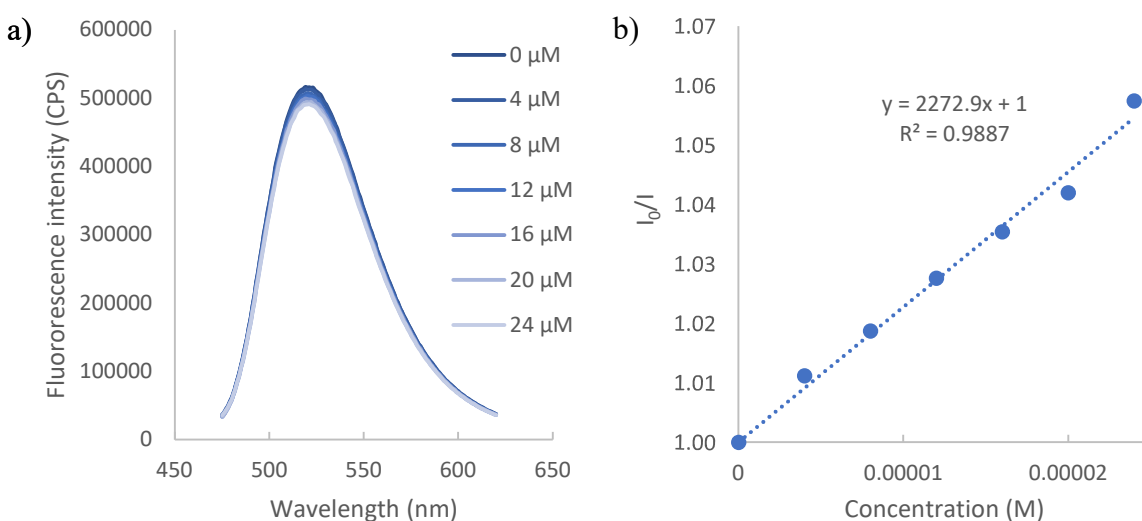


**Figure S18** Quenching study of NBD amide with 4-NO<sub>2</sub>-PhpC ethyl ester; a) Fluorescence intensities of NBD amide in different concentrations of 4-NO<sub>2</sub>-PhpC ethyl ester  $\lambda_{\text{excit}} = 465$  nm; b) Stern Volmer plot.

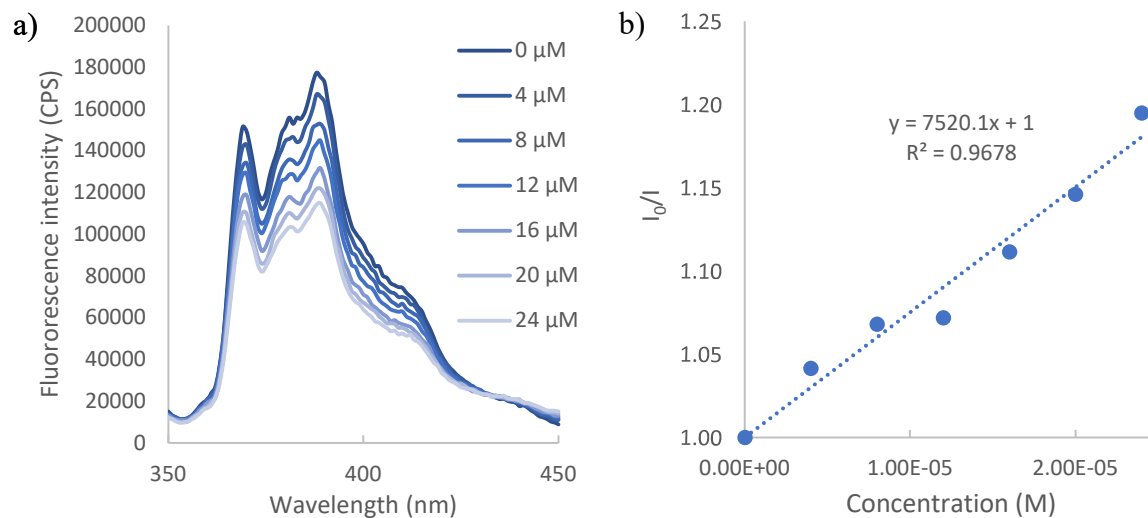


**Figure S19** Quenching study of pyrene with 4-NO<sub>2</sub>-PhEC ethyl ester; a) Fluorescence intensities of pyrene in different concentrations of 4-NO<sub>2</sub>-PhEC ethyl ester,  $\lambda_{\text{excit}} = 316 \text{ nm}$ ; b) Stern Volmer plot.

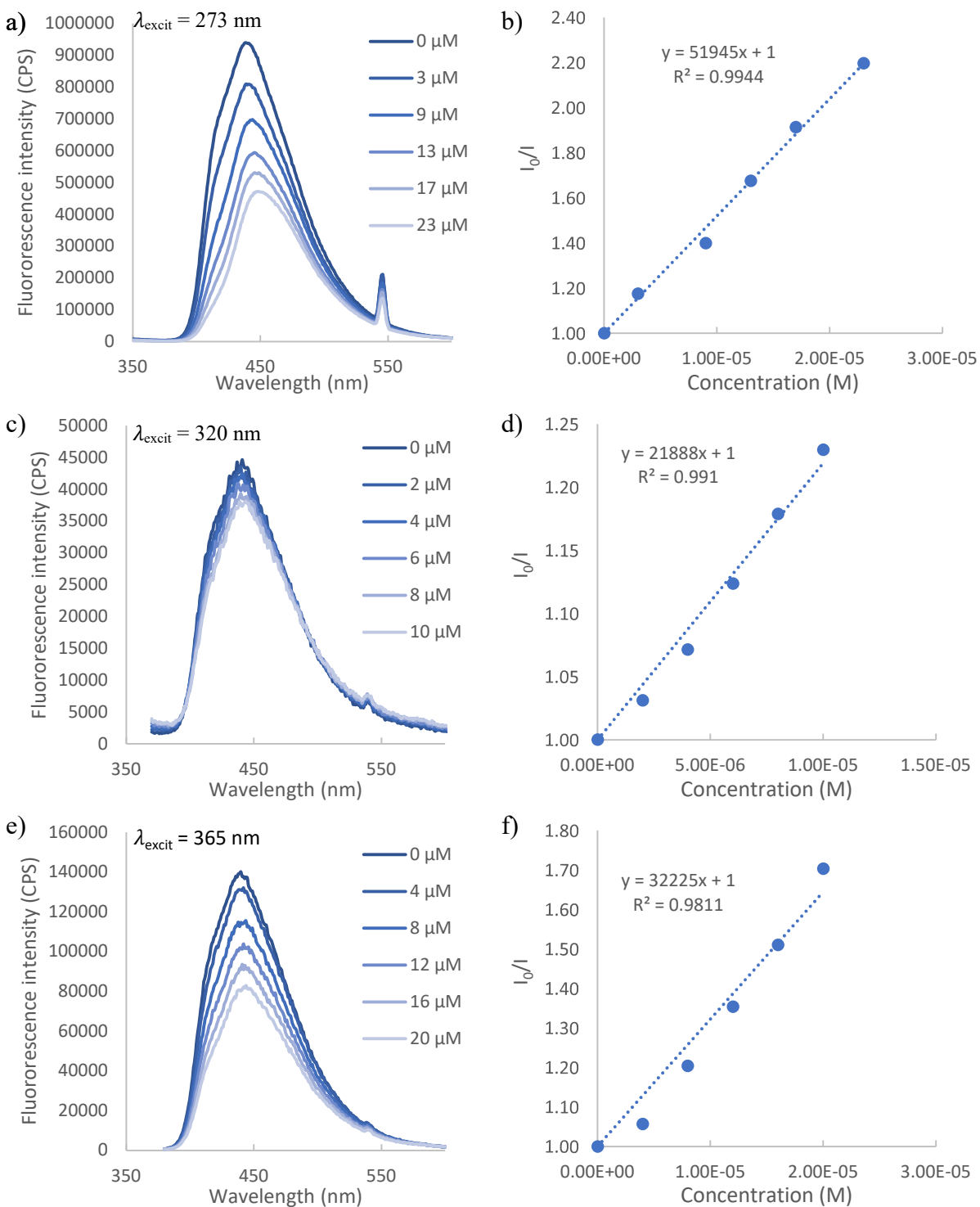


**Figure S20** Quenching study of PhpC ethyl ester with 4-NO<sub>2</sub>-PhEC ethyl ester at different excitation wavelengths; a) c) e) Fluorescence intensities of PhpC ethyl ester in different concentrations of 4-NO<sub>2</sub>-PhEC ethyl ester; b) d) f) Stern Volmer plot.

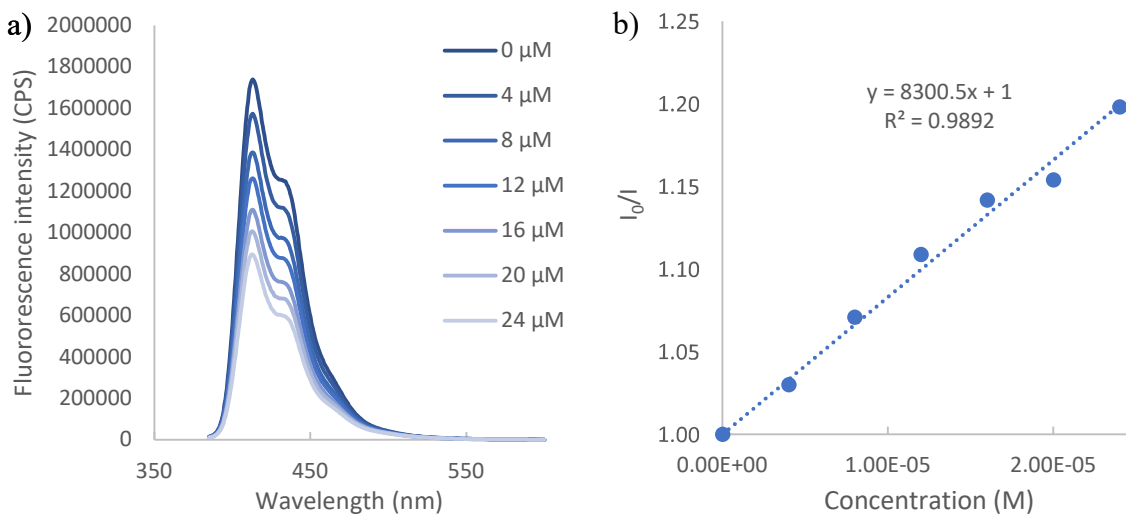


**Figure S21** Quenching study of acridone amide with 4-NO<sub>2</sub>-PhEC ethyl ester; a) Fluorescence intensities of acridone amide in different concentrations of 4-NO<sub>2</sub>-PhEC ethyl ester,  $\lambda_{\text{excit}} = 267$  nm; b) Stern Volmer plot.

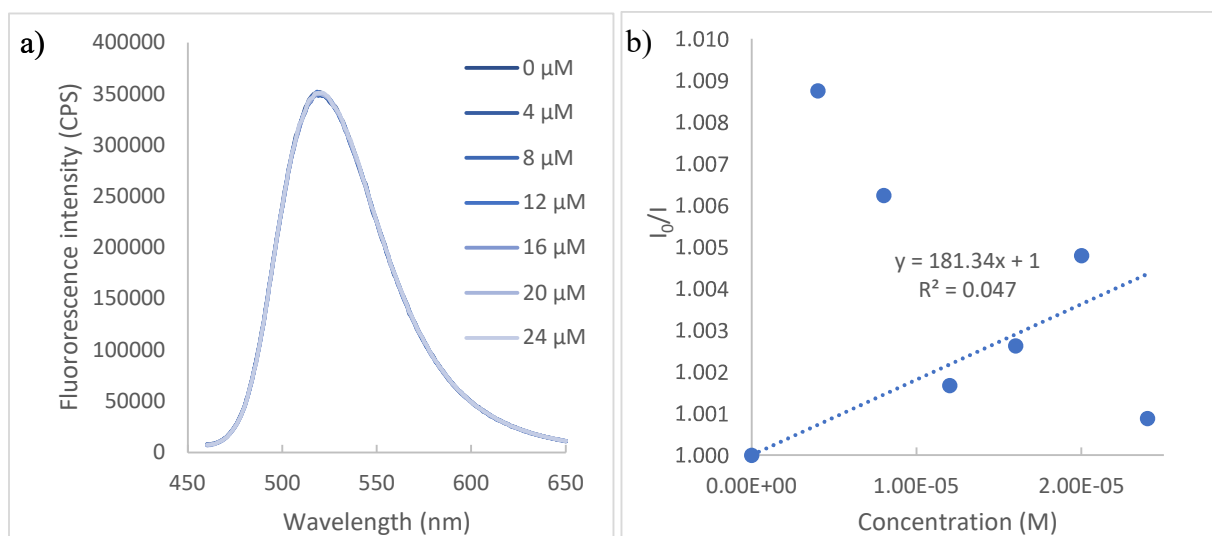


**Figure S22** Quenching study of NBD amide with 4-NO<sub>2</sub>-PhEC ethyl ester; a) Fluorescence intensities of NBD amide in different concentrations of 4-NO<sub>2</sub>-PhEC ethyl ester,  $\lambda_{\text{excit}} = 450$  nm; b) Stern Volmer plot.

## HPLC chromatograms

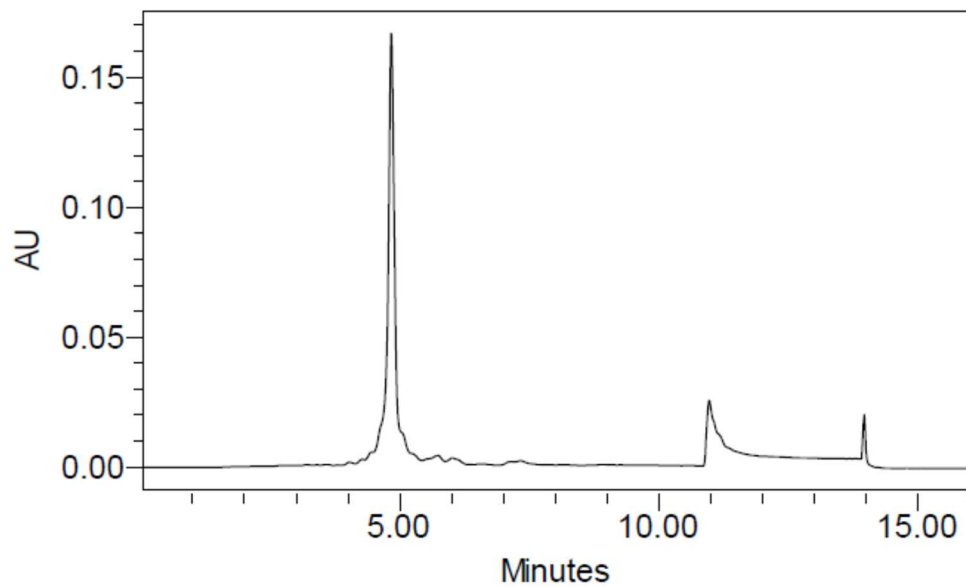


**Figure S23** HPLC trace of PNAd1 detected by UV absorption at 265 nm.

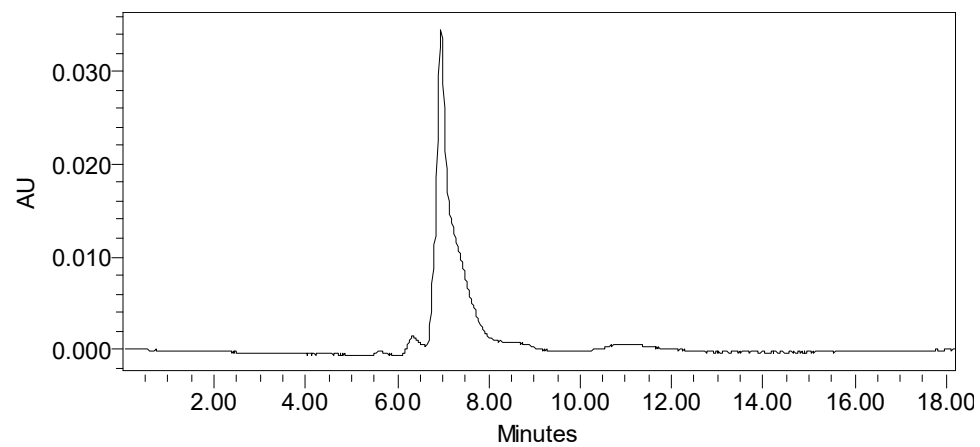


**Figure S24.** HPLC trace of PNAd2 detected by UV absorption at 265 nm.

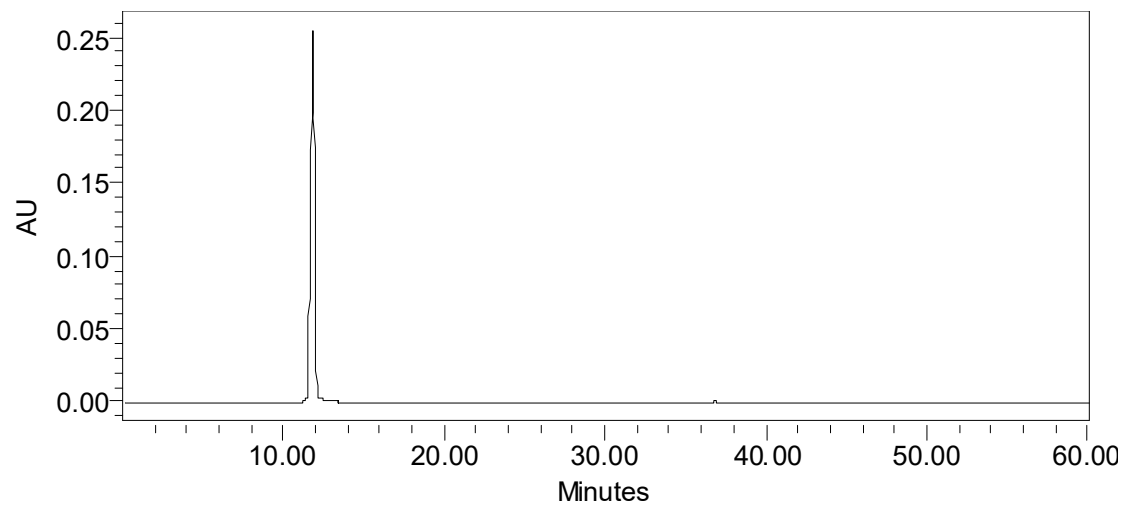


**Figure S25. HPLC trace of PNAd3 detected by UV absorption at 265 nm.**

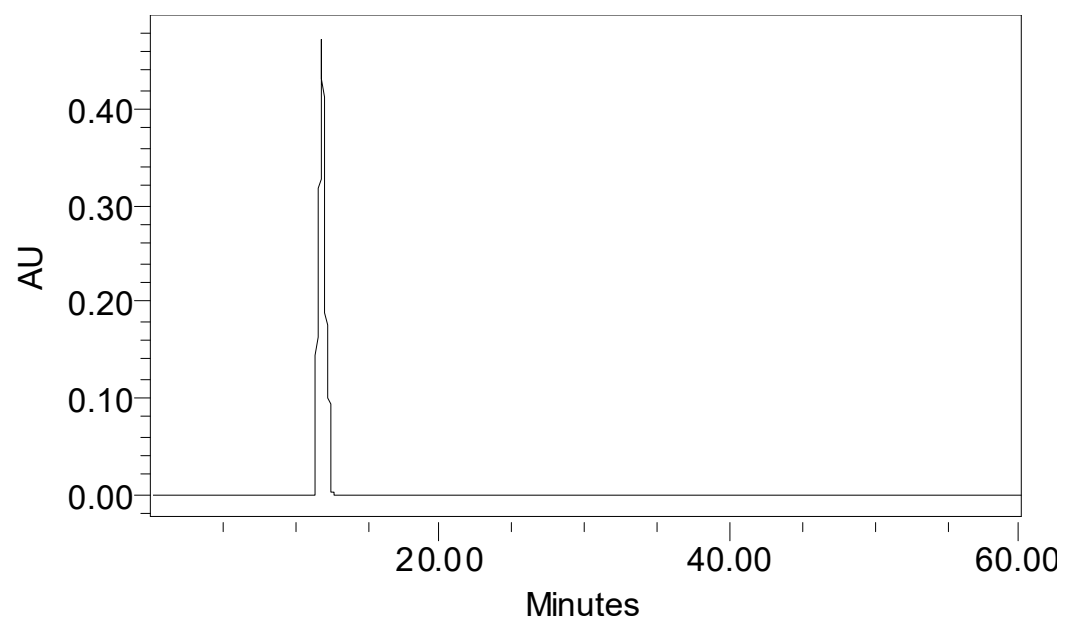


**Figure S26. HPLC trace of PNAd4 detected by UV absorption at 265 nm.**



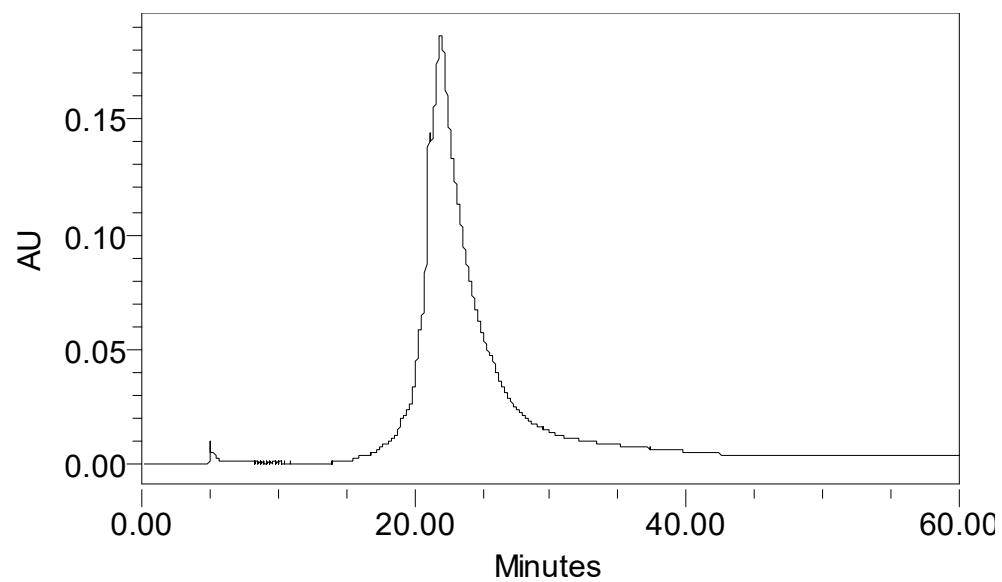


**Figure S27. HPLC trace of bisPNA1 detected by UV absorption at 265 nm.**

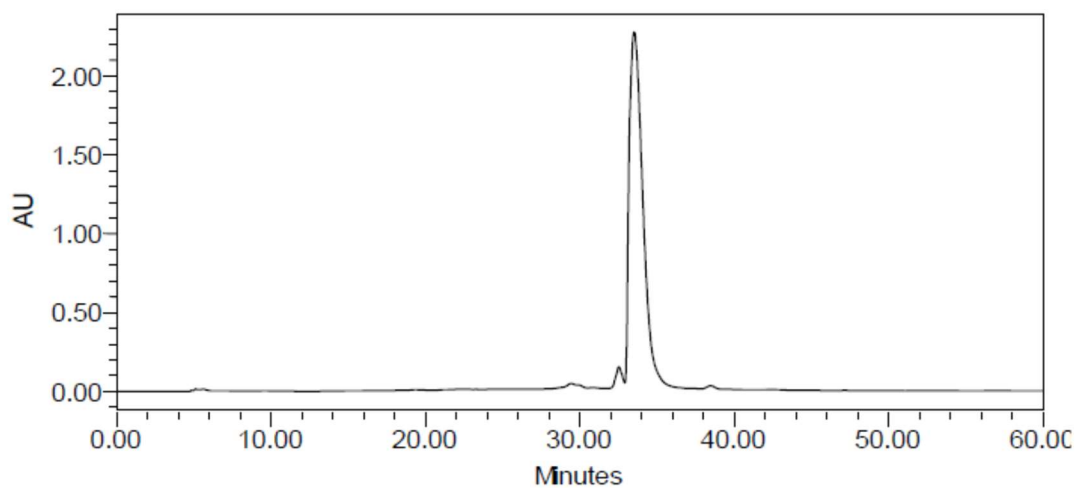


**Figure S28. HPLC trace of bisPNA2 detected by UV absorption at 265 nm.**

# NMR Spectra

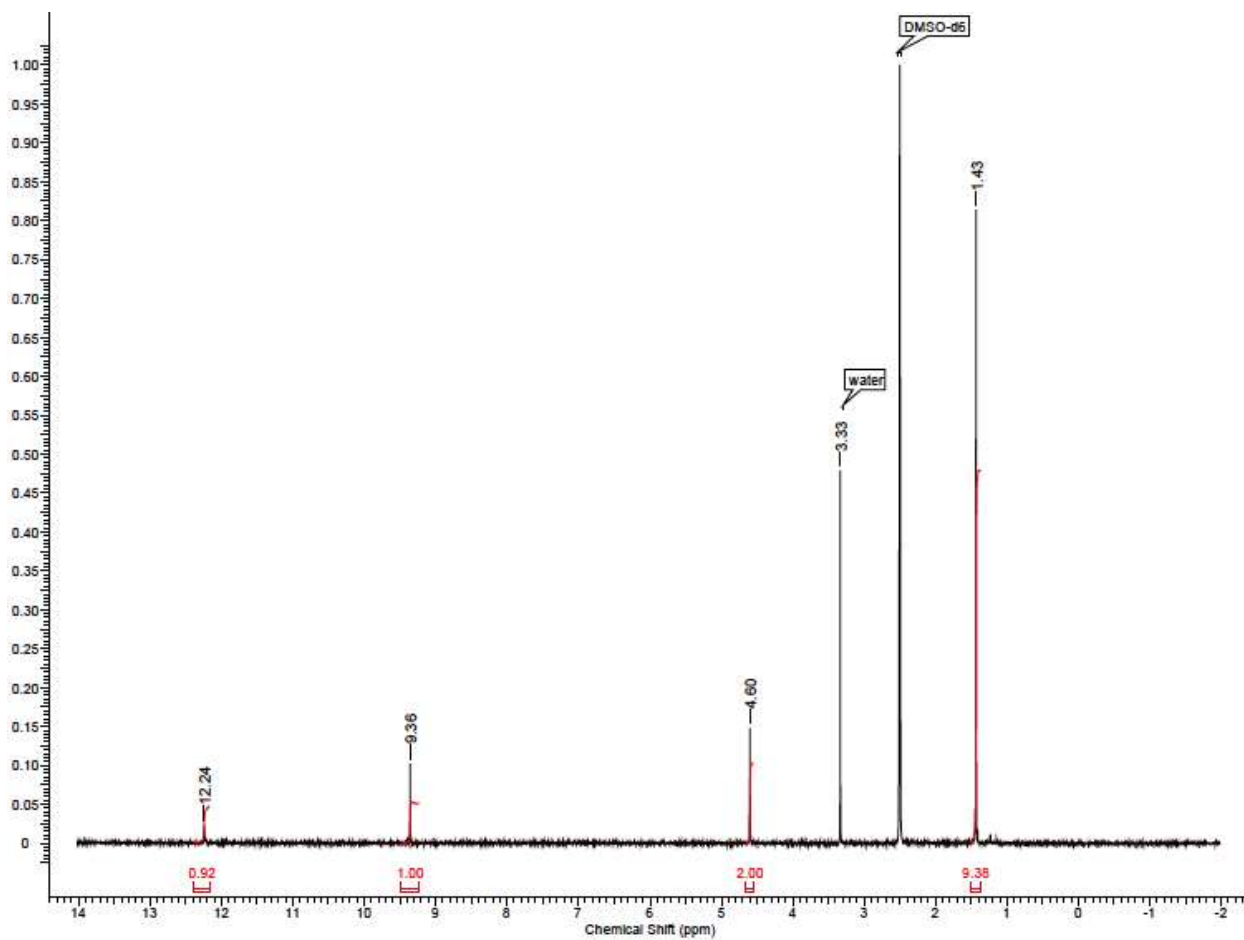


Figure S29 <sup>1</sup>H NMR of *tert*-Butyl 2-(5-nitrouracil-1-yl)acetate (II-2).

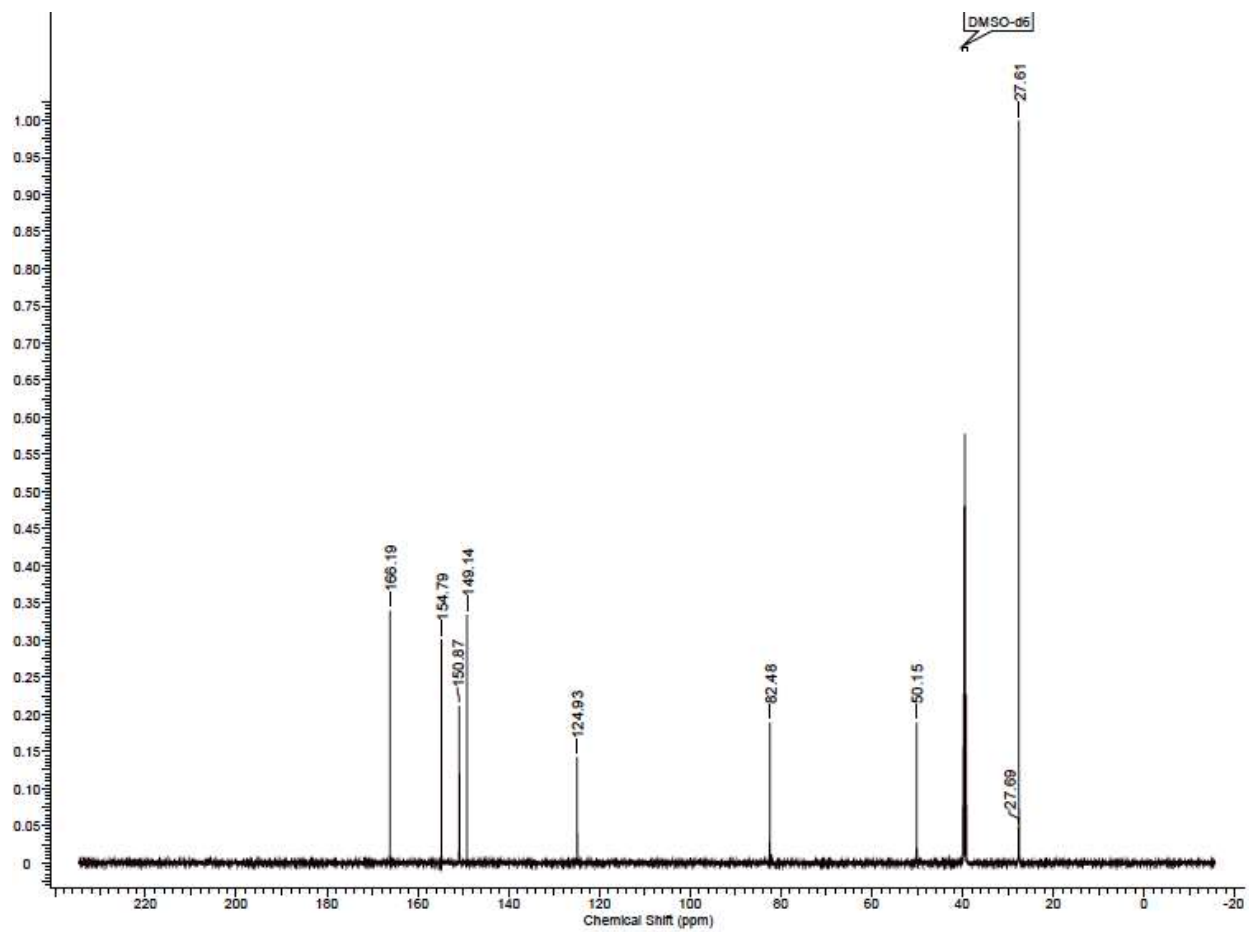


Figure S30  $^{13}\text{C}$  NMR of *tert*-Butyl 2-(5-nitrouracil-1-yl)acetate (II-2).

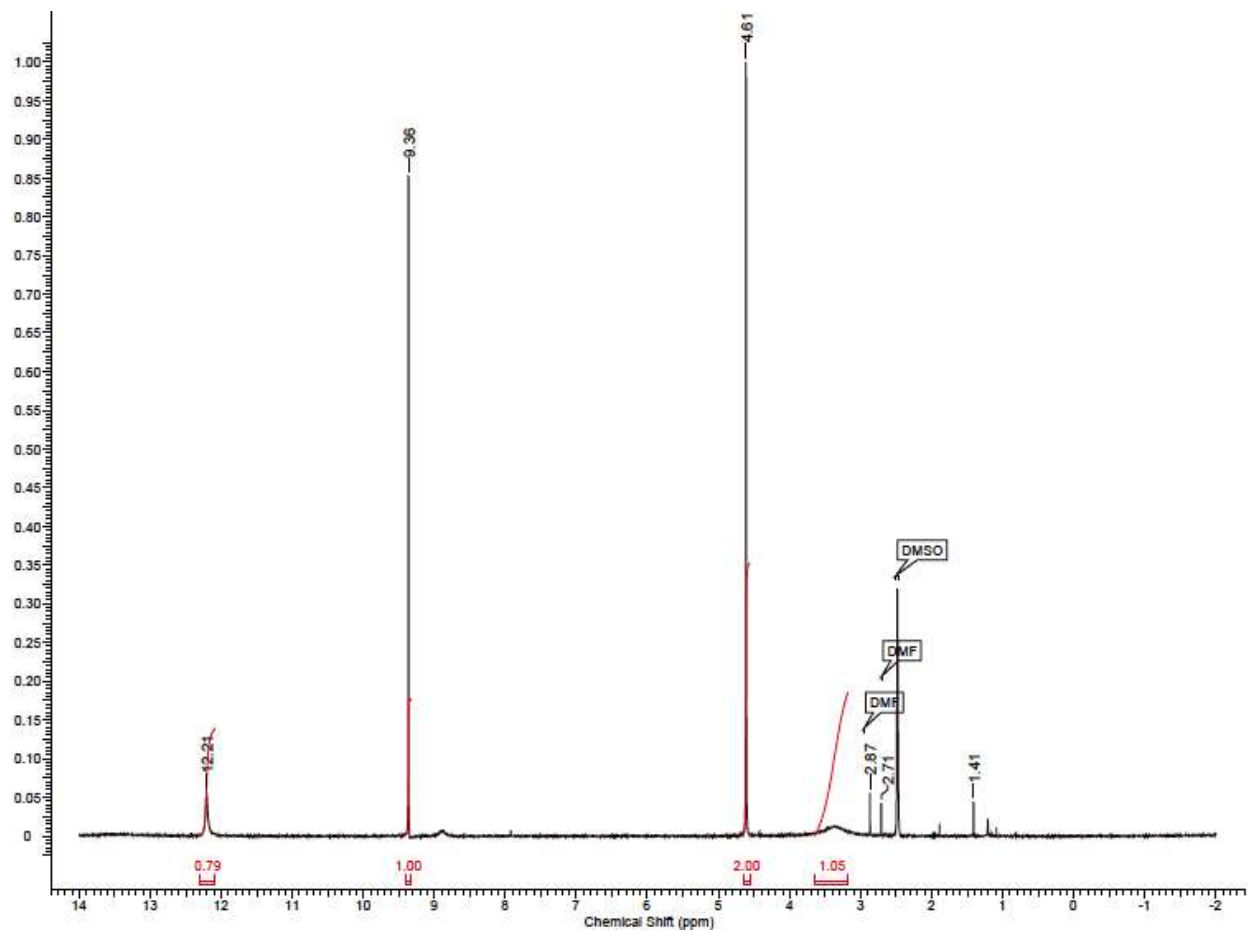


Figure S31  $^1\text{H}$  NMR of 2-(5-Ntrouracil-1-yl)acetic acid (II-3).

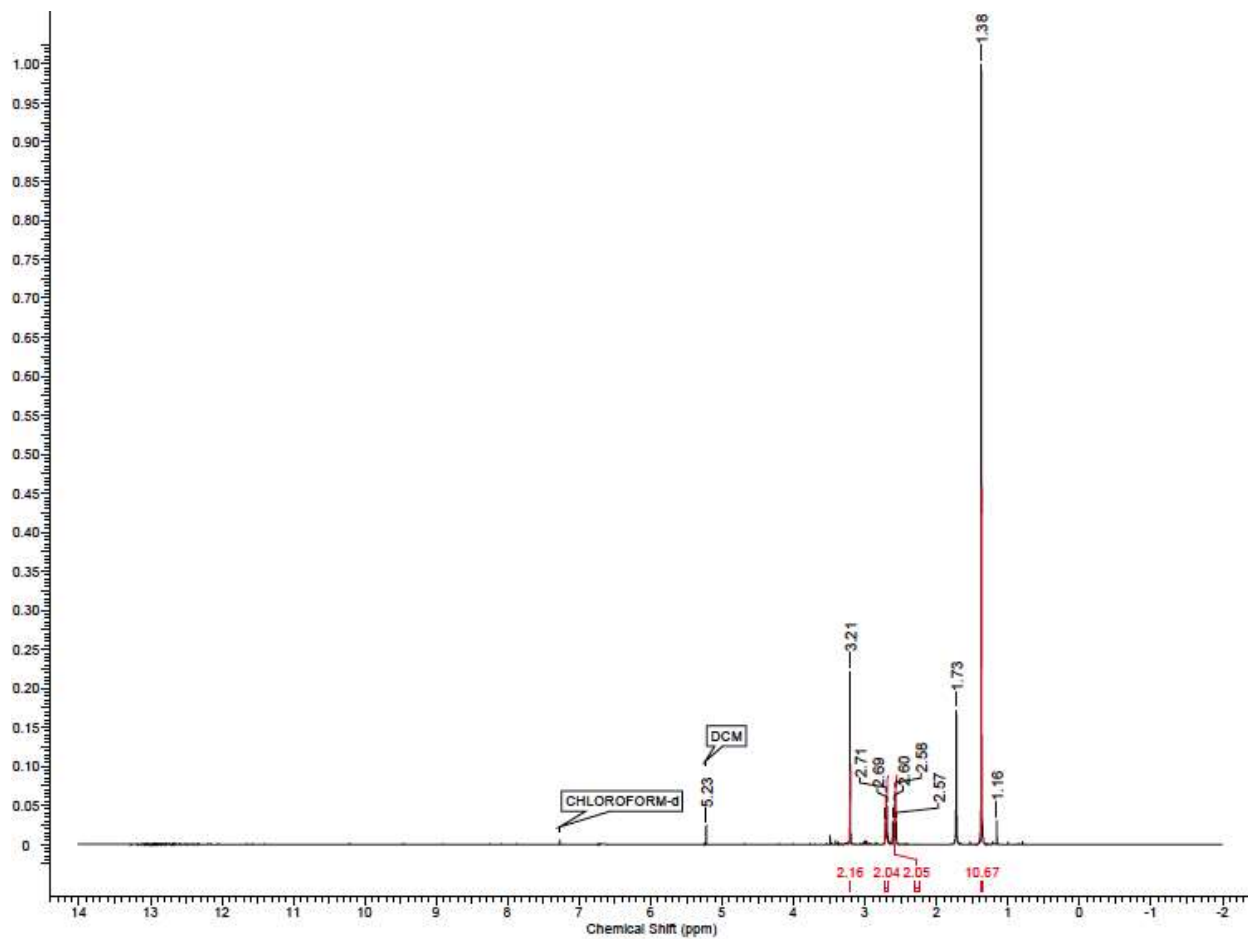


Figure S32 <sup>1</sup>H NMR of *tert*-Butyl 2-((2-aminoethyl)amino)acetate (II-5).

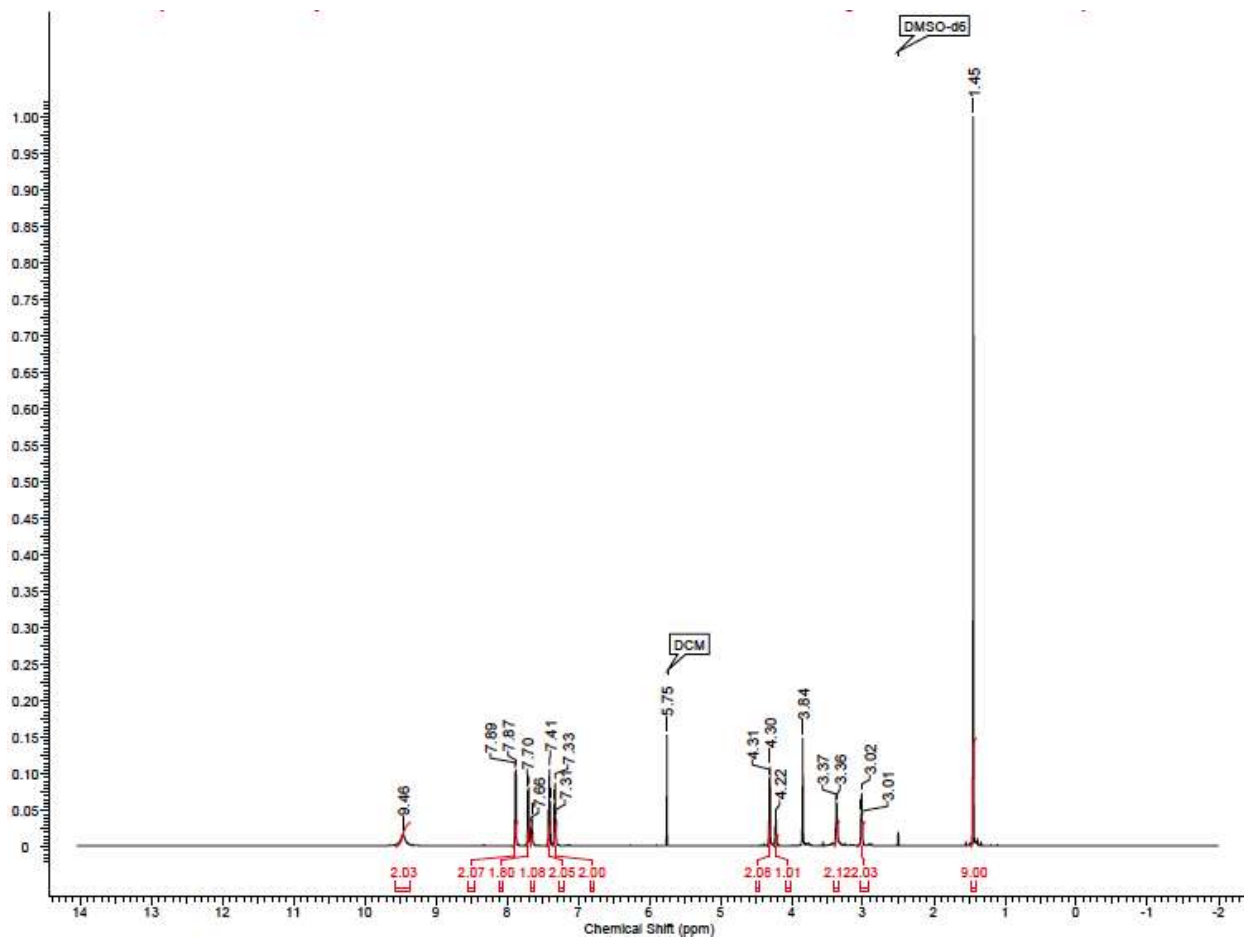


Figure S33  $^1\text{H}$  NMR of *N*-(2-(((9*H*-Fluoren-9-yl)methoxy)carbonyl)amino)ethyl)-2-(*tert*-butoxy)-2-oxoethanaminium chloride (II-6).

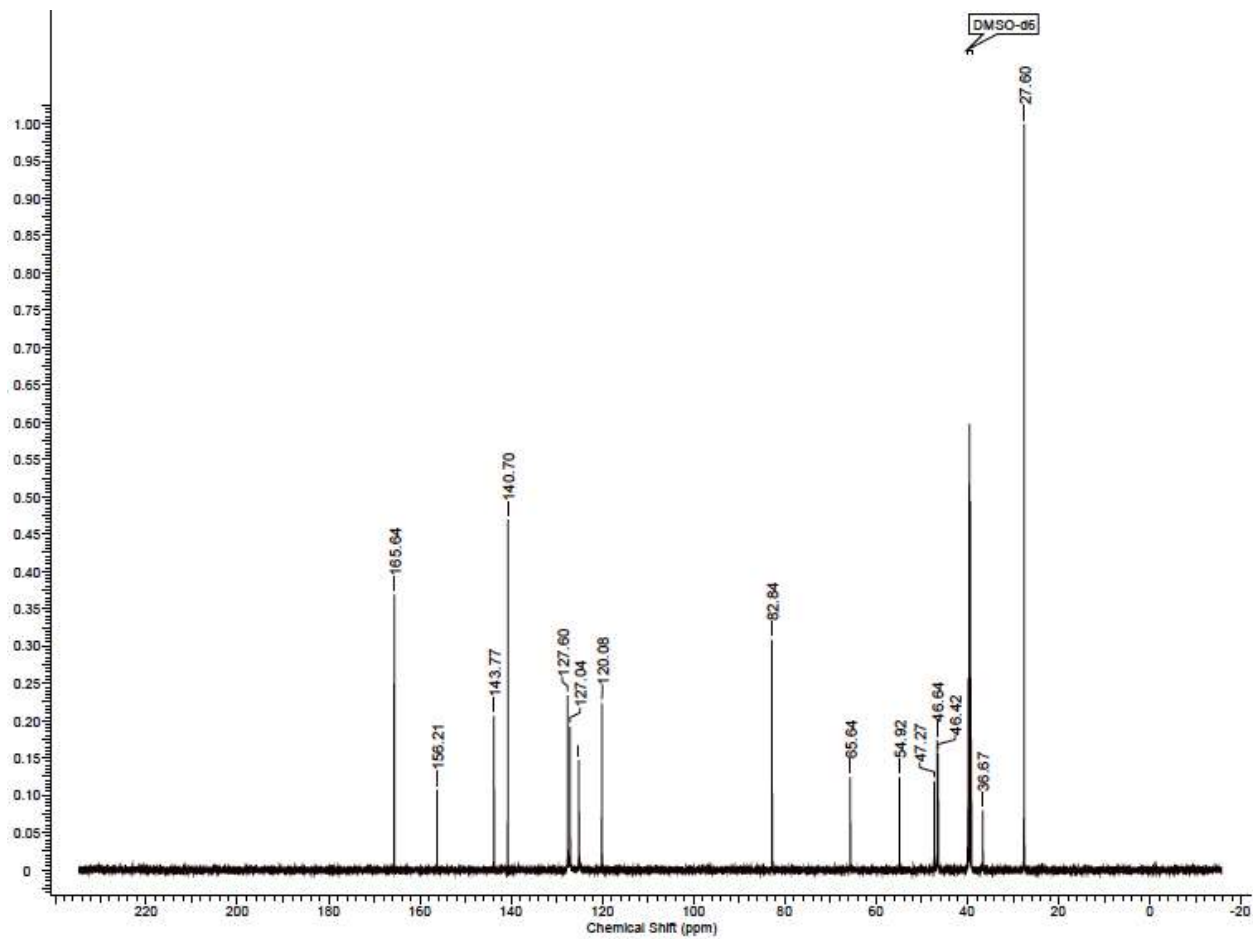


Figure S34  $^{13}\text{C}$  NMR of *N*-(2-(((9*H*-Fluoren-9-yl)methoxy)carbonyl)amino)ethyl)-2-(*tert*-butoxy)-2-oxoethanaminium chloride (II-6).

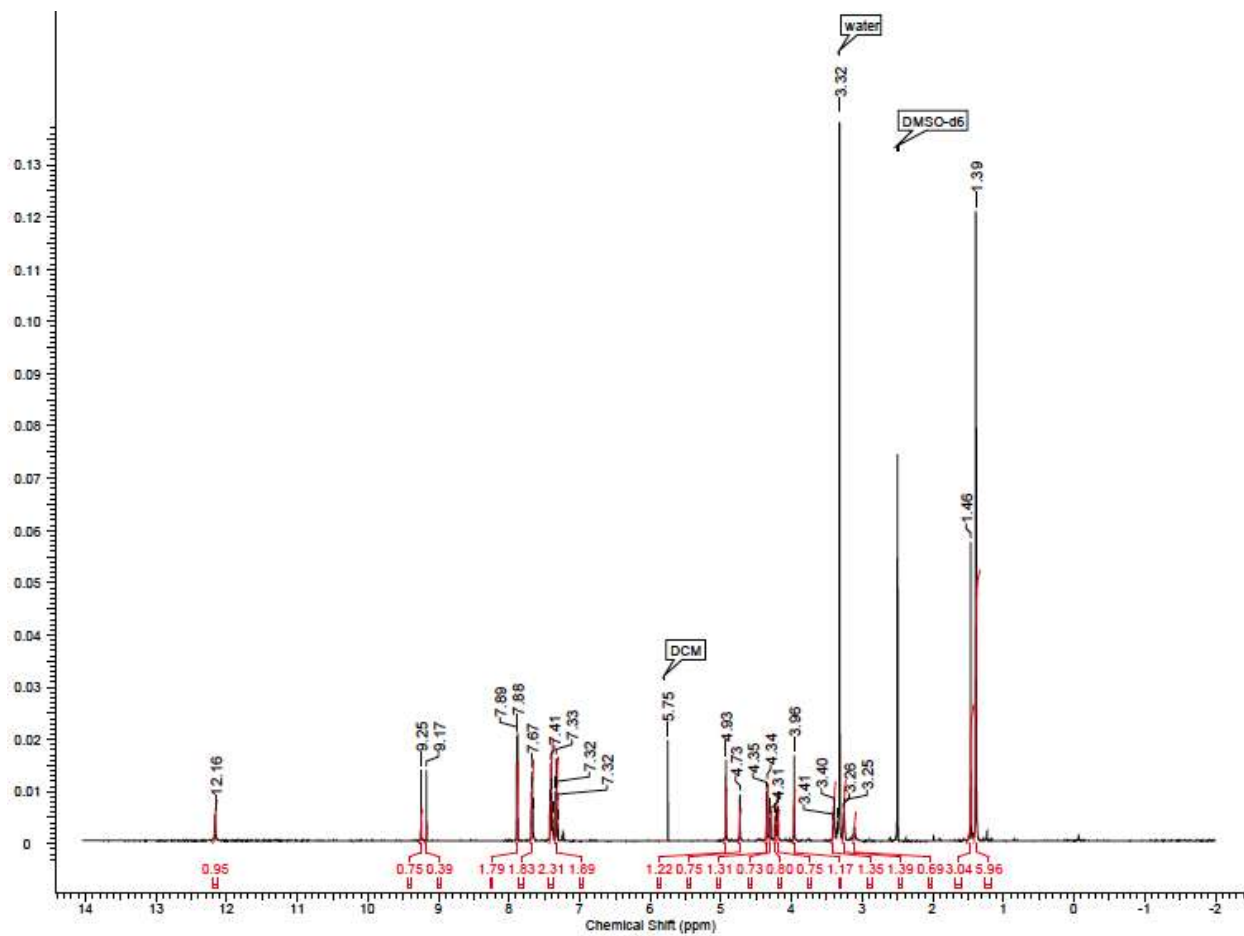


Figure S35 <sup>1</sup>H NMR of *tert*-Butyl 2-(*N*-(2-(((9*H*-fluoren-9-yl)methoxy)carbonyl)amino)ethyl)-2-(5-nitrouracil-1-yl)-acetamido)acetate (II-7).



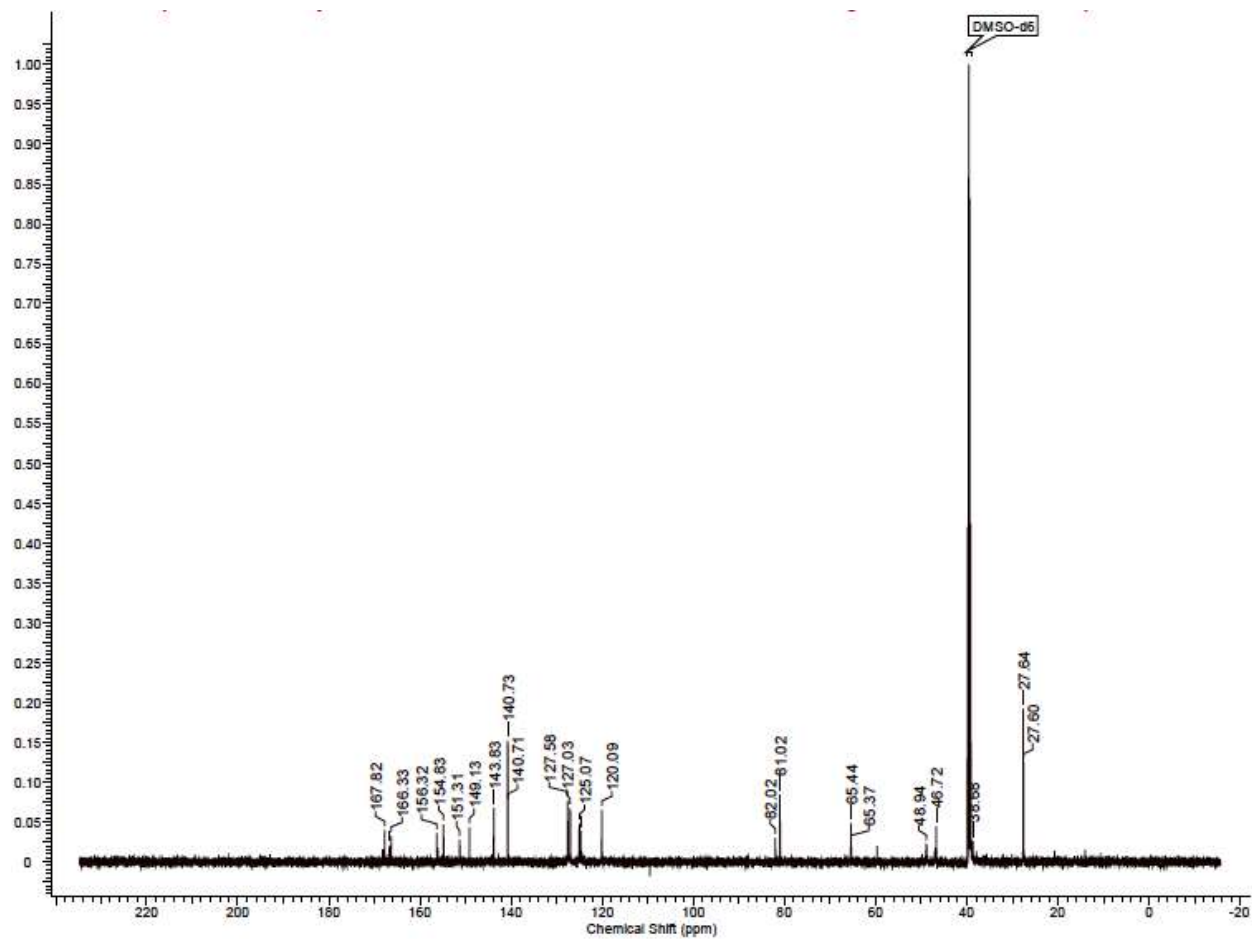
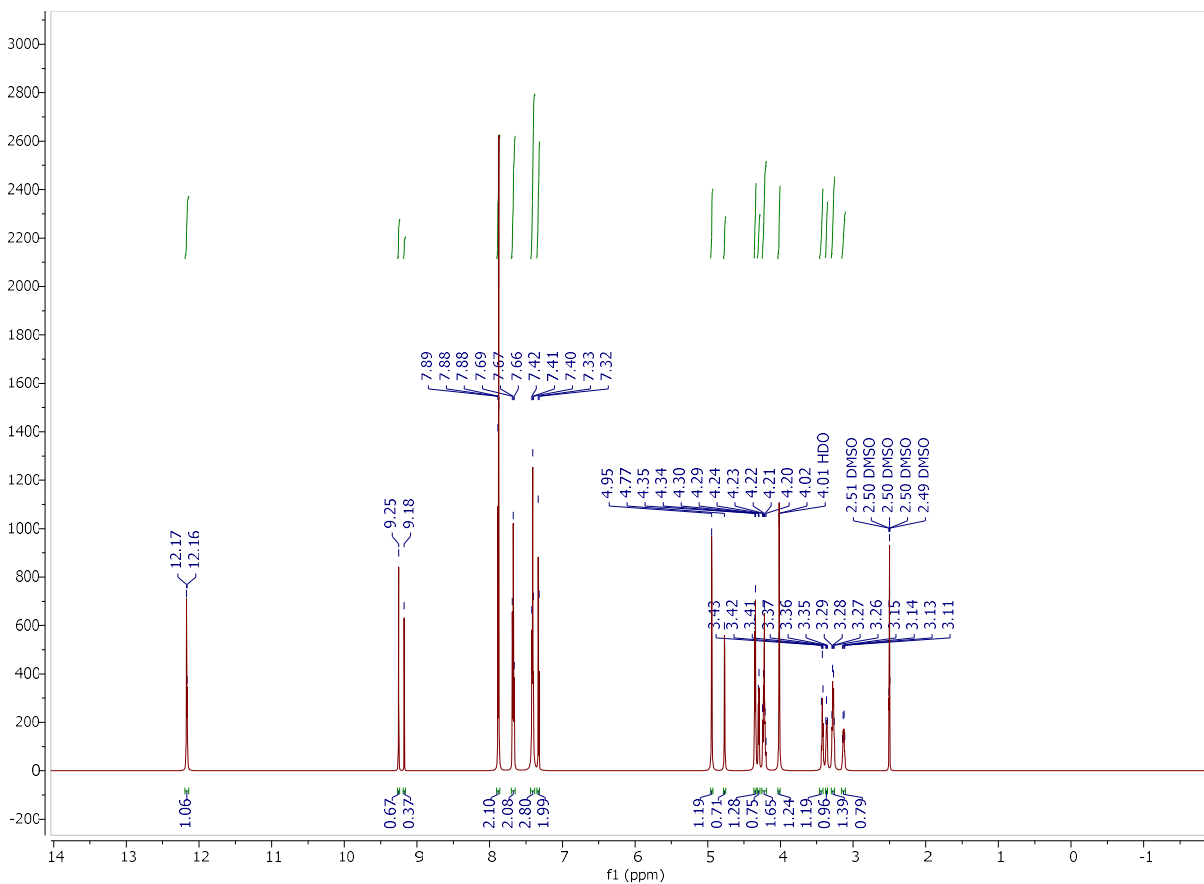


Figure S36  $^{13}\text{C}$  NMR of *tert*-Butyl 2-(*N*-(2-(((9*H*-fluoren-9-yl)methoxy)carbonyl)amino)ethyl)-2-(5-nitouracil-1-yl)-acetamido)acetate (II-7).



**Figure S37  $^1\text{H}$  NMR of 2-(N-(2-(((9H-Fluoren-9-yl)methoxy)carbonyl)amino)ethyl)-2-(5-nitouracil-1-yl)acetamido)acetic acid (II-8).**

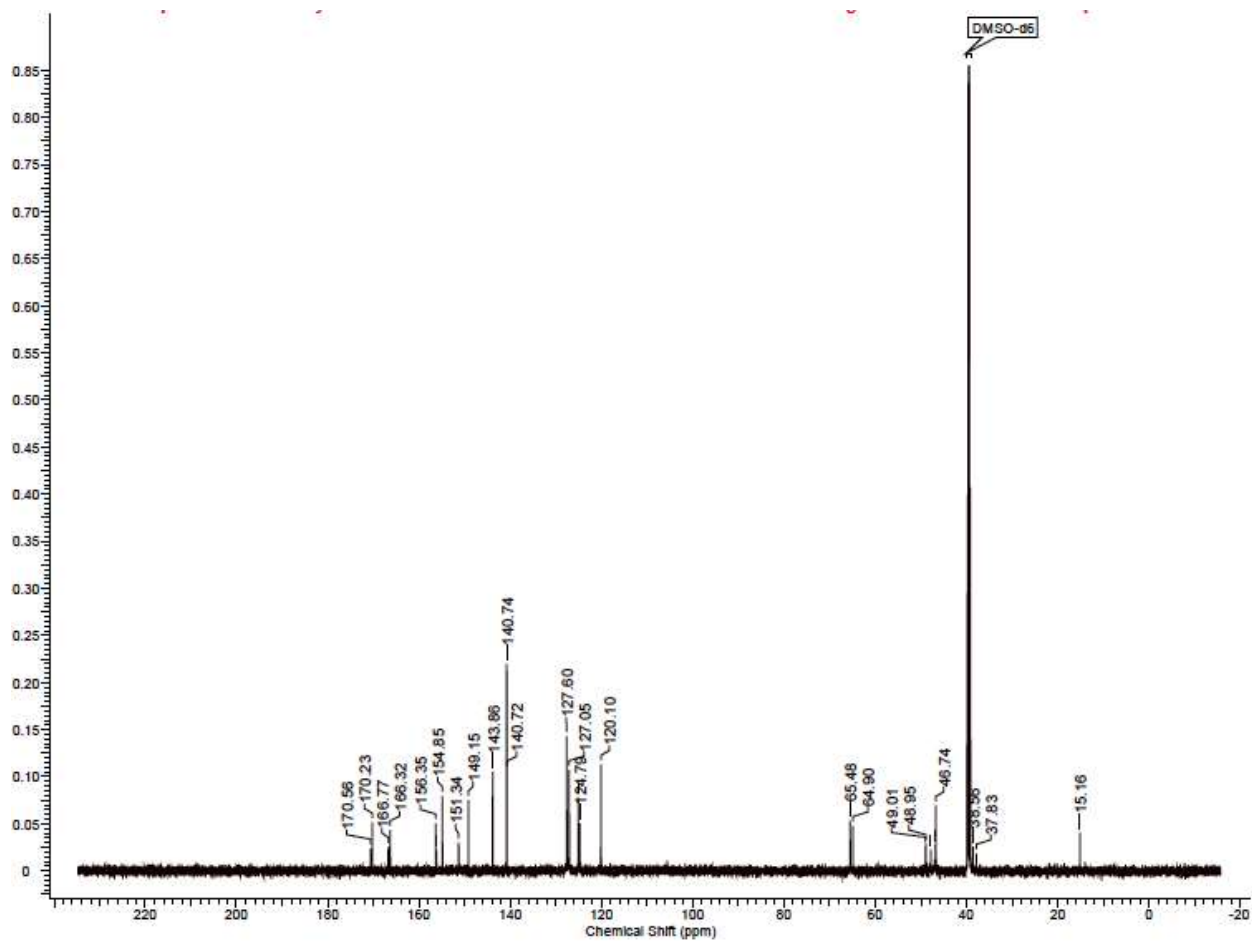


Figure S38  $^{13}\text{C}$  NMR of 2-(N-(2-(((9H-fluoren-9-yl)methoxy)carbonyl)amino)ethyl)-2-(5-nitouracil-1-yl)acetamido)acetic acid (II-8).

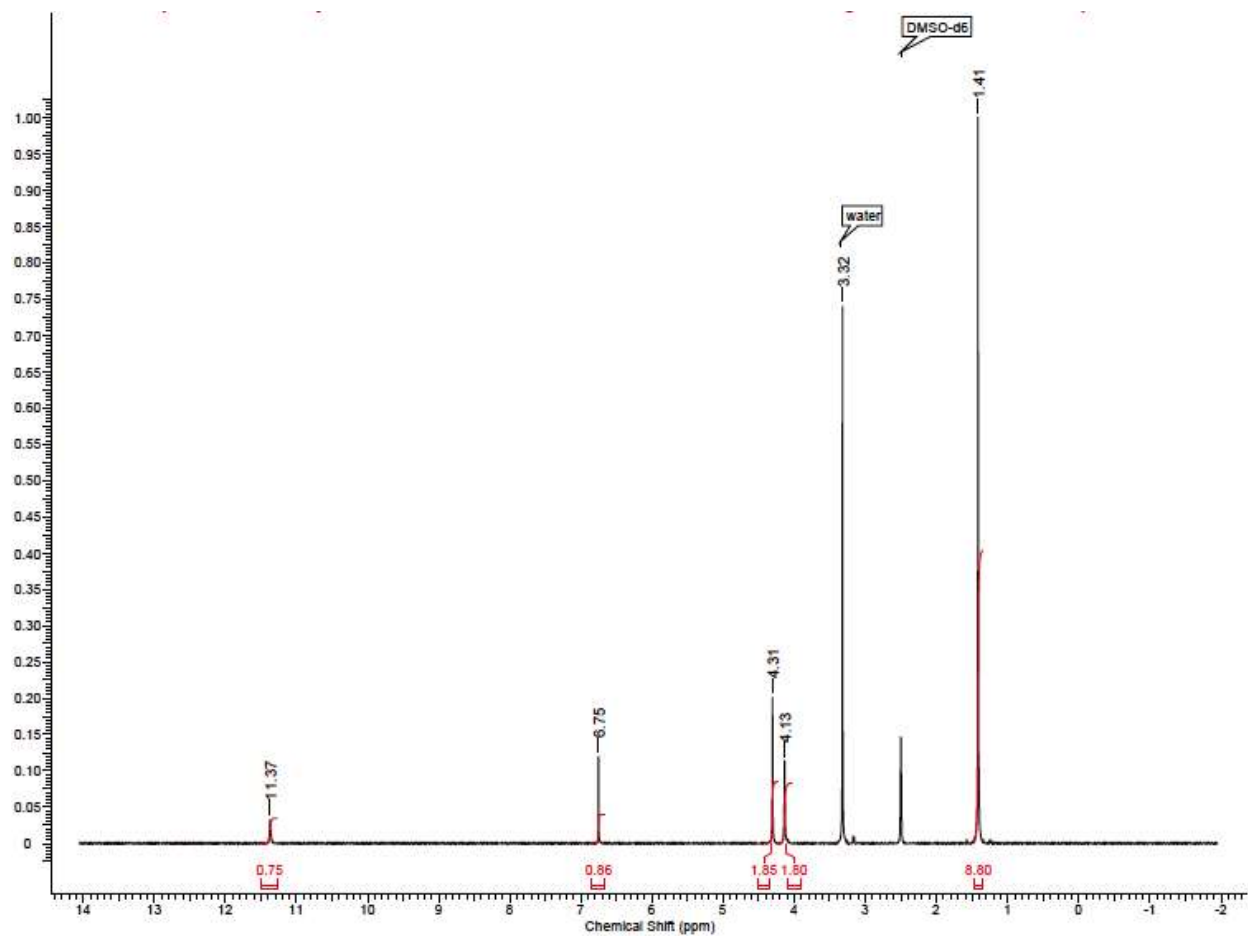


Figure S39 <sup>1</sup>H NMR of *tert*-butyl 2-(5-aminouracil-1-yl)acetate (II-9).

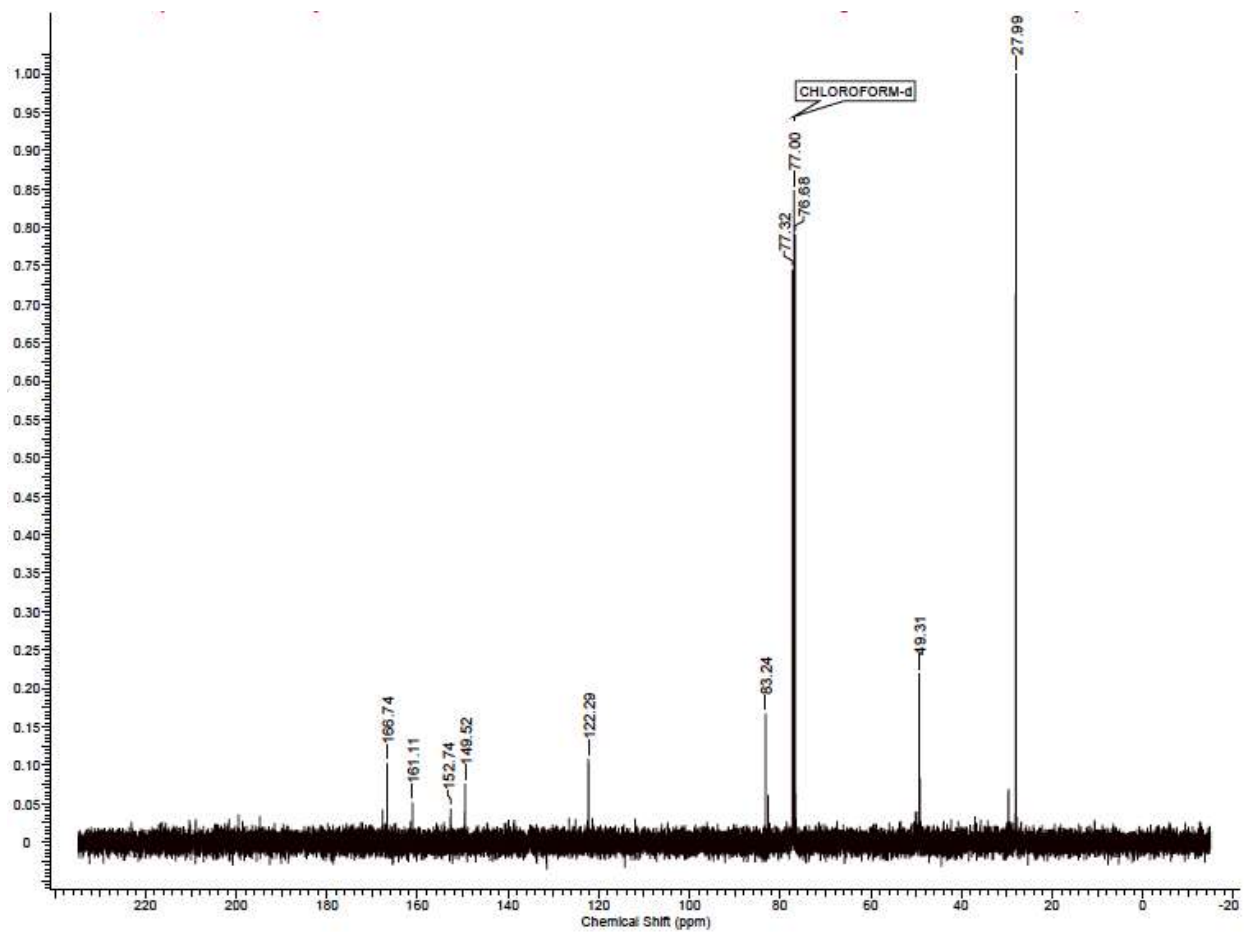


Figure S40  $^{13}\text{C}$  NMR of *tert*-butyl 2-(5-aminouracil-1-yl)acetate (II-9).

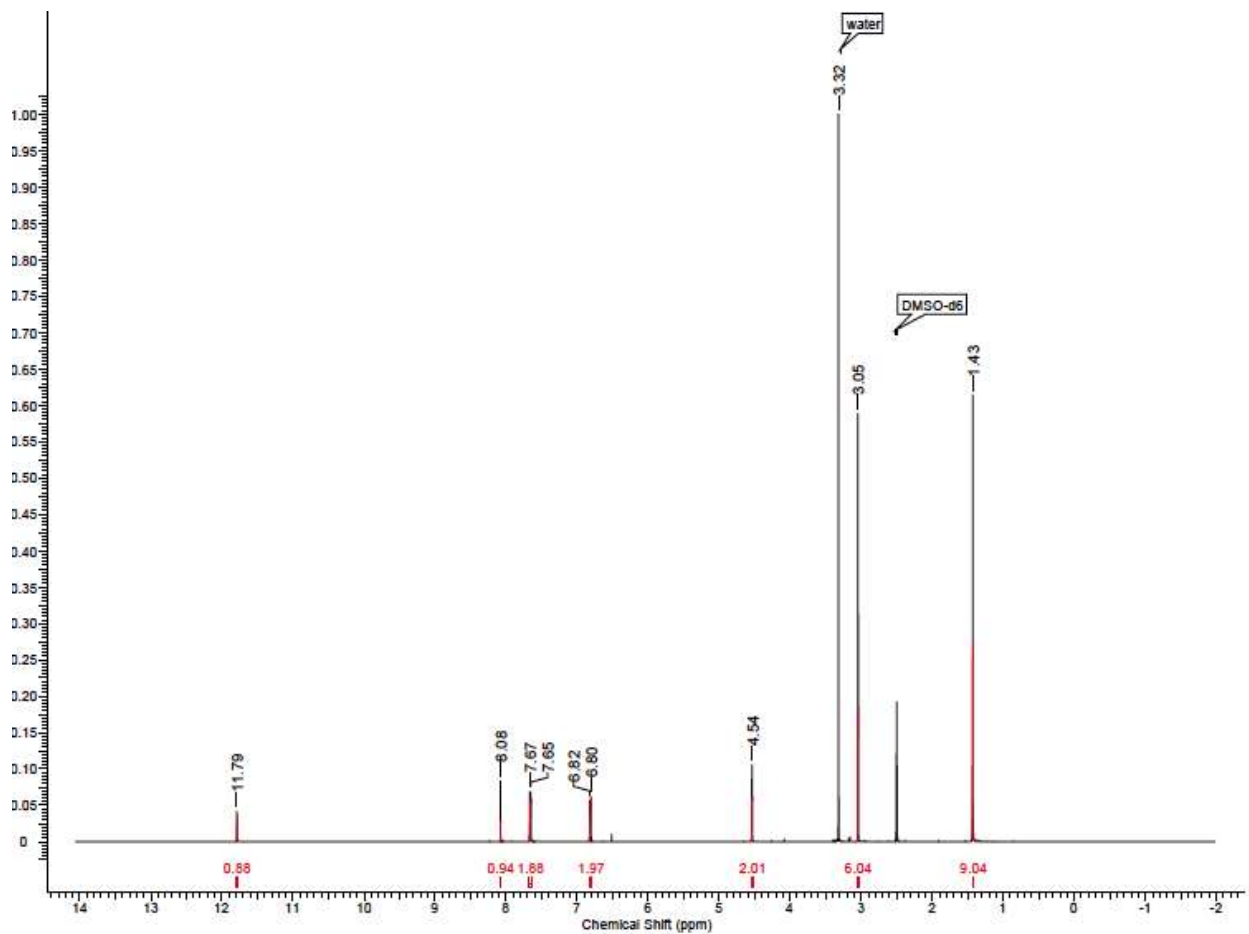


Figure S41 <sup>1</sup>H NMR of *tert*-Butyl 2-(5-[(4'(N,N-dimethylamino)phenyl)diazenyl]-uracil-1-yl)acetate (II-11).

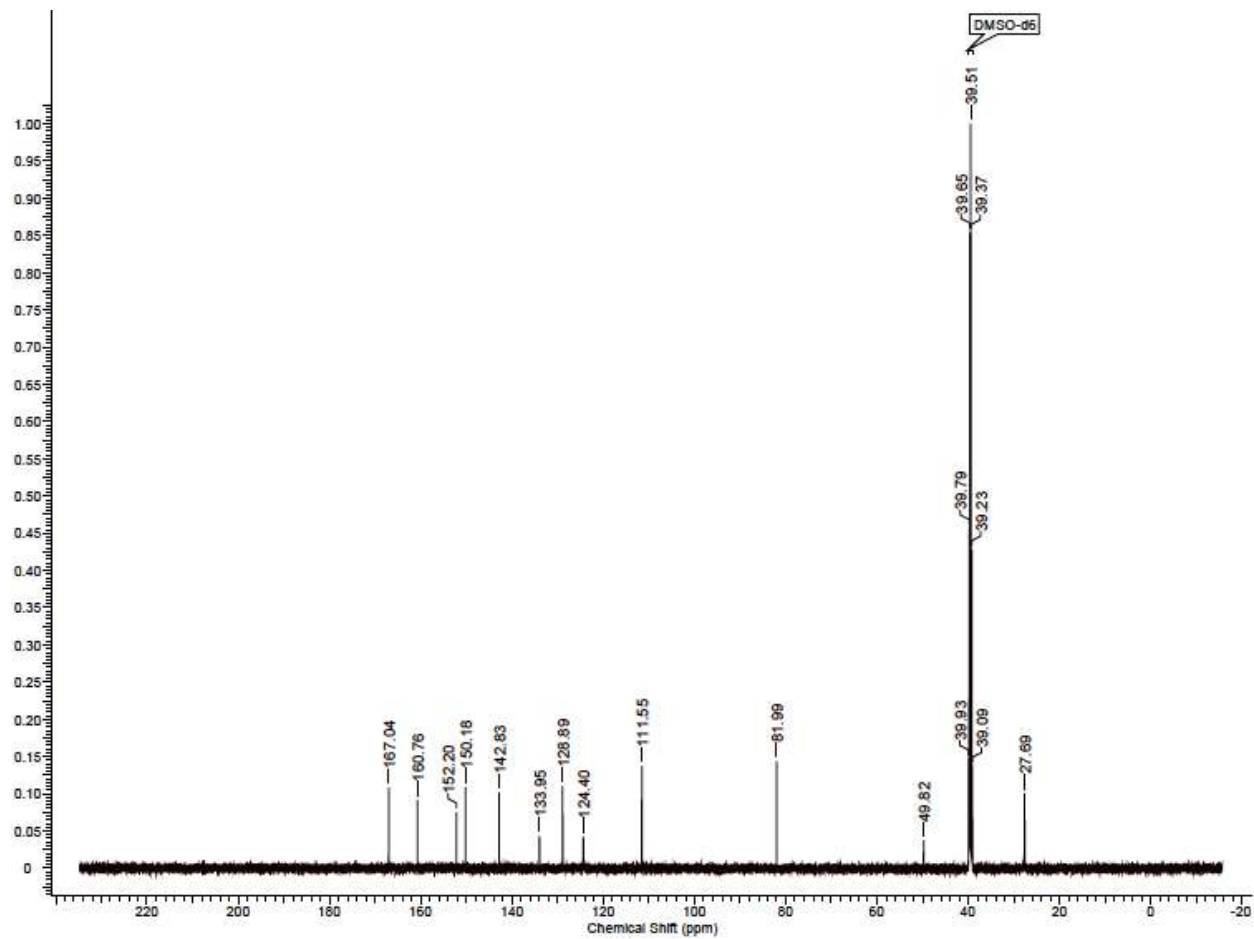


Figure S42  $^{13}\text{C}$  NMR of *tert*-Butyl 2-(5-[(4'(N,N-dimethylamino)phenyl)diazenyl]-uracil-1-yl)acetate (II-11).

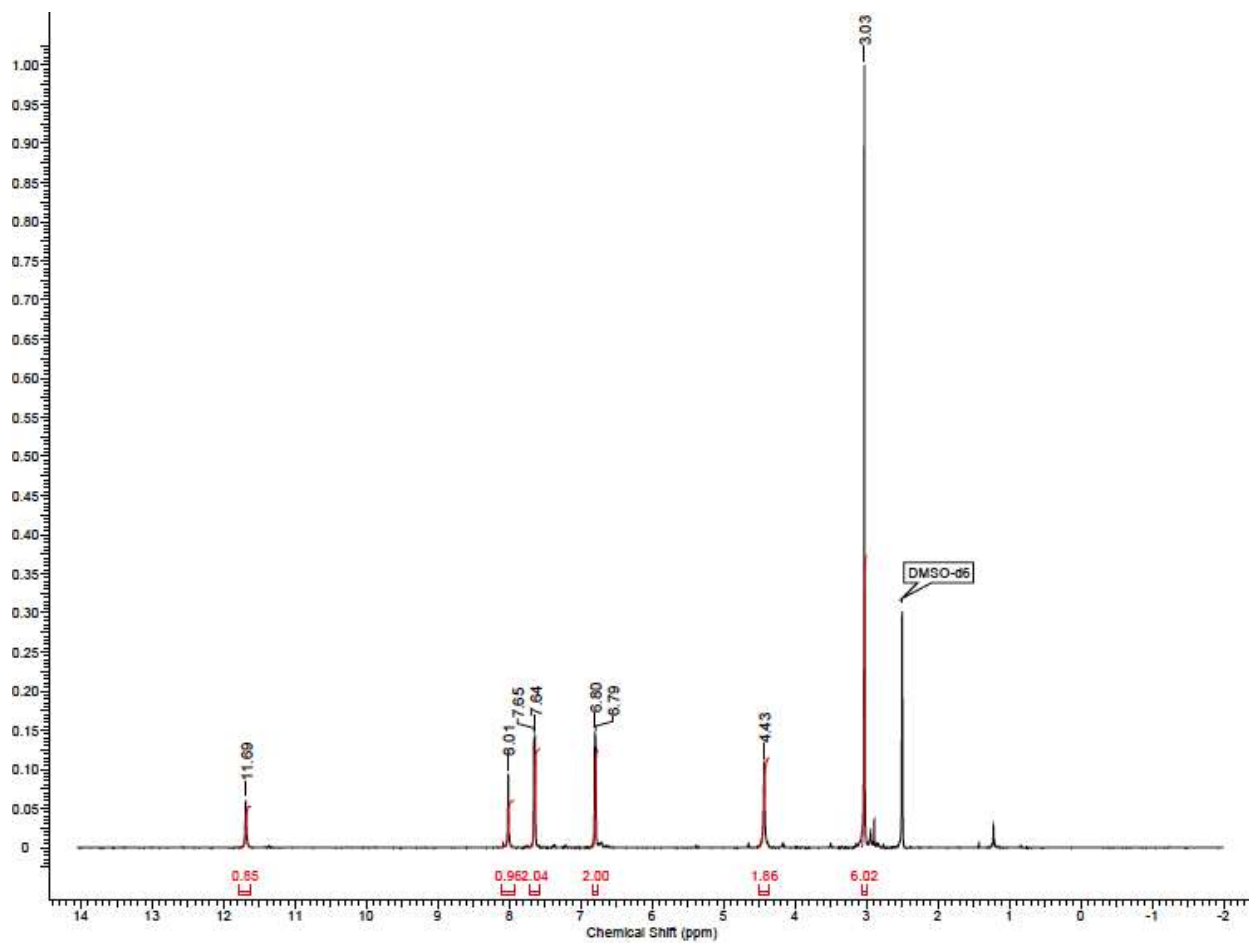


Figure S43 <sup>1</sup>H NMR of 2-(5-[(4'(N,N-dimethylamino)phenyl)diazenyl])-uracil-1-yl)acetic acid (II-12).



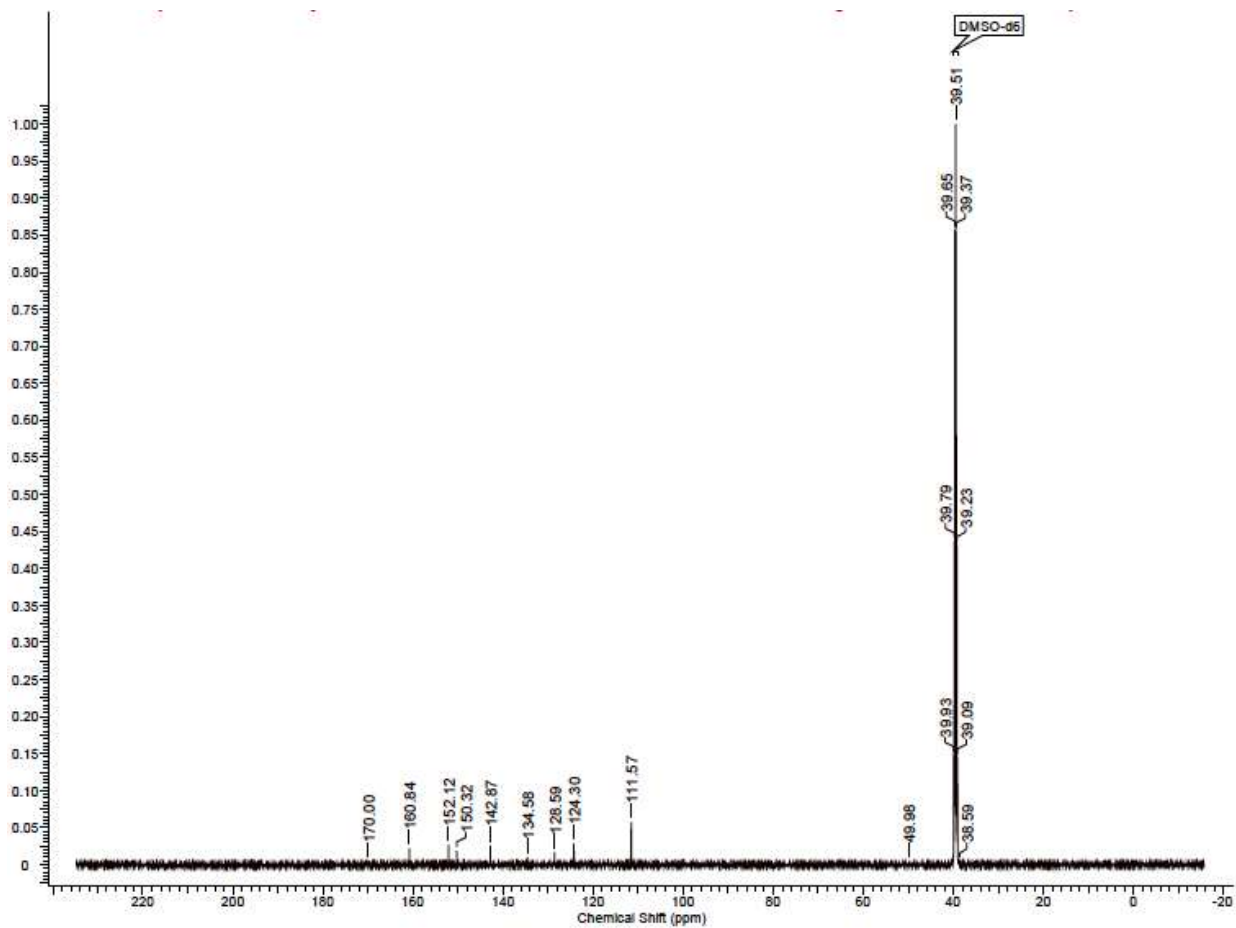
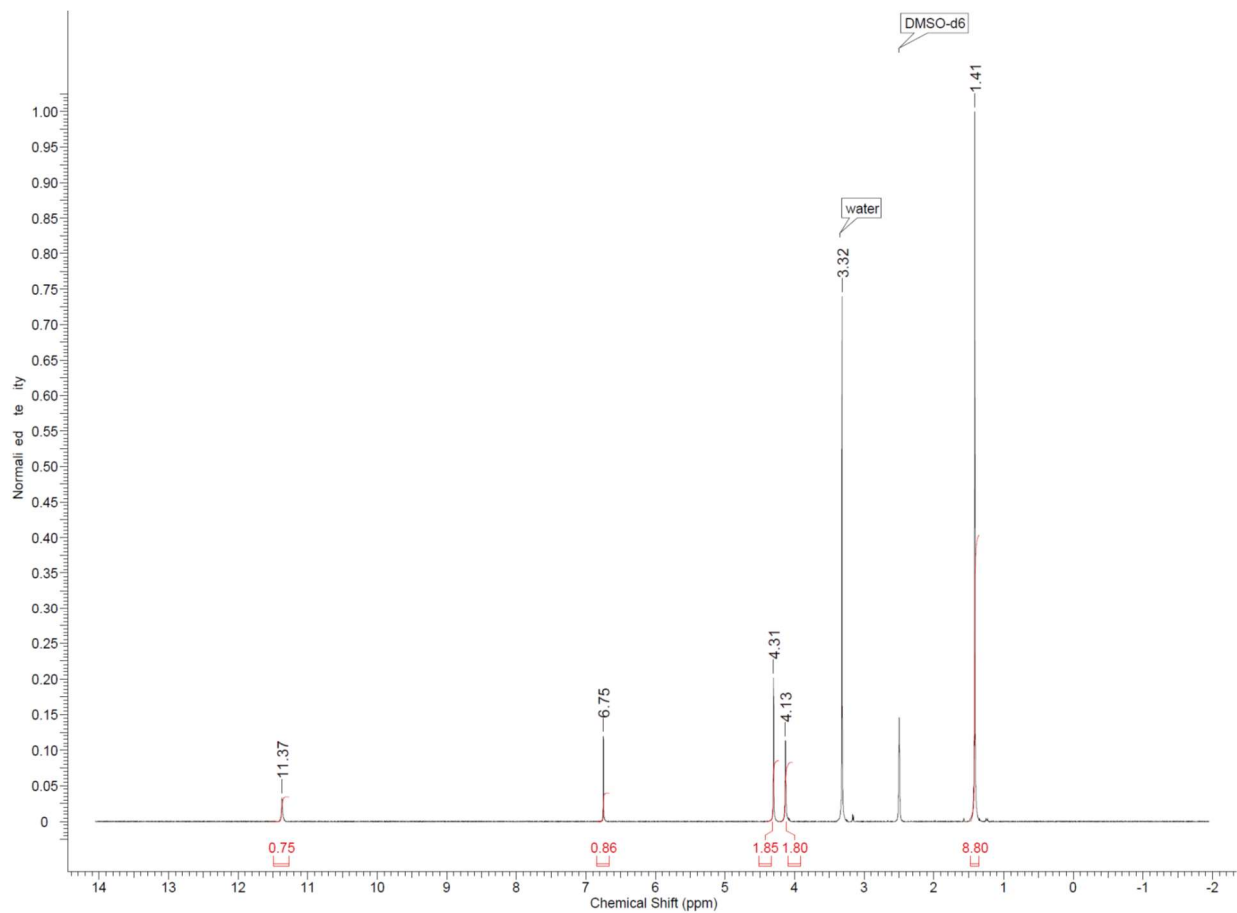


Figure S44  $^{13}\text{C}$  NMR of 2-(5-[(4'(N,N-dimethylamino)phenyl)diazenyl])-uracil-1-yl)acetic acid (II-12).



**Figure S45** <sup>1</sup>H NMR of tert-butyl 2-(5-aminouracil-1-yl)acetate (III-3).

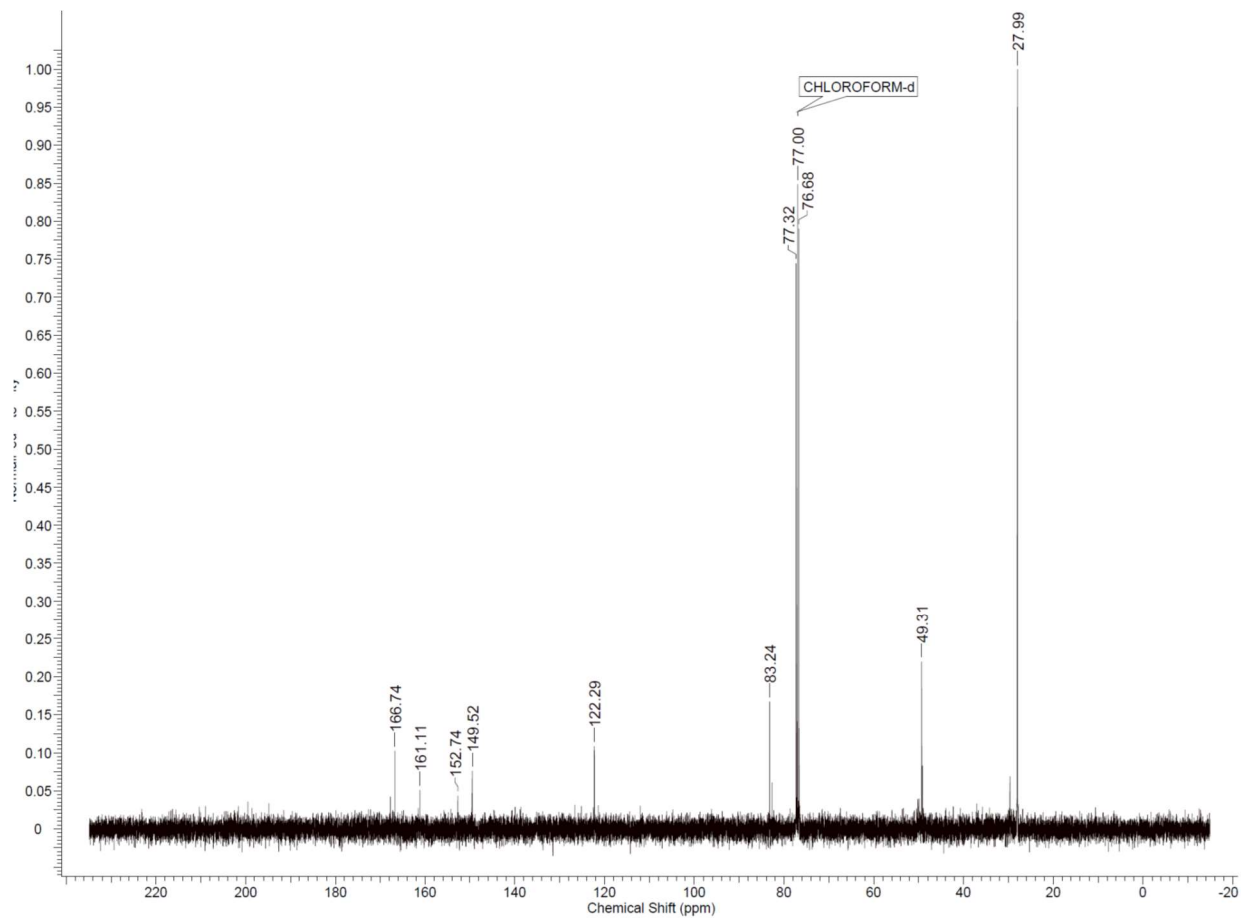
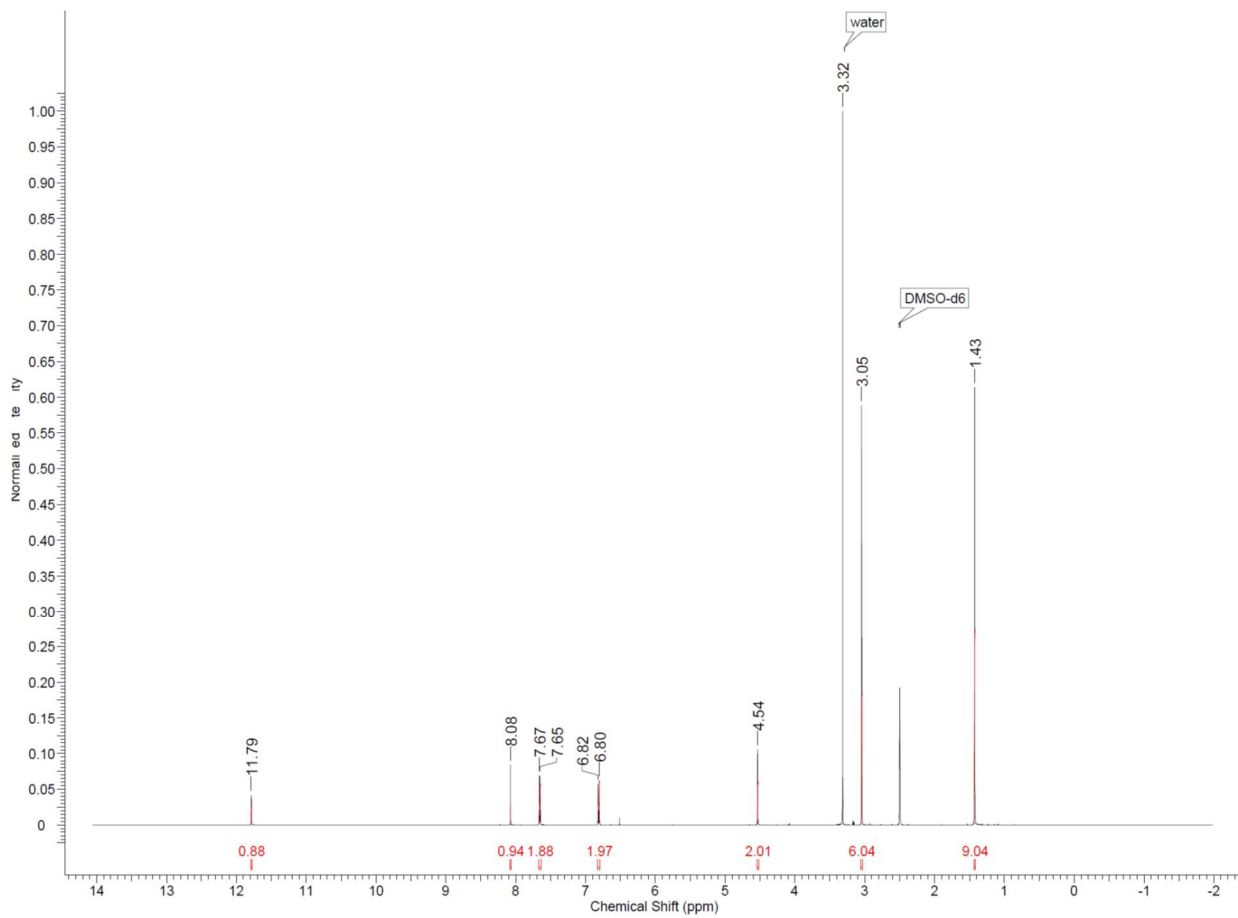


Figure S46  $^{13}\text{C}$  NMR of *tert*-butyl 2-(5-aminouracil-1-yl)acetate (III-3).



**Figure S47** <sup>1</sup>H NMR of *tert*-Butyl 2-(5-((4-(*N,N*-dimethylamino)phenyl)diazenyl)uracil-1-yl)acetate (III-5).

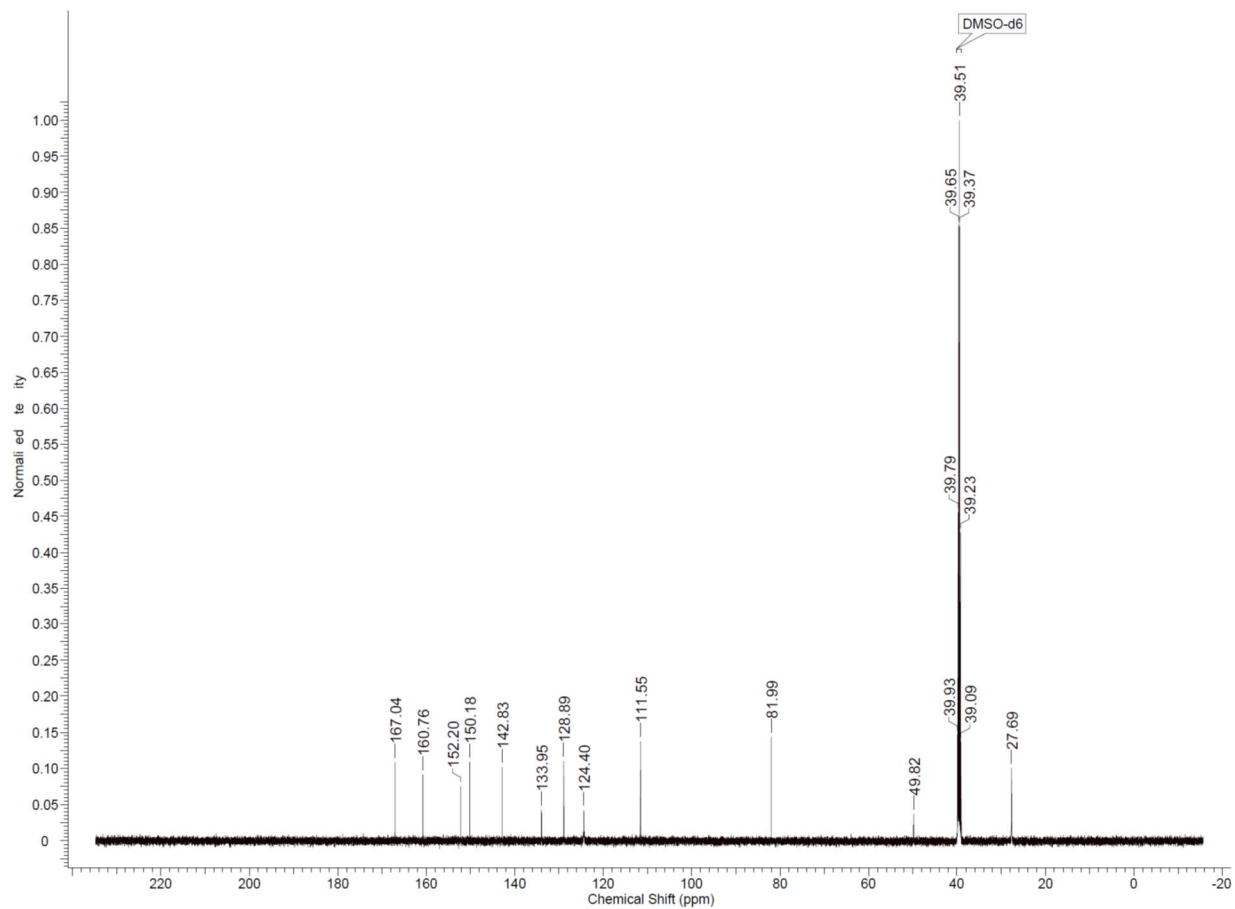
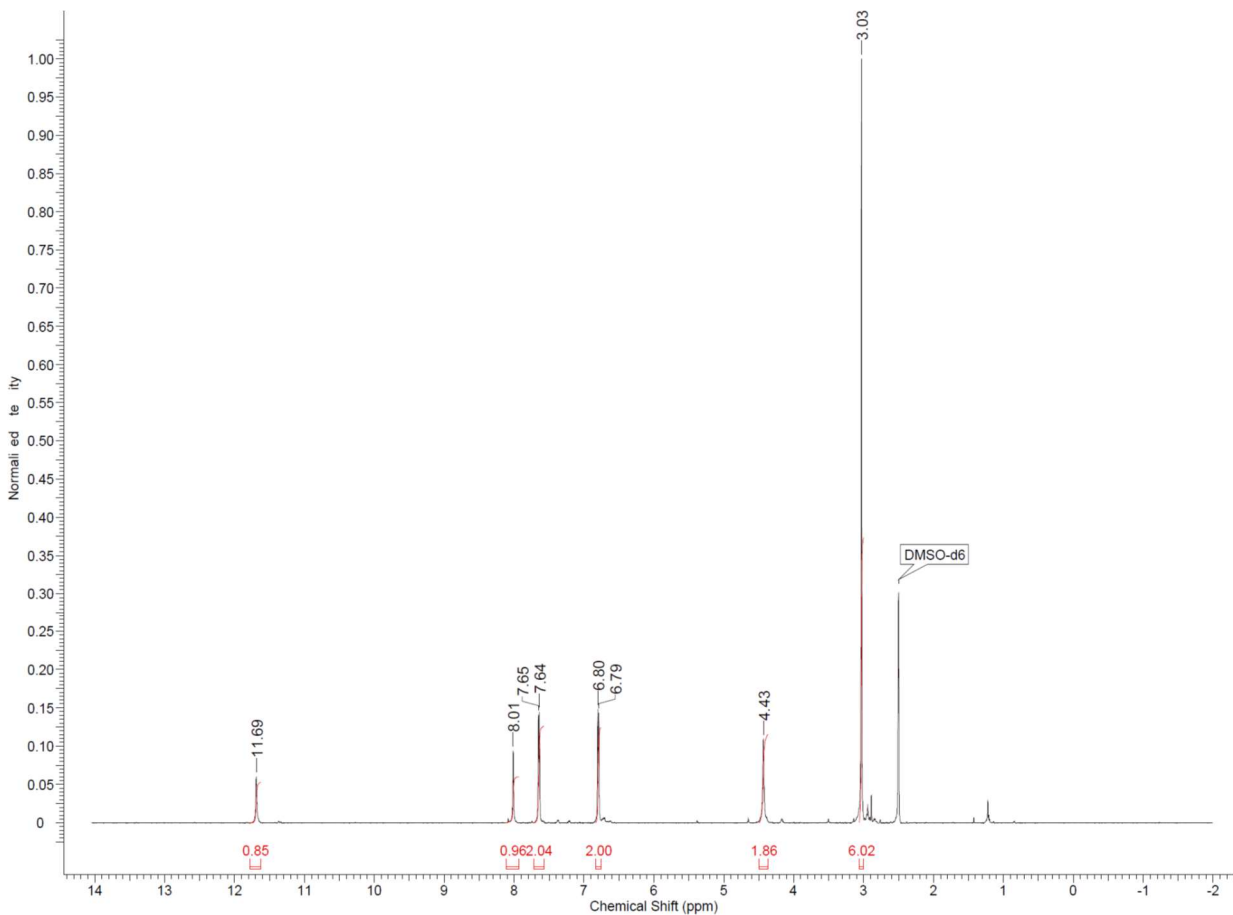
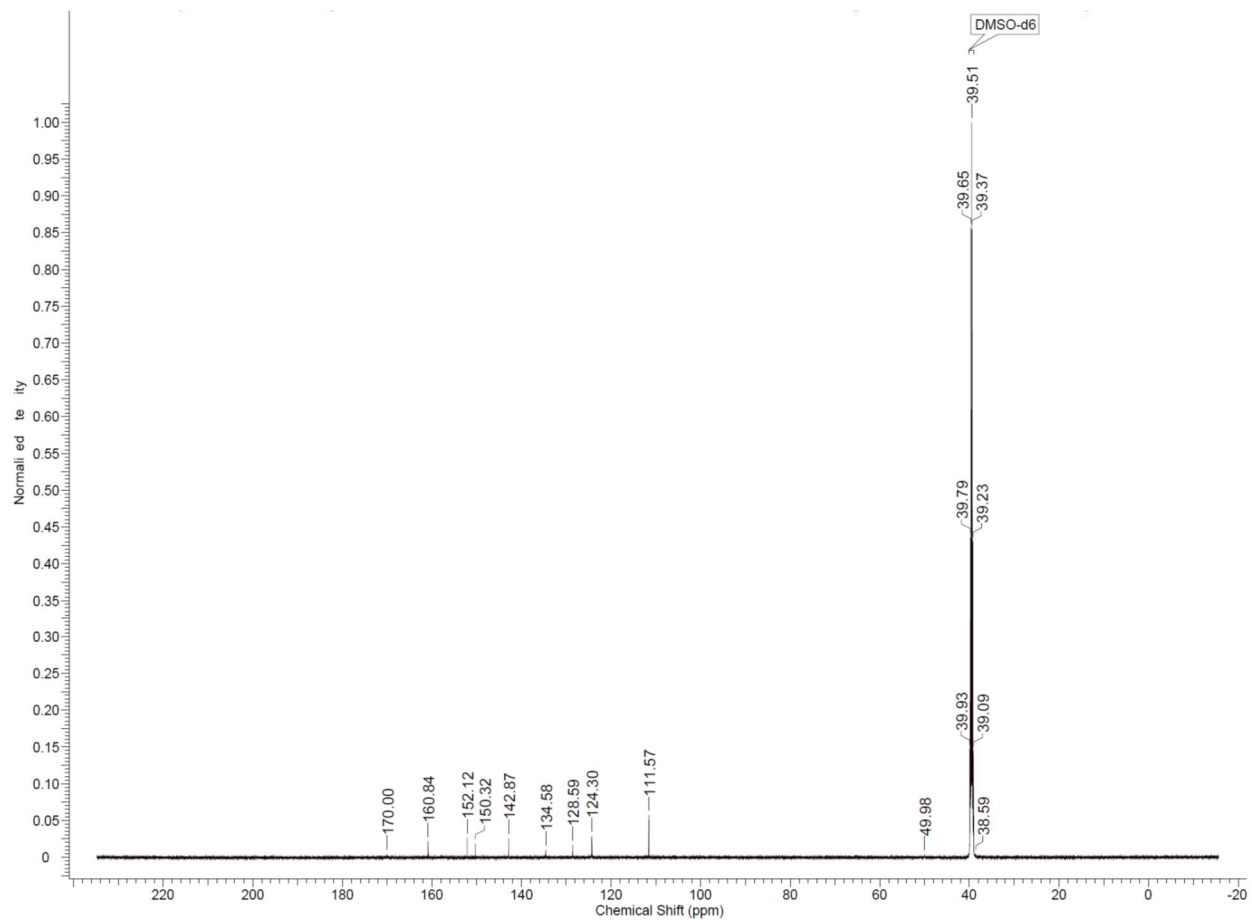


Figure S48  $^{13}\text{C}$  NMR of *tert*-Butyl 2-(5-((4-(*N,N*-dimethylamino)phenyl)diazenyl)uracil-1-yl)acetate (III-5).



**Figure S49** <sup>1</sup>H NMR of 2-(5-((4-(*N,N*-dimethylamino)phenyl)diazenyl)-uracil-1-yl)acetic acid (III-6).



**Figure S50**  $^{13}\text{C}$  NMR of 2-(5-((4-(*N,N*-dimethylamino)phenyl)diazenyl)-uracil-1-yl)acetic acid (III-6).

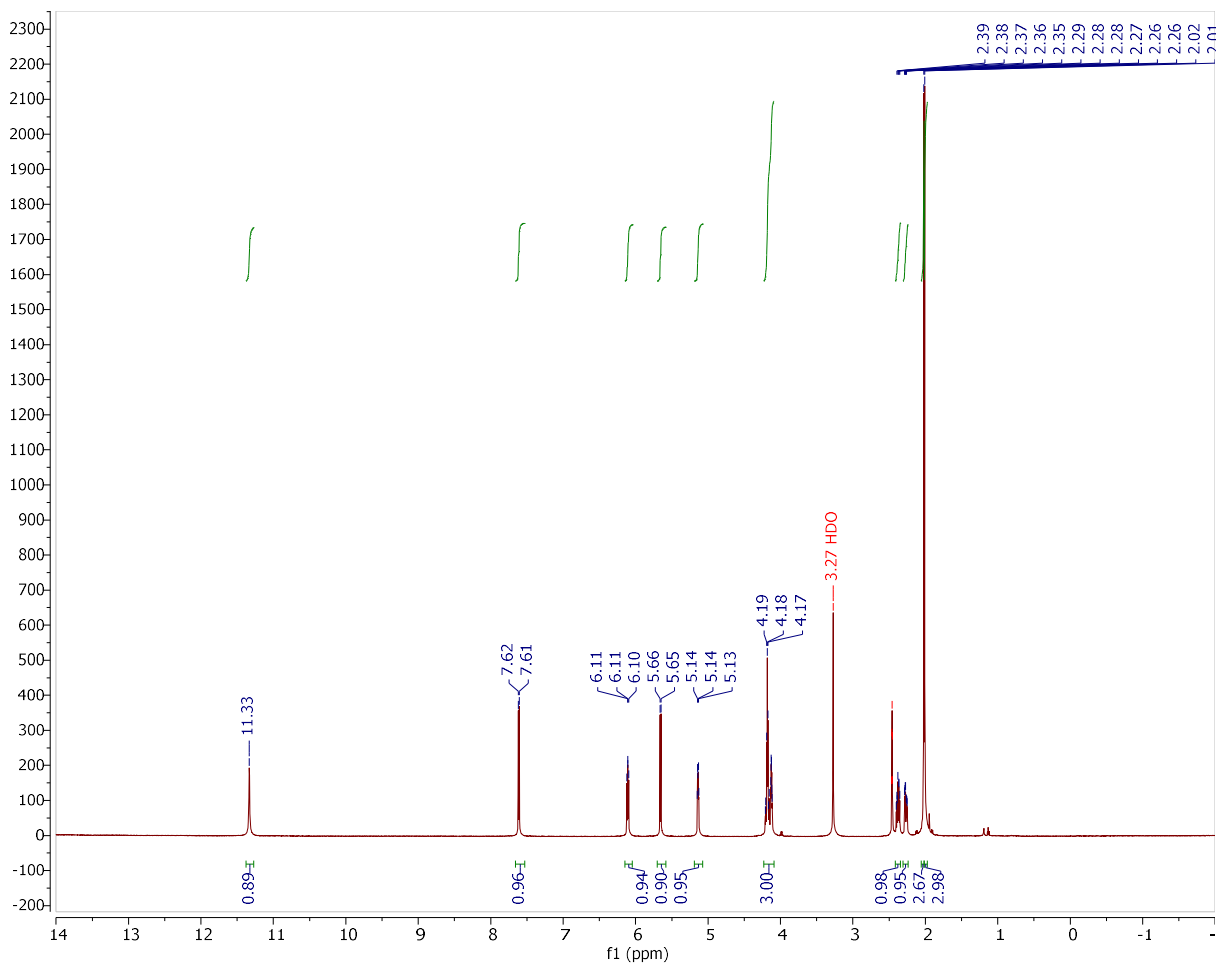


Figure S51  $^1\text{H}$  NMR of 2'-deoxyuridine-3',5'-O-diacetate (IV-2).



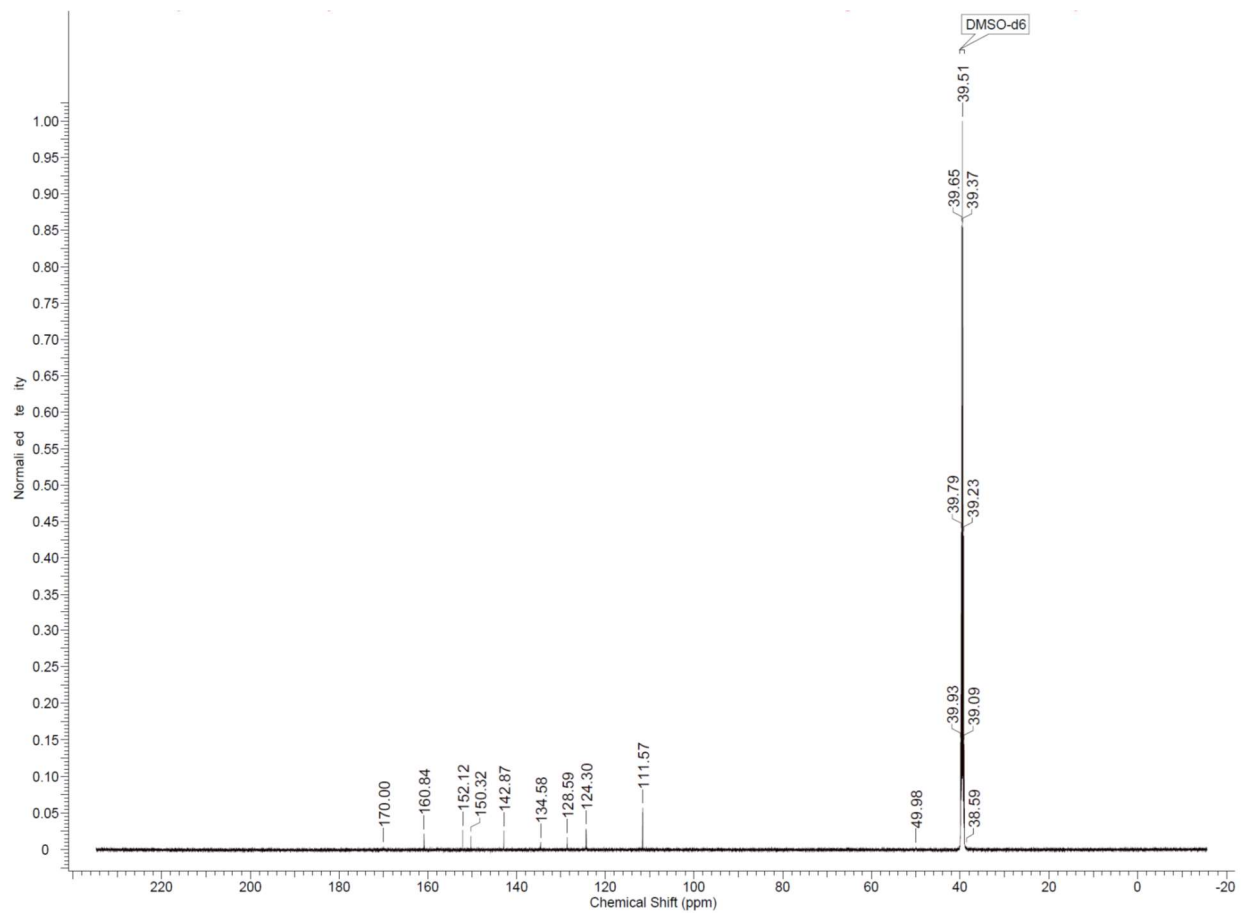


Figure S52  $^{13}\text{C}$  NMR of 2'-deoxyuridine-3',5'-O-diacetate (IV-2).

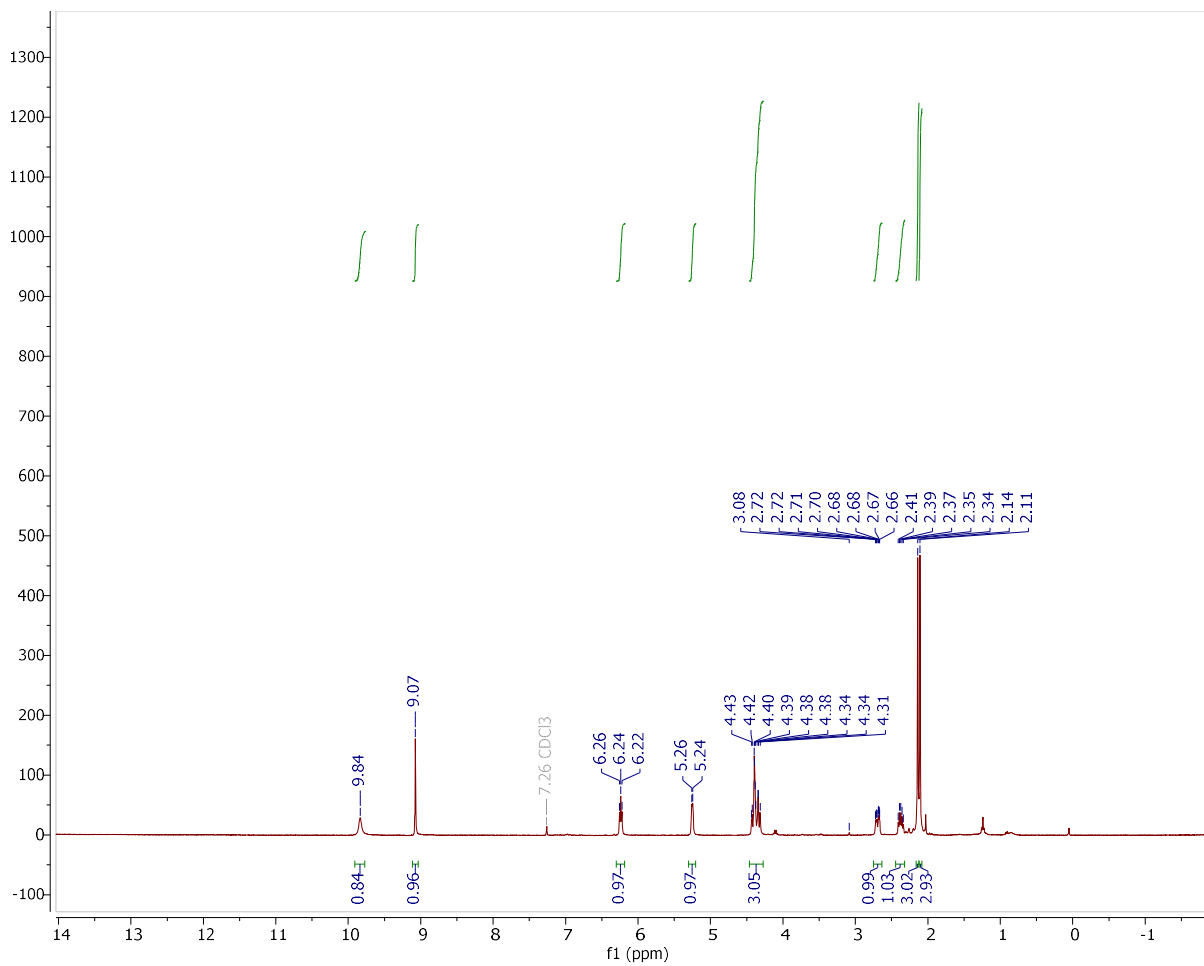


Figure S53 <sup>1</sup>H NMR of 5-nitro-2'-deoxyuridine-3',5'-O-diacetate (IV-3).

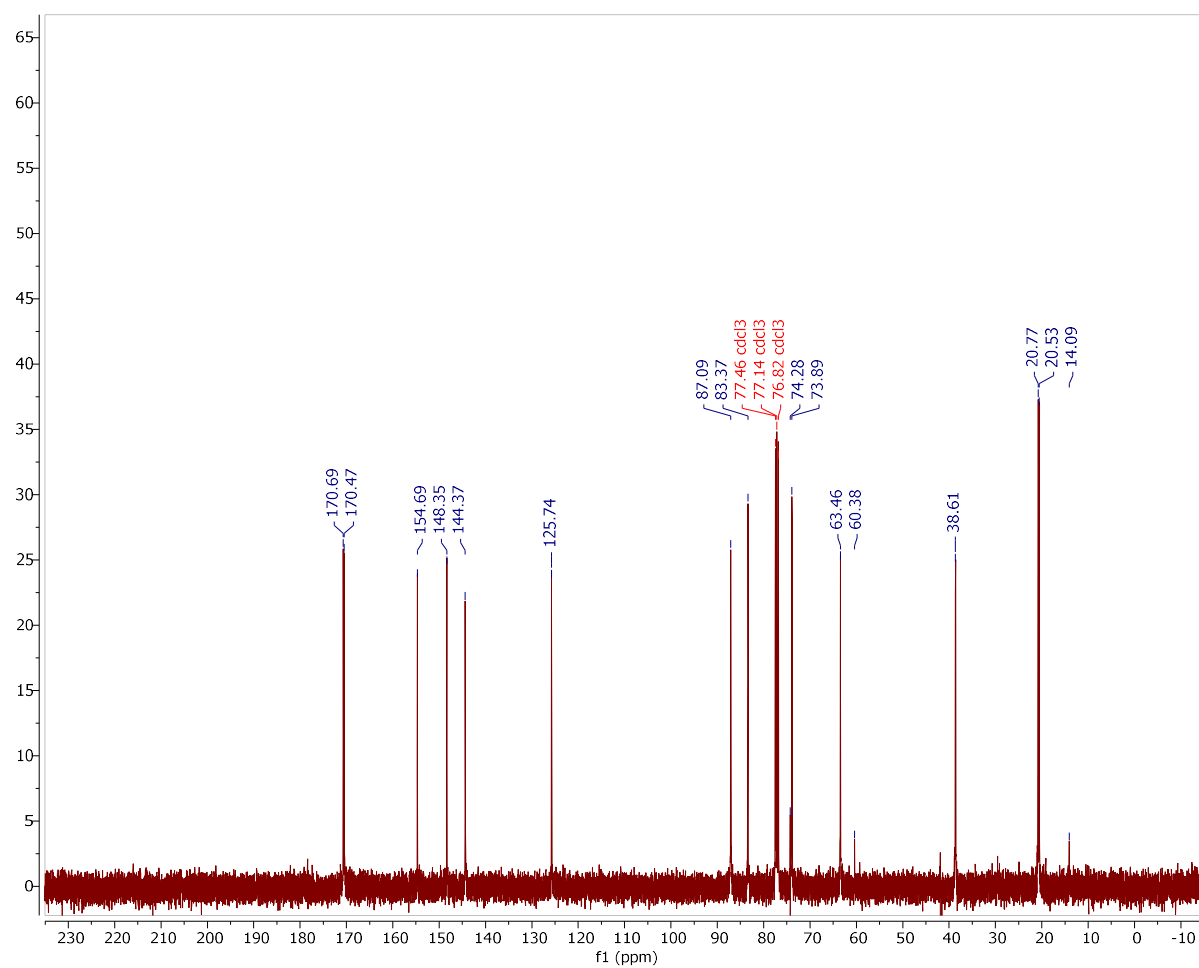


Figure S54 <sup>13</sup>C NMR of 5-nitro-2'-deoxyuridine-3',5'-O-diacetate (IV-3).

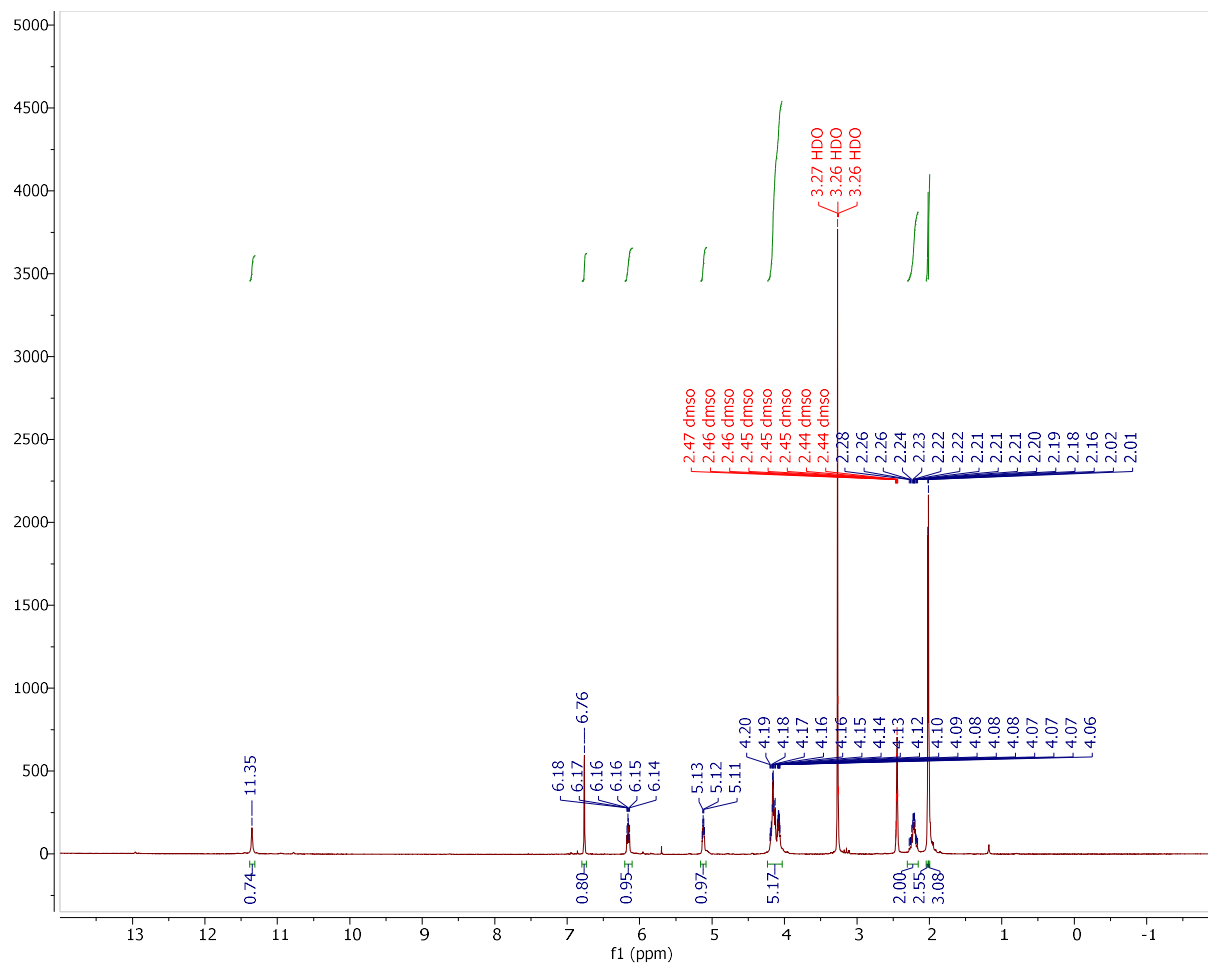


Figure S55  $^1\text{H}$  NMR of 5-amino-2'-deoxyuridine-3',5'-O-diacetate (IV-4).

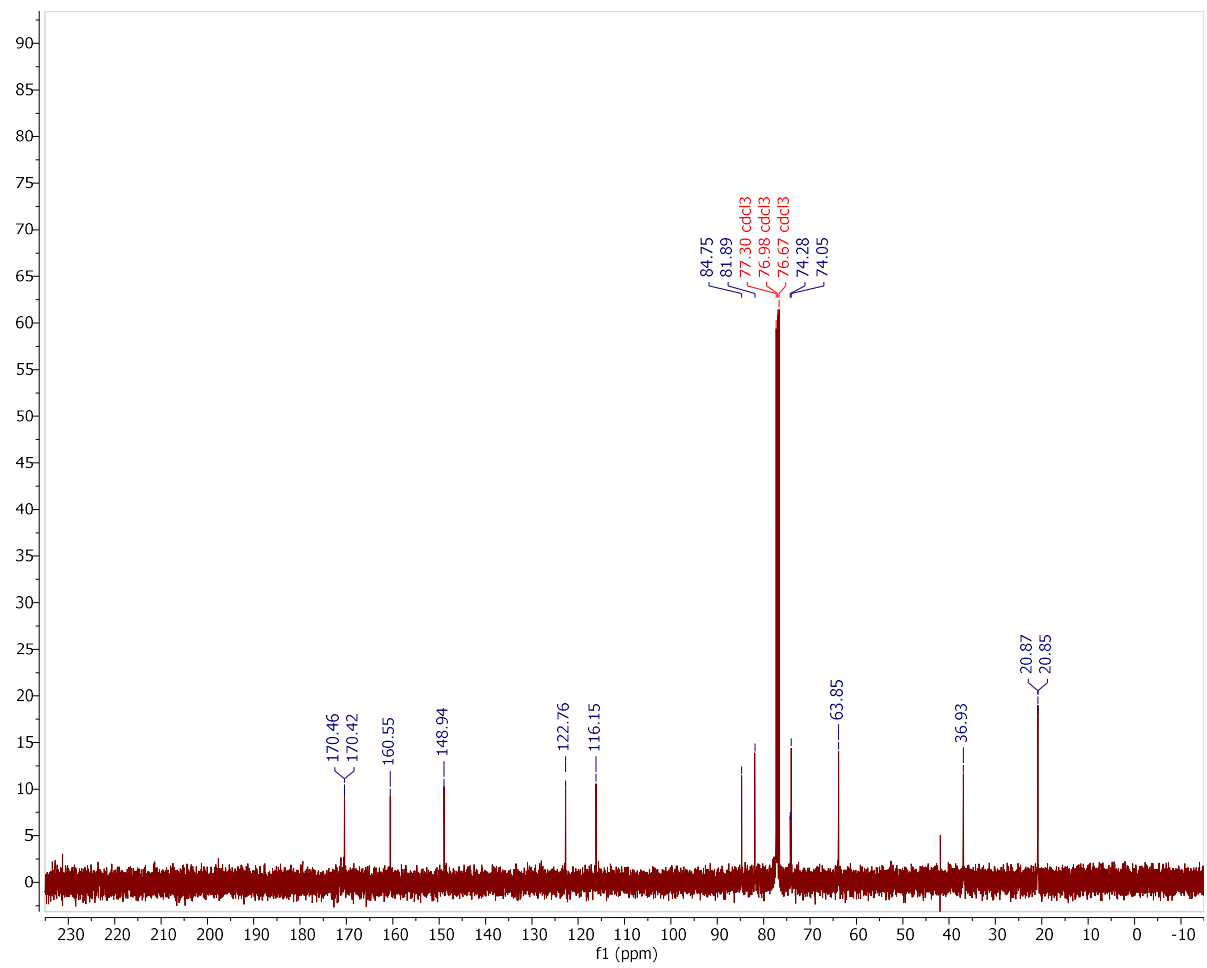
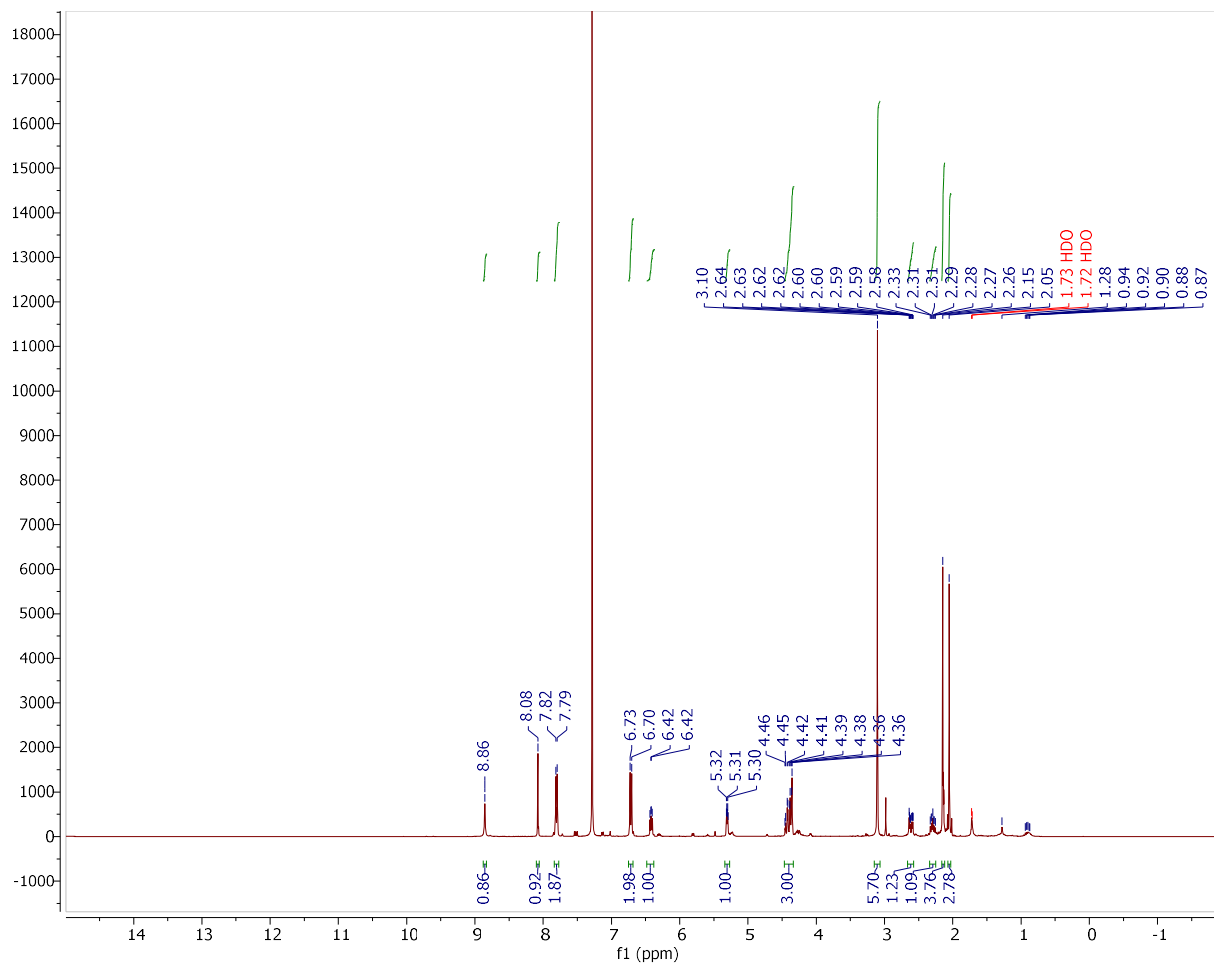
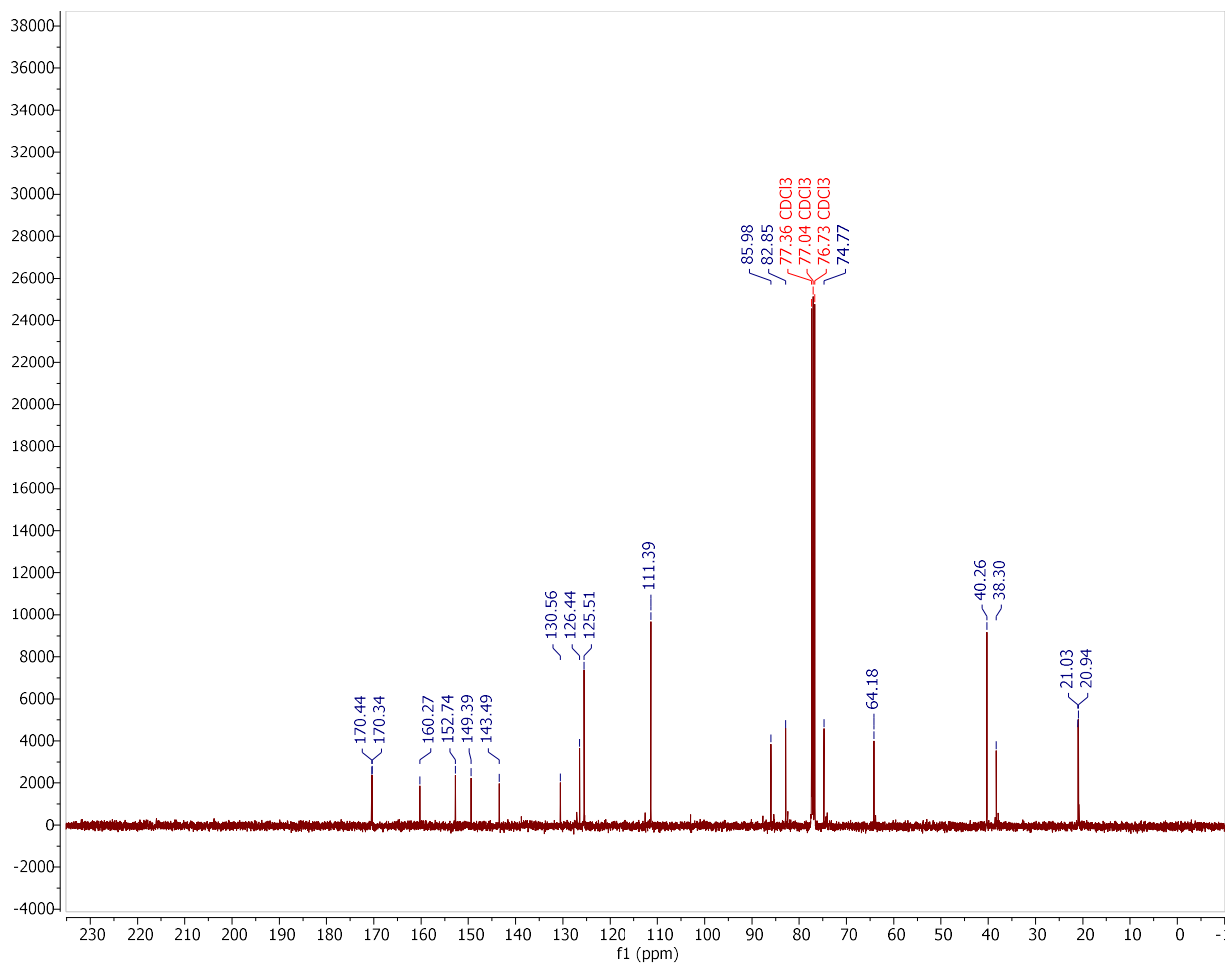


Figure S56  $^{13}\text{C}$  NMR of 5-amino-2'-deoxyuridine-3',5'-O-diacetate (IV-4).



**Figure S57**  $^1\text{H}$  NMR of 5-((4-(*N,N*-dimethylamino)phenyl)diazenyl)-2'-deoxyuridine-3',5'-*O*-diacetate (IV-5).



**Figure S58** <sup>13</sup>C NMR of 5-((4-(*N,N*-dimethylamino)phenyl)diazenyl)-2'-deoxyuridine-3',5'-*O*-diacetate (IV-5).

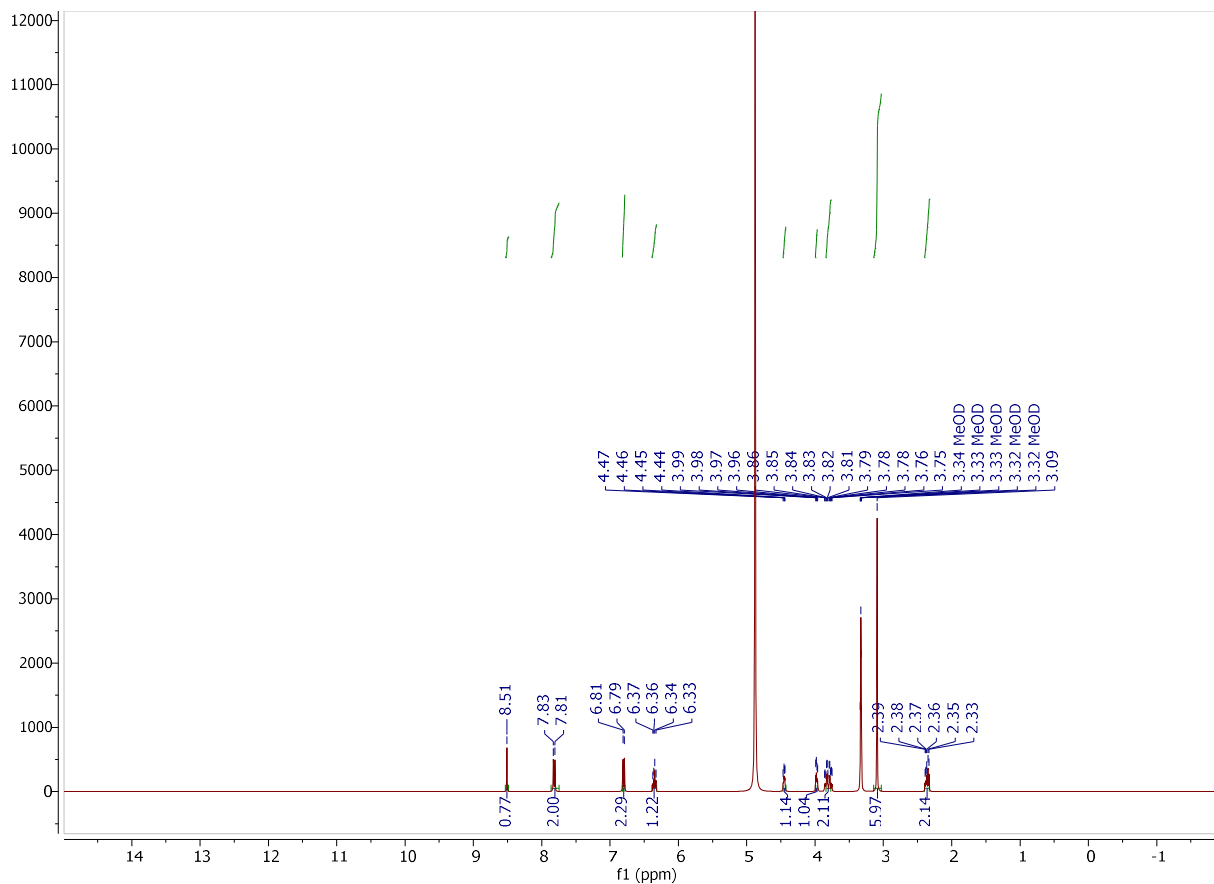


Figure S59. <sup>1</sup>H NMR of 5-((4-(*N,N*-dimethylamino)phenyl)diazenyl)-2'-deoxyuridine (IV-6).



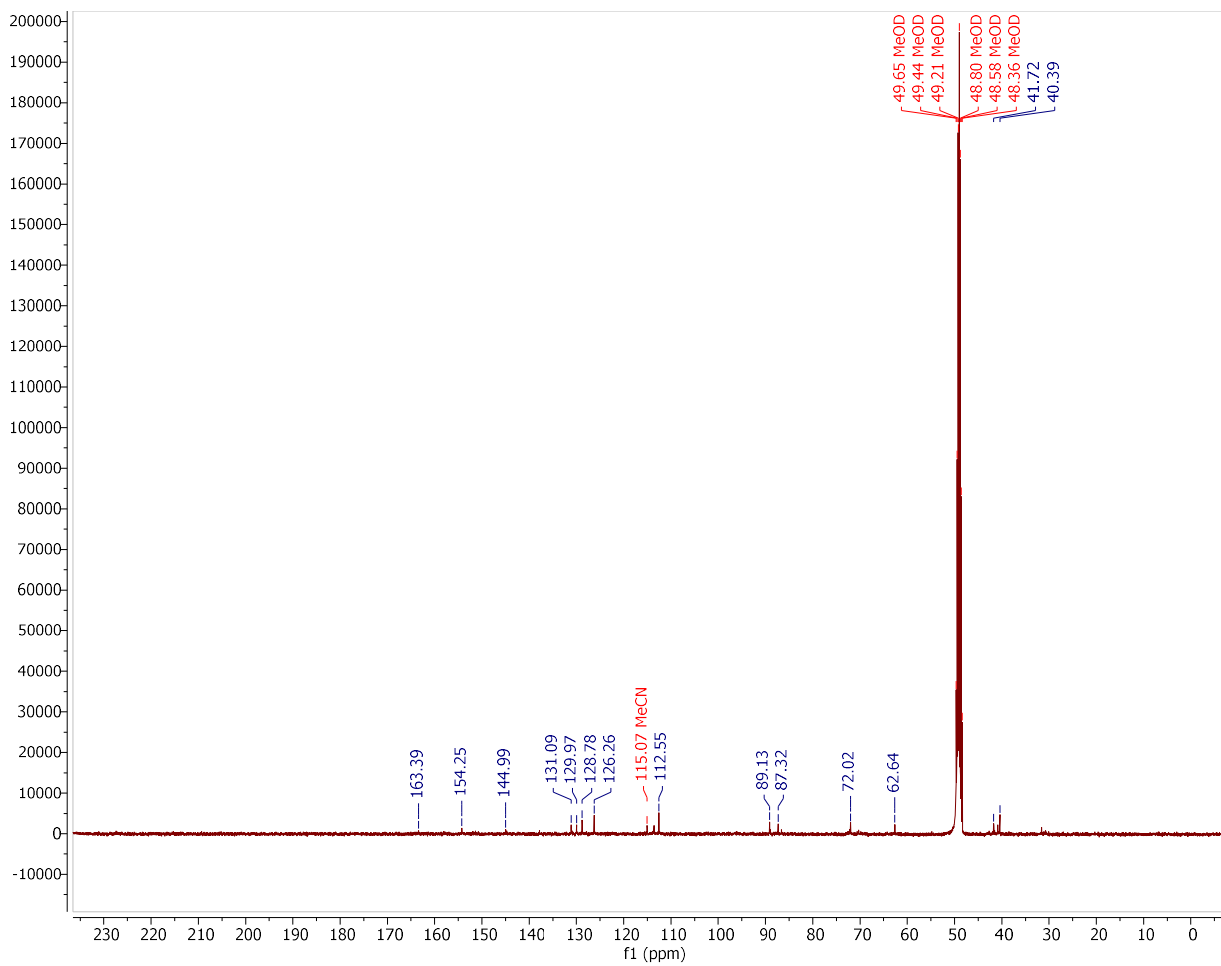


Figure S60. <sup>13</sup>C NMR of 5-((4-(*N,N*-dimethylamino)phenyl)diazenyl)-2'-deoxyuridine (IV-6)

## Incorporation of Positively Charged Linkages into DNA and RNA Backbones: A Novel Strategy for Antigene and Antisense Agents



**Author:** Moti L. Jain, Paula Yurkanis Bruice, István E. Szabó, et al

**Publication:** Chemical Reviews

**Publisher:** American Chemical Society

**Date:** Mar 1, 2012

*Copyright © 2012, American Chemical Society*

### PERMISSION/LICENSE IS GRANTED FOR YOUR ORDER AT NO CHARGE

This type of permission/license, instead of the standard Terms and Conditions, is sent to you because no fee is being charged for your order. Please note the following:

- Permission is granted for your request in both print and electronic formats, and translations.
- If figures and/or tables were requested, they may be adapted or used in part.
- Please print this page for your records and send a copy of it to your publisher/graduate school.
- Appropriate credit for the requested material should be given as follows: "Reprinted (adapted) with permission from {COMPLETE REFERENCE CITATION}. Copyright {YEAR} American Chemical Society." Insert appropriate information in place of the capitalized words.
- One-time permission is granted only for the use specified in your RightsLink request. No additional uses are granted (such as derivative works or other editions). For any uses, please submit a new request.

If credit is given to another source for the material you requested from RightsLink, permission must be obtained from that source.

[BACK](#)

[CLOSE WINDOW](#)

This is a License Agreement between Gyeongsu Park ("User") and Copyright Clearance Center, Inc. ("CCC") on behalf of the Rightsholder identified in the order details below. The license consists of the order details, the Marketplace Order General Terms and Conditions below, and any Rightsholder Terms and Conditions which are included below.

All payments must be made in full to CCC in accordance with the Marketplace Order General Terms and Conditions below.

Order Date	09-Dec-2022	Type of Use	Republish in a thesis/dissertation
Order License ID	1299191-1	Publisher	RSC Publishing
ISSN	2046-2069	Portion	Image/photo/illustration

## LICENSED CONTENT

Publication Title	RSC advances	Publication Type	e-Journal
Article Title	Nucleic acid therapeutics: basic concepts and recent developments	Start Page	16618
Date	01/01/2011	Issue	32
Language	English	Volume	4
Country	United Kingdom of Great Britain and Northern Ireland	URL	<a href="http://pubs.rsc.org/en/Journals/JournalIssues/RA">http://pubs.rsc.org/en/Journals/JournalIssues/RA</a>
Rightsholder	Royal Society of Chemistry		

## REQUEST DETAILS

Portion Type	Image/photo/illustration	Distribution	United States and Canada
Number of Images / Photos / Illustrations	2	Translation	Original language of publication
Format (select all that apply)	Electronic	Copies for the Disabled?	No
Who Will Republish the Content?	Academic institution	Minor Editing Privileges?	No
Duration of Use	Current edition and up to 10 years	Incidental Promotional Use?	No
Lifetime Unit Quantity	Up to 14,999	Currency	CAD
Rights Requested	Main product and any product related to main product		

## NEW WORK DETAILS

Title	Synthesis and studies of modified nucleobase in DNA and PNA	Institution Name	University of Western Ontario
Instructor Name	Gyeongsu Park	Expected Presentation Date	2023-02-15

## ADDITIONAL DETAILS

---

<b>Order Reference Number</b>	N/A	<b>The Requesting Person/Organization to Appear on the License</b>	Gyeongsu Park
-------------------------------	-----	--	---------------

## REUSE CONTENT DETAILS

---

<b>Title, Description or Numeric Reference of the Portion(s)</b>	An overview of general modifications and different generations of antisense oligonucleotides (AONs).	<b>Title of the Article/Chapter the Portion Is From</b>	Nucleic acid therapeutics: basic concepts and recent developments
<b>Editor of Portion(s)</b>	Sharma, Vivek K.; Rungta, Pallavi; Prasad, Ashok K.	<b>Author of Portion(s)</b>	Sharma, Vivek K.; Rungta, Pallavi; Prasad, Ashok K.
<b>Volume of Serial or Monograph</b>	4	<b>Issue, if Republishing an Article From a Serial</b>	32
<b>Page or Page Range of Portion</b>	16618	<b>Publication Date of Portion</b>	2014-04-03

## Peptide Nucleic Acid. A Molecule with Two Identities

Author: Peter E. Nielsen

Publication: Accounts of Chemical Research

Publisher: American Chemical Society

Date: Jul 1, 1999

*Copyright © 1999, American Chemical Society*



### PERMISSION/LICENSE IS GRANTED FOR YOUR ORDER AT NO CHARGE

This type of permission/license, instead of the standard Terms and Conditions, is sent to you because no fee is being charged for your order. Please note the following:

- Permission is granted for your request in both print and electronic formats, and translations.
- If figures and/or tables were requested, they may be adapted or used in part.
- Please print this page for your records and send a copy of it to your publisher/graduate school.
- Appropriate credit for the requested material should be given as follows: "Reprinted (adapted) with permission from {COMPLETE REFERENCE CITATION}. Copyright {YEAR} American Chemical Society." Insert appropriate information in place of the capitalized words.
- One-time permission is granted only for the use specified in your RightsLink request. No additional uses are granted (such as derivative works or other editions). For any uses, please submit a new request.

If credit is given to another source for the material you requested from RightsLink, permission must be obtained from that source.

[BACK](#)

[CLOSE WINDOW](#)

### PNA-nucleic acid complexes. Structure, stability and dynamics



Author: Magdalena Eriksson, Peter E. Nielsen

Publication: Quarterly Reviews of Biophysics

Publisher: Cambridge University Press

Date: Mar 17, 2009

*Copyright © Copyright © Cambridge University Press 1996*

#### License Not Required

Permission is granted at no cost for use of content in a Master's Thesis and/or Doctoral Dissertation. If you intend to distribute or sell your Master's Thesis/Doctoral Dissertation to the general public through print or website publication, please return to the previous page and select 'Republish in a Book/Journal' or 'Post on intranet/password-protected website' to complete your request.

[BACK](#)

[CLOSE](#)

## Fluorescent nucleobases as tools for studying DNA and RNA

Author: Wang Xu et al

Publication: Nature Chemistry

Publisher: Springer Nature

Date: Oct 16, 2017

**SPRINGER NATURE**

*Copyright © 2017, Nature Publishing Group, a division of Macmillan Publishers Limited. All Rights Reserved.*

### Order Completed

Thank you for your order.

This Agreement between Gyeongsu Park -- Gyeongsu Park ("You") and Springer Nature ("Springer Nature") consists of your license details and the terms and conditions provided by Springer Nature and Copyright Clearance Center.

Your confirmation email will contain your order number for future reference.

License Number 5531600630398

[Printable Details](#)

License date Apr 17, 2023

#### Licensed Content

Licensed Content Publisher	Springer Nature
Licensed Content Publication	Nature Chemistry
Licensed Content Title	Fluorescent nucleobases as tools for studying DNA and RNA
Licensed Content Author	Wang Xu et al
Licensed Content Date	Oct 16, 2017

#### Order Details

Type of Use	Thesis/Dissertation
Requestor type	academic/university or research institute
Format	electronic
Portion	figures/tables/illustrations
Number of figures/tables/illustrations	3
High-res required	no
Will you be translating?	no
Circulation/distribution	30 - 99
Author of this Springer Nature content	no

#### About Your Work

Title	Synthesis and characteristic study of modified nucleobase
Institution name	University of Western Ontario
Expected presentation date	May 2023

#### Additional Data

Portions	Figure 1 b) & c), Figure 2, Figure 5 a) & b).
----------	---

# CURRICULUM VITAE

1. **NAME: Gyeongsu Park**

2. **EDUCATION**

**Doctor of Philosophy** Sept. 2015 – June 2023  
Chemistry  
*Western University, Canada*  
Supervisor: Professor Robert H.E. Hudson

**Bachelor of Science** June 2014  
Hons. in Chemistry, Major in Medical Sciences  
*Western University, Canada*

3. **TA and OTHER RESEARCH or TEACHING RELATED EMPLOYMENT HISTORY:**

**Resource Room TA** Sept. – Dec. 2020  
Chemistry 2213: Organic Chemistry for Life Sciences Sept. 2019 – Apr. 2020  
*Chemistry Department, Western University, Canada* Sept. – Dec. 2018  
May – June 2018  
Sept. – Dec. 2017

**Laboratory TA** Sept. 2015 – Apr. 2016  
Chemistry 2213: Organic Chemistry for Life Sciences Sept. 2016 – Apr. 2017  
Chemistry 2223: Organic Chemistry of Biological Molecules Jan. – Apr. 2018  
*Chemistry Department, Western University, Canada*

4. **HONORS AND AWARDS:**

**Travel Awards** Aug. 2018  
XXIII International Round Tables on Nucleosides, Nucleotides and Nucleic acids  
*International Society of Nucleosides, Nucleotides & Nucleic Acids*

**Dean's Honor List** 2013 – 2014  
Faculty of Science  
*Western University, Canada*

5. **PUBLICATIONS:**

Park, G; Ettles, C; Charles, M; Hudson, R.H.E. Nucleobase Intrinsic Quenchers: A Fluorescence Off Switch. *Journal of Photochemistry and Photobiology A: Chemistry* **2023** (in press)

Hudson, R.H.E.; Heidari, A.; Martin-Chan, T.; Park, G.; Wisner, J. A. On the Necessity of Nucleobase Protection for 2-Thiouracil for Fmoc-Based Pseudo-Complementary Peptide Nucleic Acid Oligomer Synthesis. *The Journal of Organic Chemistry* **2019**, *84* (21), 13252–13261.



**6. PRESENTATIONS:**

**Oral presentation**

103<sup>th</sup> Canadian Chemistry Conference and Exhibition  
Virtual Conference Aug. 2021

46<sup>th</sup> International Symposium on Nucleic Acids Chemistry  
*Tokyo, Japan* Oct. 2019

102<sup>th</sup> Canadian Chemistry Conference and Exhibition  
*Quebec city, Canada* June 2019

29<sup>th</sup> Quebec-Ontario Mini-Symposium for Synthetic and Bioorganic Chemistry  
*York University, Canada* Nov. 2018

21<sup>th</sup> Chemistry and Biochemistry Graduate Research Conference  
*Concordia University, Canada* Nov. 2018

28<sup>th</sup> Quebec-Ontario Mini-Symposium for Synthetic and Bioorganic Chemistry  
*McGill University, Canada* Nov. 2017

**Poster presentation**

CAMBR(Centre for Advanced Materials and Biomaterials Research) Day  
*Western University, Canada* Apr. 2019

XXIII International Round Tables on Nucleosides, Nucleotides and Nucleic acids  
*University of California San Diego, USA* Aug. 2018

Western Research Forum  
*Western University, Canada* Mar. 2018

100<sup>th</sup> Canadian Chemistry Conference and Exhibition  
*Toronto, Canada* June 2017

**7. UNIVERSITY/SOGS ADMINISTRATIVE DUTIES:**

<b>SOGS Councilor</b> Society of Graduate Students <i>Western University, Canada</i>	Sept. 2016 – Sept. 2019
<b>Alternative SOGS Councilor</b> Society of Graduate Students <i>Western University, Canada</i>	Sept. 2015 – Aug. 2016
<b>Graduate Student Teaching Awards Committee</b> Society of Graduate Students <i>Western University, Canada</i>	Nov. 2018. – Aug 2020
<b>Health Plan Committee</b> Society of Graduate Students <i>Western University, Canada</i>	Oct 2018. – Aug 2020
<b>SOGS's 50<sup>th</sup> Anniversary Committee</b> Society of Graduate Students <i>Western University, Canada</i>	Mar. – Sept. 2018
<b>CGSA Executive Member</b> Chemistry Graduate Student Association <i>Western University, Canada</i>	Sept. 2018 – Aug 2021
<b>Safety Representative</b> Hudson Research Group, Department of Chemistry <i>Western University, Canada</i>	Sept. 2016 – Nov 2021
<b>First Aid Responder</b> 2 <sup>nd</sup> floor of Chemistry Building, Department of Chemistry <i>Western University, Canada</i>	June.2017 – Aug 2021

**8. COMMUNITY/OUTREACH SERVICE:**

**Outreach Volunteer**

March Break Open House	Department of Chemistry	Mar. 2019
O-week Liquid nitrogen ice cream	Western Chemistry Club	Sept. 2018
Science Rendezvous, Canada's National Celebration of Science	Department of Chemistry	May. 2018
Slime experiment during STEMposium/Women in Science conference	Department of Chemistry	Mar. 2018
March Break Open House	Department of Chemistry	Mar. 2018
Synthesis experiment with Saunders / Montcalm Secondary School grade 12 students	Department of Chemistry	Dec. 2017
Equilibrium experiment with A.B. Lucas Secondary School grade 12 students	Department of Chemistry	Dec. 2017
Electrochemistry experiment with East Elgin Secondary School grade 12 students	Department of Chemistry	Dec. 2017

Slime experiment with 78th Brownies, grade 1&2 students	Department of Chemistry	Dec. 2017
Fall preview day	Department of Chemistry	Nov. 2017
Synthesis experiment with secondary school grade 11 students	Department of Chemistry	July 2017
Slime experiment with Mountsfield Public School grade 1 students	Department of Chemistry	June 2017
Equilibrium experiment with Catholic Central Secondary School grade 12 students	Department of Chemistry	June 2017
Slime experiment with Arthur Ford School grade 1&2 students	Department of Chemistry	June 2017
Equilibrium experiment with A.B. Lucas secondary school grade 12 students	Department of Chemistry	June 2017
Slime experiment with Chatham Christian School grade 1 students	Department of Chemistry	May 2017
Science Rendezvous, Canada's National Celebration of Science	Department of Chemistry	May 2017
Slime experiment with S.O.A.R. program, Stratford, grade 4-6 students	Department of Chemistry	May 2017
Early Outreach Conference	Department of Chemistry	May 2017
Slime experiment during STEMposium/Women in Science conference	Department of Chemistry	Mar. 2017
March Break Open House	Department of Chemistry	Mar. 2017
Paper chromatography experiment with grade 8 students	Department of Chemistry	Feb. 2017
Calorimetry experiment with grade 10 students	Department of Chemistry	Dec. 2016
Slime experiment with grade 2 students	Department of Chemistry	Dec. 2016
Synthesis experiment with Montcalm Secondary School grade 12 students	Department of Chemistry	Dec. 2016
Fall preview day	Department of Chemistry	Nov. 2016
March Break Open House	Department of Chemistry	Mar. 2016
Synthesis experiment with Montcalm Secondary School grade 11 students	Department of Chemistry	Dec. 2015
Equilibrium experiment with A.B. Lucas secondary school grade 8 students	Department of Chemistry	Dec. 2015
Fall preview day	Department of Chemistry	Nov. 2015
National Chemistry Week	Western Chemistry Club	Oct. 2015

### Community Service

Taekwondo Instructor	Western Taekwondo Club	Sept. 2016 – Present
Taekwondo Head Instructor	Western Taekwondo Club	May 2017 – Apr. 2018
Club Executive Member	Western Taekwondo Club	May 2016 – Apr. 2017
Volunteer	Let's Talk Science at Western	Sept. 2015 – Apr. 2017